Smart TSO-DSO interaction schemes, market architectures, and ICT solutions for the integration of ancillary services from demand-side management and distributed generation

Network and market models

D2.2

Authors:

Guillaume Leclercq (N-SIDE), Marco Pavesi (N-SIDE), Thomas Gueuning (N-SIDE), Araz Ashouri (N-SIDE), Peter Sels (N-SIDE), Frederik Geth (KU Leuven/VITO/EnergyVille), Reinhilde D'hulst (VITO/EnergyVille), Hélène Le Cadre (VITO/EnergyVille)

Distribution Level	Public
Responsible Partner	N-SIDE
Checked by WP leader	Mario Džamarija (DTU) - Date: 15/02/ 2019
Verified by the appointed Reviewers	Pekka Koponen (VTT), Yelena Vardanyan (DTU) - Date: 15/02/ 2019
Approved by Project Coordinator	Gianluigi Migliavacca (RSE) - Date: 15/02/ 2019

This project has received funding from the European Union's Horizon 2020 research and innovation programme under grant agreement No 691405

Issue Record

Planned delivery date	30/06/2018
Actual date of delivery	15/02/2019
Status and version	FINAL

Version	Date	Author(s)	Notes
1.0	30/11/2018	N-SIDE and VITO	Submitted draft for internal review
1.1	27/12/2018	Pekka Koponen (VTT) and Yelena Vardanyan (DTU)	Review of the document provided to authors
1.2	8/02/2019	N-SIDE and VITO	Second version, answering the reviewers comments

About SmartNet

The project SmartNet (http://smartnet-project.eu) aims at providing architectures for optimized interaction between TSOs and DSOs in managing the exchange of information for monitoring, acquiring and operating ancillary services (frequency control, frequency restoration, congestion management and voltage regulation) both at local and national level, taking into account the European context. Local needs for ancillary services in distribution systems should be able to co-exist with system needs for balancing and congestion management. Resources located in distribution systems, like demand side management and distributed generation, are supposed to participate to the provision of ancillary services both locally and for the entire power system in the context of competitive ancillary services markets.

Within SmartNet, answers are sought for to the following questions:

- Which ancillary services could be provided from distribution grid level to the whole power system?
- How should the coordination between TSOs and DSOs be organized to optimize the processes of procurement and activation of flexibility by system operators?
- How should the architectures of the real-time markets (in particular the markets for frequency restoration and congestion management) be consequently revised?
- What information has to be exchanged between system operators and how should the communication (ICT) be organized to guarantee observability and control of distributed generation, flexible demand and storage systems?

The objective is to develop an ad hoc simulation platform able to model physical network, market and ICT in order to analyze three national cases (Italy, Denmark, Spain). Different TSO-DSO coordination schemes are compared with reference to three selected national cases (Italian, Danish, Spanish).

The simulation platform is then scaled up to a full replica lab, where the performance of real controller devices is tested.

In addition, three physical pilots are developed for the same national cases testing specific technological solutions regarding:

- monitoring of generators in distribution networks while enabling them to participate to frequency and voltage regulation,
- capability of flexible demand to provide ancillary services for the system (thermal inertia of indoor swimming pools, distributed storage of base stations for telecommunication).

Partners

Table of Contents

List of Abbreviations and Acronyms

Acronym	Meaning
AC	Alternating Current
aFRR	Automatic Frequency Restoration Reserves
AS	Ancillary Service
BFM	Branch Flow Model
BIM	Bus Injection Model
BRP	Balance Responsible Party
CHP	Combined Heat and Power
CMP	Commercial Market Party
CQCP	Convex Quadratically-Constrained Programming
CS	Coordination Scheme
DA	Day-Ahead
DC	Direct Current
DER	Distributed Energy Resource
DLMP	Distribution Locational Marginal Price
DSO	Distribution System Operator
EBGL	European Balancing guidelines
ENTSO-E	European Network of Transmission System Operators for Electricity
FACTS	Flexible Alternating Current Transmission Systems
FAT	Full Activation Time
FCR	Frequency Containment Reserve
FERC	Federal Energy Regulatory Commission
FRR	Frequency Restoration Reserve
FSP	Flexibility Service Providers
GCT	Gate Closure Time
GNE	Generalized Nash equilibrium
HV	High Voltage
HVDC	High-Voltage Direct Current
IIC	Improved Impedance Calculation
IP	Interior-Point
KCL	Kirchhoff Current Law
KVL	Kirchhoff Voltage Law
LMP	Locational Marginal Price

LP	Linear Programming
mFRR	Manual Frequency Restoration Reserve
MI	Mixed Integer
MICP	Mixed Integer Convex Programming
MILP	Mixed Integer Linear Programming
MISOCP	Mixed Integer Second-Order Cone Programming
MV	Medium Voltage
NLP	Nonlinear Programming
OLTC	On-Load Tap Changing
OPF	Optimal Power Flow
PQ	Active Power-Reactive Power
PSD	Positive Semidefinite
PTDF	Power Transfer Distribution Factors
PV	Active Power-Voltage
QC	Quadratic-Convex
QP	Quadratic Programming
RES	Renewable Energy Sources
SDP	Semidefinite Programming
SI	The International System of Units
SO	System Operator
SOC	Second-Order Cone
SOCP	Second-Order Cone Programming
SCOPF	Security-Constrained Optimal Power Flow
SOS1	Special Ordered Set type 1
SW	Social Welfare
TF	Transformer
TSO	Transmission System Operator
UPFC	Unified Power Flow Controller

Executive Summary

The increasing share of intermittent renewable energy sources (RES) [1] in the European electricity grid results in higher need for flexibility resources providing ancillary services (AS) to compensate for the power fluctuations. The imbalances introduced by RES are caused by a difference between the actual generation and the forecast values. Luckily, the rapid development of grid-connected distributed energy resources (DER) offers new sources of flexibility for the power system operators at both distribution and transmission level.

These distributed flexibilities have to be harvested in a proper way, in order to stay compatible with the current power system while avoiding the introduction of new system-imbalance, congestions, and voltage problems. It is therefore of key importance to adapt the current AS market mechanisms to allow an effective and efficient participation of DERs for providing different ancillary services.

To this end, the *Integrated Reserve* market architecture is proposed, which aims at leveraging the flexibility of DERs for providing different ancillary services to the transmission grid (ignoring cross-border exchanges) as well as local services to the distribution grid. This market aims at procuring such flexibility services in an optimal way (e.g. minimize activation costs, or maximizing welfare,...). In such a setting, DERs compete with centralized sources of flexibility, both traditional (e.g. big power plants directly connected to transmission grid) and new (e.g. large centralized electricity storages), in a level playing-field. Compared to centralized resources, DERs typically offer a better aggregated reliability (through high redundancy) in their flexibility provision, and many of them may provide a faster response time. Also, DERs are closer to the sources of power flow variations and better distributed around the grid. Liquidity could largely increase since the DER potential is huge, while the cost impact is still very unsure and dependent on the DER type. A design for the Integrated Reserve market aligned with the use cases defined and developed in deliverable D1.3 of SmartNet project [2] is provided, and the link is made to the current ancillary service markets settings in the three pilot countries investigated in the SmartNet project, namely Denmark, Italy, and Spain [3].

As shown in the figure below, the market receives bids as input (from aggregators or larger commercial players). Then, the market is cleared, i.e. quantities and prices are determined according to an algorithm (see blue block) solving an optimization problem under constraints, possibly taking into account the network model of the transmission and distribution grid (see orange blocks). In the deliverable, the market products list, network models, and clearing algorithm are described separately.

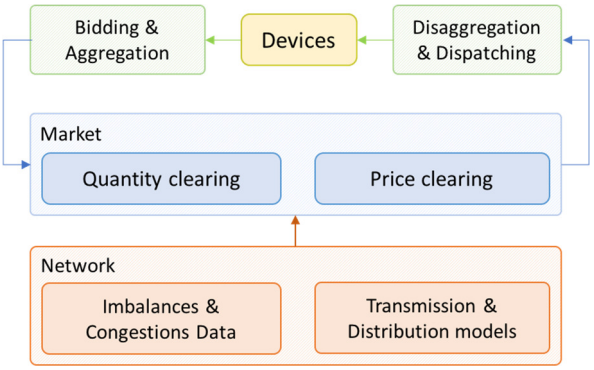

A block-diagram representing various blocks in the system.

The market products (or bids) list defines the types of bids which can be submitted to the market. The market allows both simple bids (specified by quantities and prices) and complex bids (specified by quantities, prices but also further constraints on the quantities, such as ramping constraints or exclusive bids). Complex products aim at capturing the dynamics of different flexibility resources while expressing the constraints of assets, aggregators, and system operators. The result is a catalog of products which can be optionally integrated in the market, according to the desire of system operators and regional regulations.

Transmission and Distribution network models can be used in the market clearing algorithm in order

1. to make sure that their constraints are not violated when clearing the market
2. to solve (current) congestions or other local problems (e.g. over- or under voltages)

There is a trade-off regarding the complexity of the network model to be included in the constraints of market clearing algorithm: it cannot be very simplified (otherwise it creates a big demand for countertrading because the physical constraints of network will not be taken into account in the market clearing algorithm) but it cannot be too complex (in order to maintain the algorithm computationally tractable). Therefore, a proper network model is chosen based on the type, topology, and size of the power network. The selected model is a second-order cone programming model (SOCP) model for distribution network and a direct current (DC) model for the transmission network.

In the clearing module, methods for finding the optimal values of traded quantity (of energy) and the resulting price (of the corresponding quantity) are developed. The clearings of quantity and price are not separable tasks, but rather sequential procedures belonging to the same module. The most straightforward and meaningful methods of clearing are explained.

Furthermore, various coordination schemes for the acquisition of ancillary services between the transmission system operator (TSO) and the distribution system operator (DSO) have been defined in [2]. They rely on centralized or decentralized market approaches (see Table below) where the flexibilities from the different DERs are leveraged via local and/or global (common) markets at the DSO and TSO levels. As a brief summary (see [2] for more details), there are five of them :

Centralized architecture	Decentralized market architecture
Centralized AS market	Local AS market
Common TSO-DSO AS market (centralized)	Common TSO-DSO AS market (decentralized)
Integrated flexibility market	Shared balancing responsibility model

Table showing the different TSODSO coordination schemes according to their centralized/decentralized nature

- *Centralized AS market model*: the TSO operates an AS market for both resources located at transmission and distribution level, with no or little involvement of the DSO.
- *Local AS market model*: the DSO operates a local market to solve distribution grid problems and then aggregates and offers the remaining flexibility bids to the TSO market.
- *Shared balancing responsibility model:* the balancing responsibilities are divided between TSO and DSOs according to a predefined schedule, and each SO organizes his own market. DER flexibility is not accessible by the TSO
- *Common TSO-DSO AS market model*: TSO and DSO have the common objective to minimize the total costs needed to satisfy their respective services (AS for TSO and local services for DSO). This objective can be reached with two variants of coordination
    - a common (centralized) market for both TSO and DSO needs
    - a decentralized architecture, but with a dynamic integration of a local market operated by the DSO.
- *Integrated flexibility market model*: there is one centralized market open to TSO/DSOs but also to commercial market parties (e.g. BRPs).

In this deliverable, each of these TSO-DSO coordination schemes is further explored in terms of market design and market clearing algorithms, using the Integrated Reserve architecture framework described previously. Specifically, the two main market structures, namely the centralized and the decentralized approaches are investigated, as shown in the figure below. Using the generic features developed for market products, network models and market clearing, the market clearing problem is formulated for each TSO-DSO coordination scheme.

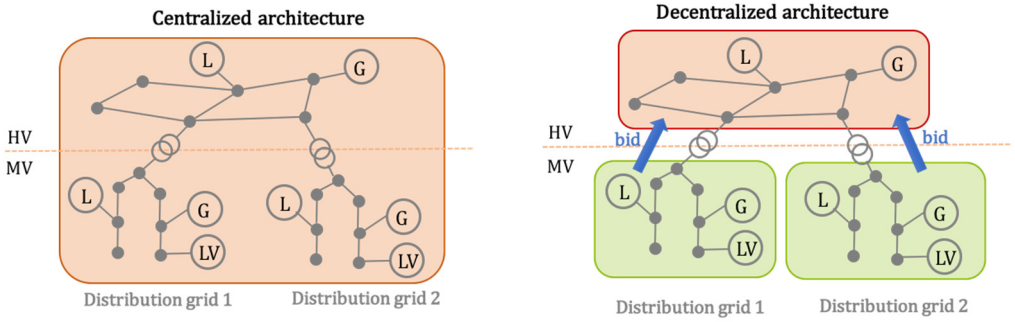

Diagrams showing centralized and decentralized market architectures.

On top of this, there are different requirements regarding the parameter settings, input/output data, and arrangement of modules for each TSO-DSO coordination schemes, as well as additional local optimization algorithms for the decentralized schemes (e.g. the aggregation procedure of the DSO, who must cluster the flexibility available in its local market to create a bid for the TSO market).

Finally, a brief discussion is made regarding the computational tractability of the market clearing algorithms, for each TSO-DSO coordination scheme. In short, taking into account the full grid model (TSO and DSO grids) and allowing many complex products comes at a cost on time to reach a solution.

1 Introduction and objectives

1.1 Context

The increasing share of Distributed Energy Resources (DERs) in the distribution grid offers new sources of flexibility which can be leveraged by both commercial market parties (e.g. a balance responsible party (BRP) trying to balance its own portfolio) and by system operators (SOs). In particular, flexible DER have the potential to provide local services to the Distribution System Operators (DSOs) and/or ancillary services (AS) to the Transmission System Operators (TSOs). The provision of AS by resources connected to the distribution grid requires the coordination between TSO and DSOs. In [2], several TSO-DSO coordination schemes have been described and analyzed. They rely on centralized or decentralized approaches where the flexibilities from the different DERs are leveraged via local and/or global (common) markets at the DSO and TSO levels. As a brief summary (see [2] for more details), there are five of them (see Figure 1-1):

- *Centralized AS market model*: the TSO operates an AS market for both resources located at transmission and distribution level, with no or little involvement of the DSO.
- *Local AS market model*: the DSO operates a local market to solve distribution grid problems and then aggregates and offers the remaining flexibility bids to the TSO market.
- *Shared balancing responsibility model:* the balancing responsibilities are divided between TSO and DSOs according to a predefined schedule, and each SO organizes his own market. DER flexibility is not accessible by the TSO
- *Common TSO-DSO AS market model*: TSO and DSO have the common objective to minimize the total costs needed to satisfy their respective services (AS for TSO and local services for DSO). This objective can be reached with two variants of coordination
    - a common (centralized) market for both TSO and DSO needs
    - a decentralized architecture, but with a dynamic integration of a local market operated by the DSO.
- *Integrated flexibility market model*: there is one centralized market open to TSO/DSOs but also to commercial market parties (e.g. BRPs,i.e. Balance Responsible Parties).

As shown in Figure 1-1, three ancillary services have been further investigated in [2], among the multiple current and future AS described in [3]: 1) frequency control (FCR), 2) balancing and congestion management (both at transmission and distribution levels), and 3) also voltage control.

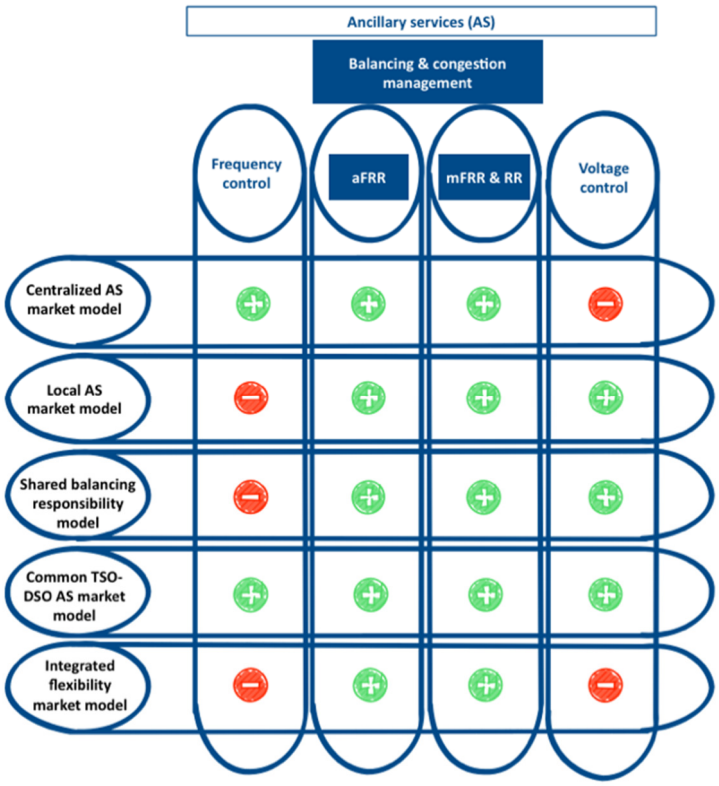

Figure 1-1 Mapping of ancillary services and coordination schemes (Figure taken from [2]*)*

It is of key importance to specify and adapt the AS market mechanisms to allow an efficient participation of DERs. The AS market should aim at leveraging in an optimal way (e.g. maximizing welfare, liquidity) the flexibility of DER. DER would compete with other centralized sources of flexibility, traditional (e.g. big power plants connected to the transmission grid, traditionally providing ancillary services) and new (e.g. large centralized energy storages).

Importantly, each of the five TSO-DSO coordination schemes is characterized by a specific market design. Some high-level features for the market design for each coordination scheme have been described in [2]:

- **market scope**: specification whether resources from distribution and transmission grid participate or not to the same market session.
- **market organization**: set of discrete auctions vs continuous market? For different reasons (see [2] for detailed explanations) like:
    - continuous markets less relevant if higher clearing frequency of discrete auctions
    - more complex to take the network constraints into account
    - more gaming possible between commercial market parties and system operators

  the choice has been made for a set of discrete auctions and continuous markets are not considered in the remainder of this deliverable.
- **market operation**: description of who runs the market

However, the detailed market design options and clearing algorithms need to be developed for each TSO-DSO coordination scheme, in light of building the SmartNet simulation platform.

1.2 Objective and scope

The main objective of this deliverable is to further define the AS market design for each TSO-DSO coordination scheme, i.e. establish a mathematical model of the market clearing algorithm needed to compute the dispatched quantities and prices of the AS market.

When designing a platform for ancillary services, two different aspects can be considered: the procurement of these ancillary services in terms of capacity (reserves) and the actual activation of these services in terms of energy. While activation of AS is by nature a real-time process, the procurement of flexibility capacity can be a yearly, monthly, weekly, daily or even closer to real-time process. Furthermore, different co-optimization mechanisms between capacity procurement and activation of AS can be considered ([4]). In the context of the SmartNet project, only the activation component is considered[1]: how to design a real-time energy market where flexibilities from DERs (at distribution level) and from assets connected at the transmission network level are activated in an optimal way. Optimal should be according to some objective function (e.g. maximize social welfare, minimize (reserve) activation costs): this is discussed in chapter 5.

Based on this choice, the FCR ancillary service (see Figure 1-1), is not further considered in the following, since it is not likely to have a real-time auction-like market for FCR activation , because the activation of this fast frequency control is based on local controllers measuring the network frequency, and correcting for any deviation. The same comment applies to aFRR, for which the activation is automatic and the update of the setpoints too frequent (5-10 sec) to allow a market to define the activation of these products at the same frequency.

Regarding voltage-control service (see Figure 1-1), the local characteristic of such service implies that a sufficient market liquidity can generally not be achieved, therefore these services were not further considered in this deliverable[2].

Instead, in this deliverable, the real-time energy market design is developed to consider the activation of balancing and congestion management services (for the latter, both for transmission and distribution levels), as illustrated in Figure 1-2. An innovative market design is proposed, in order to:

[1] It is assumed that the reserve has already been procured and/or that regulation enforces some resources to provide AS. Also, free bids can also be considered in this energy real-time market.

[2] voltage-control service will not be considered, but at distribution level (medium voltage), operational constraints on voltage will be taken into account when procuring balancing/congestion services.

- leverage flexibilities coming from both transmission grid and distribution grid resources (*geographical scope* expansion, compared to most current AS markets, see [2], [3]).
- combine multiple services in a single market: providing balancing services to the whole system, but also providing congestion management both at the level of distribution and transmission networks (*services scope* extension). In particular, this requires to take the transmission and distribution grid constraints (if any) into account in the market design.
- develop a generic timing extension (*timing scope* extension), consisting of a higher clearing frequency (if needed) and considering (the possibility of) a rolling time horizon (similar to what is already done in California for instance [5]).

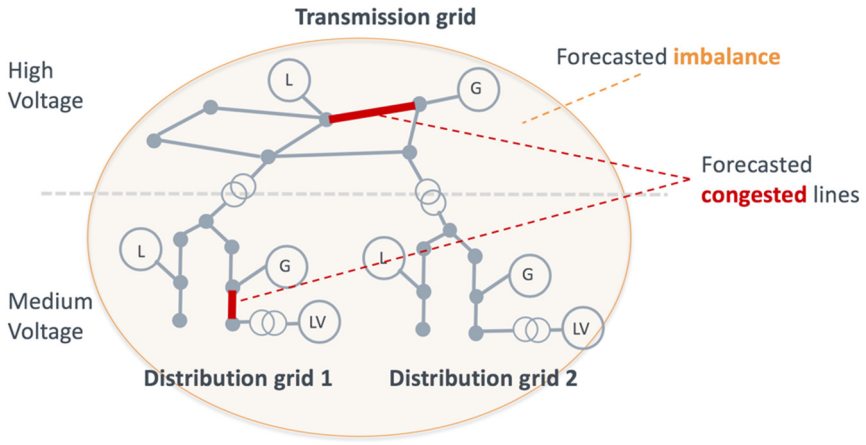

Figure 1-2 Market aims at activating services for balancing and congestion (both transmission and distribution) purposes

In this deliverable, this generic market design is called *The Integrated Reserve market design.* It is important to specify that with specific choices of settings of this market, we can reproduce the activation of existing mFRR and/or RR reserves. However, with other settings, it can rather be considered as a benchmark model, perhaps more ambitious, but still realistic in the long term. Importantly, the timing of gate closure is not determined in this deliverable, but is rather a market design parameter that can be played with (it should be with care since the interaction with intra-day and faster markets might be complex).

The key challenge of this new market design is to create an economically efficient but also computationally tractable market clearing process for the Integrated Reserve market, for each of the 5 different TSO-DSO coordination schemes (see section 1.1), such that all possible constraints can be taken into account, including for instance transmission and distribution network constraints, as well as market products and their associated constraints.

1.3 Document Structure

This deliverable aims at proposing a generic design for Integrated Reserve market, to be aligned and adapted to each TSO-DSO coordination scheme developed in [2]. The targeted market will allow TSO/DSO to leverage flexibilities from DERs in an efficient way and provide AS both at the local and global level.

In Chapter 2, a general overview of the aspects to be tackled in the market design is provided. Timing, bidding and pricing aspects are addressed together with network models. Also, optional extensions (in terms of AS and timing) are discussed, and a description of how the Integrated market reserve can fit to the current AS market settings in place in the three pilot countries (Denmark, Italy and Spain) is made.

Chapter 3 is dedicated to market products: it describes a catalogue of different possible market products to bid the flexibility of DERs in the new AS market.

In Chapter 4, several models (with varying level of complexity) of the distribution and transmission network model are considered, with the objective that they are used in the market clearing algorithm in order to take the network constraints into account.

In Chapter 5, the market clearing optimization problem is described. In particular, the acceptance procedure, the objective function, necessary network constraints, and other related elements are described in detail. Furthermore, the derivation of Distributed Locational Marginal Prices (DLMP) is explained, using the dual variables of the optimization problem described in chapter 5, providing an interpretation for these nodal prices.

Chapter 6 describes and explains the market clearing algorithms for each TSO-DSO coordination scheme (see [2]), making use of the materials developed in the previous chapters. This chapter also describes the specificities of smart DSO aggregation, used on some of the decentralized TSO-DSO coordination schemes. Also, a game theory perspective is introduced in this chapter, to reflect on some specific variations of coordination schemes.

Then, Chapter 7 investigates briefly the computational requirements of the market clearing algorithms for the different TSO-DSO coordination schemes, and provides some comparisons in terms of computational tractability between different market settings.

2 Market Design

In the previous chapter, the Integrated Reserve market concept is explained, and it was described how it differentiates from the current solutions for balancing and other ancillary services. In this chapter, the key ingredients to be considered in the market design for the Integrated Reserve market are described, regardless of the TSO-DSO coordination scheme considered, namely timing, network models, bids/market products, clearing objective and pricing. Some of them are then extensively described in the next chapters. Then, a generic description of a market clearing problem formulation is proposed. Importantly, required inputs to the market are described in the next section. Then, options are proposed, in terms of service and timing. Finally, the last section described the current AS markets situation in existing pilot countries (i.e. Spain, Italy, Denmark) and the minimal requirements required to mimic them using the market design used in this deliverable.

2.1 Timing

Some key elements of any market design lies within timing aspects. Some key timing parameters are described below and illustrated in *Figure **2**-**1***. As explained in section 1.2, discrete auction format is considered.

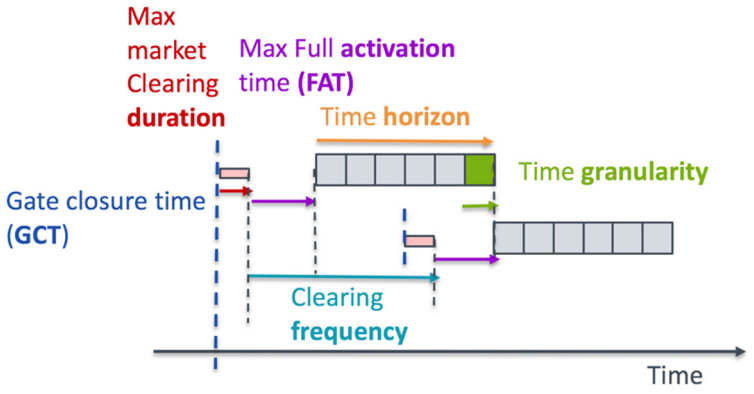

Figure 2-1 Illustration of some key market design timing parameters

- **Time horizon** (also called optimization period, or delivery window)**:** Time period considered for the market clearing (e.g. 24 hours on the Day-Ahead (DA) market).

- **Time granularity** (also called time step)**:** Time granularity for the market clearing (e.g. 1 hour on the DA market). The time granularity can be lower or equal to the time horizon. Activation decisions (i.e. quantity, price) are made for each time step. Typically, the time horizon is split into one or several time steps. Having several time steps in the market time horizon is a necessary condition to have complex market products with inter-temporal constraints (e.g. ramping constraints limiting the change in activation from one time step to the

other), as described further in section 3.5. It also allows the system operators to refine their needs at a more granular level.

- **Max market clearing duration** (also called max activation optimization function (AOF) duration): maximum time allowed to the market clearing to find a(n) (optimal) solution (e.g. 10 min for the DA market).

- **Max Full Activation Time** (FAT): time allowed to flexibility providers to react (delay) and ramp-up to the required activation they committed. This is typically used in balancing products requirements.

- **Gate Closure Time** (GCT): Time at which orders from market participants can no longer be changed and no new orders can be accepted (e.g. 11:00AM for the DA market). In theory, different GCTs could be considered for flexibility providers (sellers) and for system operators (flexibility buyers), but having different GCTs might be dangerous in leading to market inefficiencies. This option is not considered in the remainder of the document, i.e. flexibility buyers and sellers have the same GCT.

- **Frequency of clearing**: It defines how often the market is cleared (e.g. every day for the Day-Ahead market

Regarding the Integrated Reserve market, here are some considerations regarding these parameters:

If **GCT** is closer to real-time, the flexibility providers have less uncertainty on the real-time flexibility availability during the market horizon (provided the market horizon is not too long), and the system operators can have a better forecast of their network state (imbalances, congestions). However, GCT is limited by the max FAT time and the max market clearing duration. In this sense max FAT-time could be reduced as much as possible, but this can thus limit the participation of slow-to-react assets and/or assets with low ramping capabilities. Also, the maximum market clearing duration could be reduced, but there is a clear trade-off between the maximum clearing time and the possible computational complexity: if market clearing duration is short, only relatively low complexity problems can be solved

On the **time horizon**, there are two cases:

- if the time horizon comprises **a single time step**, then there is no clear interest in having a large time horizon, because it usually implies less accurate forecasts (above some given time limit, e.g. 1 hour) of both the system operators (SO) needs and of the available flexibility of assets for flexibility providers. Also, there is no granularity, which prevents the SO to express a detailed need and the flexibility providers to express inter-temporal constraints and/or varying availability over the time horizon. In summary, a short time horizon is better in this case.
- if the time horizon comprises **multiple time steps**, then it is likely beneficial to have a longer time horizon: assets can have ramp-up/down limitations or many other temporal constraints. If the time horizon is of the same order than the time duration of the inter-temporal constraints of assets, then the market will be able to optimally allocate the activation of the assets during the time horizon. However, the forecast issue remains similar, in case of a long time horizon: for example,

if the latest "acceptable" forecast is available for one hour ahead, the horizon should not be selected as two hours. But if the horizon is shorter than the latest acceptable forecast, the potential of inter-temporal constraints of flexibility providers will not be harvested.

Regarding the **clearing frequency**, a frequent clearing is much better in order to always account for the most updated forecasts (i.e. better forecast needs by SO, better estimation of the available flexibility from the pool of flexibility providers). However, as illustrated by *Figure **2-1*** (in which it is implicitly assumed that clearing is performed for non-overlapping time horizons), the market clearing frequency is limited by two elements: (1) the clearing frequency must correspond to the time horizon (e.g. DA market has a clearing every day and a time horizon of 1 day), and so it is not possible to have a high frequency and a long time horizon (which can be desirable, as explained above). (2) assuming a short time horizon makes sense (and so a high clearing frequency), a second limitation is the time between GCT and real-time (already described above): there is no point in having a very short time horizon (and so high clearing frequency), if the time between GCT and real-time is significant.

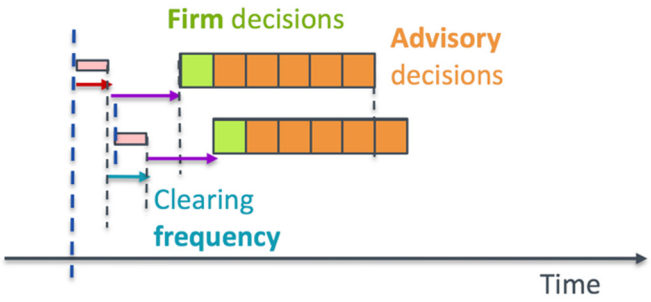

*Figure 2-2 The rolling optimization looks ahead until the end of the horizon. Dispatch and prices for the first (upcoming) time step are **firm** (green squares), while the remaining dispatch and price decisions are (mostly) **advisory** (orange squares).*

However, it is possible to decouple the clearing frequency from the time horizon, using a rolling optimization technique, as illustrated in *Figure **2-2***. In this case, it is possible to combine the advantages of a high clearing frequency, together with the advantages of a long time horizon (see above). In this rolling optimization approach, the same market time-step can be cleared in several consecutive optimizations. As the time window moves forward and the state of the system evolves, the activation decisions can be different for the same time step between two different market clearings. This raises the issue of the firmness for the activation decisions:

- For the first time-step of the considered time horizon (see *Figure **2-2***), the activation decisions generated by the market clearing are by nature firm as it is the last time that this time step is considered in the market clearing.

- For the other times steps of the considered time horizon, some of the decisions could be firm and therefore not a variable anymore for the future market clearings considering this time step (e.g. the activation of an asset with a constraint of minimum duration of activation) while other market decisions could be indicative but not binding (e.g. the exact quantity of flexibility asked to this asset for the considered time step).

In summary, the choice of timing parameters is very important. However, in this deliverable, the algorithms described can be applied to many combinations of choices of these timing parameters. In this way, a simulator of this market would be able to easily perform sensitivity analyses and/or scenarios on these timing parameters, using a single generic model.

2.1.1 Feedback from Consultation: Timing

A public consultation survey regarding various aspects of market design was carried out online [6] for a duration of 2 months. Several questions were asked and 12 participating stakeholders[3] provided their feedbacks for the survey. In general, the majority of participants believed in a future ancillary service market which is more dynamic, more extensive, and economically efficient.

In this section of the survey, 4 questions were asked. The question covered the topics of more frequent market clearing (closer to real-time), rolling-horizon optimization, and imbalance forecasting.

Among the stakeholders, none of them was opposed to a more frequent market clearing, which supported the idea of a more frequent market clearing auction. Furthermore, more than half of the participants confirmed that it is feasible to manage the inputs and outputs within 5 minutes. Some were skeptical about such a fast clearing-scheme, arguing that the system is not ready for this change yet, or claiming that it will not create any benefits for the market. In average, the answers were more supportive than opposing.

Regarding the rolling-horizon optimization, participants were quite positive. However, some participants had concerns about challenges with imbalance forecasting and transparency of decisions.

2.2 Network model

Since the idea of the integrated Reserve market is to activate flexibility bids for both balancing and congestion management (at distribution and transmission) purposes in a single market, as highlighted in **Errore. L'origine riferimento non è stata trovata.**, there is a clear need for the algorithm to take the network constraints into account. Therefore, the clearing of the considered market will be based on an appropriate mathematical representation of the transmission and distribution grids. The challenge is to find a network model which is at the same time:

[3] ACER, Clevergy, Comillas, cyberGRID, EDF, EIMV, ENEL, Epex Spot, European Commission, IBERDROLA, RTE, S&T consulting.

- Sufficiently accurate, to identify and solve the balancing and congestion issues and avoid creating voltage problems;
- Sufficiently efficient, to be tractable in the optimization problem which is solved at every time step; and
- Sufficiently simple, to include only functions that are important to build up the market algorithm and the test cases.

Chapter 4 tackles this question in details and assess different network model options for both the transmission and distribution grid.

2.2.1 Feedback from Consultation: Network

The general opinion about the integration of transmission and distribution grids in the market was questioned: the response was equally positive and negative with some neutral feedbacks. Some participants believed that these models can be added gradually, while other participants argued that it would introduce complexities and that we should take the network models out of the market clearing problem.

2.3 Bidding

The Integrated Reserve market is organized as a close-to-real-time market where the traded quantities are flexibility offers provided by resources located at transmission (e.g. conventional generators, energy intensive loads) and distribution level (DERs, see details in [7]). These flexibility offers are expressed in terms of energy (positive for injecting more active power or decreasing active power consumption, negative for injecting less active power or increasing active power consumption). The flexibilities are obtained by modifying the planned schedule/commitment on previous markets (such as day-ahead and intra-day markets), or by modifying the real-time baseline operation, depending on the nature of the assets providing flexibility [8]. The sellers (or providers) of flexibility are typically aggregators or sufficiently large flexible assets connected at transmission or distribution levels; while the buyers are the grid operators (TSO, DSO), or even commercial market parties (CMP) in one of the TSO-DSO proposed coordination schemes.

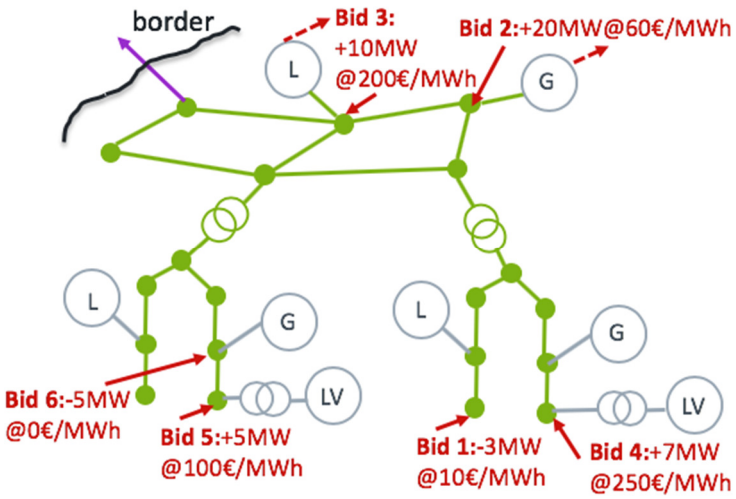

Figure 2-3 Example of location-dependent upwards (+ quantity) and downwards (- quantity) flexibility bids

Note that, as mentioned in Chapter 1, reserves (capacity) procurement for the Integrated Reserve is not considered in the SmartNet project perimeter and this report exclusively describes the market for the **activation** decision process.

Within a given market session, a flexibility provider will place a bid in the form of a price-quantity curve specifying the price asked for different levels of extra supply or consumption of energy (via the extra injection or off-take of active power). Importantly, since the Integrated Reserve market aims at solving balancing and congestion problems together, there is the necessity of having a grid model (as seen in section 2.2). Therefore, as illustrated in Figure 2-3, bids sent to the market must be detailed per node of the transmission/distribution grid models considered in the market clearing algorithm, which is a required condition for the optimization algorithm to compute and limit the power flows of the network.

A bid on the market could also include temporal or logical constraints, for example:

- Ramping constraints;
- Maximum number of activations over a time horizon;
- Minimum and maximum duration of an activation request (in terms of number of time steps);
- Minimum duration between two activations;
- and complex generation bids (e.g. the integral of energy injection over a given period).

A full description of the bidding process and the detailed mathematical definition of the catalogue of market products is carried out in Chapter 3.

2.3.1 Feedback from Consultation: Bidding

There were 4 questions about bidding aspects of market design, covering topics of allowing complex products, which actor should take the DER constraints into account, and the type of complex products.

Regarding the introduction of complex products, only two participants opposed the fundamental idea. Half of the answers suggested that such advanced products/bids may be allowed, with the concern that it would create a tradeoff between reflecting the market needs, market liquidity, and complexity of computations. Finally, four participants approved the idea by reasoning that such products will enhance the integration of distributed energy resources (DERs).

The majority of participants were leaning towards the idea that the *aggregator*, and not the market, should handle the dynamic and economic aspects of DER constraints. Only two respondents suggested that the market should take care of such constraints, without providing a strong argument.

2.4 Clearing and Pricing Aspects

Market Clearing consists in determining which flexibility offers (bids) are accepted or not, the level of the activation (in case of curtailable/divisible bids), but also determining a price to pay for these activations.

Market clearing is typically expressed as an optimization problem under constraints, i.e. optimizing some objective function, such that, e.g., 1) bids constraints are respected, 2) network constraints are respected. In our context, the objective could be maximizing the social welfare (SW), or minimizing the total activation cost for SOs for providing balancing and congestion services (all together). In the first case, it would be possible to have flexibility providers trade with each other (not providing services, but increasing the SW), while in the second case, flexibility providers can only trade with system operators (see more details in chapter 5) and not with each other. This choice is further discussed in chapter 5.

Regarding pricing, different approaches can be considered:

- The **“Pay as bid**” approach where the activated bids simply receive the price corresponding to the activated volume in the bidding curve. This approach is simple and intuitive for the different market stakeholders. However, it does not give incentive for the market participants to bid their real cost of flexibility, potentially introducing an economic distortion in the merit order and thus, creating the possibility that cost-efficient bids are not activated.
- The **“Pay as clear”** or “marginal price (MP) approach” where the activated bids receive the same price per MWh, corresponding to the most expensive activated flexibility bid. This approach removes/reduces the risk of a market participant bidding in terms of what they want to receive instead of in terms of their real cost of flexibility.

As the motivation of the Integrated Reserve market is to allow a fair and cost-efficient competition between different sources of flexibilities, including DER, it appears natural to use the most economically efficient approach of the marginal pricing [9], which is also the one favored by the Network code on Balancing [10].

Also, since networks constraints are considered, **pay as clear** pricing can be adapted to a system with network constraints in different ways (see more details in chapter 5):

- A **Nodal** approach where a price for flexibility is associated to the most granular level in our network representation i.e. to each node of the modelled grid (it depends on TSO-DSO coordination scheme)
- A **Zonal** approach where a price for flexibility is associated to a zone covering different nodes. Each zone can have a different price but the nodes in the same zone have the same price.

As the network constraints, both at the transmission and distribution levels, are of key importance for an AS market ensuring the satisfaction of congestion constraints, it is natural to account in the price mechanism for these network factors in the most accurate and economically efficient way [11]. For this reason, the nodal price is chosen in SmartNet.

With this market-design choice, the market associates a specific price to flexibility for each node of the transmission/distribution network, using the approach of distribution locational marginal prices (**nodal pricing**). This nodal price approach allows generating prices that reflect the real value of activated flexibility including the impact of these activations on congestion and voltage problems.

2.4.1 Feedback from Consultation: Clearing and Pricing

In this section of the survey, 4 questions were asked. The topics were the type and distribution of prices, as well as the type of objective function to be used (SW maximization versus a minimization of activation costs.)

Firstly, participants were asked whether they think that marginal pricing or pay-as-bid should be the methodology for pricing. There was not a single vote in favor of pay-as-bid, which was in full agreement with the choice made in the SmartNet project. There were participants who hesitated to choose, arguing that the selection should be made based on the number of bids, frequency of clearing, etc.

Secondly, the feasibility and benefits of nodal pricing was put into 3 questions. The majority of respondents confirmed that nodal prices can be implemented from a technological point of view, while not many of them think that it is economically advantageous. The reasoning behind is that further analyses should be carried out before opting for one method or another. Also, most of the participants believe that nodal pricing is acceptable from a regulatory point of view.

Finally, regarding the objective function, the majority of participants believe that maximization of

social welfare has to be used. This is justifiable from several points of view, including system security, operational and investments costs, etc. However, one participant argued that it will increase the cost of balancing.

2.5 Problem formulation and required inputs/data

In this section, a generic market clearing problem formulation is first described in the context of the Integrated Reserve market, mainly to highlight the inputs required to solve the problem. Then, different required inputs are discussed and then feedback from the consultation relative to this topic is explained.

2.5.1 Problem formulation

A generic formulation of the Integrate Reserve market clearing problem is:

maximize the social welfare or minimize the total cost of flexibility bid activations

such that:

- (forecast) imbalance is solved
- possible (forecast) congestions at distribution and transmission are solved
- voltage operational limits are not violated (at distribution level)

given:

- the transmission (and distribution) grid model (topology, electrical characteristics, network model)
- the forecast network state (e.g. what's the forecast injection/offtake at this node of the MV grid?)
- the different bids from flexibility providers at each node of the grid, and the constraints associated to these bids

2.5.2 Required inputs

Network model

A key element of the problem statement is the considered grid model, which consists of one transmission grid and/or several distribution grids connected to the transmission grid. For the purpose of the Integrated reserved market, the grid mathematical models are required (and are discussed extensively in Chapter 4). However, network data are equally important.

Network topology and characteristics

The chosen network model is built on several network data, i.e. the grid topology and the electrical element characteristics. Several elements can be listed (non-exhaustive),

- Topology describes which network nodes connect to each other (network graph), in

operational real-time conditions. Since network switches may vary over time, either the topology can change as an input to the market clearing algorithm, or the network model can explicitly include the switch state as a variable or parameter.

- Transformers characteristics (e.g. ratio).
- Line characteristics: (e.g. impedances).

Network operational limits

Other required inputs are the operational limits allowed by SO on their respective grids, for instance:

- Max apparent power (or current) allowed on any network line
- Min and max voltage magnitudes allowed at each network bus (node)

Forecast network state

For a given time step of the market, another important input for the market clearing algorithm is the forecast situation of the system, i.e. what would be the network state during each time step in the absence of any flexibility activation by the market. This highlights the need for network operators to have a view on their network state, through real-time measurements of their grid state (possibly complemented by state-estimation techniques for non-measured quantities).

In particular, in SmartNet, the network state that is considered is defined by all the active (both transmission and distribution) and reactive (only distribution) net power injections at the different nodes of the network (both transmission and distribution). For a given node, the **net nodal injection**[4] results in practice

- from outcomes of previous energy markets (e.g. day-ahead or intraday),
- from the activation by TSO and/or DSO of out-of-market ancillary services (e.g. voltage regulation), and
- from deviations (forecast errors, unpredictable events) from these previous timeframes. In practice, this last item can not be forecast perfectly, that is why we refer to **forecast net nodal injection**, which is only a forecast of the **net nodal injection**. Forecast accuracy typically gets worse with increasing lag, i.e. the imbalance forecast for the period *t* to *t+5* min is likely to be more accurate on average than the imbalance forecast for the period *t+55* to *t+60* min. The benefits of complex market clearing are lost, if used with inaccurate forecasts. This is why the market horizon cannot be too long (e.g. several hours).

It is important to note that these net nodal injections are expressed at the level of each network node but not at the resource level. The injections at each node are themselves the combinations of the individual

[4] net nodal injection = sum over all injected power at that node - sum over all power offtake at that node

behavior of many different consumers or producers of electricity, but it is not needed for the flexibility market to know these individual behaviors and to model the individual sources of imbalances.

In the context of Smartnet, it is expected that these **forecast net nodal injection** are such that:

- there is an imbalance between supply and demand, over the whole system
- there are potentially some instances of congestion problems at the lines of the considered (distribution and transmission) grids
- there are no pre-existing voltage problems, as the corresponding ancillary services have already been activated prior to the market.

Bids from flexibility providers

Last, but not least, bids from flexibility providers and their associated constraints (see section 2.3 and chapter 3), are required (in sufficient quantity) such that the market clearing algorithm can at least find a solution.

2.5.3 Feedback from Consultation: Data

The possibility of imbalance (or net node injection) forecasting was one of the questioned topic. The answers in this topic were split. While the first group believed that it is possible and even already existing, the second group doubted that it is technologically feasible and/or that it will be soon available. Some believed that imbalance forecasting will be available for the transmission grid, but not for distribution nodes. In general, such short term forecasting will generalize since they are sometimes already available and may be based on state estimation [12].

Other questions concerned the availability of data for building the network model and for providing information on nodal injection at transmission and distribution levels. We received mixed answers: on one hand, some participants believed that the required data are available (at least for the TSO) in order to make the models and that the injection forecasts are possible. On the other hand, we have participants who believed that such model data or forecasts are difficult to collect and that it is not possible to ask for such data. One participant claimed that imbalance forecasts are not even needed. In general, our take from these questions is that the possibility of having access to such data is possible, but not a given.

2.6 Potentials of Integrated Reserve

In this section, we describe a couple of optional broadenings in the market design which can extend the functionalities of the Integrated Reserve market, allowing it to fit into various applications. As a first brief

example, Integration of FCR droop coordination and FRR type market can improve efficiency and reliability of the system and the overall ancillary service markets. It could also remove the needs to develop very fast FRR

2.6.1 Optional Service Expansion: Co-optimization with Voltage Regulation

The Integrated Reserve market focuses on balancing and congestion management but includes voltage constraints and reactive power information of distribution networks. This allows the market to ensure that the activation in terms of active power, (made in order to balance the system and manage the congestion) does not create new problems in terms of reactive power and voltage.

In the Integrated Reserve market, it is not expected from the market to start from a situation with important voltage problems and to solve them, together with balancing and congestion management. However, as the network model used in the clearing mechanism takes into account the voltage constraints anyway (for distribution), it could be tempting to extend the scope of the Integrated Reserve to include also voltage regulation in the ancillary services it can provide. But to do so, a larger family of assets should participate to the market (e.g. some providing pure reactive power flexibility).

From an economical perspective, providing all the ancillary services together in the same market can increase the economic efficiency of the ancillary services decisions but at the price of more complex market products and clearing mechanism and of stronger deviation from current organization of ancillary services (even if there are exceptions).

2.6.2 Optional Timing Expansion: Finer Time-Resolution for First Time-Step

A flexibility provider will bid a price-quantity curve for different market time steps of the market time horizon.

A refinement of this approach is to consider, for the first time step, input data with a higher time resolution than the decision time step (e.g. a 1-minute input data time step and a 5-minute decision time step). Hence, we can:

- differentiate products with the same average power over the decision time step but with different and irregular power profiles at the input data step (typically different types of reactivity), and
- ensure that the imbalance is correctly matched on the input data time step, which is shorter than the decision time step.

This would likely allow to reduce the need for faster reserves, like aFRR, as the activation decision made by the Integrated Reserve allows not only to balance the system for each time step but also inside the first time step.

However, please note that in this refined approach, the market clearing frequency (e.g. 5 minutes) is not changed. Even with 30 seconds input data time step, Integrated Reserve cannot provide a response time of 30 seconds at any time (once the market is cleared, the next clearing happens 5 minutes later). For this reason, the Integrated Reserve cannot replace aFRR, which is still needed to react to unplanned events happening between two clearing events of the Integrated Reserve.

2.7 Coverage of Existing Situations in Other Regions

Existing AS markets general characteristics have been described for 8 European countries in deliverable D1.1 of the SmartNet project [3]. Since the scope of the Integrated Reserve market is mainly about the mFRR/RR reserve, the focus of this section is on these types of markets in the three pilot countries: Denmark (area DK1), Italy and Spain. In addition, the already existing advanced real-time market in California is discussed for comparison.

2.7.1 Existing Market in California

For the sake of the example and comparison, one of the most advanced markets, California ([5], [13]),is described that is already in operation, featuring high clearing frequency and a rolling window operation. ERCOT in Texas runs a similar advanced market [14]. PJM also uses nodal prices [15], like a few other markets in US.

The Real-Time Economic Dispatch (RTED) process in California has a rolling time horizon of up to 13 time-steps (of 5-minute duration), starting execution every 5 minutes at the middle of the 5-minute time steps (1.5 time steps before the dispatch). The RTED starts at approximately 7.5 minutes (1.5 time steps) prior to the start of the next dispatch interval and produces an instruction for energy injection/off-take for the next dispatch interval and advisory dispatch instructions for as many as 12 future dispatch intervals over the RTED optimization time horizon. The CAISO markets apply locational marginal prices based on a transmission grid model .

This means that thanks to this *pipelining* of input data and decision making, 1) the decision time step can be chosen shorter than the needed max market clearing time, and 2) the oldest input data used will then be one time step older than without using this trick. Using this pipeline feature, a trade-off must be made between the benefits of taking more features into account (larger networks, additional constraints or cost function terms) versus the benefits of using more recent input data.

A further aspect of the California RTED market is that bids are limited to maximum 10 segments along the quantity axis. Bids specifying both positive and negative quantities are allowed. For a bid associated to a generator, minimum and maximum energy specified in a bid are only limited to what the generator can provide.

2.7.2 Existing AS Markets in Pilot Countries

*Table **2-1*** describes detailed market settings parameters, that are representative in the current mFRR AS markets of these countries, and also some comparison with a California real-time dispatch market.

The first goal is to ensure that, even though SmartNet is trying to extend the possibilities of existing energy market operations, useful capabilities and flexibilities of current markets are not lost (last column of *Table **2-1*** explains that these settings will be considered in the description of the more general Integrated reserve market). The second goal is to state the ground and then determine the minimum extensions required for these markets to be able to leverage the flexibility of the DER in the distribution networks (e.g. for instance, in Italy, DER are not allowed yet to bid on the AS markets), and represent as such a minimum change AS market variant. Decision time steps are 60 minutes for each pilot country, and no larger prediction window is considered. Most countries specify minimum (max) bid sizes to participate to the market, as well as bid resolution.

In Italy and Spain, bids are formulated as either being upward (only) or downward (only). So, enforcing this as the only allowed bid formulations in the applicable regions has to be catered for in SmartNet. In other regions, bids with both positive and negative selectable quantities should be allowed.

In the three pilot countries, economic merit order (on price) is the first criterion for bid acceptance. In Denmark, Spain and Italy, for two bids with equal merit order, the renewable energy bids have preference over the other one (although for Italy, it applies to energy markets: DA, ID. RES and DER cannot yet bid on AS markets). Also, when there is no preference between two bids even after the renewability criteria, a bid representing high efficiency cogeneration is preferred over the other bids.

Table 2-1 Comparison of markets in the three pilot countries, California market and what is planned in the framework of SmartNet integrated reserve.

	---------- Current Practice ----------				Target
Setting/Parameter	Denmark	Italy	Spain	California	SmartNet
Current TSO-DSO coordination scheme	Centralized AS market	Centralized AS market	Centralized AS market	/	All TSO-DSO coordination schemes are considered.
Decision Time Step Size (minutes)	60	15[5]	60	5	parameter, defined in minutes
Prediction Window Size (minutes)	60	240[5]	60	55 - 65	parameter, defined in minutes
Clearing algorithm latency is larger than the decision time step?	N	N	N	Y, 1.5 time-step	[pipelining, parallelism] parameter

[5] For Italy, the decision time step is actually a set-point resolution, and the prediction window-size is the length of the window for which the set-points are calculated, which is also a market session frequency.

Lead of GCT compared to real-time (minutes)	45	n.a.	60	2.5	parameter
Min Bid size (MW)	10	1-10[6]	0-10[6]	P_{min} of generator	parameter
Max Bid size (MW)	None	n.a.	None	P_{max} of generator	parameter
Product resolution (MW)	0.1	n.a.	0.1	10 segments	parameter
Bids must have either positive or negative quantity (not both)	Y	Y	N	N	Allowing both signs of quantity in one bid when allowed.
Bids with negative quantities can only have negative prices	N	Y	N	n.a.	Allow all combinations of quantity and price (and restrict when necessary)
1. Economic Merit Order	Y	Y	Y	Y	Y
2. For equally interesting bids, renewables first	Y	n.a.	Y	n.a.	parameter + need to know in bid
3. For equally interesting bids, high-efficiency cogeneration first	Y	n.a.	Y	n.a.	parameter + need to know in bid
Non-curtailable blocks allowed?	N	n.a.	N	Y (self-dispatch)	parameter
Bid-Selection Objective	Minimum Cost	Minimum Cost	Minimum Cost	Minimum cost (demand fixed to Ca-ISO forecast)	Minimum costs or Maximum Social Welfare (with limited unnecessary activations)
Remuneration Scheme	Unified Zonal Price (Pay as clear)	Pay as Bid	Unified Zonal Price	Unified Nodal Price	Uniform Nodal Price (Pay as Clear)
Network Balancing	Y	Y	Y	Y	Y
Congestion management for transmission network	Y	Y	Y	Y	Y
Congestion management for distribution network	N	N	N	N	Y, preferably
Voltage control	N	N	N	N	N (Not aggravating voltage problems. Parameter.)

Y: Yes N: No n.a.: Data not available

In all three pilot countries, the objective function of the market clearing algorithm is to minimize activation costs. The remuneration scheme in Italy is of the pay-as-bid-type. Other regions (Denmark and Spain) are remunerating according to a uniform marginal price scheme.

Current ancillary services in European countries are mainly balancing and congestion management on the transmission network. The SmartNet project wants to take this one step further to also include congestion management for distribution networks. On top of balancing/congestion services, the market architecture will make sure that voltage problems are not created at Medium voltage (MV) level by activating balancing/congestion services.

[6] Different values are listed in [139] for RR and FRR services in Italy and Spain.

2.7.3 Requirements for Extension of Current AS-Markets

Given the current situation of mFRR/RR markets in the three pilot countries, we list the necessary required adaptations in order to minimally extend the markets and facilitate the integration of DER (

Table 2-2).

Table 2-2 List of necessary adaptations of parameter values for AS markets in pilot countries.

	Parameter	Current value →	Value after adaptation	Comment
Denmark	Decision Time Step Size (minutes)	60	5-15	More frequent clearing allows capturing the dynamics of RES and DER.
	Min Bid size (MW)	10	depends on network resolution (<< 1MW)	Allow RES and DER to participate in AS market.
Italy	Decision Time Step Size (minutes)	60	5-15	More frequent clearing allows capturing the dynamics of RES and DER.
	Use Uniform marginal price for remuneration of bidders	Pay-as-bid	Uniform nodal price	Pay-as-bid could be considered as a next step, but would deeply impact the bidding strategy defined in D2.2.
	Min Bid size (MW)	<10	depends on network resolution (<< 1MW)	Allow RES and DER to participate in AS market.
Spain	Decision Time Step Size (minutes)	60	5-15	More frequent clearing allows capturing the dynamics of RES and DER.
	Min Bid size (MW)	<10	depends on network resolution (<< 1MW)	Allow RES and DER to participate in AS market.

3 Market Products

In the previous chapter, the key market ingredients necessary for the Integrated Reserve market design have been briefly described, namely the timing, network, products/bids, objective and pricing aspects. In this chapter, first, the reason for proposing a catalogue of various market products is proposed (section 3.1). Afterwards, common bid requirements/assumptions are described (section 3.2). Then section 0 describes the different types of generic bids (i.e. with no additional constraints). Section 3.4 describes how reactive power can be included in bids (applicable for distribution networks). Sections 3.5 and 3.6 describe different complex market products, i.e. additional constraints added to a particular bid (section 3.5) or between bids (section 3.6). Finally, section 0 describes the firmness aspect of the market decisions, especially when a rolling horizon framework is used (see section 2.1).

3.1 Bidding process and need for market products

As described in the previous chapters, The *Integrated Reserve market* is a market for ancillary services aiming to leverage the flexibility from assets located both at the distribution and the transmission grid levels. The goal of this market is to solve imbalances between energy supply and demand in near real time, as well as congestions, both at transmission and distribution levels, and to support voltage control (at distribution level). Flexibility providers bid (i.e. send flexibility offers) on the market (see *Figure **3**-**1***) using the market products that are proposed in this chapter. In order to allow flexibility providers with the best way to express their constraints (e.g. ramping, minimum duration), a catalogue of market products (i.e. allowed formats of bids) is proposed. Depending on the market design, the list of market products could be restricted to a subset (e.g. design could for instance only allow simple bids, without complex constraints). In the market clearing algorithm, the bid constraints are taken into account. These market products can then be used by flexibility providers, typically aggregators, in order to aggregate the flexibility of a (large) portfolio of DERs and then to offer this flexibility on the market using some of the proposed market products (see SmartNet Deliverable D2.1 for different aggregation methods [16]).

The definition of the market products is therefore a key element for an efficient understanding of the market participants:

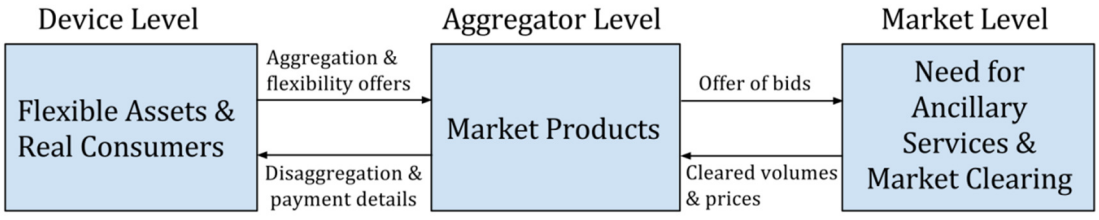

Figure 3-1 Coordination between the end user, the aggregator, and the market.

3.2 Common bid requirements

The following requirements are applicable for all type of bids described in this chapter

1. As described previously (see section 2.1), the Integrated Reserve market is a discrete/closed-gate auction market. Bids can be sent for all, or for any subset of, time steps in the market time horizon.

2. Only flexibility providers send bids to the market, i.e. all bids are flexibility **offers**. The **requestors** of flexibility, i.e. TSOs and/or DSOs, do not bid explicitly on the market, but they do send to the market their forecast network state (and so implicitly their flexibility needs), as explained in section 2.5.2. Therefore, in this deliverable, **it is assumed that TSOs and/or DSOs are price taker**.

A bid can be associated to a specific physical asset (e.g. a large power plant connected to the transmission grid) or an aggregator with aggregated portfolio of DER.

3. One of the mandatory bid attributes is the specific node of the distribution or transmission grid (as long as the node is included in the market clearing grid model!) it provides the flexibility to. As a consequence, a bid can not aggregate resources connected to different nodes of the grid. Multiple bids can be presented at a same node by multiple market.

4. A market participant can submit bids for different nodes.

5. A market participant can submit multiple bids for the same node and, by default, these bids are supposed to be completely independent. The market can accept all of them, some of them or none of them, since they are without linking constraints (see section 3.6). If two bids of the same issuer are intended to be exclusively accepted, then an exclusive-choice constraint will have to be constructed.

6. The bids are mainly expressed in terms of active power. However, reactive power capabilities of the bids may also be submitted to the market for resources at distribution level, as described in section 3.4. This is because the reactive power is accounted for in the distribution grid models (but not in transmission), as described in chapter 4. It is important to remember that the goal of Integrated Reserve market is not to optimize the reactive power flows, but to avoid additionally creating problems such as over- and under-voltages.

3.3 Type of Bids

Three main types of bids with respect to their dimension are defined, namely the UNIT-bid, the Q-bid, and the Qt-bid, as described in Figure 3-2. Each of these types can be curtailable or non-curtailable[7]. A curtailable bid allows the market to select and activate any portion of its quantity (that is the power volume), while a non-curtailable bid can either be accepted at the given quantity or be rejected. In the rest of this section, each type of the bid is described.

3.3.1 UNIT-bids

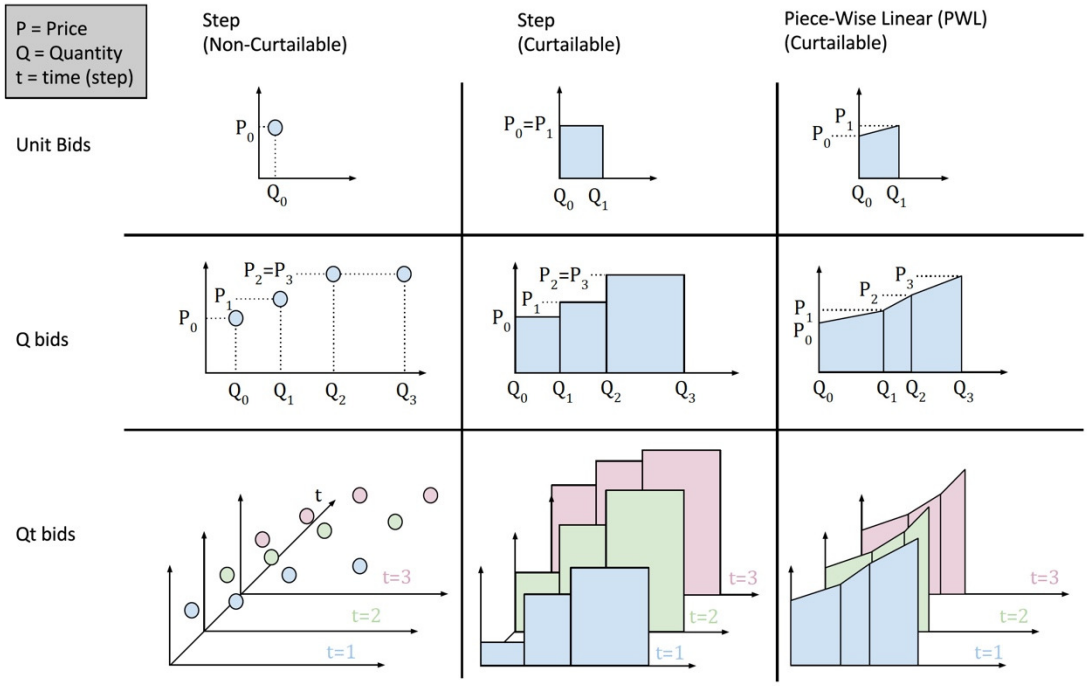

*Figure 3-2 Different types of standard bids (shown only for upward flexibility bids, i.e. with quantity **q>0**). Standard bids only mention price and quantity and form the (mandatory) basis of any bid (on top of node location). Three families of bids are considered: Unit-bids, Q-bids, and Qt-bids.*

A UNIT-bid is defined for a specific time step and is simply defined by a price and a quantity, as shown in the first row of Figure 3-2. Three sub-types of UNIT-bids are considered:

1. **Non-curtailable UNIT-bid:** This bid (see column 1 of Figure 3-2) is a simple <quantity, price> pair, $<Q_0, P_0>$ indicating to the market that it can either accept or reject the total energy quantity Q_0 at a price of P_0 or higher. This market product is called non-curtailable because either the total block is fully accepted or the

[7] in some existing markets, such bids characteristics are also called fully divisible (for curtailable) and indivisible, or regular block orders (for non-curtailable bids)

block is not accepted at all. Fractional parts of non-curtailable bids are not accepted. Price and quantity can be negative or positive. Positive quantities stand for *energy injections* into the network and negative quantities for *energy offtake* from the network. A market participant could send two separate bids, one offering an energy injection to the network node and another one offering an energy offtake from the network node.

2. **STEP curtailable UNIT-bid:** This UNIT-bid has a single price $P_0 = P_1$ for a range between two quantities Q_0 and Q_1 (see the column 2 of Figure 3-2). Here, the market operator can accept any quantity in between Q_0 and Q_1 for at least the *marginal* cost of $P_0 = P_1$ (expressed in EUR/MWh[8]).

3. **PWL (piecewise linear) curtailable UNIT-bid:** This UNIT-bid has a changing marginal price P_0 to P_1 for a range between two MW quantities Q_0 and Q_1(see the column 3 of Figure 3-2). Here, the market operator can accept any quantity in between Q_0 and Q_1 for at least the *marginal* cost on the P_0-P_1-line.

3.3.2 Q-bids

Q-bids are similar to UNIT-bids[9], but consists in multiple pairs of quantity-price (they must be monotonic in price), as shown in the second row of Figure 3-2. The objective of a Q-bid is to allow the flexibility provider to directly express an aggregated curve of flexibility with varying marginal cost.

Similar to UNIT-bids, the Q-bids can be either non-curtailable, step curtailable or piece-wise curtailable and they are associated to a specific time step of the market clearing.

3.3.3 Qt-bids

The UNIT-bids and Q-bids are associated to a specific time-step of the market time horizon and do not allow offering flexibility for consecutive time steps within a single bid.

Qt-bids essentially offer a Q-bid for a series of time steps within the market time horizon and allows the market participant expressing the availability of flexibility for the future time steps, as demonstrated in the third row of Figure 3-2.

They will also be serving as the standard bid on which additional temporal constraints (i.e. constraints linking the bids from different time steps inside a Qt-bid) can be added (see section 3.5).

The number of decision time steps in a Qt-bid is called the *bid-horizon*[10]. It must be smaller or equal to the market horizon.

[8] The energy quantities are expressed in MW (over the length of the time step) while the prices are expressed EUR/MWh .

[9] Also called **multi-part bids** in some existing markets

3.3.4 Quantity and Price Conventions

In this document, the terms buyers and sellers are avoided, and flexibility providers or requesters are rather used. The reason is that a flexibility provider can either provide **upwards** ($\boldsymbol{q} > \mathbf{0}$, by producing more or consuming less) or **downwards** flexibility ($\boldsymbol{q} < \mathbf{0}$, by producing less or consuming more). Regarding the price, we use the following convention:

$\boldsymbol{p} > \mathbf{0}$: The flexibility provider wants to receive money (at least $\boldsymbol{p}$ €/MWh)

$\boldsymbol{p} < \mathbf{0}$: The flexibility provider is OK to pay at most **-$\boldsymbol{p}$** €/MWh to provide the flexibility

In common energy markets (e.g. DA market), a generator would usually submit bids with $p > 0$, i.e. the generator wants to be paid for producing electricity, to cover its costs. However, it also happens that some generators submit bids with $p < 0$ (e.g. must-run power plants, renewables sources receiving subsidies). A consumer would usually submit a bid with $p < 0$ (the consumer is OK to pay to buy electricity up to a certain price). Similarly, flexibility providers providing upwards flexibility will likely ask to be paid, while flexibility providers providing downwards flexibility will either agree to pay for it, or asking to be paid.

3.3.5 Primitive Bid Definition

In this section, we define two primitive bid types, while section 3.3.6 explains how Q-bids are decomposed into primitive bids. Primitive bids are actually unit bids. The description is mostly adapted for curtailable bids. For non-curtailable bids, the only difference is that the bid quantity is accepted at values 0 or full.

[10] Therefore, one can consider the Q-bid as a Qt-bid with only one time-interval (or a bid horizon of one), and similarly the UNIT-bid as a Q-bid with only one quantity-price pair.

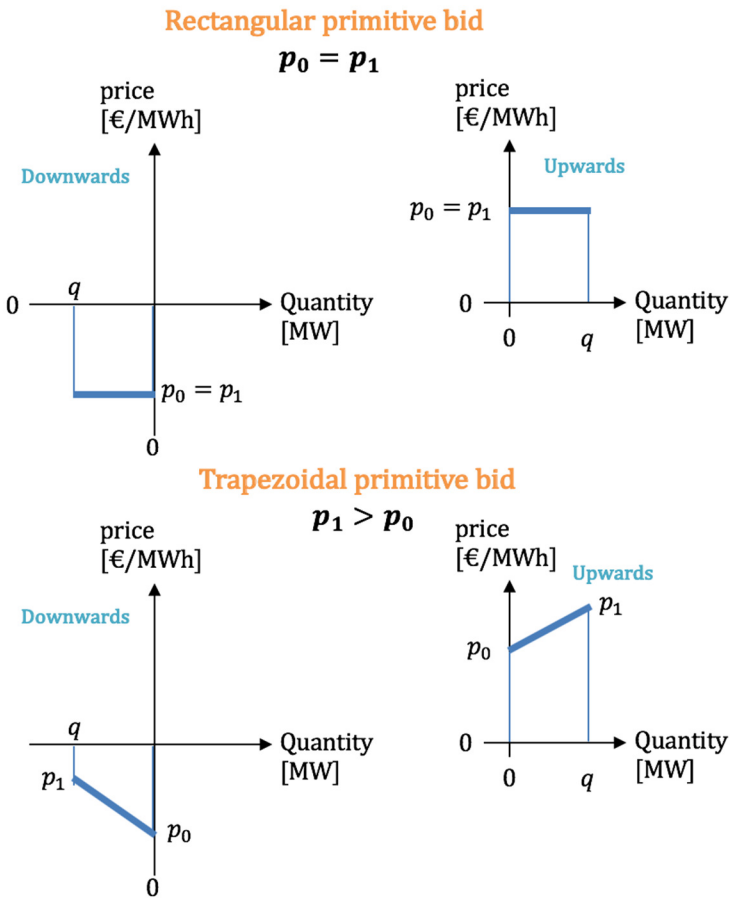

Figure 3-3 Two primitive bid types.

Two primitive bid types are defined (rectangular and trapezoidal), depending on whether a step or piecewise linear bid would be used (see *Figure **3**-**3***). Both bid types may apply to upward ($q > 0$) or downward ($q < 0$) quantities. Note that it is required in this deliverable that $p_1 \geq p_0$ (monotonic increase of price). Out of this quantity q, any fraction x between 0 and 1 can be accepted (for curtailable bids). For non-curtailable bids, x is a Boolean/binary variable (i.e. equal to 0 or 1).

For a rectangular bid (i.e. $p_0 = p_1$) and when a fraction x of q is accepted, the **flexibility cost $f(p_0, q, x)$** of this bid is equal to:

$$f(p_0, q, x) = p_0 \cdot |q| \cdot x \quad (1)$$

If $f(p_0, q, x)$ is negative, it means that the flexibility cost is negative (i.e. providing flexibility implies some revenues).

In case of upwards flexibility ($q > 0$), it means that:

- if $p_0 > 0$, the flexibility cost is positive: the flexibility provider wants to get money (at least $f(p_0, q, x)$) to compensate the cost of providing flexibility (e.g. a classical fuel power plant to cover the additional fuel costs)
- if $p_0 < 0$, the flexibility cost is negative: the flexibility provider is ok to pay money up to a point (at most - $f(p_0, q, x)$ since providing flexibility brings him money (e.g. renewable source with subsidies, even if this case is less likely).

In case of downwards flexibility ($q < 0$), it means that:

- if $p_0 < 0$, the flexibility cost is negative: the flexibility provider is ok to pay money up to a point (at most - $f(p_0, q, x)$, since providing flexibility brings him money (e.g. a classical fuel power plant saves fuel costs when reducing production)
- if $p_0 > 0$, the flexibility cost is positive: the flexibility provider wants to get money (at least $f(p_0, q, x)$) to compensate the cost of providing flexibility (e.g. a thermostatically controlled load, which has some discomfort cost for providing flexibility).

For a non-curtailable UNIT-bid, the cost is also defined as in (1), with the difference that the variable x becomes a Boolean, only accepting values 0 or 1. For a trapezoidal bid, the flexibility cost f can be expressed as:

$$f(p_0, p_1, q, x) = p_0 \cdot |q| \cdot x + \left((p_1 - p_0) \cdot x \cdot |q| \cdot {}^{x}/_{2}\right) \quad (2)$$

The cost in (2) can be considered as the more general case of (1). The same reasoning on the sign of flexibility cost can be applied as for the rectangular bid.

3.3.6 Decomposing Q-Bids into Primitive Bids

Figure 3-4 shows how a Q-bid can be decomposed into a set of rectangular and/or trapezoidal bids. This example is shown for upward bids with $\langle q > 0, p > 0 \rangle$, but the reasoning equally applies for other bid types. Note that for upwards bids, the bid curve must be monotonically increasing, while for downward bids, it must be monotonically decreasing.

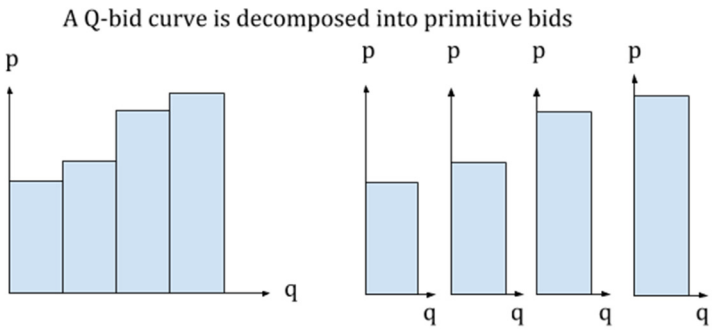

Figure 3-4 Q-bid decomposition into primitive bids.

In Figure 3-4, any block has equal or higher prices than any of the prices present in its left neighbor block. This means that they are already ordered in economic merit order, which is the order that the market will select these blocks. Therefore, there is no need to add constraints that a block will be accepted before its right neighbor block.

3.3.7 Definition of Acceptance

For different reasons, the concept of 'acceptance' of a bid needs to be defined. For instance, in order to formulate temporal constraints regarding the number or duration of activations over the time horizon of a Qt-bid (see section 3.5). Another reason to define this is to be able to construct logical relations between acceptance of Q-bids and between Qt-bids (see section 3.6).

- For UNIT-bids, acceptance of the bid simply means that a non-zero quantity is activated. On the other side, the level of acceptance (fully or partially) refers to the actual quantity which is activated.
- Q-bids are defined as 'accepted' if at least one of the Q-bid primitives bids (that the Q-bid can be decomposed into) is activated for a fraction x larger than 0.
- Qt-bids are defined as accepted if at least one of the Q-bids compositing the Qt-bid has been accepted.

For Q-bids and Qt-bids, more details can be found in Section 10.1.2.

3.4 Including Reactive Power in Bids

Since the Integrated Reserve market will consider not violating voltage operational constraints (at distribution level) by providing the congestion and balancing services, the distribution grid model takes reactive power into account (see chapter 4). Therefore, reactive power capabilities should also be described in the flexibility offers sent by market participants. In addition, an optimal management of the reactive power would allow a higher exploitation of the active power potential of distribution resources.

The relationship between the active and reactive power for a certain asset (or a group of aggregated assets) can be of different types. There are several options (see **Errore. L'origine riferimento non è stata trovata.**) to define the limitation of a bid on the active-reactive power plane:

1. Fixed power factor (a)
2. Triangular P-Q limits (b)
3. Rectangular P-Q limits (c)
4. Circular P-Q limits (d)

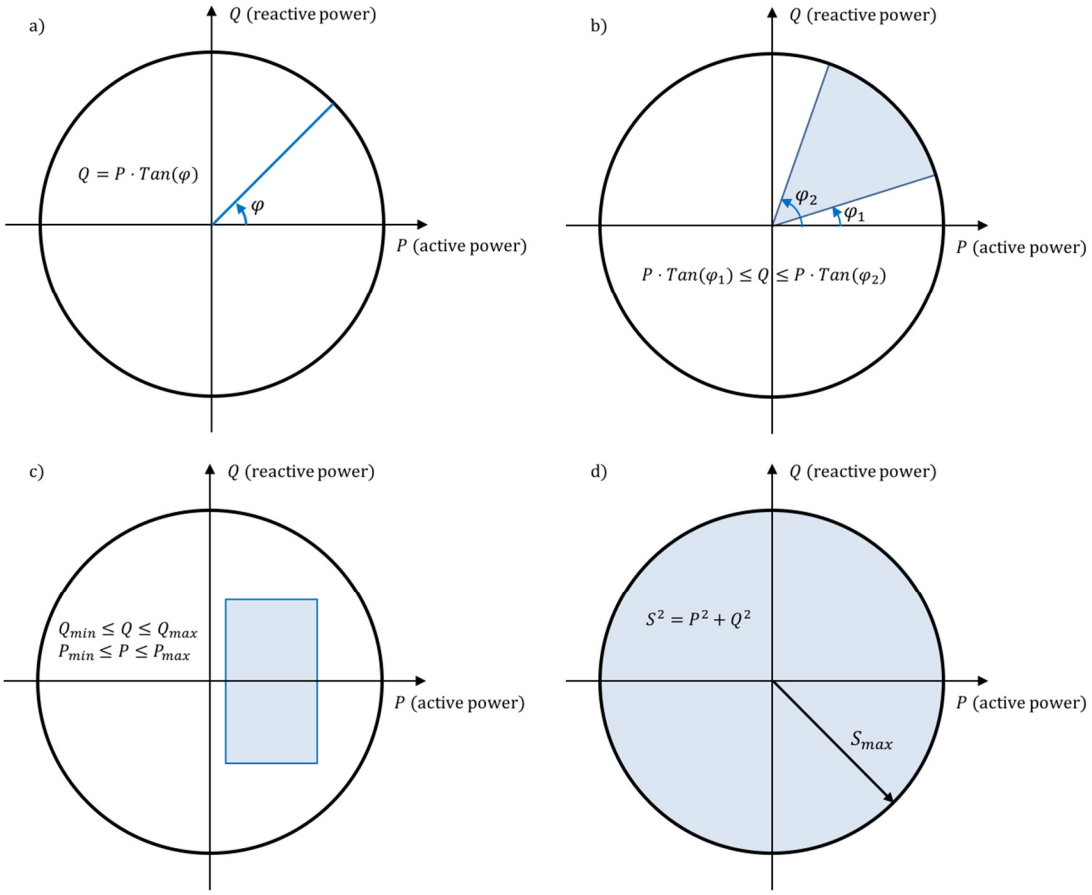

Figure 3-5 Graphical representation of various P-Q limit definition: a) fixed power factor, b) triangular limit, c) rectangular limit, d) circular limit.

Some points of attention about the provision of information on reactive power and the market clearing at the presence of reactive power bids are listed below:

- In our market design, reactive power is not priced/remunerated. Given this, the market will have the freedom of activating reactive power resources to reach feasibility without sacrificing the social welfare. It is also critical that the reactive power is activated only when it is necessary to avoid violating a constraint, even if it can also be used to reduce losses [17] :

- The provision of reactive power flexibility at zero cost is considered realistic since it is typically a mandatory service (e.g. minimum triangular capability) in some of the European countries (see [18]).
- The "activation only in necessity" is meant to avoid reactive-power exchange when it is not necessary. This can be implemented by assigning a small price to reactive-power exchange. This is not investigated in this deliverable, but could be interesting to investigate in future studies.

- The market clearing algorithm has the possibility of including reactive power in the bids:
  - Rectangular capabilities can be easily implemented.
  - Triangular and circular capabilities can be implemented, but require a conic model, which complicates the market clearing problem.
  - Implementing fixed power-factor capabilities is easy. However, only taking this category into account may lead to infeasibilities (by lack of reactive power flexibility)

In our framework, there are no guarantees on reactive power flexibility from bids (characteristics exist but market participants are free to express their constraints). However, this problem can be tackled by modeling the grid-owned assets such as capacitor banks, which can be used to compensate for the lack of reactive-power flexibility.

3.5 Intra-Bid Temporal Constraints

In this section, several types of constraints linking the different Q-bids of a single Qt-bid are described, i.e. constraints linking the bid quantities and/or bid prices across the different time steps of the market horizon. Note that such intra-bid temporal constraints do not make sense for single time step markets (i.e. market horizon = only one time step). In such a market setup, the aggregators would have to ensure themselves that all power quantities and all combinations of selectable power quantities are feasible for their assets portfolio. Having a single time step in the market horizon may severely limit the flexibility offered by market participants, since sometimes the available flexibility is conditional on future, like ramp constraints.

Since Smartnet aims at increasing the flexibility from DER in providing AS, offering different types of common temporal constraints in the market products is a way to ensure all flexibility providers (DER, or big units) can express their constraints in a way in the market. Therefore, a catalogue of market products is allowed to do so. In this way, market clearing simulations can choose to compare approaches with a more or less broad catalogue of market products.

- in one extreme case, all complex market products are allowed: this makes the market clearing algorithm more complex (computational tractability) but it allows flexibility providers to easily express their constraints.
- in the other extreme case, only simple market products are allowed (e.g. step-curtailable unit bids, see section 3.3.1), which eases the market clearing process (or allows to use a more detailed network model). But then, market participants (aggregators) need to tackle/internalize these constraints, with the risk of providing less flexibility.

In the next sections, we introduce several intra-bid temporal constraints which can be applied on a Qt-bid. Detailed mathematical formulation of each constraint is shown in the appendix in Section 10.1.3.

3.5.1 Accept-All-Time-Steps-or-None Constraint

This constraint associates to a Qt-bid and ensures that either the bid is accepted for all the time steps considered in the bid or that it is not accepted at all, as illustrated in Figure 3-6 on a Qt-bid with 4 time steps in a 6-time steps market time horizon. Depending on the type of Qt-bid, the implications are different:

- in Figure 3-6, this is a curtailable bid, and so it means a non-zero quantity must be activated for any time step of the Qt-bid.
- If the Qt-bid is a non-curtailable bid, then it means that each of the four Q-bids composing the Qt-bid should be fully accepted, or nothing.

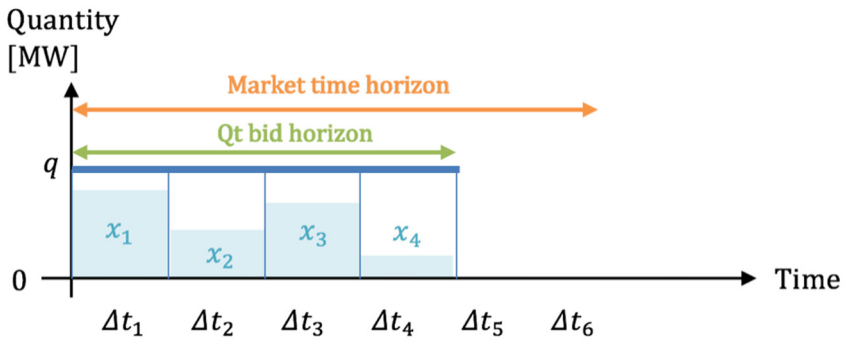

Figure 3-6 Example of a curtailable Qt-bid (where the same quantity *q* is proposed in four time steps) with a Accept-All-Time-Steps-or-None constraints

In terms of commitment, this type of product implies an anticipative commitment by the market operator, in the case a rolling optimization setting is chosen (see section 2.1): if a Qt-bid with "Accept-All-Time-Steps-or-None" constraint is accepted, then the market operator already commits to activate it for all the time steps considered in the Qt-bid.

This constraint allows, for example, to submit a specific load-profile that has to be followed when the corresponding asset is activated. Mathematical formulation of this constraint is provided in the appendix in section 10.1.3.

3.5.2 Ramping Constraints

Some generation or consumption asset may have a ramp-up or/and ramp-down energy production/consumption profile (e.g. CHPs, large power plants, some industrial processes), i.e. it can not change its generation/consumption from one market time step to the other too quickly. After aggregation of many assets this may sometimes disappear, but can sometimes still be present. Ramping constraints can be added on a Qt-bid, as illustrated by Figure 3-7.

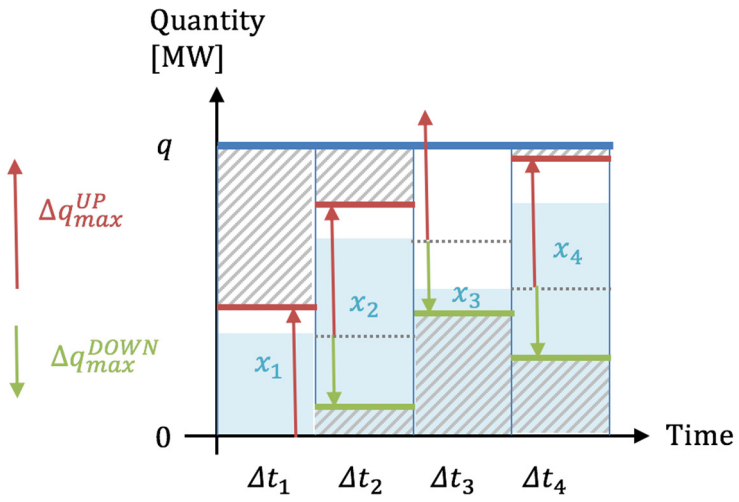

Figure 3-7 Example of a Qt-bid with both ramping up (Δq_{max}^{UP}) and ramping down (Δq_{max}^{DOWN}) constraints, limiting the UP and DOWN variations from one time step to the other. Grey striped areas represent the quantity which can not be accepted at a given time tep, due to the ramping constraints.

The maximum ramp-up (e.g. 5 MW/time-step), denoted $\Delta \boldsymbol{q}_{\boldsymbol{max}}^{\boldsymbol{UP}}$, and maximum ramp-down (e.g. -3MW/time-step), denoted $\Delta \boldsymbol{q}_{\boldsymbol{max}}^{\boldsymbol{DOWN}}$, constraints limit the possibility for the market to determine any quantity of the orignial Qt-bid, as illustrated by the striped grey lines in Figure 3-7. Note that the bid issuers are aware of the fixed decision time step and should formulate their ramping constraints accordingly. Ramping constraints can be imposed either for ramping up, or down, or both. Mathematical formulation of the ramping constraint is provided in section 10.1.3.

In the rolling optimization case, regarding commitment aspects, the activation decisions for Qt-bids are only firm for the first time-step of the rolling optimization but the ramping constraint limit what it is possible to do in the next market clearing session (i.e. the bid is stored in memory, since some activations are not decided yet).

In an interesting application, ramping constraints can be set to $\Delta \boldsymbol{q}_{max}^{UP} = \Delta \boldsymbol{q}_{max}^{DOWN} = 0$, which means that the same amount of power should be accepted for every time step within the bid-horizon of the Qt-bid. In this case, the ramping constraint implicitly includes an "Accept-All-Time-Steps-or-None" criterion, as described before.

3.5.3 Maximum Number of Activations Constraint

A bid issuer may want to restrict the number of activations within a given number of decision time steps. A typical example would be to avoid wear and tear effect on mechanical switches or on incandescent lights. This can be specified by MAX_N_ACTIVATIONS_PER_STEPS = (X, Y) where X represents the maximum number of activations and Y the considered time horizon for the bid (that can be shorter than the market time horizon if needed). Mathematical formulation of this constraint is provided in section 10.1.3.

3.5.4 Minimum and Maximum Duration of Activation Constraint

A bidder may want to restrict the activation duration to a given minimum number of decision time steps. This can be specified by

MIN_N_STEPS_PER_ACTIVATION = 5.

Suppose that a Qt-Bid contains 10 decision time steps. Then if the bid is activated, it has to be activated for at least 5 subsequent time steps within these 10 time steps. Obviously, MIN_N_STEPS_PER_ACTIVATION cannot be larger than the number of time steps contained in the Qt-bid. The default value for MIN_N_STEPS_PER_ACTIVATION is 0.

Similarly, a bidder may want to restrict the activation duration to a given maximum number of decision time steps. A typical example of this constraint is the case of an HVAC system where there is a maximum time period that the HVAC can be stopped before the discomfort level is unacceptable for the users. This can be specified by

MAX_N_STEPS_PER_ACTIVATION = 4.

The default value for MAX_N_STEPS_PER_ACTIVATION is equal to the number of decision time steps in the bid. The time a bid is active is defined between the beginning of activation and the end of that same activation. Note that a single bid can have several activations over its bid time horizon. Mathematical formulation of these constraints is provided in the appendix in section 10.1.3.

3.5.5 Minimal Delay Between Two Activations

Similar to the previous constraints, a bidder may need to specify the minimum time delay between two consecutive activations, which can be useful for example when the asset has a cool-down or start-up duration.

Mathematical formulation of this constraint is provided in the appendix in section 10.1.3.

3.5.6 Integral Constraint

For some types of flexible assets, we want to express temporal constraints in terms of the integral of injection/off-take of active power over the considered time horizon.

This constraint can force the power-integral, INTEGRAL_Target, to be at a fixed value (e.g. zero) or to be between a lower and an upper bound, specified by:

$$\text{INTEGRAL\_Target} = \text{E}$$

or

$$\text{L} \leq \text{INTEGRAL\_Target} \leq \text{U}$$

where E represents the energy target in terms of integral of active power injection/offtake over the time horizon. L and U represent the potential lower and upper bounds on this integral, respectively.

In terms of commitment, the activation decision is only firm for the first time-step but this first activation decision has implication on what can be done for the next time steps and next clearings, as we keep track of the integral constraint.

For some Qt-bids, the integral constraint may, for instance, be used to specify that the total energy consumption should remain unchanged over the bid horizon. For some loads (such as thermostatic loads), it is meant to assure that the set-point (and hence the comfort or schedule) is maintained. For storage, it can be used to set targets on the energy storage at the end of the market horizon. For some industrial processes, with shifting capabilities, it can be used to express that the energy consumption profile can be modified but only to the extent that the energy consumed over a given period remains identical. Mathematical formulation of this constraint is provided in the appendix in section 10.1.3.

3.6 Inter-Bid Logical Constraints

In the previous section, several complex products have been described, focusing on inter-temporal constraints between different time steps of a single Qt-bid. Another important family of constraints are the **logical** constraints that link the acceptance or non-acceptance of multiple bids submitted by the same market participant. This means that the logical constraints would be *inter-bid* constraints.

These constraints are applied to two or more bids and define a logical relation between those bids.

For every bid involved in a logical constraint, a Boolean variable is then used in the market clearing model. This variable represents whether a bid is accepted, partially or totally. Since inter-bid constraints need to refer to multiple different bids, we need a system to uniquely identify them.

3.6.1 Implication Constraint

It is a common practice to allow the market to select a bid only if another bid has been accepted as well (e.g. Euphemia algorithm uses linked block orders, see [19]). This could for example represent two interrelated flexible processes where the second one can be activated only if the first one is also activated.

This constraint is called the **implication constraint**. Assuming a market participants submit two bids **b1** and **b2**, but with the intention of activating b2 only if b1 is also accepted. This can be modeled by a simple Boolean constraint:

if *b2 is accepted* ***then*** *b1 must be accepted*

Implication constraints are only possible between bids submitted for the same network node and sent by the same market participant. These constraints can be applied between Qt bids, or between Q-bids (so also inside a single Qt-bid).

Looped implication constraints (i.e. the acceptance of bid 1 subject to bid 2, acceptance of bid 2 subject to bid 3, and acceptance of bid 3 subject to bid 1) are allowed, as such loops exist in today's European day-ahead electricity market. Mathematical formulation of this constraint is provided in the appendix in section 10.1.3.

3.6.2 Exclusive Choice Constraint

The exclusive choice constraint is used to indicate an exclusive acceptance between a set of bids. For example, if an aggregator has an asset that could move to a number of exclusive states during the next time step (such as an atomic load), the corresponding bids should be accompanied by an exclusive choice constraint[11]. Mathematical formulation of this constraint is provided in the appendix in section 10.1.3.

3.6.3 Deferability Constraint

If the bidder has the flexibility of deferring its bid, it can do so by specifying the maximum deferability (i.e. the maximum delay in the acceptance) in terms of the number of time steps. The market can also leverage this additional flexibility to determine the time-shift that best maximizes the optimization function.

An example is a process with a given fixed load profile (defined using a Qt-bid with one given quantity per time and an "Accept-All-Time-Steps-or-None" constraint) which has a flexible starting time, allowing the market to activate it for the current time step or shift it if needed. Mathematical formulation of this constraint is provided in the appendix in Section 10.1.3.

[11] The Exclusive Choice constraint is defined per time step and is not automatically carried on to the next time step.

3.7 Commitment of Market Decisions

In the case the market design includes a rolling horizon optimization (see section 2.1 and *Figure **2**-**2***), several aspects need further discussion and a thorough review of all these aspects is out of the scope of the deliverable, since the market simulation platform developed in the SmartNet project does not implement this rolling horizon concept. However, a brief discussion of the questions is mentioned below:

- in this framework, market participants can send **new** bids before each gate closure, for a given delivery period (e.g. at 8:45, bid 1 is sent for period 9:00-9:05 and then, at the next clearing, at 8:50, another bid is sent for the same delivery period). This is useful for market participants to adjust their *position* and make use of updated closer-to-real-time information. One danger is arbitrage/gaming by powerful market participants. In our framework, SO do not send bids, but update the forecast state of the network as an input to each market clearing session (using closer to real-time info and already binding commitments from previous market clearing sessions, e.g. bid 1 result in above example).
- are market participants allowed to update their **existing** bids from one market session to the next?
- is the commitment binding for the first market time step? or for the entire market horizon?

Table 3-1 Rolling horizon market, update bids and commitments: some options.

Rolling horizon market Options on some rules		Allow to **update bids** (from one market session to the other)	
		YES	**NO**
Commitment binding on	**first time step only**	• **simple bids** (no inter-temporal constraints): no impact compared to submiting new bids • **complex bids** (inter-temporal constraints): not very clear how to deal with quantities and prices after first time step. Allowing to update such bids might be dangerous since market would commit on some aspects (guaranteeing inter-temporal constraints) while the bid might change (price? quantities?). **Very unlikely**	• **simple bids**: no reason to send bids for more than the first time step. • **complex bids**: the inter-temporal constraints are enforced (they need to be kept in the market clearing system memory), but there is some degree of freedom left regarding exact quantity activation and pricing: this would require thorough investigations out of scope of the document.
	entire market horizon	NOT POSSIBLE since market results are binding on the entire horizon	prices and dispatched quantities well defined for each market session, for every time step • looks like DA market (Europe) in case market horizon do not overlap • in case horizons overlap, SO and market participants can still refine their position in the next market session

Table 3-1-1 represents different possible options. Usually, in the rolling optimization framework, the idea is to keep a market as reactive to system state change as possible, therefore the most likely options is that only the decisions for the upcoming first time-step are binding (Table 3-1 , second row) assuming the time step length matches the clearing frequency). If the clearing frequency is to clear every three market time steps, then the decisions (i.e. quantities, prices) are binding for the first three time steps. The activation information for the other (future) time steps are not a commitment requested by the market operator to the flexibility providers, but information about the most likely future activation decisions if everything in the system stays as planned.

4 Grid Model for Market Clearing: Trade-Offs in Tractability, Accuracy and Numerical Aspects

4.1 Introduction

The SmartNet project aims at developing a market clearing methodology that takes the physical limit of the power system into account.

In the current zonal approach (used in Europe), the part of the power system participating in the market inside a zone is considered as a copper plate, whereas the interaction with other zones is considered through a network flow approximation. To avoid problems due to the limited accuracy of such models, a post-clearing AC power flow check is performed and re-dispatch can be performed in case of expected operational difficulties. Such actions may lead to inefficiency [20]. Including a more accurate network model in the market clearing will help to avoid countertrading and the associated costs, especially when considering distribution grids.

However, taking the physics of power flow into account, while guaranteeing solution times in real time, demands pragmatic approaches. Convexification and linear approximation of the equations describing the physical system are two such approaches to improve computational tractability, which will be detailed throughout this chapter.

Generically, including the physics of the power system into a market clearing methodology implies solving an Optimal Power Flow (OPF) problem. Therefore, this chapter starts with an overview on challenges in optimal power flow calculations, and recent advances in OPF relaxations and approximations. Then, two convex relaxation methods are described further, and their impacts on several aspects is then discussed. Afterwards, approximations are discussed and compared to relaxations. Then, different methodologies to simplify/reduce the network size through equivalent networks are presented. Finally results and choices are summarized.

4.2 Challenges in Optimal Power Flow

4.2.1 Optimal Power Flow

Optimal power flow (OPF) has been a topic of interest for 50 years, with Carpentier writing his seminal paper in 1962 [21]. He, amongst other things, concluded that the convexity of the problem was to be researched further. Dommel and Tinney [22] in 1968 developed practical calculation methods, and solved case studies of 500 nodes. Alsac and Stott widened the scope of these methods in 1973 through the concept of

security-constrained OPF (SCOPF) [23], [24]. A review of recent SCOPF literature is published by Capitanescu [25].

In general, OPF encompasses any power system optimization problem with physical power flow as part of the model. This does not exclude much, therefore OPF in general can be: multiperiod, security-constrained, DC or AC, or based on approximations.

Power flow is generally considered as a complex-valued problem. Two formulations of the power flow equations have been used widely: a quadratic one, based on the rectangular-complex notation, and a polar-complex one, using sine and cosine functions. Finally, Baran and Wu developed an interesting formulation of the power flow equations in 1989 [26], which simplified power flow modeling in radial grids. This formulation of the power flow equations is called DistFlow.

4.2.2 Convex Relaxation Approaches

Since quite a while it has been understood that the true distinction between easy-to-solve and hard-to-solve problems does not align with linear programming (LP) versus nonlinear programming (NLP) problems but with convex versus nonconvex optimization. In theory and in practice, large convex problems can be solved reliably (convergence guarantees), quickly (polynomial-time) and to global optimality. With nonconvex (smooth) optimization, one largely has to choose between solving problems quickly but locally optimal or globally optimal but slowly. With the development of practical semidefinite programming (SDP) methods [27], efforts have been made to leverage their expressive power to find strong SDP approximations to nonconvex problems. A hierarchy of continuous optimization complexity classes can be developed as follows:

$$\underbrace{\mathrm{LP} \subset \mathrm{QP} \subset \mathrm{CQCP} \subset \mathrm{SOCP} \subset \mathrm{SDP}}_{\text{convex}} \subset \underbrace{\mathrm{NCQCP} \subset \mathrm{NLP}}_{\text{nonconvex}}$$

Any nonconvex quadratically constrained optimization problem (NCQCP) can be reformulated as an SDP problem with the addition of a nonconvex rank constraint. After removal of the rank constraint (Shor's relaxation [28]), a SDP problem remains, which can be solved with SDP solvers. This step of removing nonconvex constraints is referred to as the 'convex relaxation'. The power flow equations are easily written as a set of nonconvex quadratic equations; therefore, this strategy can also be followed. One thereby obtains the SDP relaxation of OPF.

Relaxations, by a process of only removing equations from the feasible set of an original problem, provide strong quality guarantees on the solution of both problems:

- if the original problem is feasible, the relaxed problem is feasible;
- if the relaxed problem is infeasible, the original problem is infeasible;
- the optimum of the relaxed problem will be a lower bound (minimization) for the optimum of the original problem.

Approximations (which cannot be shown to be relaxations), do not provide such guarantees. Nevertheless, the idea is that they are sufficiently accurate, but only under certain conditions. More generally, convex relaxations can be obtained for polynomially constrained polynomial programs, for which moment relaxation strategies have been developed [29]. Moment relaxations are tighter than the previously-discussed SDP relaxations, as this SDP relaxation is just the first-order moment relaxation.

Any SDP formulation can be relaxed further to obtain a second-order cone programming (SOCP) problem [30]. For SOCP, state-of-the-art solution methods are faster and more scalable. Furthermore, mixed-integer (MI) SOCP solvers are developed commercially whereas commercial MISDP solvers do not yet exist. Mixed-integer Linear Programming (MILP) is very commonly used for optimization of energy systems [31]. Mixed-integer convex programming (MICP) refers to the optimization of problems with integer variables, for which the continuous relaxation is convex. This generalizes MILP, MISOCP and MISDP. General solution methods for MICP are a topic in current research. For example, the solver Pajarito [32], released recently, uses lifted polyhedral relaxations to handle the convex nonlinear constraints. It is noted that any convex quadratically constrained programming (CQCP) or convex quadratic programming (QP) problem can reformulated as a SOCP problem [33].

Finally, Ben-Tal and Nemirovski developed a general (noniterative) approach to reformulate SOCP problems as LP, to an arbitrary accuracy [34]. This polyhedral relaxation technique can be used to obtain trade-offs between accuracy and speed for any SOCP problem.

4.2.3 Convex Relaxation of OPF

It can be shown that for radial grids, under balanced power flow, the SDP relaxation and the SOCP relaxation are equivalent. Related to radial grids, two formulations have been of primary interest. One has been developed in 2006 by Rabih Jabr [35], the other one is derived directly from the DistFlow formulation of Wu and Baran [26]. The Jabr's formulation belongs to the bus injection model (BIM) class, the Wu and Baran formulation belongs to the branch flow model (BFM) class. It has been shown that both approaches obtain the equivalent solution set [33], albeit in different variables.

Ultimately, it was shown that SOCP BIM and BFM formulations are exact under mild conditions in radial grids [36]. The notion of exactness refers to equivalence between the optimized decision variables of the original problem and those of the relaxed problem. Therefore, from every optimal solution of the relaxation, one must be able to recover an optimal solution to the original problem [36].

In meshed grids, SDP relaxations are tighter than SOCP. Nevertheless, they are not exact, so efforts are made to improve accuracy further. Even though computational tractability is limited, a number of publications have applied moment relaxation methodologies to OPF [37]–[39]. In the limited-size case studies that can be solved, typically, solving the second order moment relaxation is already sufficient to find the global optimum.

Jabr furthermore developed approaches to iteratively integrate angle variables [40], transformers and UPFCs [41], and grid reconfiguration [42]. Hijazi et al. extended the reconfiguration formulations to include radial and meshed grids [43], while proving bounds on optimality.

Coffrin published an archive of OPF test cases, called NESTA [44], which is commonly used to compare the effectiveness of convex relaxation methods. Authors developing stronger and more tractable relaxation methods often use this archive for benchmark purposes, e.g. [45].

Coffrin and Hijazi also developed a convex relaxation method based on the polar formulation, convexifying the sine and cosine functions directly, called the Quadratic Convex or QC relaxation [46], [47]. Furthermore, the authors developed theoretical insights in copper plate and network flow models as relaxations [48] of AC OPF.

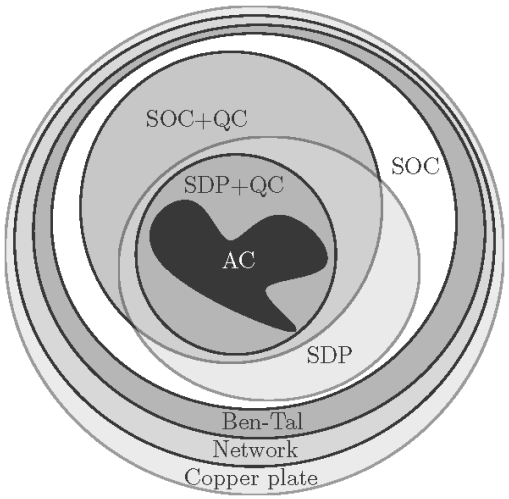

Figure 4-1: Venn diagram of the feasible sets for various relaxations to ACOPF discussed in this deliverable (not to scale).

A comparison of the tightness of different optimal power flow relaxations discussed is shown in Figure 4-1 [46]. The SOCP relaxation – exact under mild conditions in radial grids – dominates the Ben-Tal polyhedral relaxation (of the SOCP model), which in turn dominates the network flow relaxation, which in turn dominates the copper plate relaxation. If the focus is to deal with meshed grids, tighter relaxations can be considered. For instance, by adding the QC constraint set to the SOCP relaxation. The SDP relaxation dominates the SOCP relaxation, but is neither dominated by or dominates the SOCP+QC relaxation. The SDP+QC relaxation is finally the tightest relaxation discussed within the scope of this report. ***Table 4-1*** summarizes the discussed formulations.

Table 4-1 Categorization of formulations.

	Complexity	Meshed/Transmission	Exact?	Radial/Distribution	Exact?
AC	Nonconvex	Balanced polar	Y	Balanced polar	Y
		Balanced rectangular	Y	Balanced rectangular	Y
				Unbalanced rectangular [49]–[51]	Y
				Balanced DistFlow [52]	Y
				Unbalanced DistFlow [53]	Y
Rank relaxation [28]	SDP	Moment [37], [39]	Y*		
		Balanced BIM & BFM [54]–[57]	N	Unbalanced BIM & BFM [53], [58]	Y
PSD relaxation [30]	SOCP	Balanced BIM & BFM	N	Balanced BIM [36] & BFM [35], [59]	Y
Ben-Tal relaxation [34]	LP	Balanced BIM & BFM	N	Balanced BIM & BFM [60]	Y*
Convex hull	SOCP	QC [46]	N		
Linear approximation	LP	DC	N	Simplified balanced DistFlow [52]	N
	LP	LPAC [61]		Simplified unbalanced DistFlow [53]	N
Network flow	LP	Relaxation [48]	N	Relaxation [48]	N
Copper plate	LP	Relaxation [48]	N	Relaxation [48]	N

* under some conditions

4.2.4 Further Background

The upcoming paragraphs discuss a number of works which summarize and generalize a number of the previously discussed articles, as well as develop case studies based on the proposed methods.

An in-depth review of OPF methodologies was performed by FERC[12] and a series of reports was published [62], including articles such as [63]. More recently, Capitanescu published a review of developments related to AC OPF calculation, including a discussion on the effectiveness of convexification strategies [64].

Early 2015, Joshua Taylor published a book on convex optimization methods for power systems [33]. This well written work summarizes the state-of-the-art of convex OPF methods in a single formalism, which makes this book an easy entry point to the field.

Steven Low developed a convex OPF literature study [65] and published a tutorial-style article to get started with the convex OPF formulations [66]. Lingwen Gan, a former doctoral student of Low, wrote his doctoral dissertation on the application of the convexification methods in radial grids [67].

Gan and Low regularly discussed the 'exactness' of the convex formulations in [68]–[70]. Javad Lavaei focused his efforts on the SDP formulation and published an implementation of this problem for Matlab [71], in which he also develops a penalization approach. He also published some insights into the effectiveness of the convex relaxations of OPF based on insight in the physics underlying the problem [72].

[12] FERC = Federal Energy Regulatory Commission

Anya Castillo, in her doctoral dissertation, developed a number of ACOPF formulations (nonconvex, convex), methods (global, local) and case studies (storage) [73]. In his dissertation, titled 'Optimization and control of power flow in distribution networks', Masoud Farivar develops convex models for OPF in distribution grids [74]. He includes volt-var control and develops a number of case studies.

4.3 Convex Relaxation Formulations

as stated above, two main formulations of convex relaxations of the power flow equations have been of interest in the scientific literature: the bus injection model (BIM) and the branch flow model (BFM) formulation. These relaxations have been shown to be equivalent [65].

The Quadratic Convex or QC formulation, being based on a different relaxation process (combining convex hulls) [45], is not equivalent to those formulations. Therefore, adding any non-dominated QC constraint to either the BFM or BIM formulation can result in a tighter overall formulation, as the formulations can be combined.

A complete derivation of these three relaxations is given in Appendix 10.2, for an extended grid model including transformers, and switches. Table 4-2 gives an overview of all the parameters required for modelling a network using the proposed extended formulations.

Table 4-2 Parameters for grid elements

Line/cable	shunt admittance, series impedance, rated voltage level, rated current, rated power
Transformer	shunt admittance, series impedance, voltage ratio, rated voltage levels, rated currents, rated power
Tap-changing transformer	shunt admittance, series impedance, voltage ratio range, rated voltage levels, rated currents, rated power
Phase shifter	shunt admittance, series impedance, voltage ratio; shift ratio range, rated voltage levels, rated currents, rated power
Nodes	rated voltage, operational voltage bounds.

4.3.1 Compact Formulation of Extended SOCP Branch Flow Model

As a reference, the complete (compact) formulation of the SOCP branch flow model relaxation is given below. This formulation will be used in the project to include distribution grid constraints in the market clearing. All values and parameters are real-valued.

For each node *i*:

$$0 \leq (U_i^{min})^2 \leq u_i \leq (U_i^{max})^2 \leq M^2 (U_i^{rated})^2 \quad (3)$$

For each line *l = ij:*

$$0 \le a_{ij}^{min} \le a_{ij} \le a_{ij}^{max} \quad (4)$$

$$0 \le a_{ji}^{min} \le a_{ji} \le a_{ji}^{max} \quad (5)$$

$$0 \le \alpha_l^{min} \le \alpha_l \le \alpha_l^{max} \le 1, \ \ \alpha_l \in \{0,1\} \quad (6)$$

$$P_{ij}^2 + Q_{ij}^2 \le (S_{ij}^{rated})^2, P_{ji}^2 + Q_{ji}^2 \le (S_{ji}^{rated})^2 \quad (7)$$

$$-S_{ij}^{rated} \le P_{ij} \le S_{ij}^{rated}, -S_{ji}^{rated} \le P_{ji} \le S_{ji}^{rated} \quad (8)$$

$$-S_{ij}^{rated} \le Q_{ij} \le S_{ij}^{rated}, -S_{ji}^{rated} \le Q_{ji} \le S_{ji}^{rated} \quad (9)$$

$$0 \le i_{ij,s} \le M^2 \cdot (\max(I_{ij}^{rated}, I_{ji}^{rated}))^2 \quad (10)$$

$$0 \le u_i^* \le M^2 \cdot (U_{ij}^{rated})^2 \alpha_l \quad (11)$$

$$0 \le u_j^* \le M^2 \cdot (U_{ji}^{rated})^2 \alpha_l \quad (12)$$

$$0 \le (a_{ij}^{min})^2 u_i^* \le u_i' \le (a_{ij}^{max})^2 u_i^* \le M^2 \cdot (U_{ij}^{rated})^2 \quad (13)$$

$$0 \le (a_{ji}^{min})^2 u_j^* \le u_j' \le (a_{ji}^{max})^2 u_j^* \le M^2 \cdot (U_{ji}^{rated})^2 \quad (14)$$

$$-M^2 \left(U_{ij}^{rated}\right)^2 (1 - \alpha_l) \le u_i - u_i^* \le M^2 \left(U_{ij}^{rated}\right)^2 (1 - \alpha_l) \quad (15)$$

$$-M^2 \left(U_{ji}^{rated}\right)^2 (1 - \alpha_l) \le u_j - u_j^* \le M^2 \left(U_{ji}^{rated}\right)^2 (1 - \alpha_l) \quad (16)$$

$$P_{ij}^2 + Q_{ij}^2 \le (I_{ij}^{rated})^2 u_i \alpha_l \quad (17)$$

$$P_{ji}^2 + Q_{ji}^2 \le (I_{ji}^{rated})^2 u_j \alpha_l \quad (18)$$

$$P_{ij} + P_{ji} = g_{ij,sh} u_i' + r_{l,s} i_{ij,s} + g_{ji,sh} u_j' \quad (19)$$

$$Q_{ij} + Q_{ji} = -b_{ij,sh} u_i' + x_{l,s} i_{ij,s} - b_{ji,sh} u_j' \quad (20)$$

$$\left(P_{ij} - g_{ij,sh} u_i'\right)^2 + \left(Q_{ij} + b_{ij,sh} u_i'\right)^2 \le i_{ij,s} u_i' \quad (21)$$

$$u_j' - u_i' = -2\left(r_{l,s}\left(P_{ij} - g_{ij,sh} u_i'\right) + x_{l,s}\left(Q_{ij} + b_{ij,sh} u_i'\right)\right) + (r_{l,s}^2 + x_{l,s}^2) i_{ij,s} \quad (22)$$

Note that the node balance equations still need to be added in order to obtain the complete OPF problem formulation.

4.4 Impact of Formulation and Relaxation

The SOCP convex relaxations of the power flow equations (given in the appendix in Section 10.3.3), have a number of consequences on the possible result of the initial optimal power flow problem. Also, the formulations given may perform differently from a numerical point of view. A discussion of a number of these consequences is found below.

4.4.1 Numerical Stability

Lingwen Gan notes that the BFM (*DistFlow*) formulation has numerical advantages above the BIM [53] for *unbalanced* power flow formulations (SDP). This suggests that this may also be the case for balanced formulations, even though the effect may only be observed for large-scale or 'difficult' problem cases.

In the BFM formulation, the complex current and voltage variables are replaced by squared current and voltage magnitude variables. Note that the accuracy of these squared variables is impacted by the reformulation process. For instance, for a numerical accuracy of 10^{-6} of the reformulated problem in the squared current and voltage magnitude, in post-processing, an accuracy of only $\sqrt{10^{-6}} = 10^{-3}$ is obtained for the current and voltage magnitude.

4.4.2 Scaling

The scaling of the squared variables is important for numerical reasons when solving the optimization problem. Therefore, it is better to make sure that the squared variables are scaled so that they have a numerical value around 1. This is commonly performed as part of the transformation of SI[13] units to the per-unit base, but more accurate bases can be envisioned if necessary[14].

4.4.3 Variables

As current finds the path of least resistance, Kirchoff Current Law (KCL) can also be thought of as minimizing the grid losses in electric circuits [75]–[77]. In meshed AC grids, however, this is not generally as simple due to the voltage phase angle constraints (adding up to zero) that apply in loops. In the *DistFlow* derivation, the voltage angle variables are substituted out in the SOCP formulations. The SOCP formulations introduce phase shifters in any grid element, furthermore making the voltage angle constraint trivially feasible. Voltage angle variables can only be partially incorporated again through the QC feasible set.

4.4.4 Convexification Slack

The SOCP relaxation by definition introduces nonphysical solutions: those for which $(P_{ij,s})^2 + (Q_{ij,s})^2$ is strictly less than $(i_{ij,s} \cdot u_i')$ in the feasible set. Non-negligible convexification slack invalidates the overall result

[13] SI: the internal system of units

[14] For instance, due to static transformer taps (e.g. 1.1 pu), the per unit base can be off-set (e.g. nominal 20 kV) with respect to the best numerical base (e.g. closer to 22 kV).

from the physical perspective. Slack may be observed when it is beneficial to have increased losses somewhere in the grid. Slack represents 'free' nonphysical losses, on top of the normal physical power transfer losses. Such controllable 'losses', like a dispatchable load, can be used to ease the grid operation in difficult circumstances. For example, in case of overvoltage, such losses actually help you to bring down the voltage, allowing the solver to find (mathematical) solutions that 'comply' with a 'difficult' overvoltage limit. Similar effects can be observed with current and apparent power bounds. It is noted that this slack cannot be observed when the operational envelopes are absent.

If the convexified OPF is infeasible, this guarantees that the original problem is infeasible. However, infeasibility of the original problem does not guarantee that the relaxed problem returns a certificate of infeasibility. In certain cases, a numerical but nonphysical solution is returned, due to the interaction of the power flow and the operational envelope [36]. In this case, infeasibility of the underlying problem has to be confirmed.

4.4.5 Penalties

The BIM SDP and SOCP relaxation are equivalent for radial grids. Furthermore, a SOCP convex relaxation in the BFM expression is obtained by dropping a rank constraint in the non-convex quadratic constraint.

To obtain rank-1 solutions in SDP problems, rank minimization heuristics [78]–[80] were developed. The rank constraint is thereby replaced with a penalty. In some cases, a hidden rank-1 solution is recovered in the original (global) optimum, in others, some actual increase in the costs is observed due to the penalization. The application of such heuristic is illustrated by [56], [81], [82], for the balanced BIM SDP formulation.

Therefore, in case the relaxation is not exact, one can choose to penalize as such, to obtain a solution without convexification slack. It is not known which penalty makes it easiest to recover a global or near-global optimal solution. Two aspects can be considered: the formulation and scaling of the penalty, as well as the application of the penalty to a selection or to all grid elements. In the implementation, one has to choose to penalize just the lines for which the convex relaxation is not exact, versus by default penalizing all lines or no lines at all.

4.4.6 Objective

The goal is to find a solution for the cost minimization problem, where the objective is a convex cost function in the decision variables. For example, the objective is to minimize the cost of dispatch subject to the power flow physics of a distribution grid. In the convexified SOCP OPF, the original problem has to be combined with a penalization objective. This penalty is there to make sure that a solution is found on the boundary of the solution space (and is thus a feasible solution). The convexification penalties defined are convex and the feasible set is the intersection of convex cones (polyhedra, spectahedra). For radial grids, it is

known that the convex relaxation is exact and a physical solution can be recovered if it is located on the surface of the SOCs.

Therefore, the effective objective is a convex combination of the original objective Y^{cost} and the penalty $Y^{PFconvex}$. There is a challenge in fine-tuning the weight of the penalty in the problem objective. For a penalty, which is too low, the result is not physical. For a penalty, which is too high, results are physical, but the costs are suboptimal. For the lowest possible penalty for which the slack on the convexification is (close to) zero, the optimum is obtained. Note that the costs can nevertheless be constant for a wide range of penalties, which means that fine-tuning of the penalty weight may not be required in most cases. Nevertheless, in cases of overcurrent and overvoltage, it is expected that the objective may be very sensitive to the penalty weight.

A search algorithm can be used to find this penalty weight. One approach to find such a penalty weight, without use of derivatives, is the bisection method, as proposed by [82]. Note that due to the nature of interior point algorithms, it is hard to obtain solutions very close to (or on) the edge of the solution space. Conversely, simplex-based methods naturally find solutions on the edge of the solution space, but only support polyhedral feasible sets. Therefore the Ben-Tal reformulation technique, which linearizes the conic constraints into a set of polyhedra feasible sets, must be applied first.

4.5 Approximated OPF Formulations

Approximations, conversely to relaxations, do not offer strong general quality guarantees, nevertheless, they are widely used because of their simplicity. Two common approximations exist, the linearized 'DC' OPF, commonly used in transmission system modelling and the simplified DistFlow, commonly used in distribution system modelling. The feasible sets obtained in both cases are linear, allowing the direct application of the more widely understood LP modeling tools and solvers.

In SmartNet, the linearized 'DC' approximation will be used to model the physical grid constraints of the transmission grid. In linearized 'DC' OPF, voltage magnitudes are assumed to be close to 1 pu. Conduction losses are neglected. Furthermore, resistance is assumed to be small compared to reactance. Finally, voltage angle differences over grid elements are assumed to be small.

Note that power flow in distribution grids violates these assumptions: voltage margins are larger than in transmission grids, and resistance and reactance are similar in magnitude.

Coffrin and Van Hentenryck discuss the validity of the linearized OPF in [61]. They note that the 'DC' approximation works reasonably well active power flow through largely inductive lines. However, the same quality of approximation does not hold for the reactive power balance, where stronger nonlinearities are observed. Therefore, it is hard to include voltage magnitude constraints in 'DC' OPF.

In the simplified DistFlow formulation, it is assumed that the series conduction losses are negligible. Simplified DistFlow can be considered as the outcome of a low-accuracy Ben-Tal relaxation (as a reminder,

Ben-Tal linearizes the SOCP DistFlow formulation, using an arbitrary number of linear constraints to approximate the conic constraints) applied to the convex SOCP DistFlow formulation. Losses are neglected, which results in an error on the power flow of a few percents. As the power consumed by grid losses also need to be transferred to the place where it is actually lost, the voltage drops are also underestimated.

Network flow (see ***Table 4-1***) neglects all electrical physics and reduces the grid model to lossless power transfer. This approximate model is still switchable and the switching is now directly enforced on the power balance. The apparent power flow limit is typically linearized by taking the bounds. Ben-Tal or naive polyhedral approximations can be used to improve accuracy in the model of the apparent power flow constraint.

Finally, power flow can be further simplified as a copper plate (slack bus, no network), which can be also considered as a relaxation [48]. This is nevertheless out of scope due to the absence of any physical variables related to the underlying grid model.

*Table **4-3*** summarizes the properties of the power flow formulations based on the theoretical groundwork and supported by the numerical experiments.

Table 4-3 Properties of proposed formulations for radial grids (Nonlinear solvers usually have good tractability for power system optimization with only continuous variables, but tractability is low for problems including integer variables)*.

	Complexity	nature	penalty	losses	under-voltage	over-voltage	over-current	dual var.	quality	tractability	optimality	algorithm
Classic AC	Nonconvex	exact	No	exact	medium	medium	medium	hard	high*	low	local	IP
DistFlow DistFlow Ben-Tal	SOCP LP	exact	Yes	exact	easy	hard	hard	hard	high	high	global	IP IP, simplex
Simplified DisfFlow	LP	approx..	No	neglected	hard	easy	easy	easy	medium	high		IP, simplex
Linearized 'DC'	LP	approx..	No	neglected	hard	hard	hard	easy	low	high		IP, simplex

4.6 Network Simplifications

In order to reduce the dimensions of the market clearing problem (or any OPF), it can be useful to simplify the network. A number of methods to reduce the number of variables in the physical system equations are described below. These will mainly be used to model the transmission grid in the SmartNet approach.

4.6.1 External Grid Equivalent

The network areas external to the network area in focus can be modelled in different ways, according to the available data. If the external network data are available, detailed representation could be applied [83]–[85]. However, the external network data are usually not available. In the particular case of this project, the

transmission networks of the neighboring countries are not available, since the related transmission system operators are not partners of the project.

A simpler possibility is considering the boundary nodes as PQ, PV or slack nodes. The PQ nodes represent the lines in which the exchange of power is controlled. In some cases, this is true, if the power rate is controlled by the means of FACTS devices or HVDC links. The PV nodes are similar to the PQ ones, but in these cases, the reactive power can change. However, PV nodes are not present in the DC model of the network. The slack node usually represents the external network with the highest power rating. If some interconnection lines are topologically very close, then they can be considered connected to the same slack node (considering for example the external network as a copper plate). In the case of the DC power flow, if the intervention (that is the variation of power exchange in each line) of the external network is known, multiple slack busses with different weights could be considered.

Considering these simplifications, the necessary data are:

- The exchange of power with the external network in each interconnection
- The slack node, or if necessary the distribution of slack nodes
- If the exchanges of power of the interconnection change, how the variation can be evaluated

4.6.2 Network Reduction

The size of the network in focus affects the computational effort needed to solve the power flow equations. If a large area of the transmission network is addressed, it can be necessary to consider thousands of transmission lines. All these variables slow down the computational process, possibly leading to unacceptable calculation times.

However, it is usual that not all lines represent a constraint for the market clearing, since only a small percentage of them reaches high loading conditions. It is therefore possible to exclude these non-constrained lines to reduce the computational complexity of the problem. This can be done by directly simplifying the initial network topology or discarding the inactive constraints.

In case of the DC power flow, the latter is a particularly effective procedure, since it is possible to directly express the power of each line with the PTDF matrix. It is therefore possible to consider only the relevant constraints, excluding all the inactive constrains and reducing also the number of variables.

Finally, the simplification of the network or the choice of the lines with inactive constraints can be done considering the historical behavior and the normal operational conditions of the network. In this section, four methods for network reduction are examined.

Clustering Method

The clustering method, which initially reduces the complexity of the network, aggregates the nodes with similar characteristics. This method reduces directly the number of nodes and lines at the cost of higher errors in evaluating the voltages and the power flows. There are several methods to classify and reduce the nodes [83], [86]–[90], which take into account different metrics and boundary conditions.

These methods assume the knowledge of the initial state of the network, which is not necessarily available. Another problem with the application of these methods is that the information of the loading rate of each single line is lost. In fact, only the exchange of power between the clusters of nodes is preserved, but not the power flow through each line.

The clustering methods can be used in an automated way, to dynamically simplify the network, at a given frequency (e.g. once per hour). Otherwise, the basic principle expressed within the methods can be used to simplify the initial network, which would remain equal until some reconfiguration occurs.

Inactive Constraints Method

The inactive constraints methods allow to identify and then to discard the inactive constraints before the power flow calculation. These inactive constraints are the operational limits of the transmission lines that are not exceeded in any of the possible operational conditions.

These methods are well fitted for the DC power flow, in which there is a direct connection between the power of the nodes and the power flow of the lines. Simplified techniques can in some cases achieve a reduction rate above 85% [91], [92]. Other more exact techniques allow achieving high reduction rates at the cost of a more complex and heavy computational effort to find the lines with inactive constraints [93], [94].

The method “Fast identification of inactive security constraints in security constrained unit commitment problems” [89], has shown good performance and it is applied to the network (see the appendix) in some example. The method is quite simple and it uses the PTDF matrix. For each transmission line, the largest element of the PTDF is identified and the corresponding generators (in a specific load condition) are increased to the maximum rate in order to identify if the maximum power rate can be reached for the specific line.

Historical Data

A third way to identify the inactive lines is to study the historical profiles. If the loading rate of one line is always well below the limit in all the operational conditions, it is then very improbable that the line would experiment any problem in the future, unless a very important reconfiguration occurs.

Operational Experience

Another method, quite similar to the previous one, is to use the experience of the network operators. In fact, they know at first hand the network characteristics and can contribute to determine the lines with inactive constraints.

Limiting the Area of the Network

If the number of variables is still too high after network reduction has been applied, an alternative is to control only the branches on a certain zone, for example the zone of the pilot. If the method is applied and only the lines in the zone of the pilot are selected, the number of lines in focus can be significantly reduced.

4.7 Summary

The goal of this chapter was to investigate the trade-off of computational tractability versus model accuracy and complexity of integrating a physical model of the network in the market clearing process for the Integrated Reserve market.

The following recommendations are derived for including network models in market clearing algorithms:

1. Due to the fact that integer variables are required in the market clearing constraints, the approach developed to model the power flow physics needs to be tractable in combination with integer variables. Mixed-integer non-convex optimization is not tractable within the scope of the SmartNet project. The approaches proposed in this chapter depend on convex approximations of the power flow physics. This allows to develop an overall model which is mixed-integer convex, which has superior tractability.
2. The SOCP BFM (DistFlow) offers the best accuracy and very high computational tractability, but requires the tuning of a penalty term. In almost all realistic cases, optimality and feasibility of this formulation is equal to the original non-convex problem. Furthermore, in some cases, the SOCP solution (global optimum) is actually superior to those obtained by local non-convex solvers. Nevertheless, the tuning of the penalty can be cumbersome in difficult situations (overvoltage, overcurrent).
3. The simplified DistFlow formulation offers a high-quality approximation in terms of feasibility and optimality. The major advantages are that no penalty fine tuning is required in this method and that the problem formulation is immediately linear. The major disadvantage is that no guarantees can be provided on feasibility. It is noted that simplified DistFlow is the natural equivalent of linearized ‘DC’ OPF for distribution grids.

4. Applying the Ben-Tal reformulation technique selectively to the SOCP constraints is an interesting path for fine-tuning accuracy. Furthermore, Ben-Tal method provides an interesting path to leverage warm-start capability of the simplex algorithm.

5. There is no opportunity for slack in the simplified DistFlow formulation. However, due to the nature of the approximation, this results in an underestimation of the under-voltages (which results in uncleared under-voltage problems) and overcompensation of what potentially could have been over-voltages.

6. Conversely, the SOCP can be shown to be always exact with respect to under-voltage, but the slack introduced by the convexification can be misused to avoid ove-rvoltage in nonphysical ways (creating fictitious losses brings down the voltage). However, if there are sufficient controllable resources, they can be dispatched to avoid this.

7. The 'QC' feasible set can be added to the BFM formulation in a next stage if improved accuracy is sought for meshed grids. Nevertheless, the BFM generally offers a high-quality approximation of OPF in meshed grids, even without 'QC'.

Based on these observations and recommendations, the choice was made to include the BFM SOCP formulation in the market clearing process, for the distribution grids.

Transmission grids will be modeled with the traditional DC approximation, however, where suited for the foreseen simulation platform, network simplification will be applied to reduce the dimensions of the problem.

5 Clearing Algorithm and Nodal Pricing

The different ingredients of market clearing have been introduced and briefly discussed in chapter 2. In the framework of the integrated reserve market, it was chosen to include detailed grid models for both transmission and distribution (medium voltage level) in order to solve imbalances and congested lines at both transmission and distribution, while not violating the voltage constraints at distribution level. Then, a catalogue of market products was described in chapter 3 with the essential common characteristic that all bids must be specified per node (of the grid).In this chapter, the market clearing objective and pricing methodology are further discussed.

Once the bids are pre-processed and the network model is updated with the most current values, the market is ready to run the optimization process known as the "market clearing". This is the core algorithm in the heart of the market which is responsible for calculating the optimal volume of power exchange (known as the cleared quantity) and the associated value of power injection or off-take at each node (known as the cleared price).

Before discussing the market clearing algorithm, several assumptions are mentioned:

1. The transmission and distribution networks are defined as connected graphs[15]. The parameters of these graphs (i.e. the network topology and the physical characteristics of the electrical elements) are assumed to remain constant during one market clearing optimization. This implies that the power switches of the network remain in their initial state and the line parameters (e.g. impedance and reactance) do not change.

2. An actor (such as an aggregator) which offers flexibility in the market, is allowed to place a bid at the market at each time step. The minimum information in a bid are the quantity of flexibility (in terms of injection or off-take) and the corresponding (marginal cost) price.

3. The market clears over the time horizon (typically including multiple time-steps) at once. One specific option is to perform rolling-horizon optimization (see section 2.1).

4. In the rolling window configuration, it can happen that the decision for the upcoming (first) time step is related to decisions or states from the past, due to a temporal constraint. This requires the market clearing algorithm to internally store its previous decisions and constraints, regarding bids having such inter-temporal constraints.

[15] A graph is called *connected* if a path exists between any arbitrary pair of nodes.

5.1 AS market clearing objective

One of the goals of the Integrated Reserve market is *balancing*, i.e. to remove the power imbalance in the system. In the market clearing formulation, SOs do not explicitly bid their needs to solve this imbalance (as explained in section 2.5). Instead, they forecast the imbalance (for each time step over the market time horizon) at each node of the network (transmission and possibly distribution), from which they can estimate/calculate the system imbalance. Flows between the nodes are taken into account through multiple power-balance equations, which guarantees that the total amount of power injection and power off-take, also potentially considering the losses (depending on the grid model), considering the forecast network state and the accepted bids of the market, sum up to zero. This requires a coupling of market economics with the network physics: The *quantity* in the market is the same as the *power* (or nodal injection and off-take) in the network. The mathematical description of such coupling is provided in Section 10.5.1.

5.2 The Market Objective Function

The market objective function can be defined in several ways, targeting various economic and environmental measures. The most common economic objectives (which are utilized in other energy and AS markets) are minimization of (reserve) activation cost ([95], [96]) and maximization of social welfare [97]. The former aims at reducing the operating cost (resp. maximizing the benefit) in case of upward (resp. downward) activations required by the grid operator which is responsible to solve grid problems using the market products, while the latter is designed to increase the welfare for both sellers and buyers of flexibility.

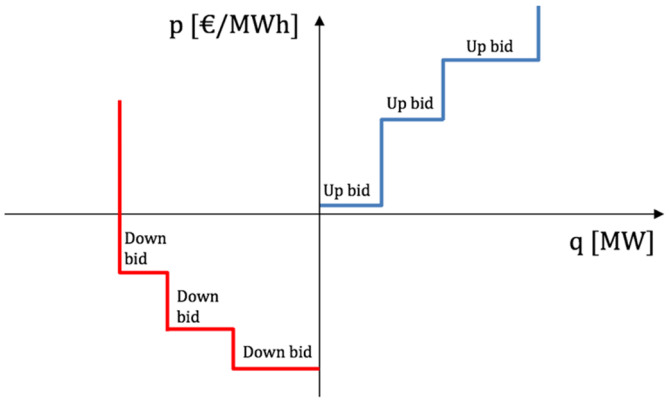

Figure 5-1 The price-quantity diagram showing the available bids for up- and down-regulation offers.

In order to better understand the two variations of market objective, let us step back and consider the situation where all bids have arrived at the market, are sorted, and are grouped based on the sign of q, as seen in Figure 5-1. As a reminder, bids with $q > 0$ correspond to an upwards regulation (hence, called an up bid), and bids with $q < 0$ represent a downward regulation (therefore, a down bid).

5.2.1 Minimization of Activation Cost

When the market objective is to minimize the (reserve) activation cost, one of the two groups of bids in Figure 5-1 are (usually) useless (unless in some cases for solving congestion problems). As shown in Figure 5-2 (right panel), in a scenario with a need for up regulation, the down-bids are neglected and the market is cleared according to the required up-regulation quantity (shown as up ask). In the opposite scenario (left panel), the need for down regulation is applied to the down bids, while the up bids are ignored. The black circles in Figure 5-2 represent the clearing point, corresponding to the cleared quantity (q^*) and the cleared price (p^*).

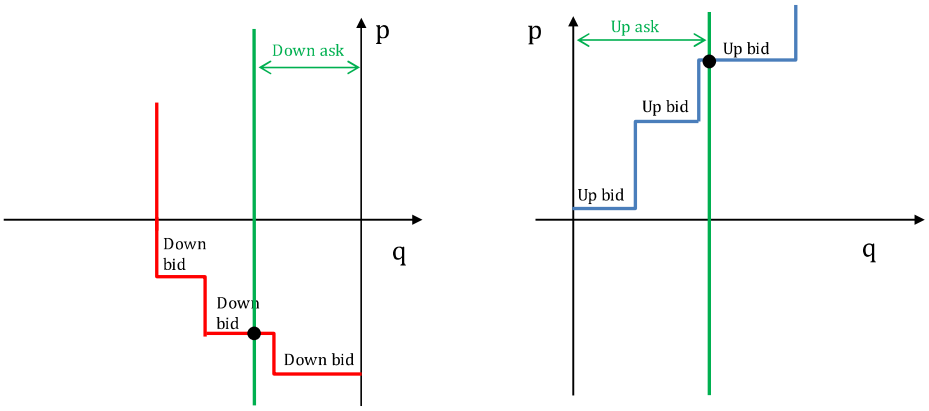

Figure 5-2 Minimization of activation costs when operator asks for up regulation (right) and for down regulation (left).

However, according to the European Balancing guidelines (EBGL ,[10]), it is recommended that the newly designed markets incorporate the *maximization of social welfare* as the objective. In addition, by defining the objective as a minimization of activation costs, a technical difficulty appears when using a pay-as-cleared approach (see section 2.4). In this setting, the activation cost is defined as the product of the absolute value of cleared quantity, q^*, and cleared price, p^*[16]:

$$UP\ regulation: \quad minimizing \sum_{\beta \in\ set\ of\ upward\ bids, q>0} f(p_{\beta,0}, p_{\beta,1}, q_\beta, x_\beta)$$

$$DOWN\ regulation: \quad minimizing \sum_{\beta \in\ set\ of\ downward\ bids, q<0} f(p_{\beta,0}, p_{\beta,1}, q_\beta, x_\beta) \qquad (23)$$

In the SmartNet context, since both congestions and balancing are considered together, we have to allow the possibility to activate bids in the same direction as the imbalance, since it might be needed in case of congestion. Therefore, we could combine the whole objective into a single minimization, across all bids,

[16] The activation-cost objective has to be *Minimized*.

$$minimizing \sum_{\beta \in \, set \, of \, downward \, bids, q<0} f(p_{\beta,0}, p_{\beta,1}, q_\beta, x_\beta) \quad (24)$$

where the variables are x_β, indicating the portion of bids (between 0 and 1) that is accepted. The sign of an f-function depends purely on the sign of the p element (see equations (1) and (2)). But then it is be strictly equivalent to maximizing the social welfare, as described in the next section.

5.2.2 Maximization of Social Welfare

If the market objective is defined as maximization of social welfare, all bids (upwards and downwards) are considered into a single objective funciton. In order to elaborate, we start by an explaining the idea of *curve-crossing* for maximizing the welfare. We want to accept bids offering the up- and down-regulation such that the total quantities match. However, the system imbalance, that is the need for up- or down-regulation has to be taken into account. For this, we introduce pseudo-bids representing such a need for flexibility: An ***up ask*** is a need for up-regulation, while a ***down ask*** is a need for down-regulation. They are called pseudo-bids because in the algorithm, the SOs do not explicitly bid: rather, they submit their forecast network state which results in needs that are represented by (hard) constraints in the optimization problem (these pseudo-bids should have vertical lines, or a arbitrarily high/low price to represent that they are price-taker). Pseudo-bids are just useful for the sake of illustration. Then, the pseudo-bids are attached to the normal bids. This is shown in Figure 5-3. Since pseudo-bids of system operators are price-takers, it is logically assumed (for the Figure) that the system operators are willing to offer a more interesting price compared to the bids in the same group, since they need the service to resolve the grid problems.

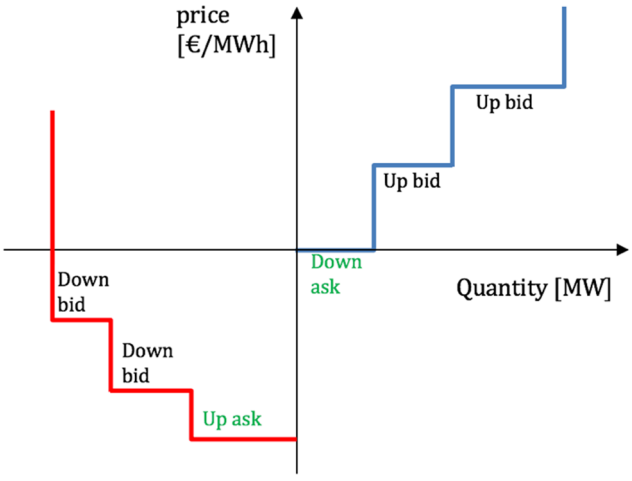

Figure 5-3 Representation of flexibility needs in the forms of pseudo-bids (or "asks").

We observe that in Figure 5-3 it is not possible to apply the curve-crossing technique, since according to the convention, the bids are not in the same half-planes of the $p-q$ diagram. Therefore, the bids on one side (in this case, on the left half-plane) are rotated to the other side. This is shown in Figure 5-4. Afterwards, the junction of two curves defines the clearing point of the market, revealing the optimal values for the cleared quantity and the cleared price. The social welfare is the area marked in green.

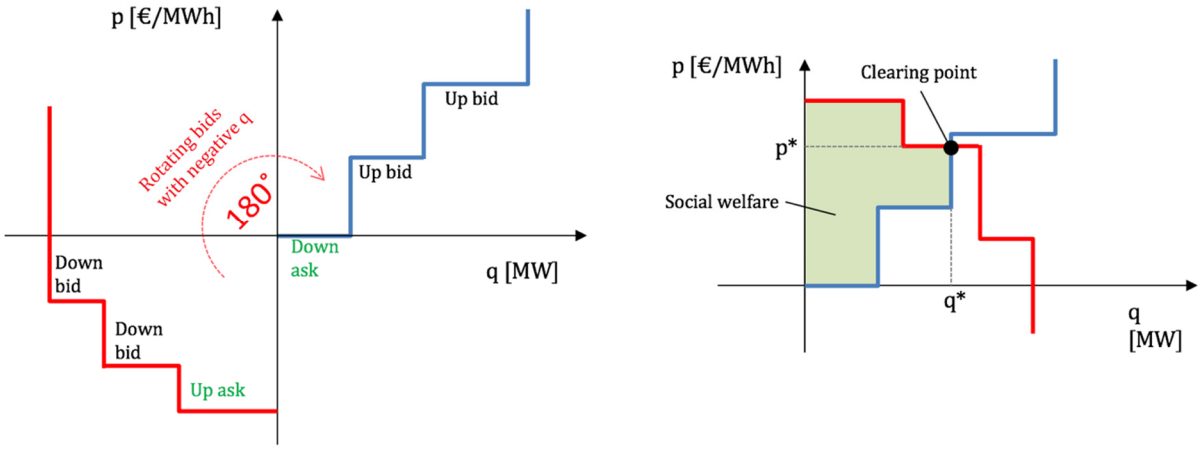

Figure 5-4 The rotation of bids, resulting in a curve-crossing. The clearing point to maximize the social welfare is located at the junction.

Using social welfare as an objective, the optimization problem has a linear objective (provided only step bids are used). The social welfare can be written as:

$$SW\ (t) = -\sum_{\beta \in\ set\ of\ all\ bids} f\left(p_{\beta,0}, p_{\beta,1}, q_{\beta}, x_{\beta}\right) \tag{25}$$

where SW is the social welfare and the variables are x_{β}, indicating the portion of bids (between 0 and 1) that is accepted[17]. The sign of an f-function depends purely on the sign of the p element (see equations (1) and (2)).

5.2.3 Multi Time-Step Objective Function

In case the market horizon is long (e.g. because a rolling horizon is used), it might be that the forecast accuracy (typically, the network state, but also the forecast of flexibility providers) between the start of the market time step and the end is different (i.e. accuracy gets worse over time). To account for this in the market clearing algorithm, one simple method is to weight differently the (social welfare) objective in time. A discount factor vector, γ_t, is introduced in the social welfare objective, for all time steps t over

[17] The social welfare objective has to be *maximized*. This objective is either linear or quadratic (which is still ok to have a convex optimization problem). It is either linear (if there exist only step bids) or quadratic (if there are also some linear bids).

the optimization horizon. Such γ_t factors may gradually decrease, starting from 1 (for t=1) and decreasing monotonically until the end of the market horizon. As a result, the time-discount weighted social-welfare over the whole time-horizon is defined as

$$SW = \sum_{t \in T} \gamma_t \, SW(t) \tag{26}$$

5.2.4 Avoiding Unnecessary Acceptance

When using a social welfare objective, it can happen that flexibility bids are matched with each other (it depends on their respective price), while the Integrated reserve market is not an energy market, but a market to solve imbalances and congestions. Therefore, it is not logical to allow unrestricted acceptation of additional bids [98], even though it may contribute to an increase of the social welfare. The reason behind this avoidance is that accepting extra bids and allowing additional trading between actors may introduce imbalances even higher than those previously existing in the network. It can also introduce the possibility of arbitrage.

In order to elaborate the issue, let us have a better look at the problem using a curve-crossing approach. In the example shown in Figure 5-5, the up-regulation need of the system operator is presented as *up ask*. If no unnecessary acceptance is allowed, the market is cleared at q_1^* (left side of Figure 5-5). In this case, none of the down bids are accepted. In contrast, if social welfare is maximized (according to (25)), the market will be cleared at q_2^* instead (right side of Figure 5-5). It can be seen than in the latter case, the social welfare is increased, but some unnecessary acceptance has occurred.

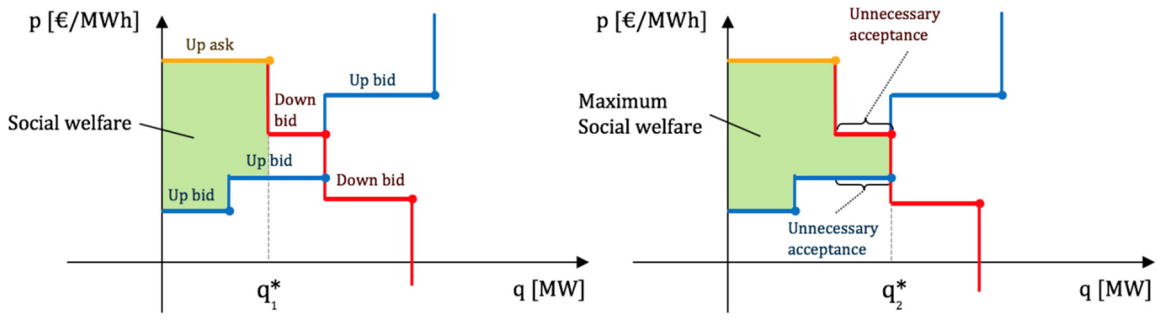

Figure 5-5 Necessary (left) and unnecessary (right) activation of bids and the corresponding social welfare.

Since minimizing activation cost requires to choose in advance between upward and downward bids, we choosed the objective as maximization of social welfare, but we introduce a technique to avoid unnecessary bid-acceptance to only allow activations really needed by SOs.

In the following, we briefly describe a technique used to adapt the prices of those bids which have a "wrong" sign of quantity (i.e. opposite to what is needed by the system). We call them “wrong bids” from

now on. The idea is to make such bids not economically interesting to be accepted, by not matching them with the bids which have a useful sign of quantity. However, if there is a non-economic reason to accept the bids (for example to solve a congestion problem), it will be allowed. The consequence would be a reduced social welfare. When adapting the prices of wrong bids, it is required that the merit order of the bids remains unchanged. Figure 5-6 shows such adaptation applied to the example of Figure 5-5.

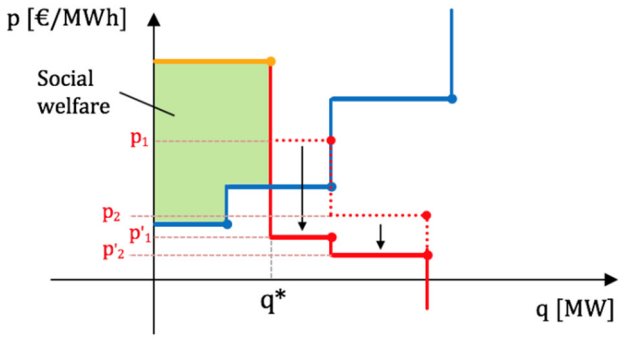

Figure 5-6 Adaptation of prices for avoiding unnecessary acceptance. The merit order is preserved.

After the prices of wrong bids are adapted, it is possible to use the standard formulation for maximization of social welfare, without the risk of unnecessary acceptance. The detailed algorithm for price adaptation is discussed in Section 10.5.3.

5.3 Nodal Physical Constraints

The network models for the transmission and distribution grid were obtained in Chapter 4. The relevant equations (such as the power balance and Kirchhoff's laws) are inserted into the market clearing optimization in the form of *constraints*.

5.4 Pricing Approach

The designed market aims not only at determining the activation of flexibilities but also to associate a price to these activations. Different pricing approaches can be considered:

- The "Pay as bid" approach where the activated bids simply receive the price corresponding to the activated quantity in the bidding curve. This approach is simple and intuitive for the different market stakeholders. However, it does not give incentive for the market participants to bid using the real cost of flexibility, creating an economic distortion in the activation decision. Some drawbacks of this approach are [9] :
    - It is even more susceptible to the exercise of market power than uniform marginal pricing
    - It tends to result in more inefficient dispatch and investments

- Pay-as-bid gives disincentives for investments and using DER for AS. Distributed AS have higher investments and much lower operational costs than centralised AS.
- It gives smaller social welfare. (higher costs and inefficiencies)

- The "Pay as cleared" or "uniform marginal price approach" where the activated bids receive the same price per MWh (or MW over a time step), corresponding to the most expensive (or the least economically interesting) activated flexibility. This approach removes the risk of market participant bidding in terms of what they want to receive instead of their real cost of flexibility.

As the motivation of the designed market is to allow a fair and cost-efficient competition between different sources of flexibilities, in particular those located at the distribution level, it appears natural to use the most economically efficient approach of the marginal pricing [9].

However, as the considered system is not a perfect copper plate, network constraints, both at the transmission and distribution levels, have to be taken into account.

Marginal pricing can be adapted to a system with network constraints in different ways, and is called Locational Marginal Price (LMP):

- A **Nodal** approach where a price for flexibility is associated to the most granular level in our network representation i.e. to each node of the distribution grid

- A **Zonal** approach where a price for flexibility is associated to a zone covering different nodes. Each zone can have a different price but the nodes in the same zone have the same price.

As the network constraints, both at the transmission and distribution levels, are of key importance for an AS market ensuring the satisfaction of congestion and voltage constraints, it is natural to encompass in the price mechanism these network factors in the most accurate and economically efficient way. Moreover, AS markets are close-to-real-time market and their decisions cannot be corrected by a market afterwards. For these reasons, a nodal approach is proposed for the considered Integrated Reserve market to be designed. Further justifications and the derivation of the distribution locational marginal prices (DLMP) for the considered network model and its interpretation is detailed in the rest of the chapter.

5.5 Nodal Marginal Pricing

The theory of nodal marginal pricing is established on the more general economic concept of marginal cost pricing, which is an approach that achieves an efficient allocation of resources under the assumption of perfect competition. The idea of marginal cost pricing is simple, and dictates that consumers with a well-defined willingness to pay for a commodity should consume as long as their incremental benefit exceeds the incremental cost of the additional production. In an economy where consumers can be stacked in order of decreasing valuation and suppliers can be stacked in order of increasing marginal cost, it is easy to

see why this system allocates resources efficiently. Consumers with the highest willingness to pay are matched with suppliers with the lowest marginal cost of production, up to the point where no additional mutual benefits from trade can be achieved.

5.5.1 Pricing over Space and Time

The complicating factor of electric power systems is the fact that marginal cost cannot be defined uniformly for all locations, or for a single time period, but instead depends on the configuration of demand over the network and the availability and physical characteristics of power generation, transmission and distribution equipment, and changes continuously (over minutes, hours, days, …). This led to the theory of spot pricing of electricity over space and time, championed by the seminal work of Schweppe, Caramanis, and Tabors [99], [100].

A major reason why marginal cost cannot be defined uniformly for all locations of a power system is the physical laws that govern power flow, losses, and limits on transmission and distribution lines. A numerical example is shown in Section 10.5.4.

5.5.2 Granularity

There has been a longstanding debate about the granularity of pricing in electricity markets. More specifically, nodal pricing has been criticized for thinning up markets and creating opportunities for the exercise of market power, as well as for creating a pricing system that is too complex or unnecessarily granular ([11], [101]). Successful experience of nodal pricing [102] in some of the largest markets worldwide, including the Pennsylvania Jersey Maryland (PJM) market which prices 8700 locations with a frequency of 15 minutes, have discarded concerns of complexity. Market power mitigation by market monitors has further softened concerns regarding the exercise of market power. Importantly, market product size must be adjusted according to the granularity. Otherwise poor liquidity and possibilities to exercise market power may result.

An alternative to nodal pricing that has been advocated on the grounds of simplicity is zonal pricing, whereby nodes are aggregated into zones with a common price (which implicitly assumes away intra-zonal congestion) and inter-zonal lines are aggregated into a single link. This aggregation creates a challenge of defining capacity and creating a proxy for the representation of power flow laws, as shown in a numerical example in Section 10.5.5. The conclusion is that a zonal model will either sacrifice efficiency or welfare, since it ignores the physical laws that govern power flow. Remedies to this issue by means of re-dispatching have exposed the market to severe gaming opportunities (including the Enron “Dec game”) [103], result in day-ahead scheduling inefficiencies [104], and create free-riding opportunities for certain zones on the transmission grids of other zones [105].

5.6 Calculating Prices

The standard definition of market equilibrium in economics is a pair of prices and quantities such that, given the prices, agents maximize profits, and prices are such that supply and demand are equal. This definition of market equilibrium implies that the price of electrical power in the optimal power flow problem can be obtained as the dual optimal multiplier of the power balance constraints[18]. These prices can be obtained by solving the dual of the optimal power flow problem, which is formulated as a set of constraints in the market clearing algorithm. Therefore, the clearing of quantities is called the "primary problem", and the clearing of nodal marginal prices is referred to as the "dual problem".

A wide range of optimization algorithms that are used in commercial applications for solving linear programs, second-order cone programs, and more generally non-linear programs, solve the dual of an optimization problem as a by-product of solving the primal problem. This implies that, in order to obtain prices, it is not necessary to solve the dual problem explicitly, since this is anyways a side-product of the optimization process. Commercial solvers (such as CPLEX) will then typically furnish primal optimal variables that are used for deciding how to dispatch an asset, how much power should flow over a line, what the voltage of a node is, as well as prices that should be assigned to an exchange of quantity.

5.6.1 Nodal Cleared Prices as Dual Variables

The nodal dual variable associated with the nodal power-balance constraint equals the marginal price of injecting/off-taking one unit of power in that node. In principle, for a linear programming (LP) problem, the cleared price p^* can be fetched by requesting the LP-solver to provide the value of the dual variable.

In reality, the market clearing problem contains binary variables. In such a case, the cleared prices need to be derived using a dedicated algorithm. The price is not explicitly present as a variable in the model of the primal problem. Further explanation is provided in Section 10.5.6.

By avoiding the situation of having prices as explicit variables in the primal problem, such difficulty is avoided. It also means that the dual problem does not have to be solved explicitly, except in the case of indeterminacies or paradoxical acceptance.

In general, indeterminacies can happen for both quantity and price. Figure 5-7 compares the situations with no indeterminacies and those with indeterminacies. In case of a quantity indeterminacy, the rule of volume maximization applies, resulting in the selection of clearing point at the end of the horizontal cross section. In case of a price indeterminacy, the rule is to choose the middle point of the vertical cross section. Section 10.5.7 explains the algorithm in more details using a numerical example.

[18] This statement is true for convex problems. Problems with binary decision variables pose deeper theoretical questions of defining what a market cleared price is, as discussed in the next section.

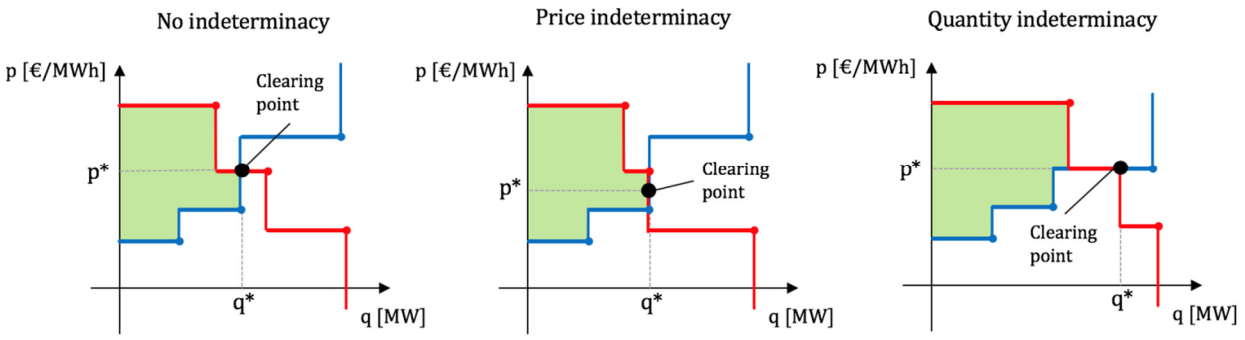

Figure 5-7 Price and quantity indeterminacies and the corresponding clearing point.

After handling the indeterminacies, there is only one more reason to solve the dual problem (for all nodes together), and that is the case of a paradoxically accepted block (PAB) in any node. These are blocks that are accepted even though they are out of the money (i.e. the bidder is losing money because of the cleared price). This situation does not occur in an LP model, but can be caused by the presence of binary variables (non-curtailable bids, out of merit-order acceptance, ramp constraints, etc.).

For example, the relaxed problem would accept 90% of a block which is in the money, but because of the binary variable representing the non-curtailability of that block, we should accept 0% or 100% of it. The problem to be solved is almost the dual problem; the difference is that, per block, a constraint is added to account for the fact that the block has to be in the form of money. However, this could make the solved problem infeasible. If that happens, some branch and bound algorithm is necessary.

5.7 Alternating-Current Power Flow

Nodal pricing theory is well developed in linearized models of transmission power flow where reactive power flows are ignored, voltage is normalized across all buses, and real power losses are ignored or simplified. By contrast, the increasingly important role of distributed resources in power system operations necessitates an explicit consideration of the non-linear power flow equations in operations. Indeed, the assumptions employed for the linearization of Kirchhoff's power flow laws, which are reasonably accurate for the high-voltage grid are not adequate for medium/low-voltage distribution grids (see chapter 4). This challend is discussed using an example in Section 10.5.8, but the important thing to note here is that the general theory of marginal pricing remains the same: one solves the optimal power flow and obtains the price at a certain node as the dual optimal multiplier of the power balance constraint at a certain node.

5.7.1 Distribution Locational Marginal Pricing

The pricing approaches used in the market clearing result in obtaining distribution locational marginal prices (DLMPs). In the early days of electricity market deregulation, locational marginal pricing in DC

networks presented interpretation difficulties, due to the fact that it deviated from simpler pricing models as a result of the linearization of Kirchhoff power flows. The interpretation of DLMPs adds a layer of complexity, since voltage, real power losses, and reactive power flows are accounted for, whereas these aspects of the problem are either simplified or ignored in DC power flow. Various methods can be used for understanding and interpreting the value of DLMPs, with the objective of justifying their value on physical grounds. In Section 10.5.9 we show three different approaches to answer the question of why DLMPs obtain the specific value furnished by the market clearing algorithm.

6 TSO-DSO Coordination Schemes

Previous sections have focused on describing the concepts and mathematical formulations needed to clear a market: market products specification, simplified network model, clearing algorithm, and pricing mechanism. In this chapter, we describe the specificities and requirements of the market architectures for the different TSO-DSO coordination schemes investigated in the SmartNet project [2]. First, the centralized vs decentralized feature is discussed (section 6.1). Then the temporal sequence of actions between actors and the market clearing specificities are described for each TSO-DSO coordination scheme, also using an example for illustration (section 6.2). Afterwards, section 6.3 describes one specific methodology for the DSO to smartly transfer/bid from local to TSO markets (needed for some decentralized architectures). Finally, a game theory perspective is explained (section 0), broadening the scope of the five TSO-DSO coordination schemes, by considering what could happen in situation where cooperation (between SOs) is not applied, leading to gaming/strategic b.

6.1 Centralized vs Decentralized Market Architectures

First of all, an important difference between TSO-DSO coordination schemes is whether a centralized or decentralized architecture (see Figure 6-1) is considered. *Table 6-1* shows which architecture is used in each coordination scheme. Acronyms are introduced for each coordination scheme (CS), to avoid lengthy naming throughout the chapter.

Table 6-1 List of centralized and decentralized architectures

Centralized architecture		Decentralized market architecture	
CS A	Centralized AS market	**CS B**	Local AS market
CS D1	Common TSO-DSO AS market (centralized)	**CS D2**	Common TSO-DSO AS market (decentralized)
CS E	Integrated flexibility market	**CS C**	Shared balancing responsibility model

In the centralized architecture, there is one (big) market, while for decentralized architecture, many local markets (managed by DSOs) co-exist with a global AS market. For the decentralized architecture, two sub-cases are considered:

- No interaction between the markets exist (*Shared balancing responsibility model*): in this case, TSO and DSOs agree in advance on a scheduled power exchange profile at their interconnection (based on the method explained in [2]).

- DSOs are responsible to transfer the bids submitted on the local markets to the global AS market in a smart way (i.e. taking the distribution grid constraints into account), as indicated by the blue arrows in Figure 6-1. This is the case for the *Local AS market* and *Common TSO-DSO AS market (decentralized)*

coordination schemes. In this circumstance, the DSO may cluster the bids having the same locational tag (i.e. connected to the same distribution network node), but also across all the distribution network nodes. Importantly, the DSO should check that networks constraints are not violated when bids are consolidated across the nodes, since there is no distribution network model in the global AS market.

Also, regarding decentralized architecture, market settings might be different for each market. As an example, the pricing scheme can be pay-as-bid in the local market and pay-as-clear in the central market [106], or the market can clear at different frequencies. This degree of freedom can be an advantage but also an inconvenience. In any case, the possibility of having different market settings does not change the mathematical description of how the markets are cleared (see previous chapters), but instead it may introduce new bidding strategies and cause a change of paradigm [107], considering the problem from a "game theory" point of view.

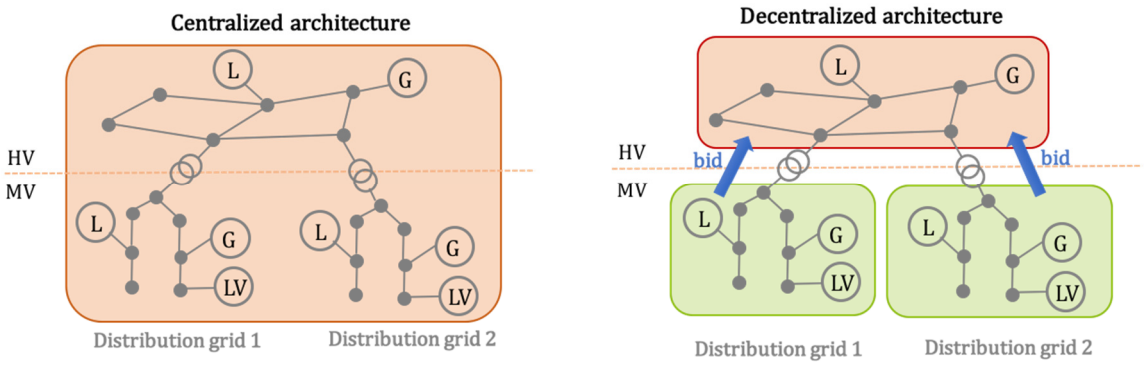

Figure 6-1 Diagrams showing centralized and decentralized market architectures

6.2 Temporal sequence and market clearing algorithm specificities

*Table **6-2*** shows some specificities regarding the market clearing for each coordination scheme. Some similarities can be seen between coordination schemes A and D1, with the difference being that in CS D1 the market considers the problem of both transmission and distribution networks. It implies that CS D1 entails the most computationally complex single-clearing problem to be solved.

Similarities are also noticeable between CS B and D2. In fact, the only difference is that the market clearing in CS B is also run to check and eventually solve local congestions, while in CS D2 all local market bids are directly submitted to the central market operator.

Table 6-2 List of TSO-DSO coordination schemes and the corresponding specifications

Coordination scheme	Specificities
CS A - Centralized AS market model	• TSO is the only buyer: No need to represent the imbalance of TSO's control area by an explicit bid. • Market objective: maximize social welfare while respecting network balances and

	operational limits (voltage profiles and line capacities) • Only transmission grid constraints are considered. • Unnecessary activations are prevented (i.e. potential trades between flexibility providers)
CS B - Local AS market model	• TSO and DSO are buyers to solve global and local problems together, with a priority for DSO to solve local problems • Need for a method to aggregate local market bids non-accepted to solve local needs into bids suited for TSO market, while taking distribution network constraints into account. • Local (central) market objective is to maximize social welfare of DSO (TSO). Unnecessary activations are also prevented.
CS C - Shared balancing responsibility model	• Local and global markets fully decoupled: easier but need for an additional input, i.e. agreed scheduled exchange profiles between TSO and DSO. • Local (central) market objective is to maximize social welfare of DSO (TSO). Unnecessary activations are also prevented.
CS D1 - Common TSO-DSO AS market model (centralized)	• TSO and DSO are buyers to solve global and local problems together • Objective is to maximize social welfare of both TSO and DSOs**.** Unnecessary activations are also prevented.
CS D2 - Common TSO-DSO AS market model (decentralized)	• TSO and DSO are buyers to solve global and local problems together • Need for a method to aggregate local market bids non-accepted to solve local needs into bids suited for TSO market, while taking distribution network constraints into account. • Objective is to maximize social welfare for TSO+DSO. Unnecessary activations are also prevented.
CS E - Integrated flexibility market	• TSO, DSO and CMP (e.g. BRP) are buyers of flexibility and compete • Objective is to maximize social welfare. Unnecessary activations are allowed. • TSO and DSO may bid explicitly.

In the next subsections, we explain how each coordination scheme, except CS E, is using the modules defined earlier in this document and also in other parts of the project. More detailed description of the coordination schemes is found in [2]. It was decided by the SmartNet consortium not to investigate CS E further, mainly for the reason that regulated and non-regulated parties are in competition to procure resources, while the priority should be for SO, so close to real-time. If priority is given to TSO and DSO compared to non-regulated market parties, then it could be thought as two sequential market sessions: one intraday session (potentially with a GCT closer to real-time) and a subsequent market session for just TSOs and DSOs, which is exactly the scope of CS D1.

Throughout the next subsections, the same example (network, flexibility providers, SO needs) is considered to illustrate the different features of each coordination scheme. Regarding the network, the

example includes a transmission grid connected to two distribution grids via HV-MV transformers, as illustrated in Figure 6-2.

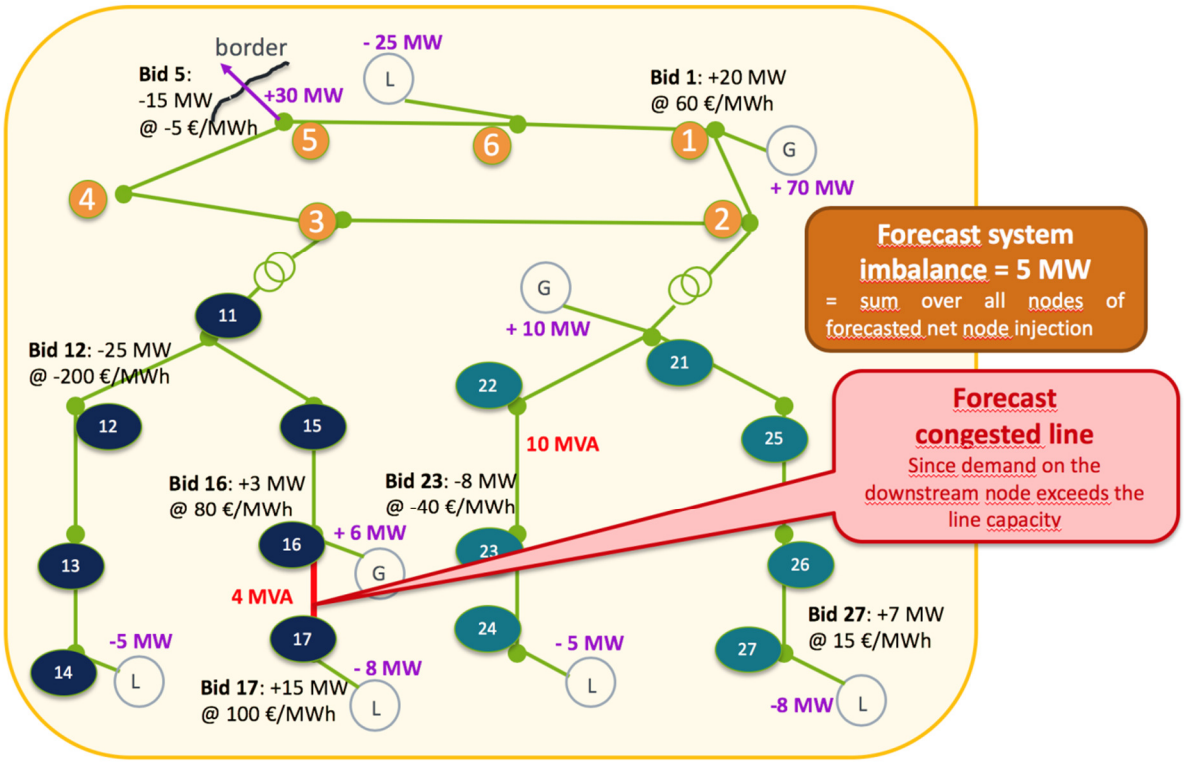

Figure 6-2: Toy example with one transmission and 2 distribution grids (nodes are numbered). Forecast net nodal injections are represented by quantities in pink (no info means 0). Specific operational limits for the example are represented in red (thermal limits on lines at distribution level). Bids used for the example(simple Q-bids) are indicated in black with the quantity (MW) and bid price (€/MWh).

At the transmission level, the active sources consist of a generating unit (at node 1) and a load (at node 2), for which the forecast injection (at the time of market GCT) is respectively an injection of 70 MW and a withdrawal of 25MW. Moreover, it is assumed that this transmission grid is connected to a neighboring zone (e.g. another country) and at this specific timestamp, an export of 30 MW is considered. As far as bids are concerned, two of them are offered at the transmission grid: bid 1 (located at node 1) is an upward bid of 20 MW at a price of 60 €/MWh, whereas bid 5 (located at node 5) is a downward bid of 15 MW at a price of -5 €/MWh. For the sake of simplicity, line parameters are assumed to be the same for all edges.

The distribution grids (denoted Dx1, on the left, and Dx2, on the right) are pretty similar in terms of setup: one generator and two loads for each of them (nodes 14,16,17,21,24,27). Three bids are offered in Dx1: one downward bid at node 12 (25 MW at -20 €/MWh) and two upwards bids (one at node 16 with 3 MW at 80 €/MWh and one at node 17 with 15 MW at 100 €/MWh). In Dx2, a downward bid at node 23

features 8 MW at -40 €/MWh and an upward bid at node 27 is offered at 15 €/MWh with a volume of 7 MW.

The input provided by SO is really about forecast net injection at each node of the network. In this example, the forecast imbalance may be approximated (i.e. losses not considered) as the sum over all nodes of the forecast net nodal injection. In this example, the forecast imbalance is +5MW (i.e. downward regulation bids are required). Finally, the main difference between the TSO and DSO networks is represented by line capacities: while the transmission grid is assumed to have "infinite" capacity and therefore no line congestions are experienced, two edges at the distribution grids are limited in their available maximum apparent power to 4 MVA (in Dx1) and 10 MVA (in Dx2). It can be noticed that the combination of the 4 MVA limit and the forecast node net injection of -8MW at the downstream node (node 17) of that line implies that there is a forecast congestion on the line (linking nodes 16 and 17). For the other line (10MVA), it is not the case. In practice, it is not always easy to detect/forecast the congestions in the network with simple rules (power flows need to be run, especially at transmission level).

In the following, the results of the market layer for this simple network are detailed and explained for each coordination scheme.

6.2.1 CS A - Centralized AS Market

The block diagram representing this coordination scheme is shown in Figure 6-3.

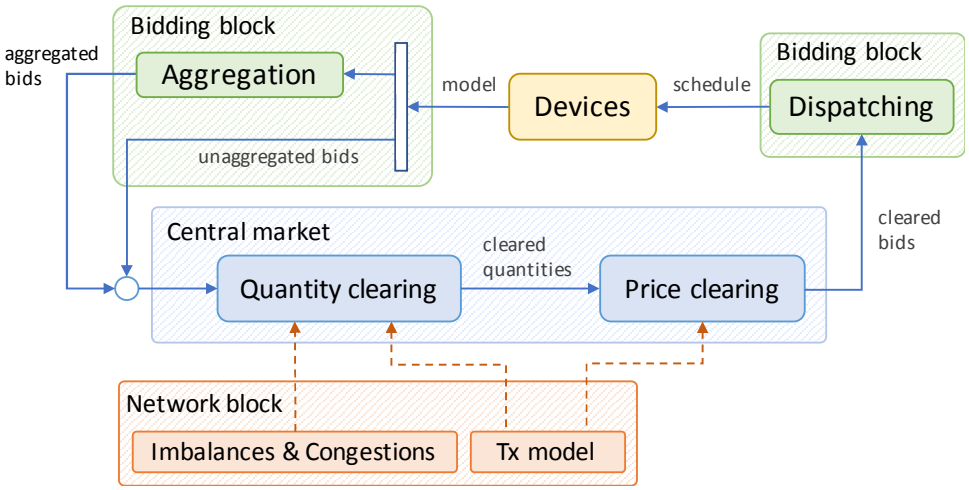

Figure 6-3 Block-diagram representing the centralized AS market

The diagram shows a set of blocks representing modules and arrows which correspond to data flows. The blocks are connected sequentially in a closed loop, implying that the procedure is repeated at each time step. Here we provide a description of each block in Figure 6-3:

- **Devices**: This block includes the models of available flexible assets in both distribution network (Dx) and transmission network (Tx). Input to this block is the dispatching schedule for the following time step. Outputs from this block are the models and parameters (including internal states) of flexible assets. More information about the contents of this block can be found in D1.2 [7].

- **Bidding**: This block contains the algorithms required for aggregation and dispatching of flexible devices. The aggregation module receives device models and produces bids, which have a locational tag related to one of the modelled transmission grid nodes. The dispatching module receives the cleared bids and generates dispatching schedules for selected flexible assets. More information about the contents of these blocks can be found in [108].

- **Network**: This block contains the network model, including:
    - network topology, line connections and parameters
    - operational limits on power flows and voltage
    - forecasts of net nodal injection at each node of the network (implicitly representing the forecast system imbalance, and potential forecast congestions).

  As described in Chapter 4, different models are considered for distribution (Dx) and transmission (Tx) grids. In this coordination scheme, only the Tx model is considered, since Dx problems are not solved in the market. This model is used in the quantity and price clearing blocks.

- **Market**: As already mentioned, in CS A, only the TSO network is considered. The sequence of actions performed by the different actors for the market clearing is described in Figure 6-4 and consists in the following steps:

1. The TSO sends the forecast grid state, per market time step, to the market operator before the Gate Closure Time (GCT): this includes forecast net nodal power injection (sum of generated power minus sum of withdrawn power at each node), operational limits, grid topology (if modified) and scheduled/agreed flow at the borders
2. Flexibility Service Providers (FSPs) send bids to the Market Operator (MO) at transmission grid nodal resolution. For our example (see *Figure 6-2*) , all bids from distribution level are grouped together, per distribution grid, and offered at the HV (High Voltage) node of the corresponding HV-MV transformer. It means that bids 12, 16 and 17 are offered at node 3, whereas bids 23 and 27 are offered at node 2.
3. The MO runs the market clearing algorithm, i.e. computes accepted bid quantities and nodal marginal prices (which, in this scheme, are only applicable to the transmission network nodes). In detail, the mathematical formulation of the optimization problem for CS A is the following:

$$\textit{Maximize}\ SW$$

Subject to:

- Nodal active power balance at Tx level
- Bids constraints
- Operational constraints (line capacities) at Tx level
- Avoid unnecessary activations

4. The MO transmits market results to the TSO
5. Finally, the MO dispatches the activated bids of FSPs

The temporal sequence diagram of the actions performed in this scheme, together with the main actors involved, is shown in Figure 6-4.

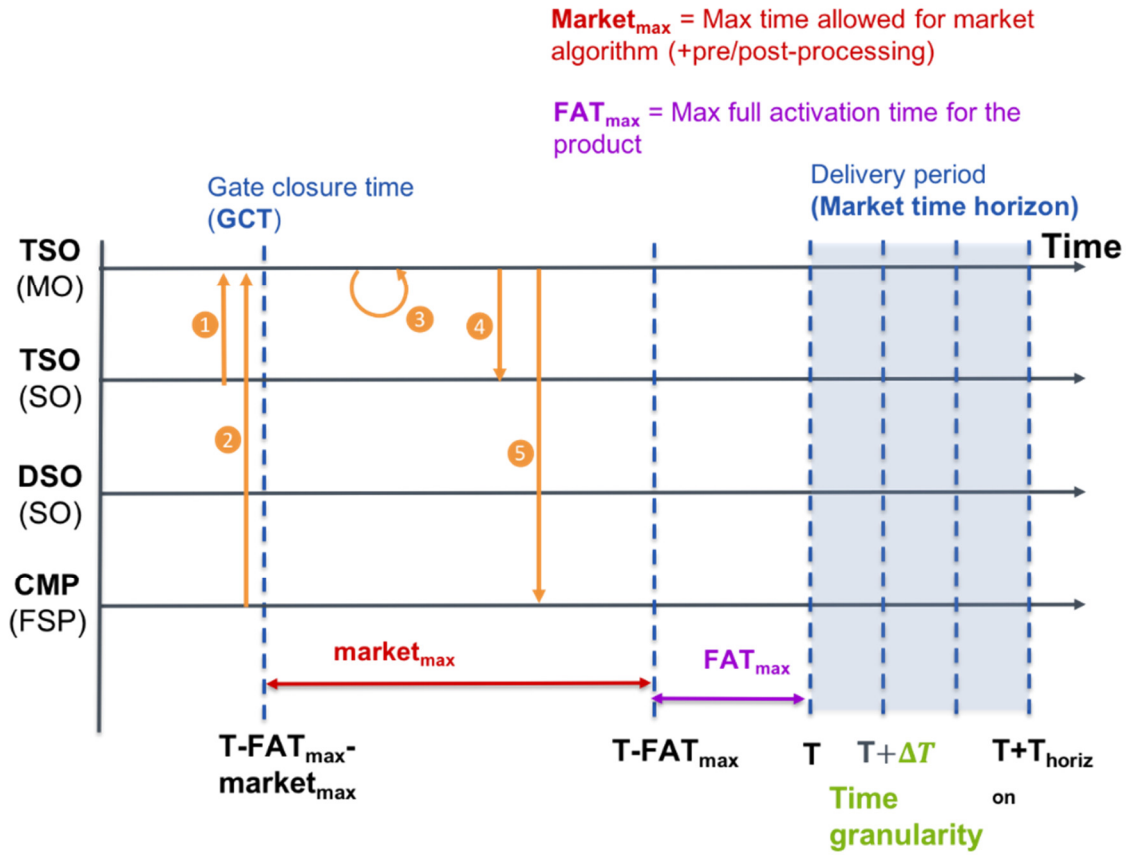

Figure 6-4: Temporal sequence diagram for CS A

The results of market clearing, in terms of nodal prices, accepted bid quantities and active power flows on transmission edges, are shown in Figure 6-5. Accepted bid quantities are displayed in blue, nodal prices in red and active power flows on the branches in light blue.

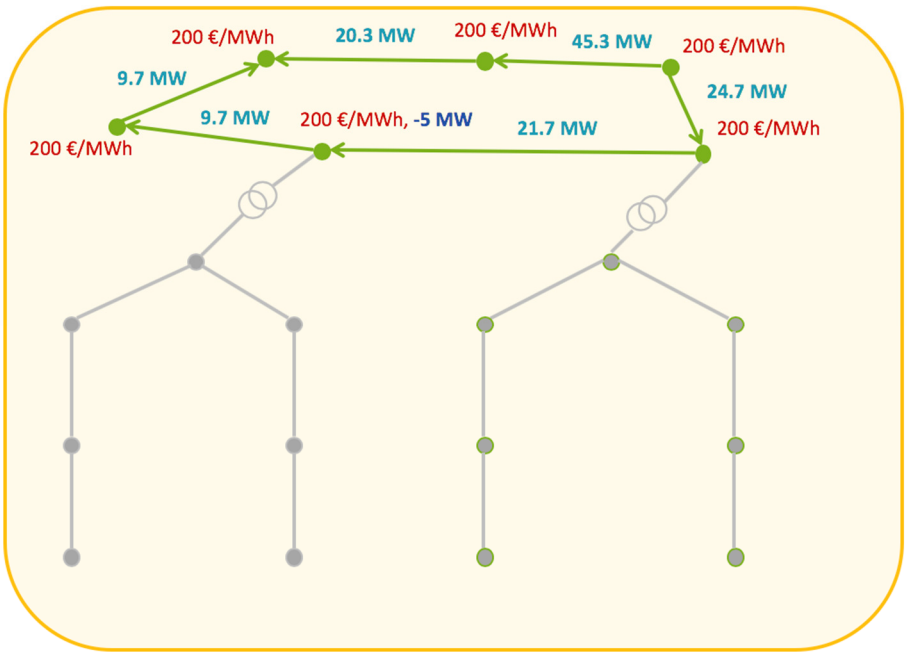

Figure 6-5: Market clearing results for CS A

Since no congestions are experienced in the transmission grid (and since the network model is a DC approximation, without voltage considerations and without losses), the market clearing price of all Tx nodes is the same and it corresponds to the marginal price of the accepted bid. Moreover, as the total system imbalance (for TSO and DSOs together) corresponds to 5 MW, the sum of accepted bid quantities is equal to this value. As the MO has at his disposal all the bids in the complete network, in this scheme all the power needed to balance the network is provided by bid 12, the cheapest provider of downward flexibility (-200 €/MWh), and consequently all nodes get a price of 200 €/MWh. Note that, using CS A, the forecast congestion on the 4MVA-capacity line in the Dx1 is not solved and re-dispatching/urgent measures will be required to be taken at DSO level.

6.2.2 CS B - Local AS Market

The block diagram representing this coordination scheme is shown in Figure 6-6. Blocks are organized into four categories as in CS A. However, alternative block connections and different sequence of running are used in this case:

- **Devices**: In this coordination scheme, Dx devices participate in the local market run by DSO, while Tx-connected devices participate in the central market run by TSO.

- **Bidding**: The bidding process is similar to the one described for CS A. However, for bids submited on the local market, the locational tag of the bid must be linked to one of the modelled distribution grid nodes. Separate dispatching steps are used for Dx and Tx devices.

- **Network**: Here, Dx and Tx models are used in the local and central market, respectively. Congestion problems are treated by the corresponding network operators in both local and central market. However, imbalances are only considered in the central market.

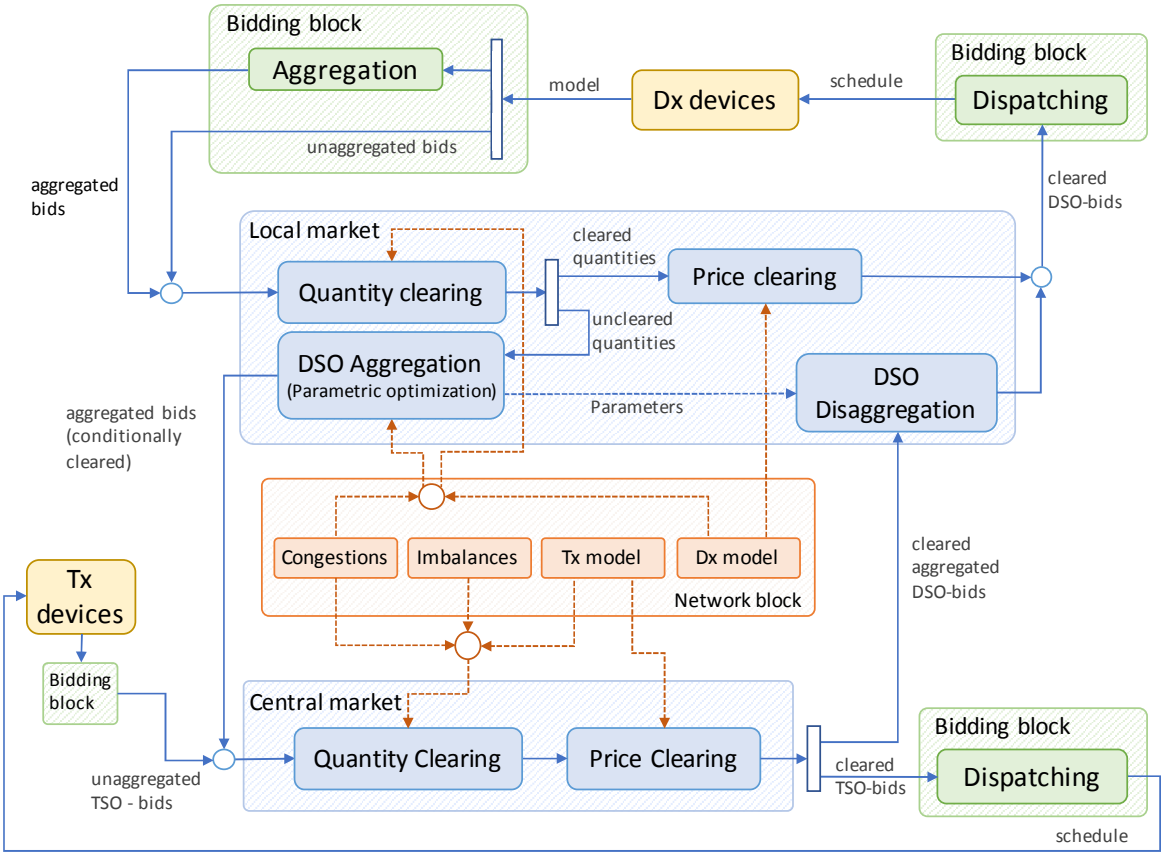

Figure 6-6 Block-diagram representing the Local AS market

- **Market:** In the market layer, the sequence of performed actions in this scheme is the following, as indicated in *Figure **6-7***:
  1. TSO and DSOs send the forecast grid state, per market time step, to their respective market operator before the GCT: this includes forecast net nodal power injection over their respective grids, operational limits, grid topology and scheduled/agreed flow at the borders
  2. Flexibility Service Providers (FSPs) send bids coming from transmission grid connected resources to the TSO MO, at transmission grid nodal resolution, and bids from distribution grid connected resources to the DSO MO, at distribution grid nodal resolution
  3. Each DSO MO runs a "pure" power flow (i.e. without having any bids at disposal) on its subnetwork and checks the presence of over- under-voltages or line congestions. In case any congestions are experienced, the available bids at this subnetwork are then considered in the

computation and the local market clearing (i.e. optimal power flow) is performed in terms of quantities.

Maximize SW

Subject to:

- Nodal active and reactive power balance at Dx level
- Bids constraints
- Operational constraints (line capacities and voltage limits) at Dx level
- Avoid unnecessary activations
- **keep the forecast flow at the HV-MV transformer unchanged** (i.e. imbalance is not changed by the local market action)

Accepted bid quantities that are used to solve those congestions and their corresponding activation costs are stored by the DSO MO for further use. At the same time, forecast net nodal power injection of DSO nodes is updated

4. Each DSO MO "smartly" aggregates remaining local market bids into one aggregated bid. The details of this aggregation are discussed in section 6.3
5. This aggregated bid is submitted to the TSO MO, before gate closure time of TSO market (GCT for DSO and TSO markets might, in general, be different)
6. TSO MO runs the market clearing algorithm (same as in CS A), i.e. computes accepted bid quantities and nodal marginal prices, having at his disposal all TSO bids together with the aggregated bid coming from the DSOs
7. The MO transmits market results to the TSO
8. The MO dispatches the activated bids of TSO FSPs and DSO MO
9. DSO MO performs the disaggregation of activated DSO bids, by running again the market clearing with a power profile at the HV-MV connection aligned with the activation of the DSO bid required by the TSO.
10. DSO MO transmits market results to the DSO
11. Finally, DSO MO dispatches the corresponding FSPs

The temporal sequence diagram of the actions performed in this scheme, together with the main actors involved, is shown in Figure 6-7.

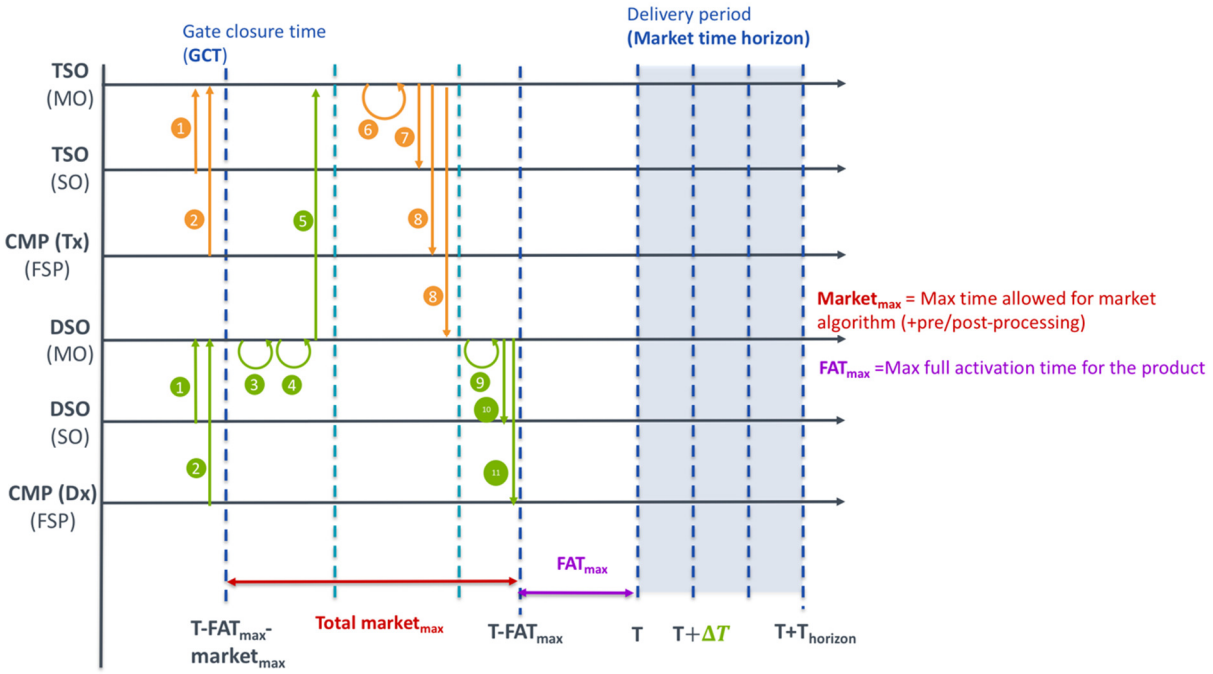

Figure 6-7: Temporal sequence diagram for CS B

The results of market clearing, in terms of nodal prices, accepted bid quantities and active power flows on transmission and distribution edges, are shown in Figure 6-8.

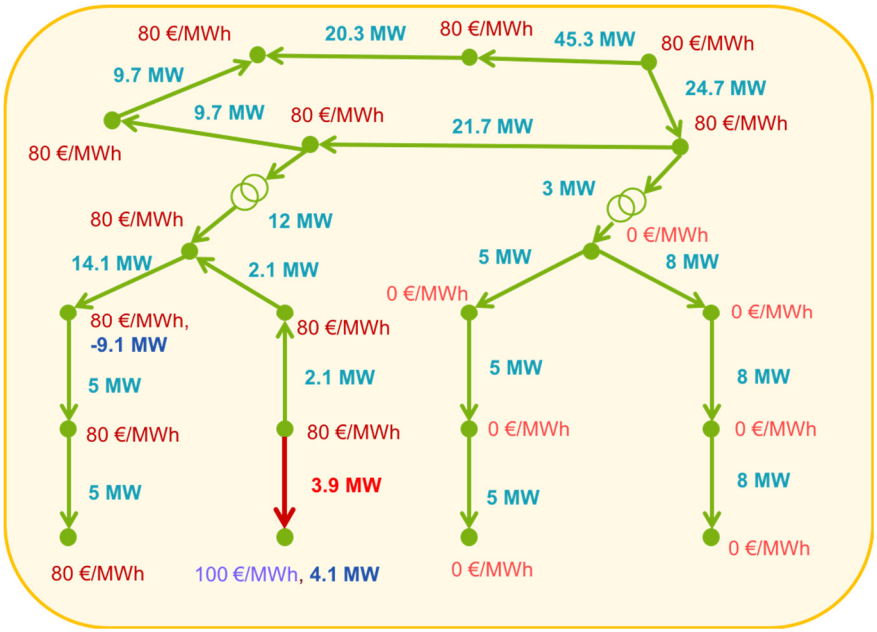

Figure 6-8: Market clearing results for CS B

It can be observed in this scheme that the flow on the branch with limited capacity of 4 MVA in Dx1 is just at the limit (reactive power flows are not displayed in the figure). Consequently, the downstream node of this branch constitutes a separate hub with respect to the rest of the distribution network and thus gets a different

price, in this case equal to the marginal price of the bid offered at this node (bid 17). The acceptance of bid 17 is necessary to solve the congestion at Dx1, whereas in the TSO market clearing problem bid 12 is accepted as the cheapest among downward bids. However, even if the price of this bid is 200 €/MWh, the cleared prices at the other nodes in Dx1 and in all TSO network is 80 €/MWh. This is due to the fact that an algorithm is introduced to avoid any unnecessary activation (see section 5.2.4): in this case, the price of downward bids in Dx 1 are modified to avoid any match between FSP, that's why the bid price is modified from 200 to 80, such that there is no trade in the local market clearing between bid 12 and bid 16 (upward bid at 80€/MWh). Also, all the nodal prices are set to 0€/MWh in Dx2, because no bid is activated in that distribution grid, and so the prices can not be properly determined.

6.2.3 CS C - Shared Balancing Responsibility

The block diagram representing this coordination scheme is shown in Figure 6-9. In this scheme, DSO and TSO solve their own congestion and imbalance problems using the devices connected to their own networks. However, additional constraints on Dx and Tx are used to schedule profiles of power exchange between Dx and Tx at connecting (HV-MV) nodes. These profiles are generated prior to any optimization using forecasts of power injection at each node of the network.

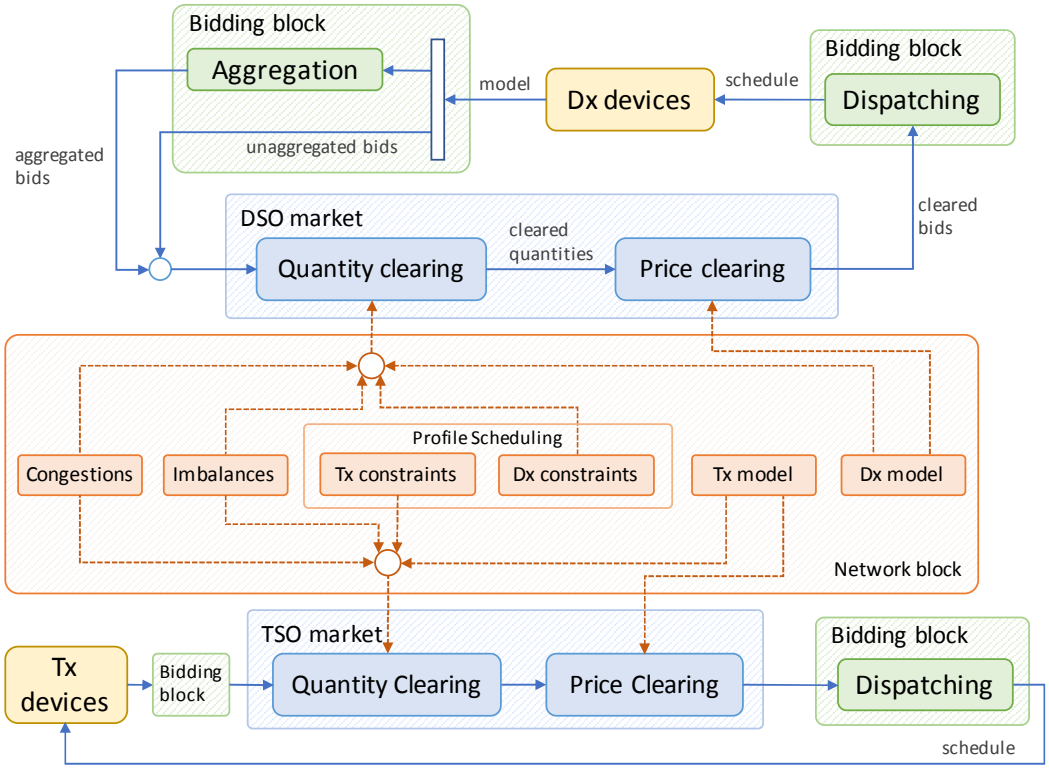

Figure 6-9 Block-diagram representing the shared balancing responsibility model.

In the market layer, the sequence of performed actions in this scheme is the following, as described in Figure 6-10:

1. TSO and DSO agree upfront in defining a schedule for the exchange of power at each primary substation (HV-MV connecting edge)
2. TSO and DSOs send the forecast grid state, per market time step, to the TSO and DSO market operator, respectively, before the GCT: this includes forecast net nodal power injection, operational limits, grid topology and scheduled/agreed flow at the borders
3. Flexibility Service Providers (FSPs) send bids coming from transmission grid connected resources to the TSO MO, at transmission grid nodal resolution, and bids from distribution grid connected resources to the DSO MO, at distribution grid nodal resolution
4. TSO MO and DSO MO run their market clearing algorithms, i.e. compute accepted bid quantities and nodal marginal prices. In detail, the mathematical formulation of the optimization problem for CS C is, for each MO, the following:

   Maximize SW

   Subject to:

   - Nodal active power balance (at MO level)
   - Nodal reactive power balance (only applicable to DSO MO)
   - Bids constraints
   - Operational constraints (line capacities, and voltage limits for DSO MO) at MO level
   - Respect the agreed schedule at HV-MW connecting edge
   - Avoid unnecessary activations

5. TSO MO and DSO MO transmit market results to the TSO
6. Finally, TSO MO and DSO MO dispatch the activated bids from FSPs

The temporal sequence diagram of the actions performed in this scheme, together with the main actors involved, is shown in Figure 6-10.

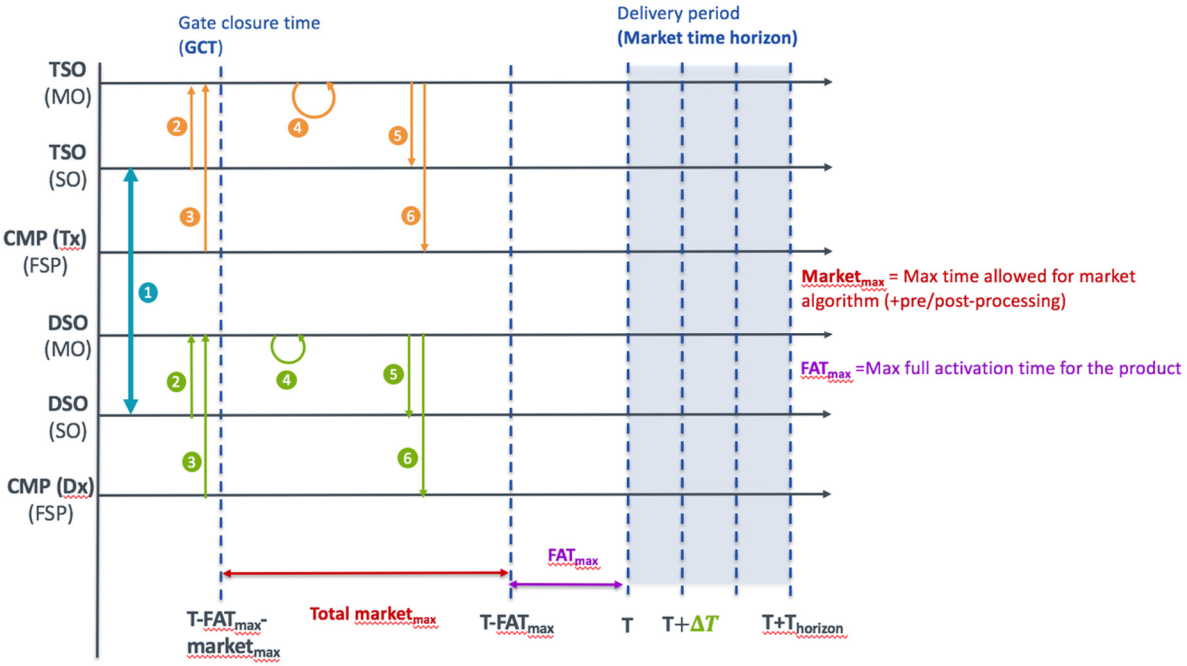

Figure 6-10: Temporal sequence diagram for CS C

The results of market clearing, in terms of nodal prices, accepted bid quantities and active power flows on transmission and distribution edges, are shown in Figure 6-11, considering a scheduled flow of 5 MW from the Tx to each Dx.

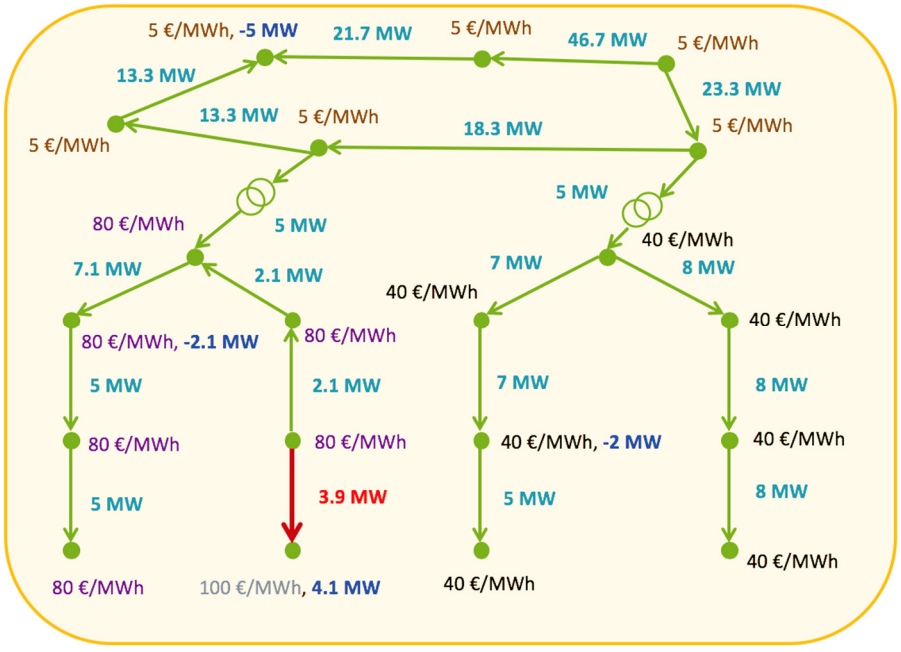

Figure 6-11: Market clearing results for CS C

Due to the fact that each system operator is only entitled to use the flexible resources connected to his own network, it can be observed that (at least) one bid for each subnetwork (Tx, Dx1 and Dx2) is activated. Moreover, for the subnetworks where no congestion is observed, the prices at all nodes are equal to the marginal price of the bids accepted in the subnetwork itself. As already noticed in CS_B, the downstream node of the limiting edge on Dx1 constitutes a separate hub with the rest of the subnetwork and, in this scheme, its clearing price is equal to the marginal price of the bid accepted at this node.

6.2.4 CS D1 - Common Centralized TSO-DSO AS Market

The block diagram representing this coordination scheme is shown in Figure 6-12. Similar to the centralized AS market scheme, in this setup a common market clears the bids from all devices in the network, in order to solve imbalance and congestion problems in both Tx and Dx.

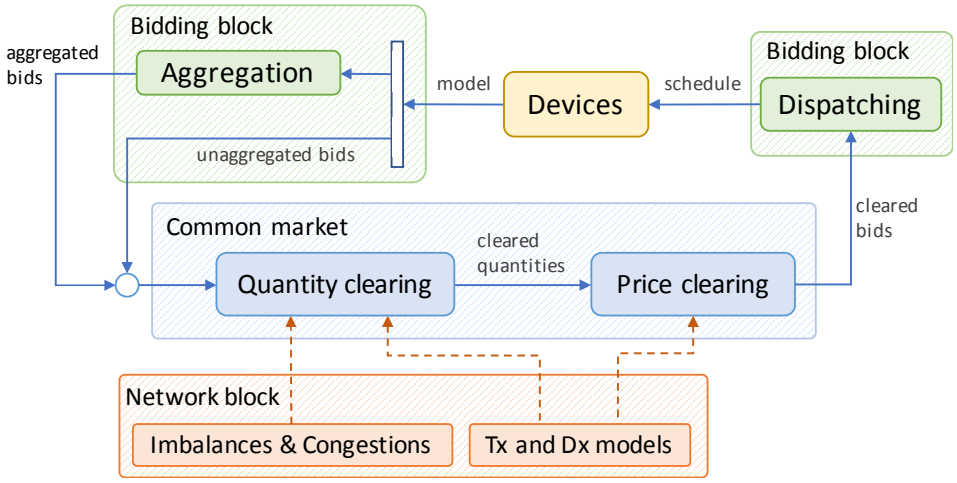

Figure 6-12 Block-diagram representing the common TSO-DSO AS market (centralized).

In the market layer, the sequence of performed actions in this scheme is the following (see Figure 6-13):

1. TSO and DSOs send their forecast grid state, per market time step, to the common MO appointed by TSO and DSOs , respectively, before GCT: this includes forecast net nodal power injection (sum of generated power minus sum of withdrawn power at each node), operational limits, grid topology and scheduled/agreed flow at the borders
2. Flexibility Service Providers (FSPs) send bids coming from both transmission grid connected resources and distribution grid connected resources to the MO, at nodal resolution.
3. The MO runs the market clearing algorithm, i.e. computes accepted bid quantities and nodal marginal prices. In detail, the mathematical formulation of the optimization problem for CS D1 is the following:

Maximize SW[19]

Subject to:

- Nodal active power balance (at Tx level and Dx level)
- Nodal reactive power balance (at Dx level)
- Bids constraints
- Operational constraints (line capacities and voltage limits) at Tx and Dx level
- Avoid unnecessary activations

4. The MO transmits market results to the TSO and DSOs
5. The MO dispatches the corresponding FSPs

The temporal sequence diagram of the actions performed in this scheme, together with the main actors involved, is shown in Figure 6-13.

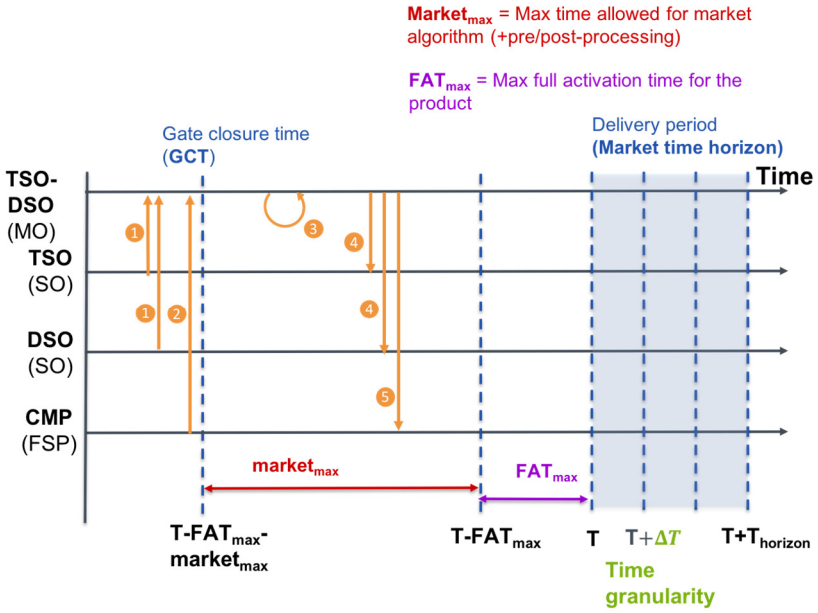

Figure 6-13: Temporal sequence diagram for CS D1

The results of market clearing, in terms of nodal prices, accepted bid quantities and active power flows on transmission and distribution edges, are shown in *Figure **6-14***.

[19] This includes both TSO and DSOs

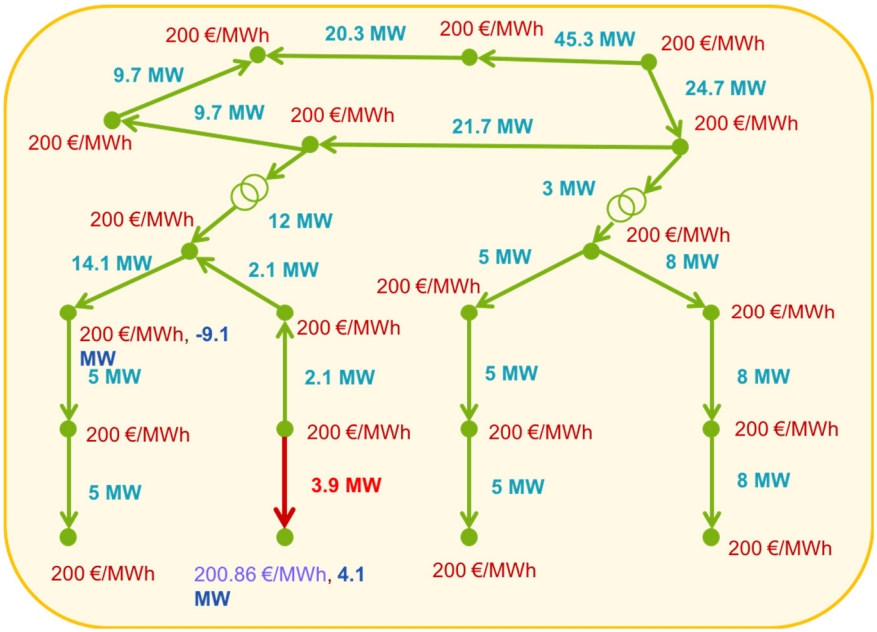

Figure 6-14: Market clearing results for CS D1

This scheme is the one where the flexibility offered at any voltage level is fully taken into account in the clearing algorithm launched by the MO. If none of the element in the complete network is at its limit, the nodal prices would be equal to the price of the marginal accepted bid. This is almost the case for our example, since the only congestion is observed in the critical branch of Dx1, for which bid 17 is used to solve the congestion. The nodal price is slightly higher than 200€/MWh, because, to avoid unnecessary activations, all bids providing upwards flexibility have been modified (set at a price slightly higher than 200, but preserving the merit order, as described in section 5.2.4) to avoid the trades between FSPs. In the rest of the network, nodal marginal prices are all equal to the marginal cost of bid 12.

6.2.5 CS D2 - Common Decentralized TSO-DSO AS Market

The block diagram representing this coordination scheme is shown in Figure 6-15. The blocks are organized in a setting similar to local AS market scheme. However, there exists only one market for DSO and TSO: the common market. In this scheme, the DSO block performs the conditional clearing using a method such as parametric optimization, without clearing any bids in order to solve the local congestion problems. Therefore, the common market is responsible to solve the imbalance and congestion problems in one clearing. Similar to local AS market scheme, a DSO disaggregation is used for post-processing of cleared aggregated DSO-bids.

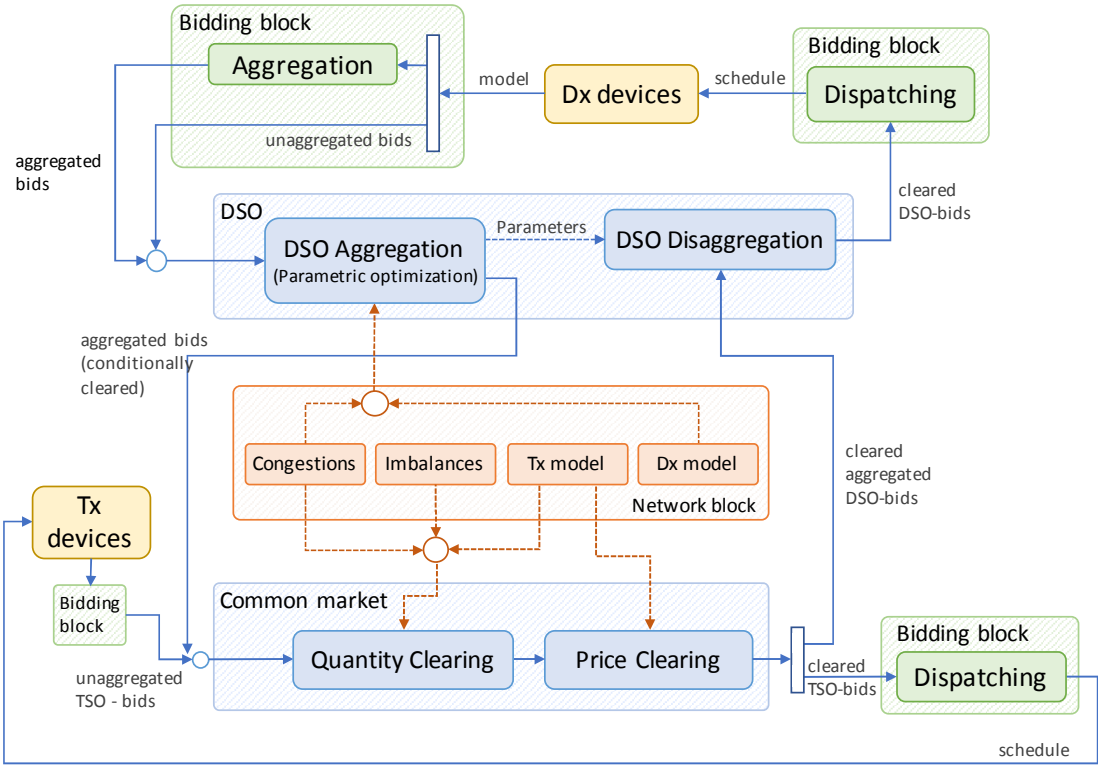

Figure 6-15 Block-diagram representing the common TSO-DSO AS market (decentralized).

In the market layer, the steps of this CS are the same as in CS B, despite the fact that congestions at the DSO level are not tackled beforehand, i.e. step 3 is missing. The results of market clearing, in terms of nodal prices, accepted bid quantities and active power flows on transmission and distribution edges, are shown in Figure 6-16.

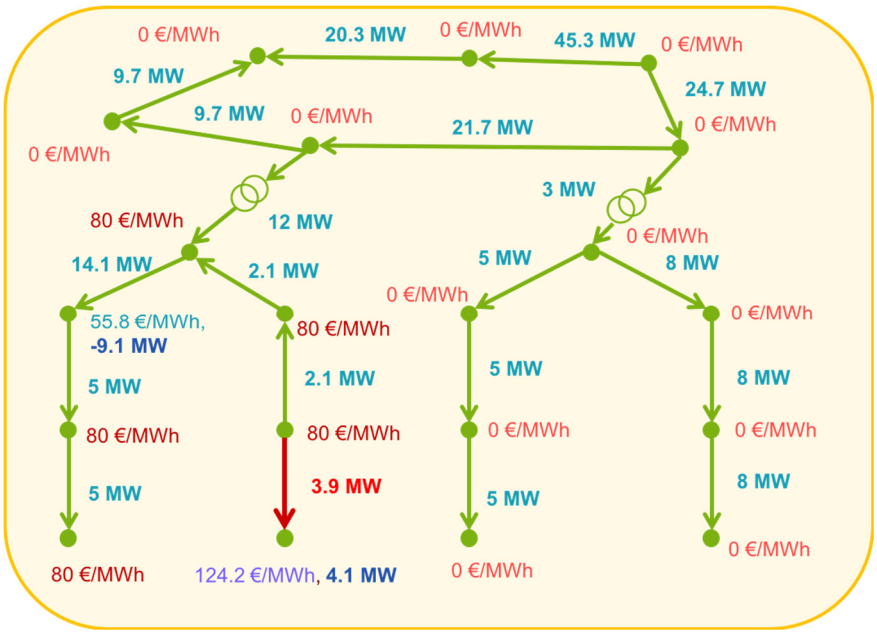

Figure 6-16: Market clearing results for CS D2

Given the strict link between schemes B and D2, it is not surprising that accepted quantities and, consequently, edge flows are the same in both cases. In our network example, the only difference lies in the prices of Tx and Dx1 grids, which are different due to the fact the bid 12 and 17 are used to solve the congestion at Dx1. However, since no bids are activated in those subnetworks, the nodal prices at all nodes are equal to zero.

6.3 Bidding from Local Markets to Central Market: Parametric Optimization

If a decentralized market architecture is used and if the local market operators (DSOs) have to transfer the (additional) flexibility, offered by DERs or by aggregators, from the local market to the central AS market, a methodology is needed on how the DSO would perform this task. In the framework of the coordination schemes, such DSO aggregation is needed in two models: Local AS market (CS B) and Common Decentralized TSO-DSO AS market (CS D2).

The DSO receives bids from DERs (aggregated or not) on the local market and is responsible to cluster them and submit one aggregated bid to the TSO market. However, a main difference with respect to commercial aggregators is that DSO needs to perform this aggregation under the condition that the distribution network constraints (such as line congestions and voltage limits) are not violated. One way to solve this aggregation problem is through parametric local market clearing. The algorithm used for the realization of such clustering and aggregation is discussed hereunder.

If no "smart" aggregation is performed, all the available flexibility at the DSO disposal would be offered to the central AS market. Conversely, considering all bids sent to the local market, the parametric local market clearing method consists in solving the local market clearing for different flexibility demands $\Delta \mathrm{P_i}$ at the HV-MV interface edge between the distribution grid and the transmission grid. $\Delta \mathrm{P_i}$ is the exchange of active power with respect to the baseline active power exchange P_{ref} at that HV-MV interface edge and is calculated as follows:

$$\Delta \mathrm{P_i} = \frac{P_{high} - P_{low}}{N_{steps}} \tag{27}$$

The boundaries P_{high} and P_{low} defining the power range on which the parametric optimization is performed are chosen by taking the lowest value between the sum of all bid quantities belonging to the same direction (i.e. upward and downward) and the remaining margin between the line capacity of the interface edge and the baseline P_{ref}. Furthermore, the number of steps N_{steps} in the parametric optimization has been made dependent on the total flexible capacity of each local market, ranging from a minimum of 2 steps to a maximum of 5.

The procedure described in Table 6-3 (derived from [109]) is iterated for each value of $\Delta \mathrm{P_i}$ as long as the local market clearing finds a solution which is compatible with the flexibility offered at the local market and which

satisfies the operational constraints of the distribution grid. For each market clearing, the goal is always to maximize social welfare while satisfying the distribution grid constraints.

<table>
<tr><th>Local AS market</th><th>Common TSO-DSO AS market (decentralized)</th></tr>
<tr><td colspan="2">• Fix the HV-MV power flow equal to $\boldsymbol{P_{ref}} + \Delta\mathbf{P_i}$</td></tr>
<tr><td colspan="2">• Run the market clearing, for which an activation cost $\boldsymbol{C_i}$ is obtained</td></tr>
<tr><td>• Prior to the aggregation step described here, the DSO runs the local market to solve local congestions. Therefore, in this step of parametric local market clearing, there are no local problems to solve</td><td>• Potential local problems are not solved as a prior step. Instead, the DSO aggregates all bids, not only obeying distribution grid constraints but also solving local problems (i.e. local problems are solved at any value of accepted quantity ΔP_i).</td></tr>
<tr><td>• For a demand of 0 MW at the HV-MV node, the cost C_0 is 0 since there is, by definition, no need to activate any flexible assets (no local problems to solve);</td><td>• In this case, the cost for a flexibility demand of 0 MW at the HV-MV node is not zero anymore, it is equal to C_0, which represents the cost to:
○ Solve local problems (e.g. congestion)
○ Correct the change in the balance using local resources such that there is no variation of power at the HV-MV node</td></tr>
<tr><td>• Thus, DSO generates bids at quantity $\Delta\boldsymbol{P_i}$ and at price $\boldsymbol{\lambda_i} = {\boldsymbol{C_i}}/{\Delta\boldsymbol{P_i}}$ [€/MWh]</td><td>• However, the TSO (buyer on the central AS market) would not want to pay a cost C_0 for activating nothing: that is why for a given power exchange ΔP_i, the total (absolute) price of bidding of DSO should be equal to $C_i - C_0$ and thus the bid price corresponding to each quantity ΔP_i will be decreased accordingly (compared to a total cost of C_i). Of course, this effect in bid price will be strongest for small offered quantities while it would be quite diluted for large quantities: $\lambda_i = {(C_i - C_0)}/{\Delta P_i}$ [€/MWh]</td></tr>
<tr><td colspan="2">• DSO submits the aggregated bid</td></tr>
<tr><td colspan="2">• In the next step, TSO clears the central AS market and provides the result to the DSO on the accepted quantity $\Delta\mathbf{P_{cleared}}$ and the clearing price $\boldsymbol{\lambda}_{\mathbf{cleared}}$</td></tr>
<tr><td colspan="2">• The DSO disaggregation step is then straightforward since in the bid-construction step the DSO has solved the local market clearing for each quantity $\Delta\boldsymbol{P_i}$, including $\Delta\boldsymbol{P_{cleared}}$</td></tr>
</table>

Table 6-3 The algorithm for parametric local market clearing

6.4 A game theory perspective

Game theory can be thought as a set of analytical tools that have been developed to enable the quantification of the output of situations of conflict involving rational decision makers, also called agents or players ([110], [111]). On the basis of the operational models described in the previous sections of this chapter (relying on power flow equations, operational constraints and bid constraints), game theory can be used to interpret the output of coordination schemes, capturing the strategic interactions between TSO and DSOs. More precisely, assuming that TSO and DSOs interact strategically, we interpret such strategic interactions using three coordination schemes (CS) that will be described below. Each of these CSes is modelled relying on parameterized optimization. The outcomes of each model corresponding to a CS is analyzed mathematically using game theory. The mathematical analysis of each CS is based on solution concepts derived from the notion of equilibrium ([110], [111]).

A simulator of TSO-DSO interactions over large-scale transmission and distribution networks, allowing nodes to provide complex bids for their flexibility activations, has been developed within SmartNet. The simulator outcome is not amenable to any analytical interpretation of the results; contrary to this section and the companion paper , in which we provide analytical conditions for the existence and uniqueness of coordination schemes outcomes and quantify for each coordination scheme the profitability, efficiency and reserve activation levels, under full and imperfect information, on a simplified instance. To that extent, our work can be seen as complementary.

6.4.1 From centralized to decentralized market designs

The need to integrate an increasing share of variable and unpredictable energy sources (such as wind and solar photovoltaic power) and the development of DERs is shifting the classical centralized market design to new market designs involving more decentralization and less communication between agents. In decentralized systems, operations/computations are performed in local markets (involving DSOs, generators and consumers) and the information based on local optimization problem output (accepted bid, prices) is shared only locally, generally in the form of messages exchanged between agents belonging to the same local market/energy community ([112], [113]). Two categories of decentralized market designs emerge: hierarchical and distributed market designs.

The first category, hierarchical design, involves agents in local markets (DSOs, generators and consumers) which perform operations/computations independently and simultaneously (e.g. run local market) and interact with other agents, known as centralized controllers, at a higher level in the hierarchical structure [113] or at lower level in the hierarchical structure (TSO or independent Market Operator, [112]). Such a hierarchical interaction can be backwards in Stackelberg game settings (leader-follower type models) under the assumption that the leaders (DSOs in the context of SmartNet) anticipate the rational reaction of the followers

(TSO in the context of SmartNet). In that case, the leaders incorporate explicitly in their optimization problems, the rational reaction functions of the followers. The closed form expression of these latter is obtained by solving first the followers (TSO)' optimization problems at the lower level of the Stackelberg game, considering as fixed the decision variables of the leaders. The leaders (DSOs), at the upper level, then incorporate the followers' rational reaction functions, expressed as functions in the leaders' decision variables only, directly in their optimization problems, therefore proceeding backwards. Alternatively, the hierarchical interaction can be forwards in case of decentralized control algorithms, assuming that a centralized controller coordinates the outputs of the local optimization problems based on the locally reported information.

The second category encompasses distributed designs where each agent communicates with its neighbors, but there is no centralized controller. This latter design is classically used to model peer-to-peer interactions in communication networks or markets involving local energy communities.

Decentralized market designs are needed because:

- Contracting DER-based generation in a centralized market may complicate market clearing procedures due to the amount and complexity of the bids and the associated coordination requirements and incentives of market participants. Typically, in the centralized co-optimization problem, an independent market operator solves a social welfare maximization problem under transmission and distribution network constraints. The resulting optimum determines the TSO and DSOs' decisions, which requires that TSO and DSOs align their own decisions with the ones implemented through the social welfare optimum that does not necessarily coincide with a Nash equilibrium (enabling them to maximize selfishly their own utility). Of course, the centralized co-optimization problem captures an ideal situation in which all the information and decisions are centralized by an independent market operator. In the rest of this section, it will be interpreted as a benchmark leading to the highest possible social welfare. All the other CSes involving various degrees of decentralization lead to some loss of efficiency, i.e., lower values for the social welfare.
- Centralized designs require that all the information is accessible to and shared with the coordinator (TSO or independent market operator), which creates communication challenges and may be impossible due to data privacy constraints.
- Centralized designs require solving large-scale mixed integer optimization problems, which creates heavy computational challenges.

Game theory is the appropriate approach to model and solve decentralized market designs that involve:

- Rational agents which have conflicting interests, captured through their utility functions (such as profit or cost functions, measured in euros) or shared variables appearing in their feasibility sets.
- Strategic agents that take into account the knowledge and anticipation that they have about the other agents' behaviors.

- Agents which have market power, meaning that their actions have an impact on the market price.

The benchmark situation as the one introduced in section 3.1 is studied as a centralized co-optimization problem. As soon as decentralization is introduced, TSO and DSOs have the possibility to play on the activated flexibility to selfishly maximize their profits (impacting a fortiori the prices in the distribution nodes). The goal of this section is to quantify mathematically the loss of efficiency that strategic interactions between TSO and DSOs can generate compared to the ideal (but not realistic) benchmark. Such results could be used by regulators to assess the efficiency loss generated by decentralization versus centralized fully integrated mechanisms and enable them to enforce economic mechanisms (relying on penalty, taxes, compensations, etc.) to correct theses efficiency losses.

Games can then be classified depending on ([110], [111]):

- The type of relation between the agents (cooperative versus non-cooperative behavior).
- The timing (simultaneous versus sequential).
- The information that is available to each agent (perfect information versus imperfect and incomplete versus incomplete information).

6.4.2 Equilibrium modeling of TSO-DSO coordination schemes

To assess how game theory can be used for TSO-DSO coordination scheme modeling, we formulate three coordination schemes (CS) between the DSOs and TSO in a game theoretic setting. Note that this setting may require to extrapolate from the initial definition of the coordination schemes introduced in the SmartNet project.

1. The first one is a co-optimization problem where DSOs and TSO are considered as belonging to a coalition operated by an independent market operator which activates jointly resources connected at the transmission and distribution grid levels. The co-optimization problem coincides with the centralized common TSO-DSO AS market. It will be used as a benchmark to assess the efficiency loss introduced by the two other decentralized coordination schemes.
2. The second one is based on a game theoretic interpretation of the shared balancing responsibility scheme. The CS is formulated in a game theoretic framework. Game theory is used to analyze the outcome of the CS (in terms of equilibrium). To model this CS, we rely on a parametrized optimization approach which is rigorously described in [112]. We approach this second scheme as a simultaneous non-cooperative game, whereby we assume 'bounded rationality' on behalf of the TSO and DSO. Under 'bounded rationality', DSO and TSO determine the reserve to activate on their networks simultaneously.
3. The last one, inspired from the local market coordination scheme [113], involves 'rational expectation' from the DSOs, which anticipate the clearing of the global market by the TSO. We

approach this last scheme as a sequential Stackelberg game, assuming DSOs with 'rational expectations' on the reaction of the TSO. In the first stage of the sequential Stackelberg game, each DSO anticipates the future reaction of the follower (TSO) (which will play in the second stage) when determining the reserves to activate on its network and sends a signal based on this activation to the TSO, which reacts optimally in the second stage.

In Table 6-4, we list the coordination schemes that we have reformulated as equilibrium models and specify the associated solution concepts to quantify mathematically their outputs. The generic framework we use for the second and third coordination schemes mentioned in the table below, is that of a strategic form game with chance moves ([111], [112]) which is classical in extensive-form and dynamic games literature. To be more precise, under such a setting, the game incorporates a chance move capturing the random aspects (Nature's moves) in the model, with possible alternatives for Nature being $\omega \in \Omega$. At the beginning of the game, Nature picks a state defined by a realization of the uncertain demand disturbances at transmission nodes and real time imbalances at distribution and interface nodes. Note that the game theoretic structure for the decentralized schemes comes from the coupling of the TSO and DSO optimization problems through interface nodes [103].

Table 6-4 - Interpretation of the coordination schemes in a game-theoretic framework.

TSO-DSO coordination scheme	Class of mathematical problem	Coupling	Solution concepts
Centralized co-optimization problem Smartnet schemes A and D1	Standard constrained optimization problem	Independent Market Operator has full control	Social welfare optimum
Shared balancing responsibility Smartnet scheme C	Non-cooperative game with bounded rational agents	Interface nodes	Generalized Nash equilibrium
Local markets Smartnet scheme B	Stackelberg game with DSOs having rational expectation on the TSO behavior	Interface nodes	Subgame Perfect (generalized) Nash equilibrium

The generic framework for the second and third coordination scheme is that of a strategic form game with chance moves introduced in ([111], [112]) . The game incorporates a chance move, with possible alternatives for Nature being $\omega \in \Omega$. At the beginning of the game, Nature picks a state defined by a realization of the uncertain demand disturbances at transmission nodes and real time imbalances at distribution and interface nodes. The detailed mathematical formulation of each of these schemes can be found in [103].

For the sake of simplicity, in what follows, we will denote $uTSO \in UTSO$ the (vector of the) decision variables of the TSO and $uDSO \in UDSO$ the (vector of the) decision variables of the DSO. We let $x \in X$ be the state of the system. In control theory, state variables are used to represent the states of a general system. The set of possible combinations of state variable values is called the state space of the system.

The utility function (profit or cost functions, measured in euros) JTSO: UTSO →ℝ for the TSO and JDSO: UDSO → ℝ, captures the system operators' total activation costs on transmission and distribution networks respectively. We also introduce the social welfare, SW(uTSO, uDSO), as the sum of the TSO and DSO utilities and consumer surplus.

Our game-theoretic setting is inspired from the operational model used as basis for SmartNet coordination scheme simulation platform, that we reformulate in the framework of Basar and Olsder [111]. Adopting system theory terminology, we differentiate the variables into two categories: we call x the (full) state of the game, while uTSO, uDSO are the TSO and DSO's decision variables. The TSO optimizes the reserve activation at each transmission node. The DSO optimizes the reserve activation, reaction power injection/consumption, and voltage at each distribution node. The (full) state variable x contains state variable characterizing the TSO (real power flow over transmission lines) and state variables characterizing the DSO (real and reactive power flows, current magnitude on each distribution line).

We prove in [103] that it is possible to express the state x as a closed form expression in the DSO and TSO decision variables, i.e., that there exists a function Ψ(.) such that x = Ψ(uTSO, uDSO). In particular, the power flows over transmission lines can be expressed as a linear matrix equation in the TSO and DSO's decision variables. The real and reactive power flows over distribution lines can be formulated as linear functions in the DSO's decision variables. The current magnitude over distribution lines is a linear function in the DSO's decision variables. The bus angles at transmission nodes can be obtained as a linear function in the TSO and DSO's decision variables. This framework is mandatory for the introduction of more complex information structures capturing TSO-DSO interactions, like the one involved in Stackelberg games for local markets. Also, such a mapping enables us to solve more efficiently large-scale parameterized optimization problems.

We introduce the feasibility set of agent a in A: $\mathbb{FS}_a(u_{a'}) := \{ u_a \in U_a \mid C_a(u_a,u_{a'}) \leq 0 \}$ where $C_a(.)$ describe agent a constraints, a, a' ∈{TSO,DSO}, a ≠a'. We let $\mathbb{FS}_{TSO}(u_{DSO})$ and $\mathbb{FS}_{DSO}(u_{TSO})$ be the feasibility sets of the TSO and DSO optimization problems, where the state has been replaced with its closed form expression in u_{TSO}, u_{DSO}. These feasibility sets are made of operational constraints and power flow equations, and contain decision variables from both the TSO and the DSO.

We now detail the generic formulation of the three coordination schemes introduced at the beginning of the section and recalled in Table 6-4 : (i) centralized co-optimization problem, (ii) shared balancing responsibility, (iii) local markets

6.4.3 Centralized co-optimization problem

This is the benchmark model. It can be formulated as a standard constrained optimization problem. The DSO/TSO entity (independent market operator) maximizes the social welfare by activating resources from the transmission and distribution grids, taking into account operational constraints and power flow equations occurring in each of these networks. Drawbacks of centralized design is that it may create computational and communication challenges due to the size of the problem (number of decision variables) and the requirements for the TSO to access all the information.

The output solution concept relies on standard (social welfare) optimum. The mathematical optimization problem is captured in Figure 6-17 .

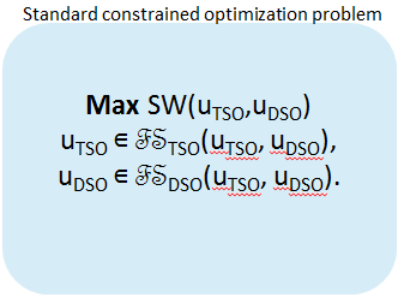

Figure 6-17 Centralized co-optimization problem formulation.

6.4.4 Shared balancing responsibility

In this scheme, we assume 'bounded rationality' of the TSO and DSOs, which act simultaneously. In practice, the TSO minimizes its activation cost by activating resources on its transmission network, taking as input the activation performed by the DSO, under a set of constraints on the transmission network, both operational and resulting from power flow equations. Simultaneously and independently, the DSO minimizes its activation cost by activating resources on its distribution network, taking as input the activation performed by the TSO, under a set of constraints on the distribution network, both operational and resulting from power flow equations. Note that these two optimization problems are coupled because transmission and distribution grids are coupled through interface nodes, which implies that the state variable, x, depends on TSO and DSO decision variables. Since x appears in both system operators' feasible sets, the optimization problems are coupled.

In this interpretation of the shared balancing responsibility scheme, we do not assume that TSO and DSO agree a priori on a scheduled exchange of power at their interface nodes. In contrast, each agent (TSO and DSO) acts selfishly, determining the reserve activation which minimizes its own activation cost while checking feasibility constraints. The output of the non-cooperative game determines the scheduled exchange of power at the interface nodes. As mentioned previously, the assumptions of section 3.1 do not hold in this section (except for the centralized co-optimization problem interpreted as an ideal benchmark). The goal of this section is to quantify the efficiency loss caused by decentralized (and strategic behaviors).

The output solution concept is that of Generalized Nash equilibrium (GNE), each agent's strategy set being dependent on the other agents' strategies through shared decision variables. The shared balancing responsibility CS interpreted in a game theoretic framework is formulated as parametrized optimization problems in Figure 6-18.

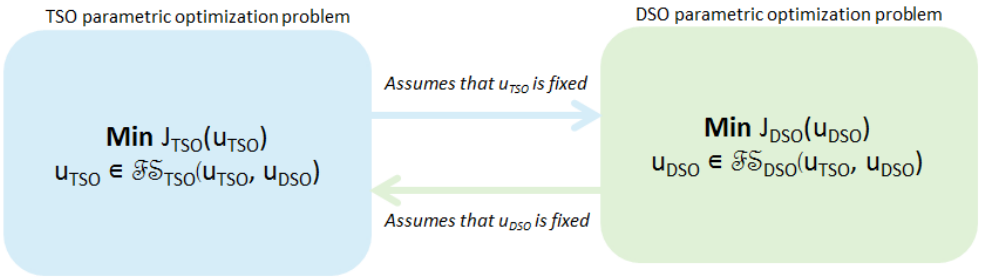

Figure 6-18 Shared balancing responsibility game formulation.

A strategy profile (u_{TSO}^*, u_{DSO}^*) is a Generalized Nash equilibrium if no player has an incentive to deviate unilaterally from its strategy u_a^* when the other agent still plays $u_{a'}$*, for any a, a' $\in A$, a $\neq a'$. Graphically, (Generalized) Nash equilibrium are obtained at the intersections of Best Response (reaction) functions of the TSO and DSO [110]. In Figure 6-19, we have represented a (Generalized) Nash equilibrium (GNE) as a pink dot obtained at the intersection of the DSO (in green) and TSO (in blue) Best Response functions. The pink dot coincides with the shared balancing responsibility Generalized Nash equilibrium outcome. In our shared balancing responsibility game, equilibrium always exist; they are unique under some conditions on the game parameter values [112].

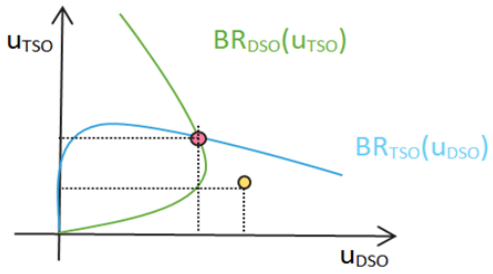

Figure 6-19 Equilibrium (pink dot) obtained at the intersection of Best Response functions. Yellow dot coincides with the outcome of the two decoupled optimization problems when DSO and TSO agree on a joint activation schedule.

In contrast, the yellow dot coincides with an optimum in u_{DSO} and u_{TSO} obtained as output of the shared balancing responsibility problem when DSO and TSO agrees on a predetermined joint schedule. In general, pink and yellow dots do not coincide.

6.4.5 Local markets

In this coordination scheme we assume that there are separate local markets managed by the DSOs. Resources from the DSO grids can only be offered to the TSO after the DSOs have selected resources needed to solve local imbalances within their periphery. The TSO is responsible for the operation of its own balancing market, where both resources from the transmission grid and resources from the distribution grids can participate. This third coordination scheme can be interpreted as sequential game involving the TSO and DSOs. We model the coordination scheme as a Stackelberg game with multiple leaders (DSOs) and one follower (TSO). This modeling requires to assume 'rational expectation' from the DSOs, a concept which is not introduced explicitely in SmartNet coordination scheme description. Stackelberg games are generally formulated as Bilevel mathematical programming problems (BLPPs, [111], [113]) . BLPPs are hierarchical optimization problems combining decisions of two decision makers, the so-called leader and the so-called follower. The leader acts first, and the follower reacts optimally on the action of the leader ([111], [113]). The goal of the leader is to find such a selection which, together with the response of the follower, minimizes its activation cost ([111], [113]).

We prove in [2] that the DSOs-TSO Stackelberg game can be reformulated as a mathematical program with complementarity constraints (MPCC), replacing the TSO problem with its KKT conditions. The constraints corresponding to the lower-level problem of BLPP provide closed form expressions for the TSO reaction function , which can be expressed as a parametric function of the DSOs' decision variables. We distinguish between three cases for the TSO's reaction function closed form expression [112]. The analytical derivations are described in more details in [112]. Since we need to compare the outcome of the shared balancing responsibility game and the local markets, we compare both games in terms of solution concepts. More formal details can be found in [112]. To find the optimum for the DSO and TSO in the local markets CS , we have the

same KKT (Karush-Kuhn-Tucker) conditions as in the shared balancing responsibility game except that the gradient of the follower's reaction function is replaced by 0 in two of the three cases derived analytically in [112] and that the constraints corresponding to the lower-level problem of BLPP are replaced by the closed form expression of the TSO optimal decision variable. Applying backward induction to the local market game is similar to applying the concept of dominance, i.e., eliminating sequentially dominated strategies, taking into account sequential rationality. Refinements of GNE which incorporate sequential rationality are called Subgame Perfect Generalized Nash equilibrium [111]. So, a Subgame Perfect Generalized Nash equilibrium is a strategy profile that specifies a Generalized Nash equilibirum in every subgame, i.e., part of the extensive form of the local market game that constitutes itself a well-defined extensive form game ([112], [111]).

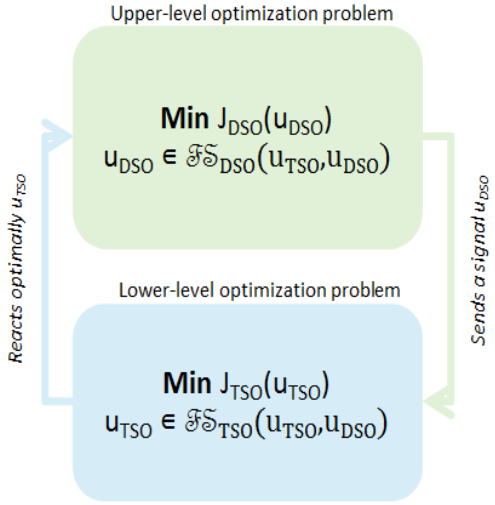

Figure 6-20 - Local market Stackelberg game formulation.

The local markets interpreted in a game theoretic framework is formulated as a BLPP in Figure 6-20.

6.4.6 Numerical comparison of the three coordination schemes on a NICTA inspired stylized network

The three coordination schemes are tested on a meshed transmission network made of three interface nodes numbered from 1 to 3. Each one of these interface nodes is itself the root of a tree capturing a distribution network containing 5 nodes. Operational parameters are calibrated based on a NICTA NESTA test case [112].

We only run tests on this stylized example for different reasons: (a) equilibrium problems are computationally difficult to tackle, (b) we want to provide a preliminary efficiency analysis on each scheme before potentially selecting the ones that should be considered for large scale instances, (c) the assumptions made on the network (meshed transmission network with DC power ow and radial distribution network with SOCP

relaxation) are common and largely used in the literature. We aim at proving concepts and showing how the schemes work in practice in this work. Large scale instances are then not considered here.

The utility of the agents are interpreted as profit, as classical in economics. Detailed expressions can be found in [112]. To make the link with the previous high-level presentation of the three CS, we set: $J_a=-\pi_a$, forall agent a in A. Therefore, at the optimum $\min J_a(u_a)=\max -\pi_a(u_a)$.

In Figure 6-21, we have represented the TSO and DSO utility functions evaluated in each coordination scheme outcome. In red, the utility functions are evaluated in the social welfare optimum obtained as output of the centralized co-optimization problem (i). As proven in [112], there exists a unique solution of the centralized co-optimization problem. In blue, the utility functions are evaluated in the set of GNE solutions of the shared balancing responsibility game (ii). Finally, in green, the utility functions are evaluated in the set of GNE solutions of the local market game (iii) formulated as a bilevel optimization problem. We observe that for the TSO it is more advantageous to behave as a follower when the DSO anticipates its follower resource activation strategy than to compete simultaneously with the TSO through a shared balancing responsibility game. This situation might be interpreted as a last-mover advantage for the TSO [112]. Furthermore, the joint activation of reserves on transmission and distribution grids through co-optimization leads to a lower profit for the TSO than under the two other decentralized coordination schemes.

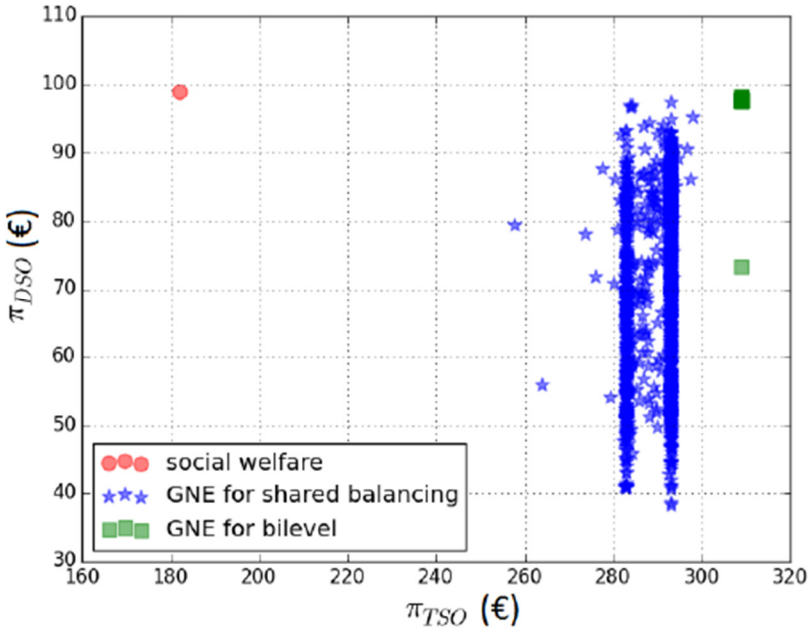

Figure 6-21 - GNE found by a parametrization approach, using random sampling.

It is also possible to compare the three coordination schemes based on other meaningful criteria to assess their relative efficiency, such as social welfare and reserve activation levels. In Figure 6-22, we have represented the TSO reserve activation level, quantified as the sum of the reserves activated on the TSO

network and at the interface nodes, and the DSO reserve activation level, quantified as the sum of the reserves activated on the DSO network, evaluated at the social optimum in red, GNE solutions of the shared balancing responsibility game in blue, and local market in green. For all the coordination schemes, the level of activated reserves is higher on the DSO network than on the TSO network; this can be explained by the fact that in our NICTA NESTA test case, activation costs of DERs are assumed to very low (close to zero because coming from RES based generators) whereas conventional generators' activation costs on the TSO network are quite high. Logically, under co-optimization, the integrated market operator activates a very low amount of reserves on the transmission network and a large quantity of reserves on the distribution network. Furthermore, more reserves are activated on the TSO network under local market coordination scheme than under shared balancing responsibility coordination scheme. This can be interpreted as a by-product of the last-mover advantage for the TSO, which gives rise to higher profitability for the TSO than the shared balancing responsibility game [112]. In Figure 6-23, we have represented the social welfare as function of the total reserve activated by TSO and DSO evaluated in the social optimum in red, GNE solutions of the shared balancing responsibility game in blue and local market in green. We observe that the centralized co-optimization coordination scheme guarantees the highest level of efficiency in terms of resource allocation, giving rise to the highest social welfare with 200 €, followed very closely by the best equilibrium of the shared balancing responsibility game with 199 €. The local market coordination scheme gives rise to a lower social welfare than the centralized co-optimization coordination scheme with values between 147 € and 153 €. However, on average (e.g., with equiprobability of all the equilibria), the local market coordination scheme provides a higher social welfare with an average value of 150 €, than the shared balancing responsibility with 143 €.

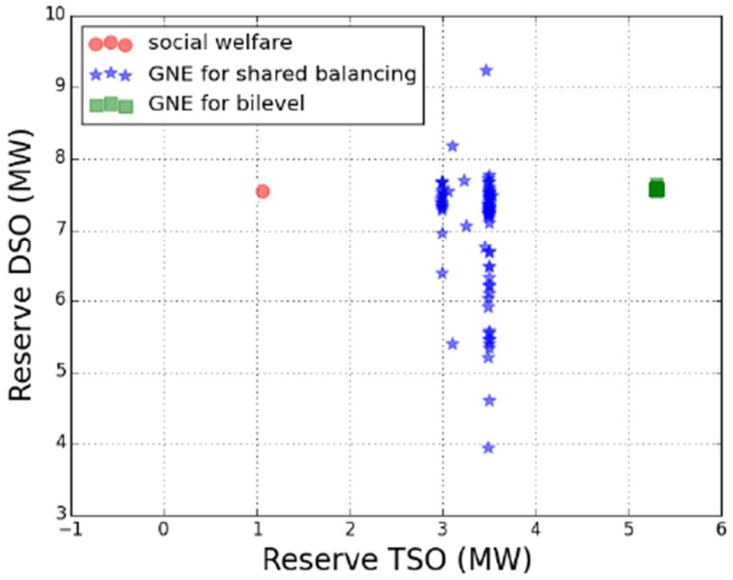

Figure 6-22 - Reserve activation levels measured as the sum of the reserves activated by the TSO and DSO.

Using our test case to assess the relative merits of our three coordination schemes, we summarize their comparison below:

- The local market coordination scheme gives rise to higher profitability for the TSO than the shared balancing responsibility coordination scheme.
- The joint activation of reserves on transmission and distribution networks through co-optimization leads to lower profit for the TSO than under the two other coordination schemes.
- More reserves are activated on the TSO network under local market coordination scheme than under the two other coordination schemes; the centralized co-optimization scheme giving rise to very low amount of reserves activated on the TSO network compared to the activation level on the DSO network.
- The social welfare is the highest when evaluated at the optimum of the centralized co-optimization problem, followed very closely by the highest value of the social welfare evaluated in the GNEs solutions of the shared balancing responsibility game. This means that the shared balancing responsibility game can reach an efficiency level very close to the centralized co-optimization problem, while enabling the introduction of strategic behaviors from the TSO and DSOs.
- The local market coordination scheme leads to a lower level of efficiency than the centralized co-optimization coordination scheme, which can be explained by the last-mover advantage of the TSO.

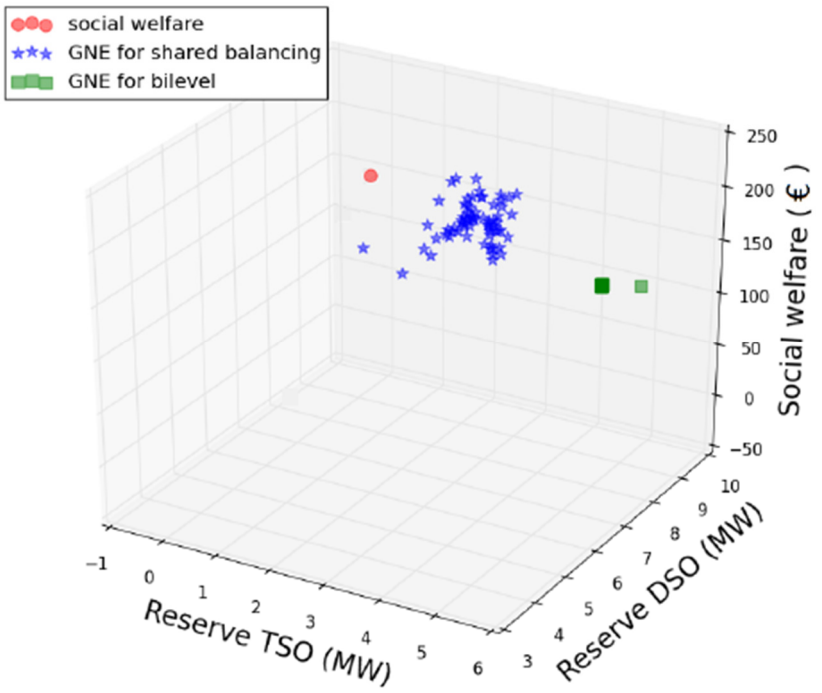

Figure 6-23 - social welfare as function of the total reserve activated by TSO and DSO.

7 Computational Tractability

In this chapter, a rough analysis of the computational tractability of each coordination scheme for the three countries of Denmark, Italy and Spain is analyzed.

Part of the computational complexity is due to the nature of the TSO-DSO coordination scheme, whether it is centralized or not, whether markets are linked (CS B, CS D2) or quite decoupled (CS C), as highlighted in Table 7-1.

Table 7-1 Qualitative assessment of the computational complexity of each TSO-DSO coordination scheme

Centralized AS market	Common TSO-DSO AS market (centralized)	Integrated flexibility market	Local AS market	Common TSO-DSO AS market (decentralized)	Shared balancing responsibility model
The **easiest** since only transmission grid	The **most difficult** since full transmission AND distribution grids in a single problem		Optimizations in parallel BUT with smart aggregation using some complexity		Many optimizations in parallel

Some factors are independent of the TSO-DSO coordination scheme: type of network model, allowed market products (complex one? with or without binary variables?). Other scaling factors/parameters (non exhaustive list) playing a significant role in determining the total computational time of the market clearing algorithm are:

- Size of Tx network
- Number of detailed distribution networks
- Average size per Dx network
- Number of binary variables in bids

Among bid constraints entailing a binary expression, the number of non-curtailable bid segments is the most impactful one. *Table **7-2*** summarizes the above-mentioned parameters for all three examined countries.

Table 7-2: Key parameters affecting computational tractability per country

	DK	IT	ES
Tx nodes	144	3648	1537
Detailed Dx networks	73	155	68
Average number of nodes per detailed Dx network	41	36	35
% non-curtailable bids	56%	45%	50%

In Figure 7-1 - Figure 7-3, the average time spent in each market session per country for all coordination schemes is reported.

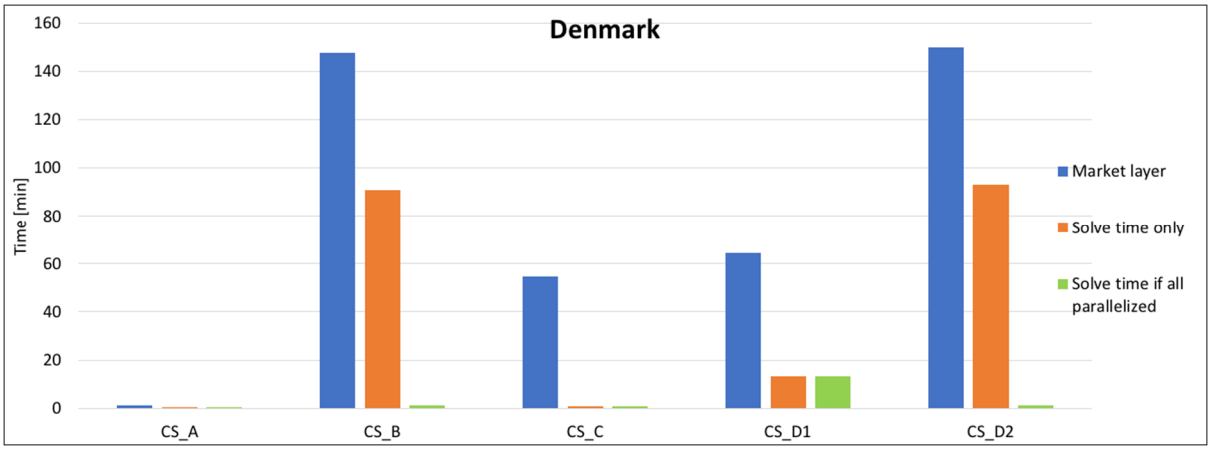

Figure 7-1: Average time complexity for Denmark

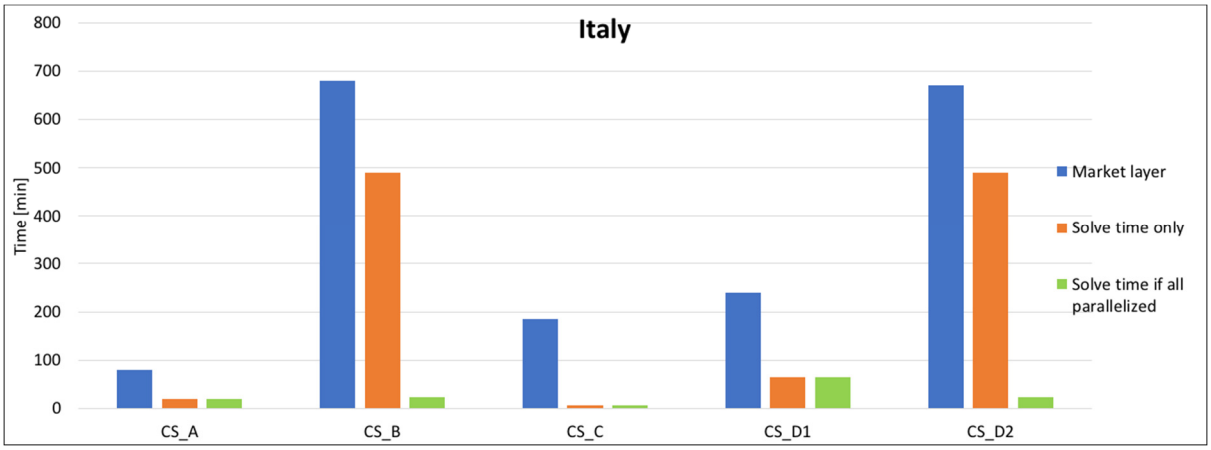

Figure 7-2: Average time complexity for Italy

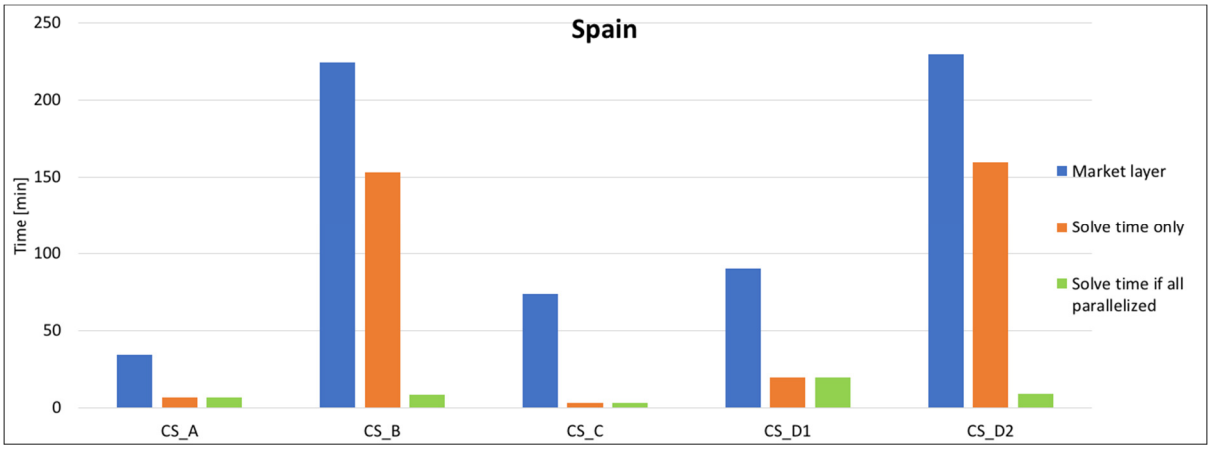

Figure 7-3: Average time complexity for Spain

For each country and each coordination scheme, three values are reported:

- average total time spent in the market layer

- average solve time
- average solve time in case a parallelization mode for the solution of the decentralized schemes would have been implemented.

Besides the solving time, the time spent on each market session is also constituted by two other main processes: writing the optimization problem (by means of one of the modelling languages like AMPL, GAMS etc..) and writing back the results in the database, the first one being the most time consuming. Moreover, it is worth re-emphasizing here that CS B and CS D2 (two of the three decentralized coordination schemes) have been run in a serial mode, i.e. one subnetwork at a time. This is not the case for CS C, where the market clearing of each subnetwork is solved in one shot and therefore the adoption of a parallel solve over different cores of the utilized machine is not too demanding to implement. For each country, the solve time in case of full parallelization has been computed by dividing the total solve time (blue bar) by the number of detailed distribution networks (reported in Table 7-1).

Analyzing the results, it does not surprise that Italy results in being the country for which the market layer, on average, spends the largest amount of time, especially due to the double value of detailed distribution networks and the large number of transmission nodes with respect to the other two. At the other extreme, Danish transmission network is represented by only 144 nodes (about 1/10 of Spain) and, despite being constituted by a larger number of detailed distribution networks and having a larger share of non-curtailable bids, it results in the country being simulated the fastest.

On the other hand, a comparison of the time spent for each coordination scheme clearly points out that, in case of serial run of CS B and CS D2, they result in being, by far, the ones for which the largest amount of time is spent in the market layer. As described in detail in the previous chapter, the parametric optimization peculiar to those two schemes is the main driving factor affecting the computational time. Moreover, as the only different feature between the two schemes lies in a check made on a possible pre-congestion of each distribution grid, the values of both schemes are almost identical.

Finally, if we now look at the solving time in case of full parallelization (green bars), given the complexity of its optimization problem, CS D1 is clearly more demanding (time consuming) than all the other CS. Then, CS B and CS D2, follow in terms of computational requirements, mainly due to the parametric optimization. Whereas the just mentioned conclusions are valid for all three considered countries, a swap between fourth and fifth position is observed for Denmark with respect to Italy and Spain. Before looking at the results, one may think that CS A, as it only entails solving a market clearing problem for one network, would always be the fastest. However, this reasoning is not considering the fact that, whereas the grid is the same, the bids considered in CS A and CS C in the transmission network are different: in CS C only bids coming from transmission network are input to the problem, whereas CS A is taking advantage of all (grouped) bids from distribution networks as well. Consequently, depending on where the largest number of binary constraints in bid formulations are

present, one might have either CS A or CS C as the fastest coordination scheme being solved by the market layer.

8 Conclusions

In this document, we provide the mathematical description of necessary modules which comprise the Integrated Reserve market, namely bidding, network, clearing, and pricing. These components can be arranged and connected in various set ups, in order to adapt the market for a specific coordination scheme between TSO and DSO. The key messages in each part are summarized below.

8.1 Bidding

In Chapter 3 we define a catalogue of market products (bids) and the accompanying constraints which are allowed in the Integrated Reserve market. The bids represent the desire to exchange a quantity of power at a given price. The accompanying constraints are used to impress those physical limitations of flexible resources which cannot be described by the bid itself. We list and formulate logical and temporal constraints which are most relevant to resources available at the moment or in foreseeable future.

8.2 Network

Chapter 4 provides the models of power network, from an optimization-oriented point of view. In addition to the mathematical modeling, several topics such as the trade-off between model complexity and level of detail, identification and estimation of network variables (power flows, voltages, etc.) and cost of modelling errors are discussed. Since integer variables exist within the market clearing constraints, the approaches proposed depend on convex approximations of the power flow physics, which allow to develop a mixed-integer convex model having superior tractability.

It is shown that in some cases, the SOCP BFM DistFlow solution (global optimum) is actually superior to those obtained by local non-convex solvers. Also, the simplified DistFlow formulation offers a high-quality approximation in terms of feasibility and optimality.

8.3 Clearing and Pricing

The mathematical formulation of market clearing and pricing algorithms, which is the core of the optimization problem, is described in Chapter 5. A first key message is that the objective of the market is highly affected by several pre-defined conventions, such as types of bids allowed (simple and complex products), quantity/price convention (whether both positive and negative quantities and prices exist), network model complexity (linearity and convexity), and the type of objective (cost minimization versus welfare maximization). Furthermore, many parameter values can affect both the behavior and the performance of the

clearing algorithm. Some important ones include the duration of time step, the length of prediction horizon, and the frequency of clearing.

In general, the pricing process, which is defined as a dual problem of the quantity clearing, can have the same complexities as the primal problem. However, there are several methods to avoid these complexities and find the locational marginal prices in a more straight-forward and intuitive way. Insights into this topic are provided in Chapter 5.

8.4 Coordination Schemes

Chapter 6 summarizes the structure of market under each TSO-DSO coordination scheme. In this schematic presentation, it is shown how different market modules can be used to create a setup suitable for each coordination scheme. The temporal sequence diagrams are described, and the focus is put on an example comparing the 5 TSO-DSO coordination schemes, as well as the optimization formulation of the different market clearing algorithms. Finally, chapter 7 briefly tackles the question of the computational tractability of the market clearing algorithms.

9 References

[1] European Environment Agency, "Renewable energy sources," Annual Indicator Report Series (AIRS), 2018.

[2] H. Gerard, E. Rivero, and D. Six, "Basic schemes for TSO-DSO coordination and ancillary services provision," SmartNet project, D1.3, 2016.

[3] J. Merino, I. Gómez, E. Turienzo, C. Madina, I. Cobelo, A. Morch, H. Saele, K. Verpoorten, E. R. Puente, S. Haninnen, P. Koponen, C. Evens, N. Helistö, A. Zani, and D. Siface, "Ancillary service provision by RES and DSM connected at distribution level in the future power system," SmartNet Project, D1.1, 2016.

[4] M. Caramanis, E. Ntakou, W. W. Hogan, A. Chakrabortty, and J. Schoene, "Co-Optimization of Power and Reserves in Dynamic T&D Power Markets With Nondispatchable Renewable Generation and Distributed Energy Resources," *Proc. IEEE*, vol. 104, no. 4, pp. 807–836, Apr. 2016.

[5] M. Kohansal and H. Mohsenian-Rad, "A closer look at demand bids in California ISO energy market," *IEEE Trans. Power Syst.*, vol. 31, no. 4, pp. 3330–3331, 2016.

[6] "SmartNet Project - Consultations - Market design," 2016. [Online]. Available: http://smartnet-project.eu/consultations/. [Accessed: 07-Dec-2017].

[7] G. Leclercq, M. Z. Degefa, G. Vigano, and J. Le Baut, "Characterization of flexible resources and distribution networks," SmartNet Project, D1.2, 2017.

[8] T. Brown, S. Newell, D. Oates, and K. Spees, "International Review of Demand Response Mechanisms," no. October, p. 83, 2015.

[9] S. F. Tierney, T. Schatzki, and R. Mukerji, "Uniform-pricing versus pay-as-bid in wholesale electricity markets: does it make a difference?," *New York ISO*, 2008.

[10] European Commission, "COMMISSION REGULATION (EU) 2017/ 2195 - of 23 November 2017 - establishing a guideline on electricity balancing," 2017.

[11] K. Neuhoff, "International Experiences of Nodal Pricing Implementation, Frequently Asked Questions," 2011.

[12] A. Mutanen, "Improving Electricity Distribution System State Estimation with AMR-Based Load Profiles," 2018.

[13] "California Independent System Operator - Part 4, Processes | Energy Central." [Online]. Available:

https://www.energycentral.com/c/pip/california-independent-system-operator-part-4-processes. [Accessed: 15-Feb-2019].

[14] P. Cramton, “Electricity market design,” 2017.

[15] PJM, “PJM Manua 11/ Energy & Ancillary Services Market Operations,” 2017.

[16] M. Dzamarija (DTU), M. Plecas (USTRATH), J. Jimeno (TECNALIA), H. Marthinsen (SINTEF-E), J. Camargo (VITO), Y. Vardanyan (DTU), M. Marroquin (ONE), D. Sanchez (ONE), F. Spiessens (VITO), G. Leclercq (N-SIDE), and N. Ruiz (TECNALIA), “Aggregation models,” SmartNet project, D2.1, 2018.

[17] M. Zamri, C. Wanik, I. Erlich, and A. Mohamed, *Intelligent Management of Distributed Generators Reactive Power for Loss Minimization and Voltage Control.* .

[18] European Commission, “COMMISSION REGULATION (EU) 2016/ 631 - of 14 April 2016 - establishing a network code on requirements for grid connection of generators,” 2016.

[19] E. S.-G.-N. P.-O.-O.-O.- TGE, “EUPHEMIA Public Description, PCR Market Coupling Algorithm,” 2016.

[20] E. Lazarczyk, “Nodal , zonal and discriminatory pricing Pär Holmberg and Ewa Lazarczyk,” no. April, 2012.

[21] J. Carpentier, “Contribution a l’etude du dispatching economique,” *Bull. la Soc. Fr. des Electr.*, vol. 3, no. 1, pp. 431–447, 1962.

[22] H. W. Dommel and W. F. Tinney, “Optimal power flow solutions,” *IEEE Trans. power Appar. Syst.*, no. 10, pp. 1866–1876, 1968.

[23] O. Alsac and B. Stott, “Optimal load flow with steady-state security,” *IEEE Trans. power Appar. Syst.*, no. 3, pp. 745–751, 1974.

[24] B. Stott and O. Alsaç, “Optimal power flow--basic requirements for real-life problems and their solutions,” in *SEPOPE XII Symposium, Rio de Janeiro, Brazil*, 2012.

[25] F. Capitanescu, J. L. M. Ramos, P. Panciatici, D. Kirschen, A. M. Marcolini, L. Platbrood, and L. Wehenkel, “State-of-the-art, challenges, and future trends in security constrained optimal power flow,” *Electr. Power Syst. Res.*, vol. 81, no. 8, pp. 1731–1741, 2011.

[26] M. E. Baran and F. F. Wu, “Optimal capacitor placement on radial distribution systems,” *IEEE Trans. power Deliv.*, vol. 4, no. 1, pp. 725–734, 1989.

[27] L. Vandenberghe and S. Boyd, “Semidefinite programming,” *SIAM Rev.*, vol. 38, no. 1, pp. 49–95,

1996.

[28] N. Z. Shor, “Quadratic optimization problems,” *Sov. J. Comput. Syst. Sci.*, vol. 25, no. 6, pp. 1–11, 1987.

[29] J. B. Lasserre, “Global optimization with polynomials and the problem of moments,” *SIAM J. Optim.*, vol. 11, no. 3, pp. 796–817, 2001.

[30] S. Kim, M. Kojima, and M. Yamashita, “Second order cone programming relaxation of a positive semidefinite constraint,” *Optim. Methods Softw.*, vol. 18, no. 5, pp. 535–541, 2003.

[31] A. Ashouri, “Simultaneous Design and Control of Energy Systems,” ETH Zurich, 2014.

[32] M. Lubin, E. Yamangil, R. Bent, and J. P. Vielma, “Extended formulations in mixed-integer convex programming,” in *International Conference on Integer Programming and Combinatorial Optimization*, 2016, pp. 102–113.

[33] J. A. Taylor, *Convex optimization of power systems*. Cambridge University Press, 2015.

[34] A. Ben-Tal and A. Nemirovski, “On polyhedral approximations of the second-order cone,” *Math. Oper. Res.*, vol. 26, no. 2, pp. 193–205, 2001.

[35] R. A. Jabr, “Radial distribution load flow using conic programming,” *IEEE Trans. Power Syst.*, vol. 21, no. 3, pp. 1458–1459, 2006.

[36] S. H. Low, “Convex relaxation of optimal power flow, part II: Exactness,” *arXiv Prepr. arXiv1405.0814*, 2014.

[37] D. K. Molzahn and I. A. Hiskens, “Mixed SDP/SOCP moment relaxations of the optimal power flow problem,” in *PowerTech, 2015 IEEE Eindhoven*, 2015, pp. 1–6.

[38] B. Ghaddar, J. Marecek, and M. Mevissen, “Optimal power flow as a polynomial optimization problem,” *IEEE Trans. Power Syst.*, vol. 31, no. 1, pp. 539–546, 2016.

[39] C. Josz, J. Maeght, P. Panciatici, and J. C. Gilbert, “Application of the moment-SOS approach to global optimization of the OPF problem,” *IEEE Trans. Power Syst.*, vol. 30, no. 1, pp. 463–470, 2015.

[40] R. A. Jabr, “A conic quadratic format for the load flow equations of meshed networks,” *IEEE Trans. Power Syst.*, vol. 22, no. 4, pp. 2285–2286, 2007.

[41] R. A. Jabr, “Optimal power flow using an extended conic quadratic formulation,” *IEEE Trans. power Syst.*, vol. 23, no. 3, pp. 1000–1008, 2008.

[42] R. A. Jabr, R. Singh, and B. C. Pal, “Minimum loss network reconfiguration using mixed-integer convex programming,” *IEEE Trans. Power Syst.*, vol. 27, no. 2, pp. 1106–1115, 2012.

[43] H. L. Hijazi and S. Thiébaux, "Optimal AC distribution systems reconfiguration," in *Power Systems Computation Conference (PSCC), 2014*, 2014, pp. 1–7.

[44] C. Coffrin, D. Gordon, and P. Scott, "Nesta, the NICTA energy system test case archive," *arXiv Prepr. arXiv1411.0359*, 2014.

[45] C. Coffrin, H. Hijazi, and P. Van Hentenryck, "Strengthening the SDP Relaxation of AC Power Flows with Convex Envelopes, Bound Tightening, and Lifted Nonlinear Cuts," pp. 1–26, 2015.

[46] C. Coffrin, H. L. Hijazi, and P. Van Hentenryck, "The QC relaxation: Theoretical and computational results on optimal power flow," *arXiv Prepr. arXiv1502.07847*, 2015.

[47] H. Hijazi, C. Coffrin, and P. Van Hentenryck, "Convex quadratic relaxations for mixed-integer nonlinear programs in power systems," *Math. Program. Comput.*, pp. 1–47, 2014.

[48] C. Coffrin, H. L. Hijazi, and P. Van Hentenryck, "Network Flow and Copper Plate Relaxations for AC Transmission Systems," *arXiv Prepr. arXiv1506.05202*, 2015.

[49] R. Berg, E. S. Hawkins, and W. W. Pleines, "Mechanized calculation of unbalanced load flow on radial distribution circuits," *IEEE Trans. Power Appar. Syst.*, no. 4, pp. 415–421, 1967.

[50] T.-H. Chen, M.-S. Chen, K.-J. Hwang, P. Kotas, and E. A. Chebli, "Distribution system power flow analysis-a rigid approach," *IEEE Trans. Power Deliv.*, vol. 6, no. 3, pp. 1146–1152, 1991.

[51] C. S. Cheng and D. Shirmohammadi, "A three-phase power flow method for real-time distribution system analysis," *IEEE Trans. Power Syst.*, vol. 10, no. 2, pp. 671–679, 1995.

[52] M. E. Baran and F. F. Wu, "Network reconfiguration in distribution systems for loss reduction and load balancing," *IEEE Trans. Power Deliv.*, vol. 4, no. 2, pp. 1401–1407, 1989.

[53] L. Gan and S. H. Low, "Convex relaxations and linear approximation for optimal power flow in multiphase radial networks," in *Power Systems Computation Conference (PSCC)*, 2014, pp. 1–9.

[54] D. K. Molzahn, J. T. Holzer, B. C. Lesieutre, and C. L. DeMarco, "Implementation of a large-scale optimal power flow solver based on semidefinite programming," *IEEE Trans. Power Syst.*, vol. 28, no. 4, pp. 3987–3998, 2013.

[55] X. Bai, H. Wei, K. Fujisawa, and Y. Wang, "Semidefinite programming for optimal power flow problems," *Int. J. Electr. Power Energy Syst.*, vol. 30, no. 6, pp. 383–392, 2008.

[56] R. Madani, S. Sojoudi, and J. Lavaei, "Convex relaxation for optimal power flow problem: Mesh networks," *IEEE Trans. Power Syst.*, vol. 30, no. 1, pp. 199–211, 2015.

[57] J. Lavaei, S. Member, and S. H. Low, "Zero Duality Gap in Optimal Power Flow Problem," vol. 27, no.

1, pp. 92–107, 2012.

[58] L. Gan and S. H. Low, "Chordal relaxation of OPF for multiphase radial networks," in *2014 IEEE International Symposium on Circuits and Systems (ISCAS)*, 2014, pp. 1812–1815.

[59] S. Bose, S. H. Low, T. Teeraratkul, and B. Hassibi, "Equivalent relaxations of optimal power flow," *IEEE Trans. Automat. Contr.*, vol. 60, no. 3, pp. 729–742, 2015.

[60] S. Mhanna, G. Verbic, and A. Chapman, "Tight LP Approximations for the Optimal Power Flow Problem," *arXiv Prepr. arXiv1603.00773*, 2016.

[61] C. Coffrin and P. Van Hentenryck, "A linear-programming approximation of AC power flows," *INFORMS J. Comput.*, vol. 26, no. 4, pp. 718–734, 2014.

[62] Federal Energy Regulatory Commission, "FERC - optimal power flow and formulation papers." 2013.

[63] A. Castillo and R. P. O'Neill, "Survey of approaches to solving the ACOPF (OPF Paper 4)," *US Fed. Energy Regul. Comm. Tech. Rep*, 2013.

[64] F. Capitanescu, "Critical review of recent advances and further developments needed in AC optimal power flow," *Electr. Power Syst. Res.*, vol. 136, pp. 57–68, 2016.

[65] S. H. Low, "Convex relaxation of optimal power flow, part I: Formulations and equivalence," *arXiv Prepr. arXiv1405.0766*, 2014.

[66] S. H. Low, "Convex relaxation of optimal power flow: a tutorial," in *2013 IREP Symposium Bulk Power System Dynamics and Control-IX Optimization, Security and Control of the Emerging Power Grid*, 2013.

[67] L. Gan, "Distributed load control in multiphase radial networks," California Institute of Technology, 2015.

[68] L. Gan, N. Li, U. Topcu, and S. H. Low, "Exact convex relaxation of optimal power flow in tree networks," *arXiv Prepr. arXiv1208.4076*, 2012.

[69] L. Gan, N. Li, U. Topcu, and S. Low, "On the exactness of convex relaxation for optimal power flow in tree networks," in *2012 IEEE 51st IEEE Conference on Decision and Control (CDC)*, 2012, pp. 465–471.

[70] L. Gan, S. H. Low, and C. EAS, "Convexification of AC optimal power flow," in *Proc. of the 18th Power Systems Computation Conference (PSCC), Wroclaw, Poland*, 2014.

[71] R. Madani, M. Ashraphijuo, and J. Lavaei, "SDP solver of optimal power flow users manual," 2014.

[72] S. Sojoudi and J. Lavaei, "Physics of power networks makes hard optimization problems easy to solve," in *2012 IEEE Power and Energy Society General Meeting*, 2012, pp. 1–8.

[73] A. Castillo and others, "Essays on the ACOPF Problem: Formulations, Approximations, and Applications in the Electricity Markets," Johns Hopkins University, 2016.

[74] M. Farivar, "Optimization and Control of Power Flow in Distribution Networks," California Institute of Technology, 2016.

[75] D. Mayer, "Hamiltons Principle and Electric Circuits Tudory," *Adv. Electr. Electron. Eng.*, vol. 5, no. 1–2, p. 185, 2006.

[76] H. Andrei, P. C. Andrei, G. Oprea, and B. Botea, "Basic equations of linear electric and magnetic circuits in quasi-stationary state based on principle of minimum absorbed power and energy," in *Fundamentals of Electrical Engineering (ISFEE), 2014 International Symposium on*, 2014, pp. 1–6.

[77] H. Andrei and F. Spinei, "An extension of the minimum energy principle in stationary regime for electric and magnetic circuits," *Rev. Roum. des Sci. Tech. Ser. Electrotech. Energ.*, vol. 52, no. 4, p. 419, 2007.

[78] J. E. Prussing, "The principal minor test for semidefinite matrices," *J. Guid. Control. Dyn.*, vol. 9, no. 1, pp. 121–122, 1986.

[79] M. Fazel, H. Hindi, and S. P. Boyd, "Log-det heuristic for matrix rank minimization with applications to Hankel and Euclidean distance matrices," in *American Control Conference,. Proceedings of the*, 2003, vol. 3, pp. 2156–2162.

[80] K. Mohan and M. Fazel, "Reweighted nuclear norm minimization with application to system identification," in *Proceedings of the 2010 American Control Conference*, 2010, pp. 2953–2959.

[81] R. Louca, P. Seiler, and E. Bitar, "A rank minimization algorithm to enhance semidefinite relaxations of optimal power flow," in *Communication, Control, and Computing (Allerton), 2013 51st Annual Allerton Conference on*, 2013, pp. 1010–1020.

[82] R. Madani, M. Ashraphijuo, and J. Lavaei, "Promises of conic relaxation for contingency-constrained optimal power flow problem," *IEEE Trans. Power Syst.*, vol. 31, no. 2, pp. 1297–1307, 2016.

[83] D. Shi, "Power system network reduction for engineering and economic analysis," Arizona State University, 2012.

[84] D. Dobrijevic and D. Popovic, "An unified external network equivalent in steady-state security assessment," *Facta Univ. - Ser. Electron. Energ.*, vol. 23, no. 2, pp. 179–189, 2010.

[85] F. Milano and K. Srivastava, "Dynamic REI equivalents for short circuit and transient stability analyses," *Electr. Power Syst. Res.*, vol. 79, no. 6, pp. 878–887, 2009.

[86] K. Van Den Bergh, E. Delarue, and W. D'haeseleer, "DC power flow in unit commitment models," no. May, 2014.

[87] D. Shi and D. J. Tylavsky, "An improved bus aggregation technique for generating network equivalents," in *2012 IEEE Power and Energy Society General Meeting*, 2012, pp. 1–8.

[88] T. Pang-Ning, M. Steinbach, V. Kumar, and others, "Introduction to data mining," in *Library of congress*, 2006, vol. 74.

[89] N. Muller and V. K. Quintana, "A sparse eigenvalue-based approach for partitioning power networks," *IEEE Trans. power Syst.*, vol. 7, no. 2, pp. 520–527, 1992.

[90] M. Gavrilas, O. Ivanov, and G. Gavrilas, "REI Equivalent Design for Electric Power Systems with Genetic Algorithms," vol. 7, no. 10, pp. 911–921, 2008.

[91] Q. Zhai, X. Guan, J. Cheng, and H. Wu, "Fast identification of inactive security constraints in SCUC problems," *IEEE Trans. Power Syst.*, vol. 25, no. 4, pp. 1946–1954, 2010.

[92] R. Fernández-Blanco, J. M. Arroyo, N. Alguacil, and X. Guan, "Incorporating Price-Responsive Demand in Energy Scheduling Based on Consumer Payment Minimization," *IEEE Trans. Smart Grid*, vol. 7, no. 2, pp. 817–826, 2016.

[93] A. J. Ardakani and F. Bouffard, "Identification of umbrella constraints in DC-based security-constrained optimal power flow," *IEEE Trans. Power Syst.*, vol. 28, no. 4, pp. 3924–3934, 2013.

[94] A. J. Ardakani and F. Bouffard, "Acceleration of umbrella constraint discovery in generation scheduling problems," *IEEE Trans. Power Syst.*, vol. 30, no. 4, pp. 2100–2109, 2015.

[95] A. Papavasiliou and I. Mezghani, "Coordination Schemes for the Integration of Transmission and Distribution System Operations," in *2018 Power Systems Computation Conference (PSCC)*, 2018, vol. 32, no. i, pp. 1–7.

[96] M. Sarfati, M. Hesamzadeh, and P. Benedicto Martinez, "A probabilistic spot market design for reducing real-time balancing costs," in *2014 IEEE PES General Meeting | Conference & Exposition*, 2014, pp. 1–5.

[97] "Public consultation document for the design of the TERRE (Trans European Replacement Reserves Exchange)," 2016.

[98] A. Zani and G. Migliavacca, "Pan-European balancing market: Benefits for the Italian power system," in *AEIT Annual Conference-From Research to Industry: The Need for a More Effective*

Technology Transfer (AEIT), 2014, 2014, pp. 1–6.

[99] F. C. Schweppe, M. C. Caramanis, R. D. Tabors, and R. E. Bohn, *Spot pricing of electricity*. Springer Science & Business Media, 2013.

[100] R. E. Bohn, M. C. Caramanis, and F. C. Schweppe, "Optimal pricing in electrical networks over space and time," *Rand J. Econ.*, pp. 360–376, 1984.

[101] L. Hirth, "Nodal Pricing Some Pros and Cons," 2018.

[102] F. A. Wolak, "Measuring the Benefits of Greater Spatial Granularity in Short-Term Pricing in Wholesale Electricity Markets," *Am. Econ. Rev.*, vol. 101, no. 3, pp. 247–252, May 2011.

[103] S. S. Oren, "Market Design and Gaming in Competitive Electricity Markets."

[104] A. Ehrenmann and Y. Smeers, "Inefficiencies in European congestion management proposals," *Util. policy*, vol. 13, no. 2, pp. 135–152, 2005.

[105] E. Bjorndal, M. H. Bjorndal, H. Cai, and E. Panos, "Hybrid Pricing in a Coupled European Power Market with More Wind Power," *NHH Dept. Bus. Manag. Sci. Discuss. Pap.*, no. 2015/28, 2015.

[106] S. Oren, "When is a pay-as bid preferable to uniform price in electricity markets," in *Power Systems Conference and Exposition*, 2004, vol. 3, pp. 1618–1620.

[107] M. Marracci and D. Poli, "Analysis of the Possible Impact of Complex Bids in the Italian Electricity Spot Market," in *International Conference on Energy, Environment, Devices, Systems, Communications, Computers*, 2011.

[108] M. Dzamarija, "Aggregation models," 2017.

[109] M. Mashhour, M. A. Golkar, and S. M. Moghaddas-Tafreshi, "Extending market activities for a distribution company in hourly-ahead energy and reserve markets--Part I: Problem formulation," *Energy Convers. Manag.*, vol. 52, no. 1, pp. 477–486, 2011.

[110] M. J. Osborne and A. Rubinstein, *A Course in Game Theory*. MIT Press, 1999.

[111] T. Başar and G. J. Olsder, *Dynamic noncooperative game theory*. SIAM, 1999.

[112] H. Le Cadre, I. Mezghani, and A. Papavasiliou, "A game-theoretic analysis of transmission-distribution system operator coordination," *Eur. J. Oper. Res.*, vol. 274, no. 1, pp. 317–339, Apr. 2019.

[113] H. Le Cadre, "On the efficiency of local electricity markets under decentralized and centralized designs: a multi-leader Stackelberg game analysis," *Cent. Eur. J. Oper. Res.*, pp. 1–32, Jan. 2018.

[114] J. Lofberg, "YALMIP: A toolbox for modeling and optimization in MATLAB," in *Computer Aided Control Systems Design, 2004 IEEE International Symposium on*, 2004, pp. 284–289.

[115] B. De Tandt, "EN50160 -- Voltage characteristics of electricity supplied by public distribution systems," *Eur. Comm. Electrotech. Stand.*, 1999.

[116] G. Andersson, "Modelling and analysis of electric power systems," *EEH-Power Syst. Lab. Swiss Fed. Inst. Technol. (ETH), Zürich, Switz.*, 2004.

[117] M. Fazel, H. Hindi, and S. P. Boyd, "A rank minimization heuristic with application to minimum order system approximation," in *American Control Conference, 2001. Proceedings of the 2001*, 2001, vol. 6, pp. 4734–4739.

[118] S. Kolodziej, P. M. Castro, and I. E. Grossmann, "Global optimization of bilinear programs with a multiparametric disaggregation technique," *J. Glob. Optim.*, vol. 57, no. 4, pp. 1039–1063, Dec. 2013.

[119] "Phase Shift Transformers Modelling," no. May, pp. 1–27, 2014.

[120] D. Povh and others, "Load flow control in high voltage power systems using FACTS controllers," *Cigre TF*, pp. 1–38, 1996.

[121] F. Li and R. Bo, "DCOPF-based LMP simulation: algorithm, comparison with ACOPF, and sensitivity," *IEEE Trans. Power Syst.*, vol. 22, no. 4, pp. 1475–1485, 2007.

[122] R. D. Zimmerman, C. E. Murillo-Sánchez, and R. J. Thomas, "MATPOWER: Steady-state operations, planning, and analysis tools for power systems research and education," *IEEE Trans. power Syst.*, vol. 26, no. 1, pp. 12–19, 2011.

[123] K. Purchala, L. Meeus, D. Van Dommelen, and R. Belmans, "Usefulness of DC power flow for active power flow analysis," in *IEEE Power Engineering Society General Meeting, 2005*, 2005, pp. 454–459.

[124] E. M. L. Beale and J. J. H. Forrest, "Global optimization using special ordered sets," *Math. Program.*, vol. 10, no. 1, pp. 52–69, Dec. 1976.

[125] R. A. Jabr, "Polyhedral formulations and loop elimination constraints for distribution network expansion planning," *IEEE Trans. Power Syst.*, vol. 28, no. 2, pp. 1888–1897, 2013.

[126] F. Geth, C. del Marmol, D. Laudy, and C. Merckx, "Mixed-integer second-order cone unit models for combined active-reactive power optimization," in *2016 IEEE International Energy Conference (ENERGYCON)*, 2016, no. 1, pp. 1–6.

[127] K. Heussen, S. Koch, A. Ulbig, and G. Andersson, "Unified System-Level Modeling of Intermittent

Renewable Energy Sources and Energy Storage for Power System Operation," *IEEE Syst. J.*, vol. 6, no. 1, pp. 140–151, Mar. 2012.

[128] M. Farivar, C. R. Clarke, S. H. Low, and K. M. Chandy, "Inverter var control for distribution systems with renewables," in *Smart Grid Communications (SmartGridComm), 2011 IEEE International Conference on*, 2011, pp. 457–462.

[129] F. Pilo, G. Pisano, S. Scalari, D. Dal Canto, A. Testa, R. Langella, R. Caldon, and R. Turri, "ATLANTIDE—Digital archive of the Italian electric distribution reference networks," in *Integration of Renewables into the Distribution Grid, CIRED 2012 Workshop*, 2012, pp. 1–4.

[130] S. Diamond and S. Boyd, "CVXPY: A Python-embedded modeling language for convex optimization," *J. Mach. Learn. Res.*, vol. 17, no. 83, pp. 1–5, 2016.

[131] A. Domahidi, E. Chu, and S. Boyd, "ECOS: An SOCP solver for embedded systems," in *Control Conference (ECC), 2013 European*, 2013, pp. 3071–3076.

[132] R. Lincoln, "PYPOWER 5.0.1." 2015.

[133] A. Papavasiliou, "Optimization Models in Electricity Markets."

[134] W. W. Hogan, "Contract networks for electric power transmission," *J. Regul. Econ.*, vol. 4, no. 3, pp. 211–242, 1992.

[135] P. R. Gribik, W. W. Hogan, and S. L. Pope, "Market-clearing electricity prices and energy uplift." December, 2007.

[136] R. P. O'Neill, P. M. Sotkiewicz, B. F. Hobbs, M. H. Rothkopf, and W. R. Stewart, "Efficient market-clearing prices in markets with nonconvexities," *Eur. J. Oper. Res.*, vol. 164, no. 1, pp. 269–285, 2005.

[137] M. Madani and M. Van Vyve, "Computationally efficient MIP formulation and algorithms for European day-ahead electricity market auctions," *Eur. J. Oper. Res.*, vol. 242, no. 2, pp. 580–593, 2015.

[138] A. Papavasiliou, "Analysis of Distribution Locational Marginal Prices," *IEEE Trans. Smart Grid*, pp. 1–1, 2017.

[139] IndustRE, "Deliverable 2.2: Regulatory and Market Framework Analysis." .

10 Appendices

10.1 Formulation of Bids and Constraints

10.1.1 Nomenclature

In this section, constants (parameters, sets) and variables which are used to define the constraints and the objectives are listed.

Constants (Scalars, Sets and Mappings)

1. δt: duration of a time step in the market time horizon [hours]
2. T: number of time steps considered in one rolling window optimization.
3. N^+: the set of all nodes in the network (graph). For the considered tree-shaped distribution sub-networks, N denotes the set of nodes of the tree-shaped network, except for the root node.
4. γ_t: time discount factor that, in the objective function, weighs near-future time slot objective terms higher than far-future time slots.
5. A_n : the set of actors (aggregators or agents) at node $n \in N^+$.
6. $\forall n \in N^+, \forall a \in A_n$:
   (a) B_{na}: set of bids.
   (b) I_{na}: set of pairs of bids with an 'implication' constraint.
   (c) X_{na}: set of sets of bids with 'exclusive choice' constraints.
7. $\forall n \in N^+, \forall a \in A_n, \forall b \in B_{na}$:
   (a) PF_{nab}: power factor.
   (b) $\underline{x}_{nab}$: the minimal acceptance fraction for the variable x_{nab}.
   (c) $a_{nab,-1}$: the assumed current state of activation of the offered bid.
   (d) $\overline{\alpha}_{nab}$: maximal number of activations (start-ups) in the optimization window.
   (e) $\underline{\delta}^{\alpha}_{nab}$: minimal activation duration (number of time steps)
   (f) $\overline{\delta}^{\alpha}_{nab}$: maximal activation duration (number of time steps)

(g) $\underline{\delta}^{\omega}_{nab}$: minimal deactivation duration (number of time steps) in which the bid must be deactivated. The parameter $\underline{\delta}^{\omega}_{nab}$ has 0 as its default value.

(h) $\alpha_{nab,\tau}$: Booleans indicating the start of activation prior to current time step. These must be defined if constraint (e) or (f) exists. For constraint (f), $\tau \in \left\{-\overline{\delta}^{\alpha}_{nab}+1, \dots, -2, -1\right\}$, and for constraint (e), $\forall\tau \in \left\{-\underline{\delta}^{\alpha}_{nab}+1, \dots, -2, -1\right\}$.

(i) $\omega_{nab,\tau}$: Booleans indicating stop of activation (i.e. deactivation) prior to current time step. These must be available if constraint (g) exists, in which case $\tau \in \left\{-\underline{\delta}^{\omega}_{nab}+1, \dots, -2, -1\right\}$.

(j) $\underline{\Delta q}_{nab}$: maximal decrease of power from any time step to the next one.

(k) $\overline{\Delta q}_{nab}$: maximal increase of power from any time step to the next one.

(l) $\underline{e}^{i}_{nab}$: Minimum energy that needs to be delivered by the Qt-bid with integral constraint, if activated. [MWh]

(m) $\overline{e}^{i}_{nab}$: Maximum energy that needs to be delivered by a Qt-bid with an integral constraint, if activated. [MWh]

(n) T_{nab}: set of (consecutive) time steps in a Qt bid.

8. $\forall n \in N^{+}, \forall a \in A_n, \forall b \in B_{na}, \forall t \in T_{nab}$:

(a) q_{nabt}: maximal available quantity of active power for a primitive bid (step/linear).

(b) p_{nabt}: bidding price at chosen quantity (corresponding to the marginal costs of the bidder).

(c) $m_{nabt}: \mathbb{R} \to \mathbb{R}$: mapping of power quantity q to marginal cost (price) p. It implies that $p = m_{nabt}(q)$

(d) $\Pi = \Pi_{nabt}$: set of primitive bids that a Q-bid can be decomposed into

(e) Π^{right}: subset of Π, including common bids with the right sign of q (useful for elimination of system imbalance).

(f) Π^{wrong}: subset of Π, including common bids with the wrong sign of q (not useful for elimination of system imbalance).

Variables

Variables can be real or binary (or integer, to be more general). Binary variables take values in $\{0,1\}$.

1. $\forall n \in N^{+}, \forall a \in A_n, \forall b \in B_{na}$:

(a) aa_{nab} (binary) is equal to 1 if the bid is activated for any time step within the horizon. Then we call the bid 'accepted'.

2. $\forall n \in N^+, \forall a \in A_n, \forall b \in B_{na}, \forall t \in T_{nab}$:

(a) a_{nabt}(binary) which equals 1 if the bid is activated for the time step *t*.

(b) α_{nabt} (binary) which equals 1 for time step at which the bid goes from non-activated to activated (activation begins).

(c) ω_{nabt} (binary) which equals 1 for time step at which the bid goes from activated to non-activated (activation ends).

3. $\forall n \in N^+, \forall a \in A_n, \forall b \in B_{na}, \forall t \in T_{nab}, \forall \beta \in \Pi_{nabt}$:

(a) $x_{nabt\beta}$ (real): $0 \leq x_{nabt\beta} \leq 1$: fraction of quantity $q_{nabt\beta}$ of primitive bid β that is activated.

10.1.2 Definition of Acceptance

Acceptance of a Q-bid

A Q-bid is defined as 'accepted' if at least one of its primitives bids (that the Q-bid can be decomposed into) is activated for a fraction x larger than 0. The Boolean variable a_{nabt} indicates whether the bid is activated or not. Whether this is the case or not can be derived from the acceptance of its composing primitive bids by the constraints

$$a_{nabt} \cdot \underline{x}_{nab} \leq \left(\sum_{\beta \in \Pi_{nabt}} x_{nabt\beta} \right) \leq a_{nabt} \cdot |\Pi_{nabt}| \tag{28}$$

where $|\Pi_{nabt}|$ is the number of primitive bids composing the Q-bid and $\underline{x}_{nab}$ is the optional minimum acceptance fraction specified by a bidder (e.g. $\underline{x}_{nab} = 0.7$ to ensure a minimum activation of a bid, if any). Constraint (28) only needs to be specified in the optimization problem if $\underline{x}_{nab} > 0$ or if the Boolean variable is explicitly needed (e.g. exclusive constraint) in another bid constraint, otherwise it can be computed ex-post, based on $x_{nabt\beta}$ values: $\underline{a}_{nabt} = 1 \; if \; \max_{\beta \in \Pi_{nabt}} x_{nabt\beta} > 0 \; and \; 0 \; otherwise$.

Acceptance of a Qt-bid

A Qt-bid is defined as accepted if at least one of its Q-bids has been accepted. This is imposed by the following constraints:

$$aa_{nab} \cdot \underline{x}_{nab} \leq \left(\sum_{t \in T_{nab}} a_{nabt} \right) \leq aa_{nab} \cdot |T_{nab}|. \tag{29}$$

When $aa_{nab} = 0$, the right-hand side forces a_{nabt} to be 0 for all $t \in T_{nab}$. When $aa_{nab} = 1$, the left-hand side is larger than zero, so at least one a_{nabt} has to be equal to 1 (accepted). The constraint is only part of the optimization problem if $\underline{x}_{nab} > 0$ or if aa_{nab} is explicitly needed in another bid constraint (e.g.

exclusive constraint). Otherwise, it can be computed ex-post, based on a_{nabt} values: $\underline{a}_{nab} = 1\ if\ \max_{t \in T_{nab}} x_{nabt} > 0\ and\ 0\ otherwise.$

10.1.3 Formulation of Bid Constraints

Helper Activation and Deactivation Pulse Variables

To be able to define some specific constraints in the next sections, some additional helper Booleans can be defined: α_{nabt} , equal to 1 when a bid starts to be activated at time t, and ω_{nabt}, equal to 1 when the bid is deactivated (i.e. stopped) at time t. These variables relate with the activation Boolean variable a_{nabt} in the following way:

$$\forall t \in T_{nab} \backslash \{0\}, \qquad a_{nabt} = a_{nab,t-1} + \alpha_{nabt} - \omega_{nabt} \tag{30}$$

To avoid that both α_{nabt} and ω_{nabt} are true for the same time step, we add the constraint

$$\alpha_{nabt} + \omega_{nabt} \leq 1 \tag{31}$$

When required by some specific bid constraints (see subsections below), equations (30) and (31) are added to the optimization model. This relation is graphically represented for some example waveforms in Figure 10-1. It shows a first pulse on α_{nabt} marked as 1, which leads to a_{nabt} going from 0 to 1. The first pulse on ω_{nabt} marked as 1, makes a_{nabt} going down again from 1 to 0. The first activation period is marked as a_1. Similar start and end pulses occur for the subsequent activations marked as a_2 and a_3.

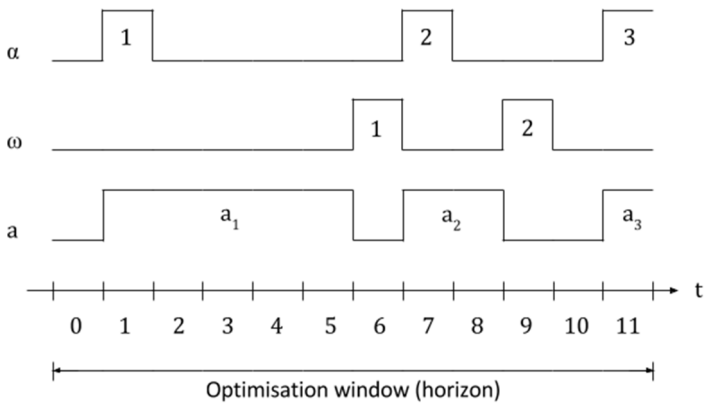

Figure 10-1 Relation of pulses $\boldsymbol{\alpha_{nabt}}$ and $\boldsymbol{\omega_{nabt}}$ to activation level $\boldsymbol{a_{nabt}}$.

Accept-All-Time-Steps-or-None Constraint

When the actor specifies that the bid is 'Accept-All-Time-Steps-or-None', the following constraint is applied (minimum duration of activation must be equal to the number of time steps in the bid horizon) :

$$\underline{\delta}^{\alpha}_{nab} = \#T_{nab} \quad (32)$$

where $\#T_{nab}$ is the number of time-steps in the Qt-bid. Note that all $\delta's$ are constant parameters and not variables.

Ramping Constraints

Ramping constraints are exactly the same for every two consecutive time steps of the bid. It holds that:

$$q_{nab,t} \leq q_{nab,t-1} + \overline{\Delta q}_{nab} \text{ (ramp-up limit)} \quad (33)$$

and

$$q_{nab,t} \geq q_{nab,t-1} + \underline{\Delta q}_{nab} \text{ (ramp-down limit)} \quad \text{i(34)}$$

Maximum Number of Activations Constraint

To be able to count the number of starts and stops of activations during the bid time span, the previously defined variables α_{nabt} and ω_{nabt} are used. The constraint limiting the number of new activations during the time horizon can be written as:

$$\sum_{t \in T_{nab}} \alpha_{nabt} \leq \overline{\alpha}_{nab} \quad (35)$$

Minimum and Maximum Duration of Activation Constraint

The following equation may be used to enforce a minimum activation duration of $\underline{\delta}^{\alpha}_{nab}$ time steps

$$\forall \tau \in \{0, \ldots, |T_{nab}| - \underline{\delta}^{\alpha}_{nab}\} : \left(\sum_{t=\tau}^{t+\overline{\delta}^{\alpha}_{nab}-1} a_{nab,t} \right) \geq \underline{\delta}^{\alpha}_{nab} \alpha_{nab\tau} \quad (36)$$

This means that if, for a certain τ, $\alpha_{nab\tau}$ is 1 (beginning of activation), $a_{nab,t}$ will be equal to 1 (active) for at least the $\underline{\delta}^{\alpha}_{nab}$ following time slots. The activation must happen during the Qt-bid time horizon, thus, the time at which the activation can begin, τ, is comprised between 0 and $|T_{nab}| - \underline{\delta}^{\alpha}_{nab}$. The minimum duration $\underline{\delta}^{\alpha}_{\text{nab}}$should be at least two time steps, otherwise it does not make sense to have such a constraint.

As for the maximum duration, the condition that $a_{nab,\tau}$ should not be 1 any longer than $\overline{\delta}^{\alpha}_{nab}$ consecutive time steps, can simply be enforced by:

$$\forall \tau \in \left\{0, \ldots, |T_{nab}| - \overline{\delta}^{\alpha}_{nab} - 1\right\} : \left(\sum_{t=\tau}^{t+\overline{\delta}^{\alpha}_{nab}} a_{nab,t} \right) \leq \overline{\delta}^{\alpha}_{nab} \quad (37)$$

Indeed, the left-hand side of eq. (37) is a sum of $\overline{\delta}^{\alpha}_{\text{nab}} + 1$ binary variables and should sum up to at most $\overline{\delta}^{\alpha}_{\text{nab}}$ so at least one of them needs to be equal to 0, ensuring that the maximum duration of activation is at

most $\overline{\delta}^{\alpha}_{nab}$. The maximum duration $\overline{\delta}^{\alpha}_{nab}$should be strictly smaller than $|T_{nab}|$, otherwise it does not make sense to have such a constraint.

Minimal Delay Between Two Activations

Similar to the constraint the minimum duration of activation, the constraint expressing a minimum delay of $\underline{\delta}^{\omega}_{nab}$ time steps between the end of an activation and the beginning of the next activation can be written as:

$$\forall \tau \in \{1, \ldots, |T_{nab}| - \underline{\delta}^{\omega}_{nab}\} : \left(\sum_{t=\tau}^{t+\underline{\delta}^{\omega}_{nab}-1} (1 - a_{nab,t}) \right) \geq \underline{\delta}^{\omega}_{nab} \omega_{nab\tau} \quad (38)$$

This means that if, for a certain τ, $\omega_{nab\tau}$ is 1 (end of an activation), $a_{nab,t}$ will be equal to 0 (not active) for at least the $\underline{\delta}^{\omega}_{nab}$ following time steps. τ must be at least 1 since the stop of an activation can not be at the first time step. The minimum duration $\underline{\delta}^{\omega}_{nab}$ should be at least two time steps and strictly smaller than the Qt-bid time horizon $|T_{nab}|$, otherwise it does not make sense to have such a constraint.

Integral Constraint

In the more general form, the integral constraint can be formulated as:

$$\underline{e}^{i}_{nab} a_{nab,t} \leq \sum_{t \in T_{nab}} (q_{nabt} \cdot \delta t) \leq \overline{e}^{i}_{nab} a_{nab,t} \quad (39)$$

where $\underline{e}^{i}_{nab}$ and $\overline{e}^{i}_{nab}$ respectively represent the lower and upper bounds on the energy that the bid should deliver, if activated. When the lower and upper bounds are equal, a single equality constraint results. As a special case, when the bounds are set to zero, the integral constraint guarantees that the asset (usually a thermal or electrical storage) returns to its initial value at the end of the bid-horizon (without accounting for efficiency losses), or its energy content remains within the pre-defined bounds. Note that the binary variables can be removed in the constraint formulation when $\underline{e}^{i}_{nab} \leq 0$ and $\overline{e}^{i}_{nab} \geq 0$. Also, it is possible to specify a restricted time interval $T_{int\ constraint} \subseteq T_{nab}$ on which the integral constraint applies.

Implication Constraint

The implication constraint can be defined on a set of pairs of Qt-bids $\mathrm{I_{na}} \subset \mathrm{B_{na}} \times \mathrm{B_{na}}$. It is formulated as:

$$\forall_{b \neq b'} (b, b') \in I_{na}, \qquad aa_{na,b} \leq aa_{na,b'} \quad (40)$$

If $\mathrm{aa_{na,b}} = 1$ then $\mathrm{aa_{na,b'}}$ is forced to be 1. If $\mathrm{aa_{na,b}} = 0$, then nothing is enforced on $\mathrm{aa_{na,b'}}$. Therefore, the implication $\mathrm{b} \rightarrow \mathrm{b'}$ holds. Similarly, the implication constraint can be defined on a set of pairs of Q-bids, independently of whether they are part of the same Qt-bid or not (of course, they need to belong to the same actor *a*).

Exclusive Choice Constraint

This limitation is setup by first creating a sublist l within a list $\mathrm{X_{na}}$ of Qt bid-identifiers, and then within the sublist, requiring that at most one bid can be accepted. This is enforced by the following constraint:

$$\forall l \in X_{na}, \qquad \left(\sum_{b \in l} aa_{nab}\right) \leq 1 \tag{41}$$

Also, as highlighted by the sub-list indices, this constraint can only be enforced between bids at the same node *n* and belonging to this bidder *a*. Similarly, the exclusive choice constraint can be defined on a list of Q-bids independently whether they are part of the same Qt-bid or not.

Deferability Constraint

There is no need in formulating an independent constraint for deferability, since it can be done (in the algorithm) by creating as many Qt-bids, being different shifted versions of the original Qt-bid, as the max deferability number. Then, an exclusive-choice constraint can be used on this list of bids to ensure that at most one of the shifted versions of the bid is accepted.

To ease the process for market participant, we propose a product that allows expressing the deferability explicitly using:

DEFERABILITY = Max.

This field describes the number of decision time steps that the offered bid could be maximally delayed. The value is bounded by the optimization horizon T.

10.2 Network Modeling

10.2.1 Nomenclature

Grid Element Parameters	
$z_{l,s}$	Series impedance (Ω)
$r_{l,s}$	Series resistance (Ω)
$x_{l,s}$	Series reactance (Ω)
$y_{l,s}$	Series admittance (S)
$g_{l,s}$	Series conductance (S)
$b_{l,s}$	Series susceptance (S)
$z_{ij,sh}$	Shunt impedance (Ω)
$r_{ij,sh}$	Shunt resistance (Ω)
$x_{ij,sh}$	Shunt reactance (Ω)
$y_{ij,sh}$	Shunt admittance (Ω)
$g_{ij,sh}$	Shunt conductance (S)
$b_{ij,sh}$	Shunt susceptance(S)
Grid Element Bounds	
a_{ij}^{min}	Min tap ratio (-)
a_{ij}^{max}	Max tap ratio (-)
φ_{ij}^{min}	Min phase shift (rad)
φ_{ij}^{max}	Max phase shift (rad)
α_l^{min}	State bound of section (0,1)
α_l^{max}	State bound of section (0,1)
Grid Element Ratings	
U_{ij}^{rated}	Voltage rating at side I (V)
I_{ij}^{rated}	Current rating at side I (A)
S_{ij}^{rated}	Apparent power rating at side i (VA)
Grid Element Variables	
P_{ij}	Active power flow (W)
Q_{ij}	Reactive power flow (var)
P_l^{loss}	Active power loss (W)
Q_l^{loss}	Reactive power loss (var)
I_{ij}	Grid Element current (A)
I_{ij}^{re}	Real current (A)
I_{ij}^{im}	Imaginary current (A)

Node Variables	
U_i	Node voltage magnitude (V)
U_i'	Node voltage magnitude (V)
U_i^*	Node voltage magnitude (V)
θ_i	Node Voltage angle (rad)
θ_i'	Node Voltage angle (rad)
θ_i^*	Node Voltage angle (rad)
S_i	Aggregated apparent power (VA)
P_i	Aggregated active power (W)
Q_i	Aggregated reactive power (var)
I_i	Aggregated current (A)
Node squared variables	
u_i	Node squared voltage (V²)
u_i'	Node squared voltage (V²)
u_i^*	Node squared voltage (V²)
Sets	
$\mathcal{U}$	Sets of units
$\mathcal{I}$	Sets of nodes
$\mathcal{I}_{SB}$	Sets of slack nodes
$\mathcal{I}_{nonSB}$	Sets of non-slack nodes
$\mathcal{J}$	Sets of grid elements
Other symbols	
M	big M
Grid element squared variables	
$I_{l,s}^2$	Squared series current magnitude (A²)
$i_{ij,s}$	Variable squared series current magnitude
Node Parameters	
U_i^{ref}	Voltage reference (V)
θ_i^{ref}	Voltage angle reference (rad)
Node Bounds	
U_i^{min}	Min bound on voltage magnitude (V)
U_i^{max}	Max bound on voltage magnitude (V)

$I_{ij,s}$	series current (A)	Node ratings	
$I_{ij,sh}$	shunt current (A)	U_i^{rated}	Node voltage rating (V)
θ_{ij}	Voltage angle difference (rad)		
α_{ij}	state indicator for grid element (0,1)		
a_{ij}	instantaneous voltage transformation ratio (-)		
φ_{ij}	phase shift (rad)		

10.2.2 Notation

With the exception of Yalmip [114] and CVX[20], common algebraic modelling languages only support real-valued variables. Intermediately, complex variables will be used in derivations, but ultimately, real-valued constraint sets are formulated. Note that quadratic representation of SOCP constraints is used, but these can be converted to the 2-norm vector representation.

$$x_1{}^2 + x_2{}^2 \leq x_3{}^2, x_3 \geq 0 \Leftrightarrow \sqrt{x_1{}^2 + x_2{}^2} \leq x_3 \Leftrightarrow \left\| \begin{bmatrix} x_1 \\ x_2 \end{bmatrix} \right\|_2 \leq x_3 \tag{42}$$

Finally, a typographic distinction is made between scalar variables, e.g. W_{ij} and matrix variables, e.g. **W**. Valued indexes are subscripted and stylized in a specific font, e.g. '*i*', whereas descriptive indexes are superscripted and stylized as normal text, e.g. 's'.

10.2.3 Physics of Power Flow

In power system modeling, the system is typically represented as a *single-wire diagram*. This representation matches nicely with the concept of *mathematical graphs*. Mathematical graphs are composed of nodes/vertices/buses and edges/arcs/lines. To convert circuits to mathematical graphs, edge models for conducting elements are developed.

Grid nodes and elements are assigned indexes as follows:

- Grid nodes *i; j* ∈ $\mathcal{I} = \mathcal{I}_{SB} \cup \mathcal{I}_{nonSB}$
- Slack bus nodes *i* ∈ $\mathcal{I}_{SB}$
- Non-slackbus nodes *i* ∈ $\mathcal{I}_{nonSB}$
- Grid elements *l,ij* ∈ $\mathcal{J}$

For symmetric variables and parameters, the index *l* is preferred to *ij* or *ji*.

[20] CVX is a Matlab software for convex programming

Nodes are connected to each other through conductive elements. Conducting grid element technologies include: overhead lines, underground cables, classic transformers, on-load tap-changing transformers, phase-shifting transformers, switches, and breakers.

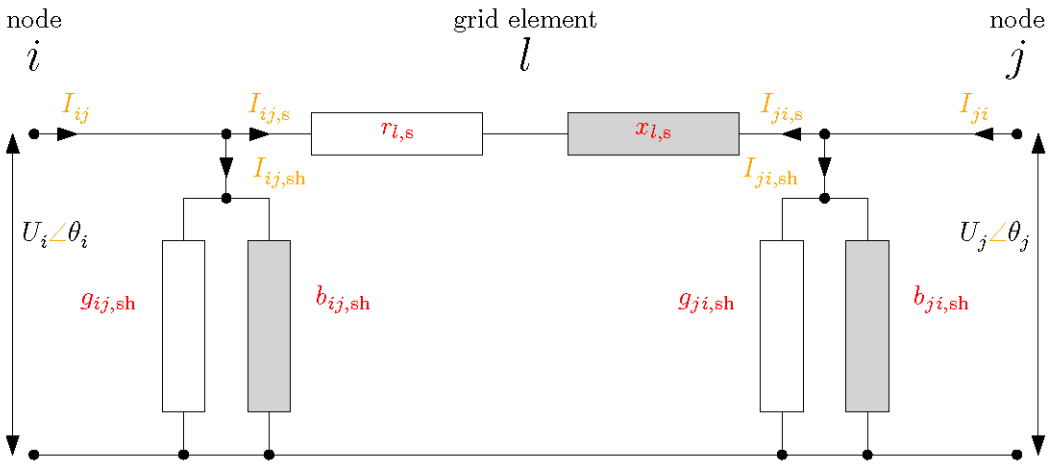

Figure 10-2 Circuit representation of the classic π-element

10.2.4 Grid Elements

In this section, the focus is on cables and lines; in upcoming sections, switches and transformers will be added. Natural notation is series *impedance*, $z_{l,s}$, and shunt *admittance,* $y_{l,sh}$. Nevertheless, admittance forms can be freely converted to impedance forms and vice versa, except for degenerate cases (negligible admittance / impedance). It is noted that in the scientific literature, papers switch the sign of $b_{l,sh}$ (e.g. $y = g + jb$ [41] vs. $y = g - jb$ [35]).

Figure 10-2 displays the circuit representation of the classic π-element, which is commonly used to represent lines & cables. The series impedance (symmetric *ij = ji = l*) is defined as:

$$z_{l,s} = r_{l,s} + j \cdot x_{l,s} \tag{43}$$

The shunt admittance is defined as:

$$y_{l,sh} = g_{l,sh} + j \cdot b_{l,sh} \tag{44}$$

Generally, the shunts are assumed to be symmetric, divided equally to the *i* and *j* side of the π-element.

10.2.5 Kirchhoff's Circuit Laws

The Kirchhoff voltage law (KVL) states that the voltage drops in any (circuit) loop add up to zero. The Kirchhoff current law (KCL) states that the currents at any node add up to zero. This article uses polar notation

for voltage variables, with U_i the voltage magnitude and θ_i the voltage angle. For currents, the variables are $I_{ij} = |I_{ij}|\angle I_{ij}^{\angle} = I_{ij}^{\mathrm{re}} + jI_{ij}^{\mathrm{im}}$.

$$\left((U_i\angle\theta_i) - (U_j\angle\theta_j)\right) = I_{ij,s}z_{l,s} \tag{45}$$

$$I_{ij,sh} = y_{ij,sh}(U_i\angle\theta_i) \tag{46}$$

$$I_{ji,sh} = y_{ji,sh}(U_j\angle\theta_j) \tag{47}$$

$$I_{ij} = I_{ij,s} + I_{ij,sh} \tag{48}$$

$$I_{ji} = I_{ji,s} + I_{ji,sh} \tag{49}$$

$$I_{ij,s} + I_{ji,s} = 0 \tag{50}$$

Here we have Ohm's law (45), the current to the shunt elements (46)-(47), and Kirchhoff's current law (48)-(50). As is easily verified, Kirchhoff's circuit laws are linear in voltage and current for constant impedances. Note that this describes only one grid element. In meshed grids, KVL also has to be applied in the mesh loops.

10.2.6 Power Flow

As the purpose of the grid is to transport *energy*, stakeholders are interested in quantities of energy, power, and cost. Power in AC grids considered as complex rectangular variable S_{ij} , with P_{ij} the active power and Q_{ij} the reactive power. The complex conjugate operator is a superscripted '*'. Even though KLs applied to π-element results in a linear set of equations in current and voltage, adding equations to model (complex) power flow makes the set of equations nonconvex:

$$S_{ij} = P_{ij} + jQ_{ij} = (U_i\angle\theta_i)I_{ij}^{*} \tag{51}$$

Historically, OPF has been based on the static approximation to the power flow equations. This means that in the power flow equations, there are no time derivatives.

Voltage angles and reactive power do not have any useful meaning in the DC power flow domain. Nevertheless, the equations remain valid (with $\theta_{ij} = 0; Q_{ij} = 0 ; x_{l,s} = 0; b_{ij,sh} = 0$).

With interacting DC and AC grids, AC-DC converter models (for reactive power control of the AC-DC converter) need to be included.

10.2.7 Nodes

Any Node

Nodal aggregate power is the sum of all the power flows away from node *i* to any connected node *j*:

Voltage bounds can be applied at any node. These user supplied bounds can be used to reflect quality of supply standards such as EN50160 [115].

$$U_i^{min} \leq U_i \leq U_i^{max} \tag{52}$$

Normal Nodes

Complex power flows P_i and Q_i are determined by the units connected to the node. Voltage $U_i \angle \theta_i$ consequently varies. Some units may have controllers which regulate the voltage. Commonly, the buses that have generators with such controllers, are called PV buses. Typically, then, reactive power dispatch is changed to keep the voltage steady. More generally, active power dispatch can also be adapted to regulate the voltage.

Voltage angle reference node

One node is required to have a voltage angle reference:

$$\theta_i^{ref} \leq \theta_i \leq \theta_i^{ref} \tag{53}$$

Often, a slack node is used instead of just a voltage angle reference bus.

Slack node

A slack node is not required in general. However, in a radial grid, the slack node is used to represent the interaction with the external nodes, e.g. the transmission system. As the interface with the transmission system is generally stronger than the distribution grid connected to it, it is assumed that the slack bus can support a large complex power flow at a fixed voltage. Conversely, in a microgrid, one can choose not to include a slack node, but merely a voltage angle reference node.

It generally makes sense not to connect any loads or generators directly to this node, as these units do not influence the power flow physics. At a slack node, voltage magnitude and angle are fixed, but there are free variables (slack) for the complex power flow:

$$\theta_i^{ref} \leq \theta_i \leq \theta_i^{ref} \tag{54}$$

$$U_i^{ref} \leq U_i \leq U_i^{ref} \tag{55}$$

$$-\infty \leq P_i \leq \infty \tag{56}$$

$$-\infty \leq Q_i \leq \infty \tag{57}$$

10.2.8 Classic Power Flow Formulations

The power flow derivation in this section is based on the classic π-element representation as depicted in Figure 10-2. Three formulations are derived: rectangular, polar and DistFlow. Any of those formulations can be used straightaway in NLP solvers. Commonly, the polar formulation is implemented.

Power Flow Rectangular

The power balance and series and shunt currents are defined as the product of complex numbers.

$$P_{ij} + jQ_{ij} = (U_i \angle \theta_i)(I_{ij,sh} + I_{ij,s}) \tag{58}$$

$$I_{ij,s} = ((U_i \angle \theta_i) - (U_j \angle \theta_j))y_{l,s} \tag{59}$$

$$I_{ij,sh} = (U_i \angle \theta_i)y_{ij,sh} \tag{60}$$

Combining the equations above results in the rectangular formulation of power flow:

$$P_{ij} + jQ_{ij} = (U_i \angle \theta_i)\left((U_i \angle \theta_i)^* - (U_j \angle \theta_j)^*\right)y_{l,s}^* + U_i^2 y_{ij,sh}^* \tag{61}$$

Rectangular power flow Feasible Set I: (61)

Power Flow Polar

The power flow equations are formulated in polar form with trigonometric functions

$$\theta_{ij} = \theta_i - \theta_j \tag{62}$$

$$P_{ij} = (g_{l,s} + g_{ij,sh})U_i^2 - g_{l,s}U_iU_j\cos(\theta_{ij}) - b_{l,s}U_i U_j\sin(\theta_{ij}) \tag{63}$$

$$Q_{ij} = -(b_{l,s} + b_{ij,sh})U_i^2 + b_{l,s}U_iU_j\cos(\theta_{ij}) - g_{l,s}U_i U_j\sin(\theta_{ij}) \tag{64}$$

Polar power flow Feasible Set II: (62)-(64)

The phase angle difference over any section is generally limited to 90° :

$$-\pi/2 \le \theta_i^{min} \le \theta_{ij} \le \theta_i^{max} \le \pi/2 \tag{65}$$

Power Flow DistFlow

The *DistFlow* reformulation process takes the square of Ohm's law, and derives in a nonconvex quadratic equation in the variables of U_i; P_{ij} ;Q_{ij} and $I_{ij,s}$.

$$U_j^2 = U_i^2 - 2\left(r_{l,s}P_{ij,s} + x_{l,s}Q_{ij,s}\right) + (r_{l,s}^2 + x_{l,s}^2)I_{l,s}^2 \quad (66)$$

DistFlow power flow Feasible Set III: (66)

In the DistFlow reformulation, the voltage angle variables get substituted out. The voltage magnitudes and either end of a grid element can be related purely based on complex power flow and current magnitude observations. Such approximation does not change the results of the power flow in a radial grid, as the voltage angle variables can still be recovered through a process which gives a unique solution. However, in meshed grids this is not the case due to voltage angle constraint applying to any loop.

The power balance equations are derived as follows:

$$0 \leq P_{ij} + P_{ji} = P_l^{loss} = P_{l,sh}^{loss} + P_{l,s}^{loss} \quad (67)$$

$$Q_{ij} + Q_{ji} = Q_l^{loss} = Q_{l,sh}^{loss} + Q_{l,s}^{loss} \quad (68)$$

$$P_{l,s}^{loss} = r_{l,s}I_{l,s}^2 \quad (69)$$

$$Q_{l,s}^{loss} = x_{l,s}I_{l,s}^2 \quad (70)$$

$$P_{l,sh}^{loss} = g_{l,sh}U_i^2 \quad (71)$$

$$Q_{l,sh}^{loss} = -b_{l,sh}U_i^2 \quad (72)$$

$$I_{ij,s}^2 = (P_{ij}^2 + Q_{ij}^2)/U_i^2 \quad (73)$$

Note that U_i and $|I_{ij,s}|$ only appear as squared variables. The voltage angles should satisfy:

$$\theta_{ij} = \theta_i - \theta_j = \angle(U_i\angle\theta_i)((U_i\angle\theta_i) - z_{l,s}I_{ij,s})^* \quad (74)$$

$$\sum_{loop} \theta_{ij} = 0 \; mod \; 2\pi \quad (75)$$

The voltage angles in any loop have to add up to 0 mod 2π, which is trivially satisfied in a radial grid but which requires additional treatment in meshed grids [59], [74].

Operational Envelopes

10.2.8.1.1 Grid element ratings

Bounds on apparent power, current magnitude and voltage magnitude related to lines:

$$0 \leq |S_{ij}| \leq S_{ij}^{rated} \quad (76)$$

$$0 \leq |I_{ij}| \leq I_{ij}^{rated} \quad (77)$$

$$0 \leq U_i \leq M \cdot U_{ij}^{rated} \quad (78)$$

It is noted that the ratings do not need to be symmetric (ij ≠ ji), e.g. voltage ratings being different with transformers. It is furthermore noted that such voltage ratings, (which are generally always known, i.e. the rating depends on the cable material, insulation level, etc.), can be used to derive generic bounds on the voltages, but only by application of a big M.

Grid element ratings Feasible Set IV: (76)-(78)

10.2.8.1.2 Node ratings

Bounds voltage related to nodes:

$$0 \leq U_i^{min} \leq U_i \leq U_i^{max} \leq M \cdot U_i^{rated} \quad (79)$$

Again, it is assumed that the voltage rating (voltage level) to which nodes belong, is always known, i.e. U_i^{rated} . This can be used to define an upper bound on the voltages, even in absence of user-supplied bounds $\mathrm{U_i^{min}}, U_i^{max}$.

Node rating and bound Feasible Set V: (79)

10.3 Extended OPF Formulation

A commonly used model for the conducting elements is the π-element, as discussed in the previous section, which includes a series impedance and shunt admittances at each end of the line. This π-element can again be generalized to include voltage transformation, phase shifting and switching [116]. Such a formulation will be developed in this work and is referred to as the 'extended symmetric π-element' representation, as depicted in Figure 10-3. Figure 10-4 furthermore displays the complex-valued graph representation corresponding to the extended symmetric π-element. Finally, Figure 10-5 illustrates the real-valued graph representation.

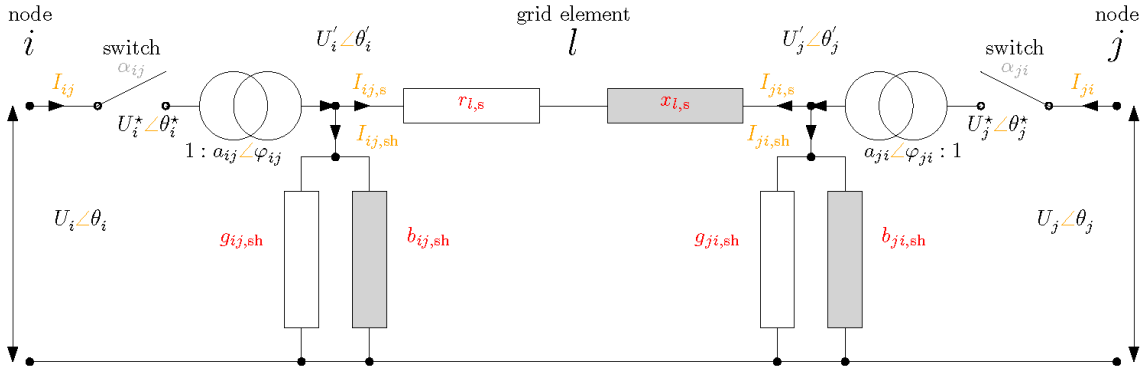

Figure 10-3 Balanced π-element-representation of a conducting element.

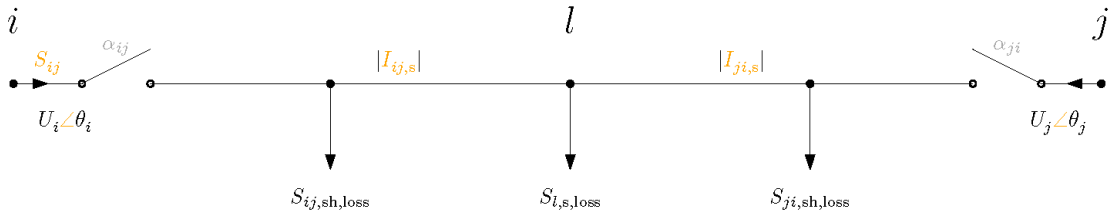

Figure 10-4 Complex-valued graph representation of the extended balanced π-element-representation.

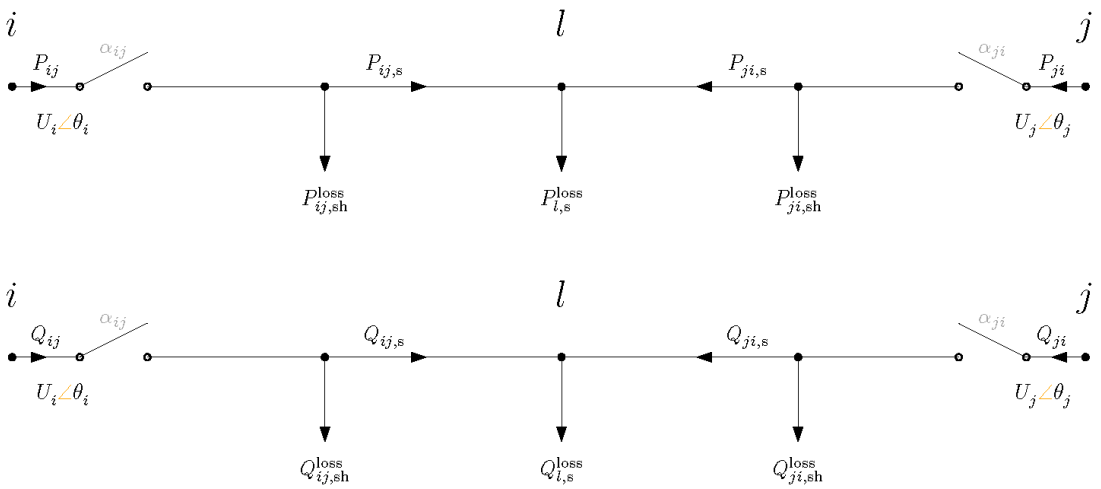

Figure 10-5 Real-valued graph representations of the extended balanced π-element-representation.

10.3.1 Transformer

The effective transformation ratio is defined as:

$$a_{ij} = {U_i'}/{U_i^*} \tag{80}$$

$$a_{ji} = {U_j'}/{U_j^*} \tag{81}$$

This voltage transformation ratio is bounded by a minimum and maximum value:

$$0 \le a_{ij}^{min} \le a_{ij} \le a_{ij}^{max} \tag{82}$$

$$0 \le a_{ji}^{min} \le a_{ji} \le a_{ji}^{max} \tag{83}$$

To operate at a known ratio, the lower a_{ij}^{min} ; a_{ji}^{min} and upper bounds a_{ij}^{max}; a_{ji}^{max} are given equal values. Minimum and maximum phase shifts are defined as:

$$0 \le \varphi_{ij}^{min} \le \varphi_{ij} \le \varphi_{ij}^{max} \tag{84}$$

$$0 \le \varphi_{ji}^{min} \le \varphi_{ji} \le \varphi_{ji}^{max} \tag{85}$$

$$\theta_i' = \theta_i^* + \varphi_{ij} \tag{86}$$

$$\theta_j' = \theta_j^* + \varphi_{ji} \tag{87}$$

To operate at a known phase shift, the lower φ_{ij}^{min} ; φ_{ji}^{min} and upper bounds φ_{ij}^{max} ; φ_{ji}^{max} are given equal values. Negative phase shifts can be handled by assigning the shift to the corresponding side of the element. A negative phase shift from i to j corresponds to a positive phase shift from j to i.

Having a transformer at each end allows to:

1. define the impedance model in any reference base
2. separate voltage transformation and tap changing
3. model tap changing at either side of the transformer.

10.3.2 Switch

For each grid element to have an interpretable state variable, switches are required at both ends. If only one switch is used, power may still flow in the grid element due to the contributions of the shunt elements. Only if switching occurs at both sides, power flow is guaranteed to be interrupted.

State α_l = 0 means both switches are in open position and the grid element does not conduct. State α_l = 1 means the switches are in closed position and the grid element does conduct. A disjunctive formulation is developed, which requires an upper bound on the voltage ('big M' notation used). In state α_l = 0, the voltage U_i^* is forced to 0, and U_i' is independent from U_i^*. In state α_l = 1, the voltage U_i^* is not forced to 0, but equality of U_i' with U_i^* is enforced. Forcing U_i^* to 0 is sufficient to stop power flow through the element.

$$\alpha_l \in \{0,1\} \tag{88}$$

$$0 \leq U_i^* \leq M \cdot \alpha_l \cdot U_{ij}^{rated} \tag{89}$$

$$0 \leq U_j^* \leq M \cdot \alpha_l \cdot U_{ji}^{rated} \tag{90}$$

$$0 \leq U_i - U_i^* \leq M(1-\alpha_l) \cdot U_{ij}^{rated} \tag{91}$$

$$0 \leq U_j - U_j^* \leq M(1-\alpha_l) \cdot U_{ji}^{rated} \tag{92}$$

If a switch is in the closed position, the voltage angles at either end of the switch are equal. If the switch is open, the voltage angles are not related.

$$-\pi/2 \cdot M \cdot (1-\alpha_l) \leq \theta_i - \theta_i^* \leq \pi/2 \cdot M(1-\alpha_l) \tag{93}$$

$$-\pi/2 \cdot M \cdot (1-\alpha_l) \leq \theta_j - \theta_j^* \leq \pi/2 \cdot M(1-\alpha_l) \tag{94}$$

$$-\pi/2 \cdot M \cdot \alpha_l \leq \theta_i' \leq \pi/2 \cdot M \cdot \alpha_l \tag{95}$$

$$-\pi/2 \cdot M \cdot \alpha_l \leq \theta_j' \leq \pi/2 \cdot M \cdot \alpha_l \tag{96}$$

Switches are dynamic elements and switching actions contribute to operational costs. The following types of constraints are often considered in this context:

- switch ramp rates
- switch costs
- switching restricted to certain time slots

To fix the state of the switch, bounds α_l^{min} and α_l^{max} can be used:

$$0 \leq \alpha_l^{min} \leq \alpha_l \leq \alpha_l^{max} \leq 1 \quad (97)$$

It is noted that the switch position does not need to be considered as a variable (through fixing the bounds and elimination and substitution), even though it can be used as a variable. Nevertheless, the variable switch formulation is also used in the modelling of discrete transformer taps, see further for details on this.

10.3.3 Branch Flow Model Formulation: DistFlow

Substitution

The complex current and voltage variables are replaced by squared current and voltage magnitude variables. There are no variables for current or voltage angles.

$$0 \leq i_{ij,s} = \left|I_{ij,s}\right|^2 \quad (98)$$

$$0 \leq i_{ij} = \left|I_{ij}\right|^2 \quad (99)$$

$$0 \leq u_i = U_i^2 \quad (100)$$

$$0 \leq u_i' = U_i'^2 \quad (101)$$

$$0 \leq u_i^* = U_i^{*2} \quad (102)$$

SOCP Convex Formulation

The *DistFlow* equations are reformulated in the squared variables:

$$0 \leq P_{ij} + P_{ji} = P_l^{loss} = P_{l,sh}^{loss} + P_{l,s}^{loss} \quad (103)$$

$$Q_{ij} + Q_{ji} = Q_l^{loss} = Q_{l,sh}^{loss} + Q_{l,s}^{loss} \quad (104)$$

$$P_{l,s}^{loss} = r_{l,s} i_{l,s} \quad (105)$$

$$Q_{l,s}^{loss} = x_{l,s} i_{l,s} \quad (106)$$

$$P_{l,sh}^{loss} = g_{l,sh} u_i' \quad (107)$$

$$Q_{l,sh}^{loss} = -b_{l,sh} u_i' \quad (108)$$

$$(P_{ij,s}^2 + Q_{ij,s}^2) \leq u_i' \cdot i_{l,s} \quad (109)$$

$$(u_i' - u_j') = -2(r_{l,s} P_{ij,s} + x_{l,s} Q_{ij,s}) + \left|z_{l,s}\right|^2 \cdot i_{l,s} \quad (110)$$

With respect to the nonconvex formulation, the convexification is the replacement of the equality symbol in (73) by the inequality in (109), obtaining a second-order cone. Basically, (110) reflects Ohm's law / KVL. Furthermore, KCL is reflected in the complex power balance equations (103)-(108) and (109) links the power, voltage and current variables together through the convex relaxation.

SOCP DistFlow

Feasible Set VI: (103)-(110)

Switch constraints are reformulated in the squared variables:

$$\alpha_l \in \{0,1\} \tag{111}$$

$$0 \le u_i^* \le M^2 \cdot \alpha_l \cdot (U_{ij}^{rated})^2 \tag{112}$$

$$0 \le u_j^* \le M^2 \cdot \alpha_l \cdot (U_{ij}^{rated})^2 \tag{113}$$

$$0 \le u_i - u_i^* \le M^2(1-\alpha_l) \cdot (U_{ij}^{rated})^2 \tag{114}$$

$$0 \le u_j - u_j^* \le M^2(1-\alpha_l) \cdot (U_{ij}^{rated})^2 \tag{115}$$

The power flow through the switch therefore satisfies:

$$P_{ij}^2 + Q_{ij}^2 \le (I_{ij}^{rated})^2 \cdot U_i^2 \cdot \alpha_l \tag{116}$$

This formulation effectively limits the total current magnitude $|I_{ij}|$ to a maximum of I_{ij}^{rated}, but doesn't require an explicit variable for the total current or total current magnitude. As the current rating isn't necessarily symmetrical, the equation is also considered for *ji*. This equation, after substitution, can be formulated in the new variables as:

$$P_{ij}^2 + Q_{ij}^2 \le (I_{ij}^{rated})^2 \cdot u_i \cdot \alpha_l \tag{117}$$

This convex expression is a rotated second-order cone.

Switching in squared voltage magnitude variables (MILP)

Feasible Set VII: (111)-(117)

Finally, the voltage magnitude transformation is reformulated in an exact manner as:

$$(a_{ij}^{min})^2 u_i^* \le u_i' \le (a_{ij}^{max})^2 u_i^* \tag{118}$$

$$(a_{ji}^{min})^2 u_j^* \le u_j' \le (a_{ji}^{max})^2 u_j^* \tag{119}$$

It is noted that all the constraints only contain real-valued variables and parameters, therefore no additional reformulation is required. In post-processing, complex-valued variables $I_{ij}, U_i \angle \theta_i$; S_{ij} are again obtained.

This relaxation can be penalized, to make sure $i_{ij,s}$ and u_i' lay on the cone surface:

$$\min Y^{PFconvex} = \frac{1}{n_{\mathcal{J}}} \sum_{l \in \mathcal{J}} \frac{i_{ij,s}}{(I_{ij}^{rated})^2} \quad (120)$$

Note that $P_{ij,s}$ or $Q_{ij,s}$, also in (109), cannot be easily penalized due to their unknown sign. The objective $Y^{PFconvex}$ is considered as a penalty in OPF problems with a wider scope, e.g. a multiperiod OPF with operational cost minimization. For more insights on the penalization of the SOCP relaxation, see section 4.4.5.

Operational Envelopes

The voltage, current and complex power envelopes are representable in the squared variables by taking the square of the original bounds.

$$(U_i^{min})^2 \leq u_i \leq (U_i^{max})^2 \quad (121)$$

$$0 \leq u_i' \leq M^2 \cdot (U_{ij}^{rated})^2 \quad (122)$$

$$0 \leq i_{ij,s} \leq M^2 \cdot (I_{ij}^{rated})^2 \quad (123)$$

$$P_{ij}^2 + Q_{ij}^2 \leq (S_{ij}^{rated})^2 \quad (124)$$

Extended SOCP DistFlow envelopes Feasible Set VIII: (118)-(120), (121)-(124)

Note that the apparent power flow bound on complex power flow (83) is a circular area constraint ($x_1^2 + x_2^2 \leq r^2$), which is convex and representable as a SOCP constraint. Note also that by including expression (123) an explicit formulation for the current bound is added to the constraint set.

Ultimately, the overall feasible set is derived:

Extended SOCP DistFlow Feasible Set IX: VI, VII, VIII

Post-Processing

The slack on the convexification is defined as follows:

$$\epsilon_{ij}^{PFconvex} = i_{ij,s} \cdot u_i' - P_{ij,s}^2 - Q_{ij,s}^2 \quad (125)$$

If $\epsilon_{ij}^{PFconvex} \approx 0$ then a physically meaningful optimum is obtained. Due to numerical effects, the slack will not be 0 exactly, and can even be slightly negative. If $\epsilon_{ij}^{PFconvex} \not\approx 0$ then the results are not physical. Slack on the convexification implies artificially increased grid losses.

The voltage angle difference must add up to zero in any cycle in a meshed grid [74].

$$\theta'_{ij} = \theta'_i - \theta'_j = \angle\left(u'_i - z_{l,s} S_{ij}\right) \tag{126}$$

$$\sum_{ij \in loop} \theta_{ij} = 0 \; mod \; 2\pi \tag{127}$$

This condition is trivially satisfied in a radial grid, but the error has to be checked when this formulation is applied to a meshed grid.

No post-processing is required for P_{ij} , Q_{ij} , α_l. The optimized variables $u_i, u_i^*, u'_i, i_{ij,s}$ need to be mapped back to the original variables $U_i, U_i^*, U'_i, \theta_i,\ \theta_i^*,\ \theta'_i,\ I_{ij}$. A possible procedure for post-processing is the following. Start from slack bus, and solve grid element by grid element, while walking down the tree of the network.

It is noted that a generic power flow solver can also be used to recover the results. Power flow solvers take as input the optimized dispatch of generators and loads $(P_u; Q_u)$ and the grid model (topology and parameters), to calculate voltages and currents throughout the system.

10.3.4 Bus Injection Model Formulation

Substitution

The complex voltage variables are replaced by cross-products of node voltages. There are no variables for voltage angles and current. Complex-valued variables Wij are elements in the matrix **W** (note that this implies $i, j \in \mathbb{N}^+$). The elements are assigned the products of voltage variables ($U'_i \angle \theta'_i$) and ($U'_j \angle \theta'_j$):

$$W_{ij} = 0 + 0j \quad \forall ij \notin \mathcal{J} \tag{128}$$

$$W_{ij} = \left(U'_i \angle \theta'_i\right)\left(U'_j \angle \theta'_j\right)^* \quad \forall ij \in \mathcal{J} \tag{129}$$

$$W_{ij} = (U'_i)^2 \tag{130}$$

Nonexistent connections ij have Wij set to zero (128). Therefore, the matrix $\boldsymbol{W}$ is sparse if the network is not too meshed. Note that this $n \times n$ matrix is Hermitian $\boldsymbol{W} \in \mathbb{H}^n$, as it satisfies $W_{ij} = W_{ji}^*$. This equality between the natural voltage variables and Wij (129)-(130) can also be formulated as constraints on this matrix variable:

$$\boldsymbol{W} \succcurlyeq 0 \tag{131}$$

$$rank(\boldsymbol{W}) = 1 \tag{132}$$

The positive semi-definiteness is encoded as (131) and the rank-1 requirement as (132). The power balance can be formulated as follows:

$$S_{ij} = (y_{l,s} + y_{ij,sh})^* W_{ii} - (y_{l,s}) W_{ij} \quad (133)$$

Overall, this formulation then is a rank-constrained SDP problem. Only due to the rank constraint, the problem is nonconvex. To obtain the SDP formulation, the rank constraint is simply dropped. Similar to Jabr formulation [41], the variables R_{ij} and T_{ij} are used to model the real and imaginary parts of the voltages, as follows:

$$W_{ij} = R_{ij} + jT_{ij} \quad (134)$$

$$R_{ij} = Re(W_{ij}) = U_i' U_j' \cos(\theta_{ij}') \quad (135)$$

$$T_{ij} = Im(W_{ij}) = U_i' U_j' \sin(\theta_{ij}') \quad (136)$$

It is noted that due to the substitution, the phase-shift variables are not explicit in the convex formulation. Furthermore, voltage angles relate by the following nonlinear equation:

$$\theta_i' - \theta_j' = atan2 \frac{T_{ij}}{R_{ij}} \quad (137)$$

A phase angle difference (PAD) constraint can therefore be formulated in these variables as follows:

$$\tan(\theta_{ij}'^{min}) R_{ij} \leq T_{ij} \leq \tan(\theta_{ij}'^{max}) R_{ij} \quad (138)$$

To obtain a tight convex hull, bounds implied on R_{ij} and T_{ij} , through bounds on W_{ii}, where W_{ii} are derived from (134)-(136), assuming $\theta_{ij} \in [-\pi/2, \pi/2]$:

$$0 \leq R_{ij} \leq M^2 \cdot U_{ij}^{rated} U_{ji}^{rated} \quad (139)$$

$$-M^2 \cdot U_{ij}^{rated} U_{ji}^{rated} \leq T_{ij} \leq M^2 \cdot U_{ij}^{rated} U_{ji}^{rated} \quad (140)$$

The voltage bounds are reformulated as

$$0 \leq (U_i^{min})^2 \leq W_{ii} \leq (U_i^{max})^2 \leq M^2 (U_i^{rated})^2 \quad (141)$$

SDP Convex Relaxation

It consists in dropping rank constraint (132) from the feasible set. If this relaxed formulation satisfies $rank(W) = 1$ in post-processing, the global optimum is found. The dropped rank constraint can be replaced with a rank minimization heuristic penalty, based on the trace of the matrix [117]:

$$\min tr(\boldsymbol{W}) = \sum_{i \in \mathcal{I}} W_{ii} \quad (142)$$

$$\min Y^{PFconvex} = \sum_{i \in \mathcal{I}} \frac{W_{ii}}{(U_i^{rated})^2} \quad (143)$$

SDP BIM

Feasible Set X: (131), (133)

SOCP Convex Relaxation

The positive semi-definiteness (PSD) matrix constraint can generally not be represented in SOCP in an exact manner. Another representation is developed for the squared voltage magnitude:

$$W_{ij}W_{ij}^{*} = (U_i'\angle\theta_i')(U_j'\angle\theta_j')^{*}(U_i'\angle\theta_j')^{*}(U_j'\angle\theta_i') \tag{144}$$

$$|W_{ij}|^2 = W_{ii}W_{jj} \tag{145}$$

This nonconvex equation is consequently relaxed:

$$|W_{ij}|^2 \leq W_{ii}W_{jj} \tag{146}$$

The above constraint is a rotated second-order cone. Note that this formulation is equivalent to a PSD constraint on 2 x 2 principal minors [30], [78] (for all effective lines *ij*) in the original matrix W:

$$\begin{bmatrix} W_{ii} & W_{ij} \\ W_{ij}^{*} & W_{jj} \end{bmatrix} \succcurlyeq 0 \Leftrightarrow |W_{ij}|^2 \leq W_{ii}W_{jj} \tag{147}$$

The resulting real-valued power flow equations are:

$$P_{ij} = (g_{l,s} + g_{ij,sh})W_{ii} - g_{l,s}R_{ij} - b_{l,s}T_{ij} \tag{148}$$

$$Q_{ij} = (-b_{l,s} + g_{ij,sh})W_{ii} + b_{l,s}R_{ij} - g_{l,s}T_{ij} \tag{149}$$

$$W_{ii}W_{jj} \geq R_{ij}^2 + T_{ij}^2 \tag{150}$$

SOCP BIM

Feasible Set XI: (148)-(150)

Note that $R_{ij} = R_{ji}$ but $T_{ij} + T_{ji} = 0$. Therefore, this relaxation can be penalized as follows:

$$\min Y^{PFconvex} = \frac{1}{n_{\mathcal{J}}}\sum_{i\in\mathcal{J}} R_{ij} \tag{151}$$

Post-processing

The slack on the convexification is defined as follows:

$$\epsilon_{ij}^{PFconvex} = W_{ii}W_{jj} - \left(R_{ij}^2\right) - (T_{ij}^2) \quad (152)$$

No post-processing is required for P_{ij}, Q_{ij} , α_l. The optimized variables R_{ij} , T_{ij} ,W_{ii} need to be mapped back to the original variables U_i, θ_i , I_{ij} . Start from slack bus, and calculate line by line, while walking down the tree of the network.

10.3.5 QC relaxation

The Quadratic Convex or QC formulation is based on the use of convex hulls of the sine and cosine function. Notation ⟨f(.)⟩ is used to indicate the convex hull of the function f(.). Instead of variables being bound by functions in equalities, variables can also be formulated as lying in the convex hull of nonlinear functions. As the original function is contained within that convex hull, through this methodology, a relaxation of the original problem is performed.

$$W_{ii}\epsilon\langle(U_i')^2\rangle \quad (153)$$

$$R_{ij}\epsilon\,\langle\langle U_i'U_j'\rangle\langle\cos(\theta_{ij}')\rangle\rangle \quad (154)$$

$$T_{ij}\epsilon\,\langle\langle U_i'U_j'\rangle\langle\sin(\theta_{ij}')\rangle\rangle \quad (155)$$

Convex Hull for Cosine Function

Tight convex hulls of sine, cosine and quadratic functions are derived in [45], [47]. The phase angle difference over any section is considered limited to 90°:

$$-\pi/2 \le \theta_{ij}'^{min} \le \theta_{ij}' \le \theta_i'^{max} \le \pi/2 \quad (156)$$

$$\theta_{ij}'^{absmax} = \max(\left|\theta_{ij}'^{min}\right|, \left|\theta_{ij}'^{max}\right|) \quad (157)$$

A visualization of the convex hull of the cosine function is shown in Figure 10-6. Variable c_{ij} models the result of the cosine function.

$$\langle\cos\left(\theta_{ij}'\right)\rangle \equiv \quad (158)$$

$$\begin{cases} c_{ij} \le 1 - \left(\dfrac{1-\cos(\theta_{ij}'^{absmax})}{(\theta_{ij}'^{absmax})^2}\right)\theta_{ij}'^2 \\ c_{ij} \ge \cos\left(\theta_{ij}'^{max}\right) + \dfrac{\cos\left(\theta_{ij}'^{min}\right) - \cos\left(\theta_{ij}'^{max}\right)}{\theta_{ij}'^{min} - \theta_{ij}'^{max}}(\theta_{ij}' - \theta_{ij}'^{min}) \end{cases}$$

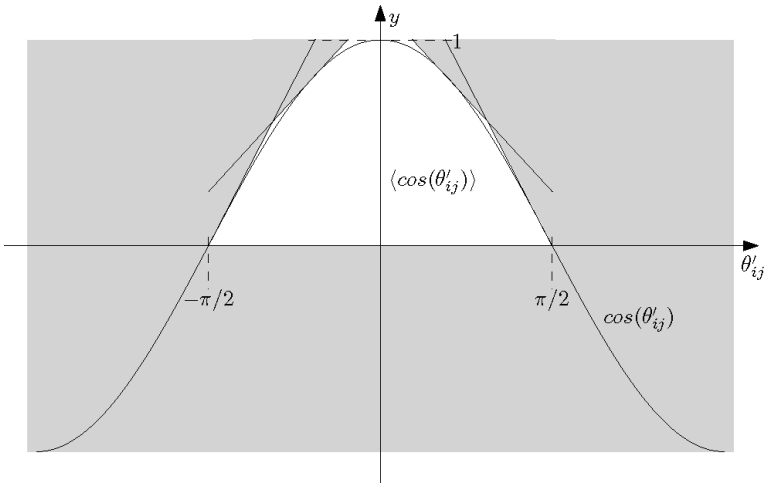

Figure 10-6 Polyhedral convex hull of cosine function in the range $-\frac{\pi}{2} \leq \theta'_{ij} \leq \frac{\pi}{2}$ [47].

It is noted that this constraint set is SOC-representable. Note that the tangent lines to the cosine in this domain can be represented as

$d \in 1,2, \ldots,$ (159)

$$td = \frac{2\theta_{ij}^{\prime max}}{h+1} \tag{160}$$

$$td \in \left[-\frac{\pi}{2}; \frac{\pi}{2}\right] \tag{161}$$

$$c_{ij} = -\sin(td)\left(\theta'_{ij} - td\right) + \cos(td) \tag{162}$$

Therefore, a polyhedral relaxation of the cosine function can be defined as:

$$\langle \cos(\theta'_{ij}) \rangle \equiv \tag{163}$$

$$\begin{cases} c_{ij} \leq -\sin\left(td - \theta_{ij}^{\prime max}\right)\left(\theta'_{ij} - td + \theta_{ij}^{\prime max}\right) + \cos(td - \theta_{ij}^{\prime max}) \\ c_{ij} \geq \cos\left(\theta_{ij}^{\prime max}\right) + \frac{\cos\left(\theta_{ij}^{\prime min}\right) - \cos\left(\theta_{ij}^{\prime max}\right)}{\theta_{ij}^{\prime min} - \theta_{ij}^{\prime max}}\left(\theta'_{ij} - \theta_{ij}^{\prime min}\right) \end{cases}$$

It is noted that another polyhedral relaxation can be obtained through the application of the Ben-Tal polyhedral relaxation technique to the SOCP representation of the quadratic convex terms.

Convex Hull for Sine Function

A visualization of the convex hull of the sine function is shown in Figure 10-7. Variable s_{ij} models the sine function:

$$\langle \sin(\theta'_{ij}) \rangle \equiv \tag{164}$$

$$\begin{cases} s_{ij} \le \cos\left(\frac{\theta_{ij}^{'absmax}}{2}\right)\left(\theta_{ij}' - \frac{\theta_{ij}^{'max}}{2}\right) + \sin(\frac{\theta_{ij}^{'absmax}}{2}) \\ s_{ij} \ge \cos\left(\frac{\theta_{ij}^{'absmax}}{2}\right)\left(\theta_{ij}' + \frac{\theta_{ij}^{'max}}{2}\right) - \sin(\frac{\theta_{ij}^{'absmax}}{2}) \\ s_{ij} \ge \sin(\theta_{ij}^{'min}) + \frac{\sin(\theta_{ij}^{'min}) - \sin(\theta_{ij}^{'max})}{\theta_{ij}^{'min} - \theta_{ij}^{'max}}(\theta_{ij}' - \theta_{ij}^{'min}) \;\; if\; \theta_{ij}^{'min} \ge 0 \\ s_{ij} \le \sin(\theta_{ij}^{'min}) + \frac{\sin(\theta_{ij}^{'min}) - \sin(\theta_{ij}^{'max})}{\theta_{ij}^{'min} - \theta_{ij}^{'max}}(\theta_{ij}' - \theta_{ij}^{'min}) \;\; if\; \theta_{ij}^{'max} \ge 0 \end{cases}$$

It is noted that this constraint set is polyhedral.

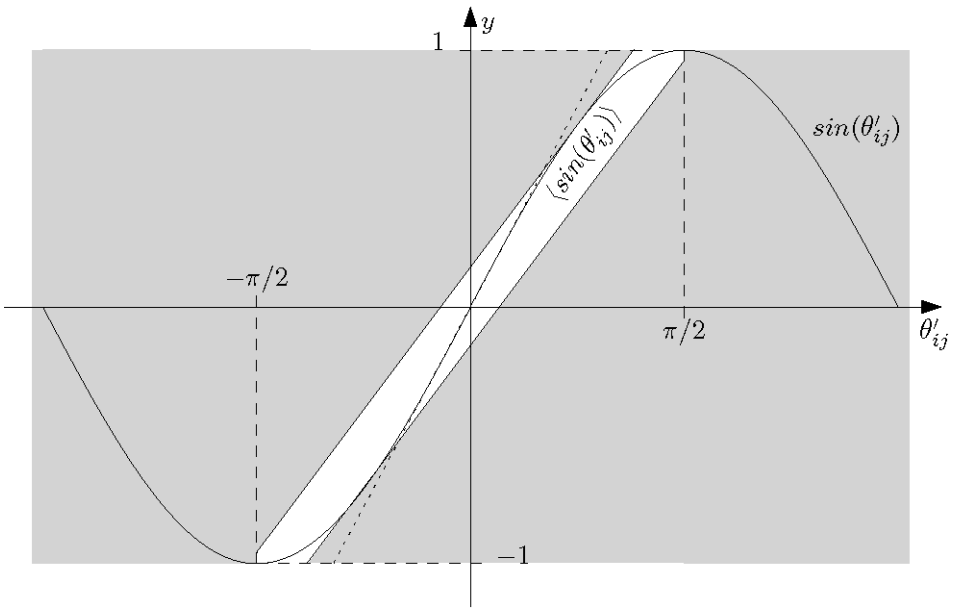

Figure 10-7 Polyhedral convex hull of sine function in the range $-\frac{\pi}{2} \le \theta_{ij}' \le$ [47]. *Note that* $\sin\theta_{ij}' = \theta_{ij}'$ *only lies within the convex hull for small angles.*

Convex Hull for Quadratic Variables

A visualization of the convex hull of the quadratic function is shown in Figure 10-8.

$$x^L \le x \le x^U \tag{165}$$

$$\langle x^2 \rangle \equiv \begin{cases} z \le x^2 \\ z \ge (x^L + x^U)x - x^L x^U \end{cases}$$

It is noted that this constraint set is SOC representable.

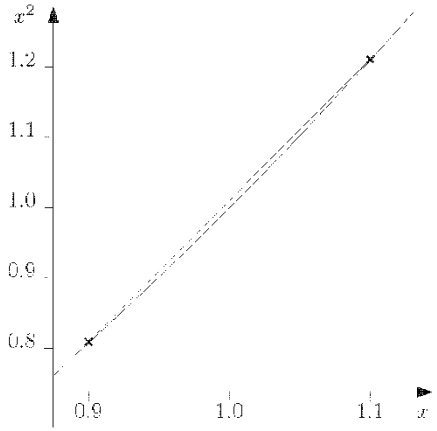

Figure 10-8 Convex hull of quadratic function [47] *illustrated in the domain* $x \in [0.9;\ 1.1]$.

McCormick's Envelopes for Bilinear Terms

$$x_1^L \le x_1 \le x_1^U \tag{166}$$

$$x_2^L \le x_2 \le x_2^U$$

$$\langle x_1 x_2 \rangle \equiv \begin{cases} y \ge x_2^U x_1 + x_1^U x_2 - x_1^U x_2^U \\ y \le x_2^L x_1 + x_1^U x_2 - x_1^L x_2^U \\ y \le x_2^U x_1 + x_1^L x_2 - x_1^U x_2^L \\ y \ge x_2^L x_1 + x_1^L x_2 - x_1^L x_2^L \end{cases}$$

Variable y models the result of the bilinear multiplication [118]. It is noted that this constraint set is polyhedral.

Overall QC Formulation

$$P_{ij} = (g_{l,s} + g_{ij,sh})u_{ii} - g_{l,s} r_{ij} - b_{l,s} t_{ij} \tag{167}$$

$$Q_{ij} = -(b_{l,s} + b_{ij,sh})u_{ii} + b_{l,s} r_{ij} - g_{l,s} t_{ij} \tag{168}$$

$$u_{ii} \in \langle U_i'^2 \rangle \tag{169}$$

$$u_{ij} \in \langle U_i' U_j' \rangle \tag{170}$$

$$c_{ij} \in \langle \cos(\theta_{ij}') \rangle \tag{171}$$

$$s_{ij} \in \langle \sin(\theta_{ij}') \rangle \tag{172}$$

$$r_{ij} \in \langle u_{ij} c_{ij} \rangle \tag{173}$$

$$t_{ij} \in \langle u_{ij} s_{ij} \rangle \quad (174)$$

The tighter the angle bounds $\theta_{ij}^{'min}$; $\theta_{ij}^{'max}$ are set, the tighter is the formulation.

QC Feasible Set XII: (154)-(174)

It is noted that the LPAC formulation [61] uses a convex-hull formulation of the cosine terms, in combination with a linearization of the sine terms. A piecewise linearization of this convex hull is used, which can be considered as a polyhedral relaxation of the quadratic hull proposed here. This LPAC approximation has a strong correlation with the NLP AC formulation in transmission systems, and is superior to the linearized 'DC' OPF formulation.

10.3.6 OPF Approximation: Linear DC Formulation

The linear 'DC' approximation is used in SmartNet to describe the transmission grid physical constraints in the market-clearing algorithm.

Model Formulation

The DC formulation has the following assumptions.

- Branches can be considered lossless. In particular, if branch parameters $r_{l,s}, b_{l,sh}$ and $g_{l,sh}$ are negligible:

$$y_{l,s} = \frac{1}{r_{l,s} + jx_{l,s}} \approx \frac{1}{jx_{l,s}}, \quad b_{l,sh} \approx 0, \quad g_{l,sh} \approx 0 \quad (175)$$

- All bus voltage magnitudes are close to one p.u.

$$U_i \approx 1 \quad (176)$$

- Voltage angle differences across branches are small:

$$\sin(\theta_i - \theta_j + \varphi_{ij}) \approx \theta_i - \theta_j + \varphi_{ij} \quad (177)$$

- All the shunt elements can be considered as PQ load at constant voltage (e.g. nominal voltage) and added to the loads vector.

The approximate real power flow is then:

$$P_{ij} \approx \frac{a_{ij}}{x_{l,s}} (\theta_i - \theta_j + \varphi_{ij}) \quad (178)$$

As expected, given the lossless assumption, a similar derivation for the power injection at the *two* ends of the line leads to $P_{ij} = -P_{ji}$.

10.3.6.1.1 HVDC Links

The HVDC links can be modelled by the use of generators with opposite injection. The losses within the DC cable, in first approximation, can be neglected.

10.3.6.1.2 FACTS Approximations

In the DC approximation, all reactive power control devices are disregarded. Other devices that are used only for specific applications (e.g. oscillation damping or the increase of the transmission capability) are also neglected in the DC approximation. The only devices to be modelled are those who directly affect the active power flow. There are different models which can be used for each single device [119], [120]. However, from the point of view of the DC model, the effect of the active phase shifters is to change the active power flow of a line, independently from the particular model or control scheme. Then, for the DC model it is only necessary to know the active power or the equivalent phase shifting as shown in [83], [86], [121].

Including Losses

Including the active power losses gives a better alignment of the AC and DC models. It was shown that a significant part of the error of the DC approximation comes from not considering the contribution of network losses.

It is possible to improve the DC model including a first approximation of the losses. The main problem to include them is that it is necessary to know them before calculating the power flow. Either the losses are already known from conventional values (based on the operational experience), or it is necessary to calculate a complete AC power flow, which considers both the reactive power flow and the resistance of the lines. Once the losses are known, it is possible to take them into account, either by increasing the loads or by decreasing the generator power injections.

If only the total amount of losses is known, it is possible to scale all the loads or generators (usually with a proportional multiplication factor). If the specific losses of every single line are known, it is possible to assign the losses of a line directly to the loads or generators of the two busses between which the specific line is connected [83], [122].

The final procedure to include the losses in the platform calculations will depend also on the available data and on the structure of the platform itself. To show the effectiveness of the procedure five methods of considering the network losses are addressed here.

10.3.6.1.3 Method 1 - Flat Loss-Profile

Method 1 uses a flat loss-profile, which is added proportionally to the load. The value of the flat loss-profile parameter is selected to a fixed value, e.g. 2.5% (e.g. this value represents the percentage of losses in the Spanish transmission network under normal conditions).

10.3.6.1.4 Method 2 - Flat Loss-Profile Recomputed

The previous method fails when the losses are different with respect the fixed value, in these cases the error is concentrated particularly in the slack bus. Then the losses are recomputed for each particular scenario.

10.3.6.1.5 Method 3 - Losses Proportional to each Bus

In method 3, the losses of each line in the DC power flow are assigned to the loads at the two busses connected by the line with a 50% distribution. This method should reduce the error of the DC approximation, since it conserves the geographic location of the losses.

10.3.6.1.6 Method 4 - Error Proportional to each Gen

It is like the method 2, but in this case the losses are assigned proportionally to the generator productions.

10.3.6.1.7 Method 5 - Error Proportional to Each Gen and Generator in Half

It is like the method 2, but in this case the losses are assigned 50% proportionally to the generator productions and 50% to the load.

Improved Impedance Calculation

It is possible to use the following approximation in the DC power flow:

$$y_{l,s} = -j\frac{x_{l,s}}{r_{l,s}^2 + x_{l,s}^2} \approx \frac{1}{jx_{l,s}}, \quad b_{l,sh} \approx 0, \;\; g_{l,sh} \approx 0 \tag{179}$$

This equation represents the Improved Impedance Calculation (IIC) and it should give a more accurate behavior since it also takes the resistance of the lines into account. However, the achievable improvement depends on the structure and the parameters of the network.

DC Model Accuracy

It is impossible to evaluate a priori the accuracy of the DC model: it depends from the particular network and scenario considered. However, some considerations can be made in order to know where the errors come from [122].

- Neglecting the losses brings an error of a few percent. However, if the network is big and there is only one slack bus, the error in the proximity of the slack bus can increase considerably. Then it is necessary to distribute the losses to all the network busses.

- The maximum angle difference between two busses is usually 40°, then the errors between $\sin(\theta)$ and θ is usually less than 8.6%.

- If the voltage limits are taken in the range of 0.75 to 1.4 pu, the maximum error is about 44%.

- The error of neglecting the resistance of the lines depends on the r/x ratio of the lines. For r/x ratios of about 1/3 the error is about 11%, which increases for higher ratio. However usually the error of a DC model is much lower and the accuracy of the DC power flow is around 5% of the AC power flow, but in particular lines the error can greatly increase [86]. In particular if the r/x ratio is smaller than 0.25, then the error in the power flows across the lines, when considering AC and DC solution, does not exceed 5% for the vast majority of lines [123]. This because usually the r/x ratio is very small and similar for all the lines, then the flows in the DC model divide themselves in the same way of the AC model. Besides that, the voltage and angle differences between two consecutive busses are usually low. These approximations are not true with particular non-linearities of the AC model (e.g. voltage dependence of the load, effects of shunt elements, differences in high meshed network…). These errors can be usually neglected for the market applications [83].

10.3.7 A few extensions

Additional models and their feasible sets are developed in this section.

Partial Slack Node to Link DistFlow with Linearized OPF

In linearized 'DC' OPF, active power flow and voltage angles are represented, but reactive power and voltage magnitudes are not modelled. Therefore, to link the linearized 'DC' formulation, used for transmission grid modeling, with the DistFlow formulation, used in distribution grid modeling, a new slack node type is defined at their common interface:

$$U_i^{ref} \leq U_i \leq U_i^{ref} \tag{180}$$

$$-\infty \leq Q_i \leq \infty \tag{181}$$

A voltage angle reference node can still be defined at any node in the model of the transmission system.

OLTC Transformer with Discrete Steps

An on-load tap changing (OLTC) transformer is already modelled in a continuous way using the formulations developed in Section 10.3.1. Often, tap changers have a limited number of discrete settings, e.g. $a_{ij} \in \{0.90, 0.92, \ldots, 1.08, 1.10\}$. Such integrality constraint is considered as a 'special ordered set of type 1'

(SOS1) constraint [124], a MILP formulation technique which models stepwise functions. One adds, for each possible tap setting *l*, the switch state variable α_l:

$$\alpha_l \in \{0,1\} \tag{182}$$

$$\sum_l \alpha_l = 1 \tag{183}$$

For each tap, one also adds a transformer to the optimization model with a known tap $a_{ij}^{min} = a_{ij}^{max} \in \{0.90, 0.92, \ldots, 1.08, 1.10\}$. All these transformers are virtually put in parallel. The SOS1 constraint enforces that only one of those transformers will actually be used. The fact that the *values* in the tap set have an order can be exploited by certain solvers.

ZIP Load Models

Generic load behavior, defined by a reference P_u^{ref} is often described in terms of constant impedance (Z), current (I) and power (P) parts (hence the ZIP name), respectively through parameters a_u^{zP} ; a_u^{IP} ; a_u^{PP}.

Such ZIP load model is (for active power) formulated as follows:

$$0 \le a_u^{zP} \le 1 \,; 0 \le\ a_u^{IP}\ \le 1;\ 0 \le a_u^{PP} \le 1 \tag{184}$$

$$a_u^{zP} + a_u^{IP} + a_u^{PP} = 1 \tag{185}$$

$$P_u = \left(a_u^{zP} \left(\frac{U_u}{U_u^{ref}} \right)^2 + a_u^{IP} \frac{U_u}{U_u^{ref}} + a_u^{PP} \right) P_u^{ref} \tag{186}$$

Here, U_u is the voltage magnitude seen by the unit, namely the voltage of the node U_i the unit is connected to (there exists a mapping of *u* to i). From this formulation, it can be immediately seen that the Z and P components are compatible with the convexified AC OPF formulations previously developed. Therefore, with a_u^{IP} = 0, the model is exact in those variables. Nevertheless, there is no variable representing the voltage magnitude U_u in that set of variables, only a variable for $(U_u)^2$. An approximation $U_u^{lin} \approx U_u$ is developed based on the Taylor series in the neighborhood of U_u^{ref}.

$$U_u^{lin} = U_u^{ref} + \frac{1}{2U_u^{ref}}(u_u - (U_u^{ref})^2) \tag{187}$$

The approximated ZIP formulation then becomes:

$$P_u = \left(a_u^{zP} \left(\frac{u_u}{(U_u^{ref})^2} \right) + a_u^{IP} \frac{U_u^{lin}}{U_u^{ref}} + a_u^{PP} \right) P_u^{ref} \tag{188}$$

This formulation is linear in the squared voltage magnitude variable u_u. It is noted that ZIP models are inherently approximate in any case, as it abstracts behavior of individual consumers and distributed generation units. An equivalent ZIP formulation is sometimes developed for reactive power.

Radiality Enforcement in Reconfiguration

If the grid element state variables are free, one can develop optimization formulations for reconfiguration. A common objective for grid reconfiguration is minimization of grid (energy) losses.

$$\min P^{loss} \tag{189}$$

It is noted that equivalent formulations exist to enforce the radiality [125], which could be more computationally efficient, depending on the case. Such constraint sets include 'single commodity flow', 'multi-commodity flow', and 'spanning tree' [125]. Below, the spanning tree formulation is illustrated. Grid elements are either active, inactive, or the switch states can be optimized (190). Only limited number of grid elements are active at the same time, to satisfy a necessary condition for radiality: the number of lines equals the number of nodes minus one (191). For each line, there is a parent node indicator variable which is binary (192). A line has at most one parent node (193) and if it has a parent node, then the line is in the state "ON". Every non-slack node is a parent node once (194) - (195).

$$0 \leq \alpha_l^{min} \leq \alpha_l \leq \alpha_l^{max} \leq 1 \tag{190}$$

$$\sum_{l \in \mathcal{J}} \alpha_l = n_{\mathcal{J}} - 1 \tag{191}$$

$$\beta_{ij} \in \{0,1\}, \beta_{ji} \in \{0,1\} \tag{192}$$

$$\beta_{ij} + \beta_{ji} = \alpha_l \tag{193}$$

$$\forall i \in \mathcal{I}_{d,SB}: \beta_{ij} = 0 \tag{194}$$

$$\forall i \in \mathcal{I}_{d,nonSB}: \sum \beta_{ij} = 1 \tag{195}$$

As the binary nature of α_l is already guaranteed due to the integrality constraint (190), the integrality constraint (192) can be removed.

Unit Modeling Approaches

Frameworks for MILP and MISOCP unit models, for convex multiperiod OPF, are developed in [126], [127]. Furthermore, volt-var control can be incorporated in the models of inverters or synchronous machines [126], [128].

10.3.8 Network modeling formulation extra's

Definition atan2

atan2 is a variation on the arctangent function with two arguments instead of one. This allows to distinguish the sign of both arguments.

$$atan2(y,x) = \tag{196}$$

$$\begin{cases} \arctan\left(\frac{y}{x}\right) & if\ x > 0 \\ \arctan\left(\frac{y}{x}\right) + \pi & if\ x < 0\ and\ y \geq 0 \\ \arctan(y,x) - \pi & if\ x > 0\ and\ y > 0 \\ +\frac{\pi}{2} & if\ x = 0\ and\ y > 0 \\ -\frac{\pi}{2} & if\ x = 0\ and\ y < 0 \\ undefined & if\ x = 0\ and\ y = 0 \end{cases}$$

Rotated SOCP

The 2-norm representation of a rotated SOC is the following

$$x_1^2 + x_2^2 \leq x_3 x_4, \quad x_3 \geq 0, x_4 \geq 0 \tag{197}$$

$$\Leftrightarrow \left\| \begin{bmatrix} 2x_1 \\ 2x_2 \\ x_3 - x_4 \end{bmatrix} \right\| \leq x_3 + x_4$$

$$(2x_1)^2 + (2x_2)^2 + (x_3 - x_4)^2 \leq (x_3 + x_4)^2$$

$$(2x_1)^2 + (2x_2)^2 + (x_3^2 - 2x_3x_4 + x_4^2) \leq (x_3^2 + 2x_3x_4 + x_4^2)$$

A quadratic constraint $(x_1)^2 + (x_2)^2 \leq x_3$ with $x_3 \geq 0$ can be written as such a rotated SOC with $x_4^{ref} \leq x_4 \leq x_4^{ref}$.

10.4 Illustration of power flow approximations and relaxations: calculation results

This section describes the results obtained by the optimal power flow calculations using the different options for approximation or relaxation described above.

10.4.1 Objective

The objective for the optimal power flow problems dealt with in the case studies discussed below is to determine the minimal curtailing cost while still maintaining the branch power flows and bus voltages within their respective ratings. The assumptions of the curtailment flexibility in the case studies are assumed to be the following:

- The active power of the generators in the network can be curtailed up to 50% of its initial value. The bounds on the reactive power output of the generators are set to be the reactive output at a power factor of 0.8 at the initial, i.e. maximal, active power generation. The constraints on the generated power are implemented as box constraints with the upper and lower bounds of active and reactive power specifying the box edges.

- The curtailable loads can be curtailed up to 20% of their initial value. The curtailable loads are assumed to have a constant power factor; hence their reactive power consumption is dependent on the active power consumption.

The minimal curtailment cost (€) is expressed as:

$$\boldsymbol{K_{cost}} = \sum_{\boldsymbol{u \in \mathcal{U}}} (\boldsymbol{c_u^{curt,P}} \left| \boldsymbol{P_u} - \boldsymbol{P_u^{ref}} \right| + \boldsymbol{c_u^{curt,Q}} \left| \boldsymbol{Q_u} - \boldsymbol{Q_u^{ref}} \right|) \tag{198}$$

The objective used in the optimization problem Y_{cost} is normalized as follows:

$$Y_{cost} = \frac{K_{cost}}{\sum_{u \in \mathcal{U}} (c_u^{curt,P} P_u^{ref} + c_u^{curt,Q} Q_u^{ref})} \tag{199}$$

with P_u^{ref} and Q_u^{ref} the initial power (active and reactive) consumption of the $u \in \mathcal{U}$ flexible units (here: dispatchable generators and curtailable loads). Curtailing costs are assumed to be equal for each curtailable load and generator ($c_u^{curt,P}$ = 10€/MW curtailed). A curtailing cost is also applied for a change in reactive power output of the generators ($c_u^{curt,Q}$ = 10€/MVAr adapted). This cost function is convex.

10.4.2 Case Studies

The OPF calculations are applied on different case studies. All case studies build on an adaptation of the Atlantide test grid, i.e. a MV distribution network provided by ENEL Distribuzione through the Atlantide project [129]. It is a typical radial distribution network where commercial, residential and industrial customers are connected. The radial network has 101 AC lines connecting the 100 AC buses with 15 kV as rated voltage. The total length of the lines is 120.42 km, divided in overhead lines (53.32 km) and cables (67.10 km). A total of 128 loads are connected to the network, divided in residential, commercial and industrial loads. In addition to this, 28 generators are connected to the network, they are either rotating (3 wind generators and 3 CHPs) or static (22 photovoltaic solar panel installations) generators. A schematic of the network is shown in Figure 10-9, the generators are indicated as blue circles, the loads as greenhouse-shaped nodes. Some of the loads are curtailable; these are indicated as light-green loads.

Three case studies were defined: 'undervoltage', 'overvoltage' and 'overcurrent'. Depending on the case study, the power demand and generation of each load/generator is adapted so that the grid suffers from bus voltages below the voltage limit, above the voltage limit and/or branch powers exceeding branch ratings, if no curtailing would be applied. Figure 10-10 shows the calculated bus voltages in each case study, Figure 10-11 shows the calculated branch powers, and Figure 10-12 shows the number of each type of constraint violation (undervoltage, overvoltage or power limit excess).

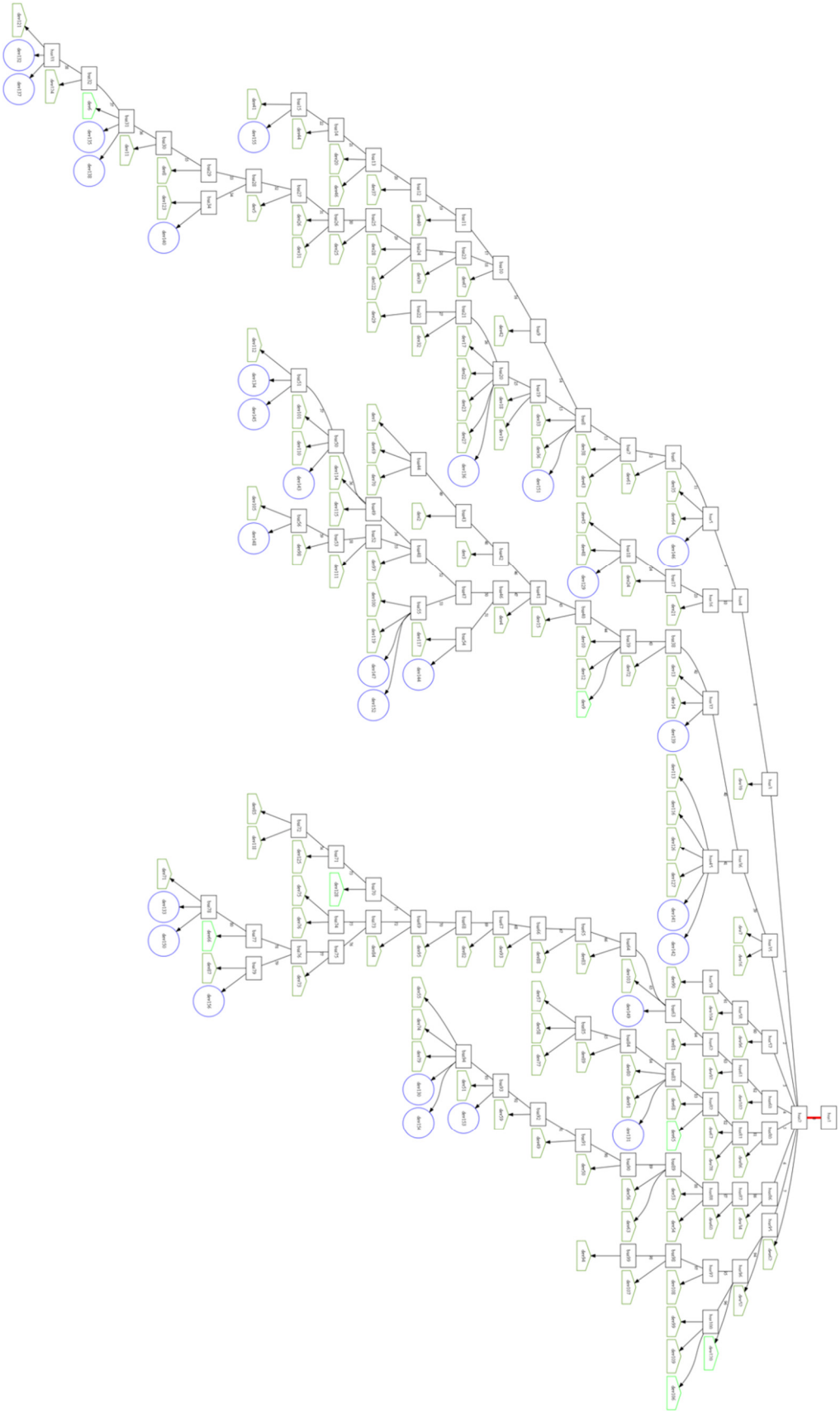

Figure 10-9 Schematic of the adapted Atlantide MV distribution grid.

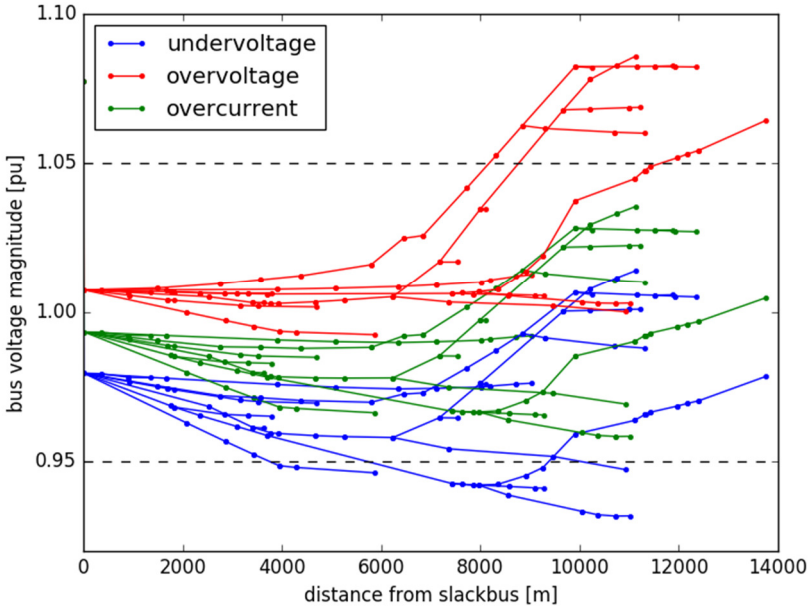

Figure 10-10 Bus voltages for each case study (without curtailing).

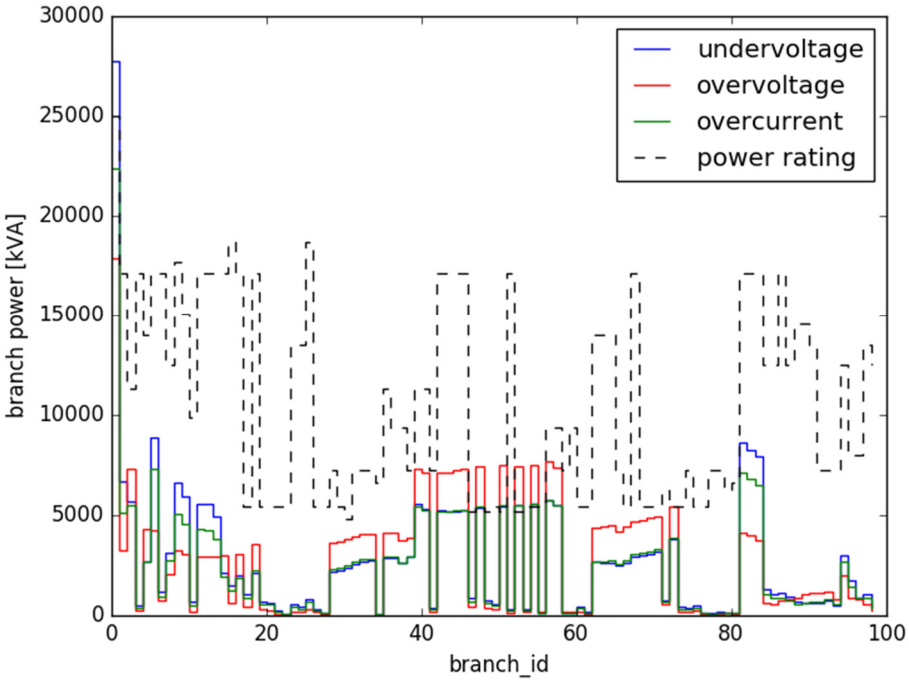

Figure 10-11 Branch power for each case study (without curtailing).

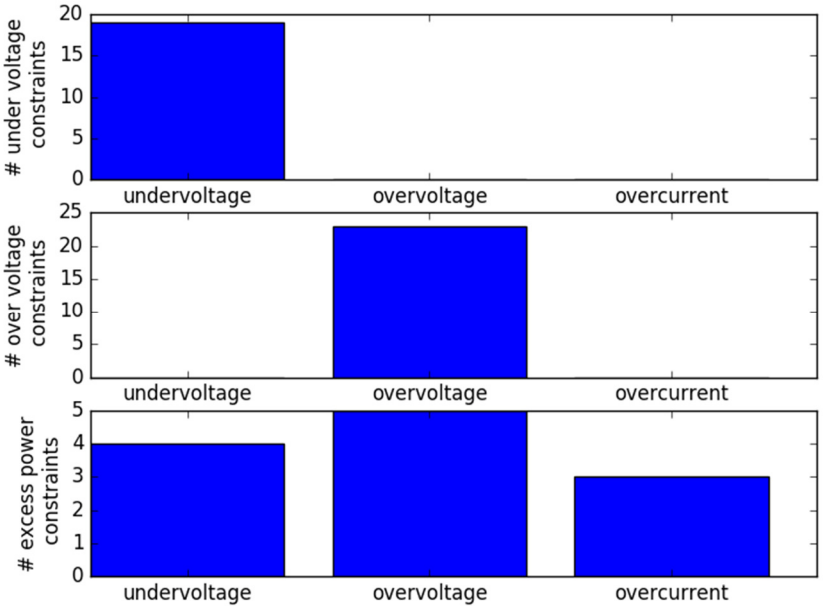

Figure 10-12 The number of constraint violations for each scenario.

10.4.3 Tool Chain

All power flow and optimal power flow calculations are implemented in Python. All variables and parameters are expressed in pu-values, with a power base equal to the rated power of the substation transformer (25 MVA), and a voltage base equal to the rated voltage of the MV network (15 kV).

The optimal power flow calculations using a convex relaxation or linear approximation are implemented using CVXPY [130], with ECOS [131] used as solver. PYPOWER [132] is used to calculate the nonconvex AC optimal power flow result. The PYPOWER package includes the MIPS (Mixed Integer Programming) solver, which is an implementation of an interior-point method for nonconvex problems. MIPS only guarantees that the solution is locally optimal. Following the optimization, the obtained result, i.e. the obtained active and reactive power output from curtailable loads and generators, is fed into a power flow calculation, also provided by PYPOWER [132]. This load flow result is used to check the feasibility of the optimization result. The tool-chain and calculation methodology are illustrated in Figure 10-13.

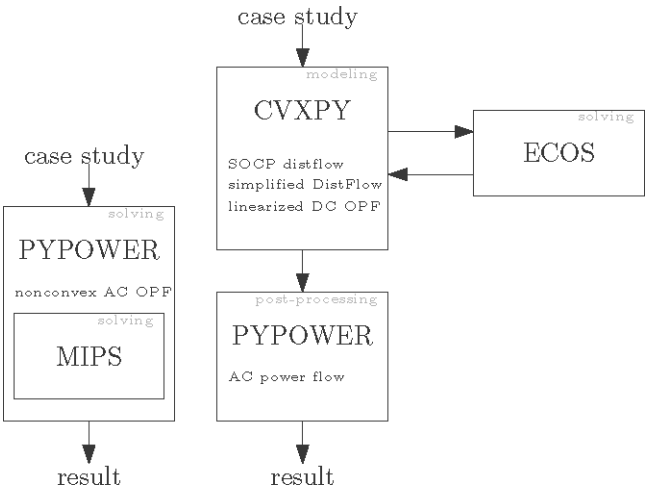

Figure 10-13 Illustration of tool-chain & methodology

The following formulations are compared in the upcoming section with numerical results:

- *AC – NLP*
- *DistFlow - SOCP*
- *DistFlow Ben-Tal - LP*
- *Simplified DistFlow - LP*
- *Linearized 'DC' – LP*

10.4.4 Numerical Comparison of OPF Formulations

Scaling of SOCP Penalty Factor

As indicated in Section 4.3, a penalization factor $w \cdot Y^{PFconvex}$ needs to be added to the optimization objective of the SOC relaxation of the optimal power flow, so that the obtained result lies on the cone surface. The SOCP result is then physically meaningful and hence a feasible result (when applied to radial grids). In order to test if an obtained result is feasible, the total relaxation 'slack' $\epsilon^{PFconvex}$ is calculated. If the calculated slack $\epsilon^{PFconvex} \approx 0$, the optimization result lies on the cone surface. Computational tests were performed to see how sensitive the obtained results are for the weight w that is given to the penalty factor in the optimization objective function. The penalization factor used in the tests is:

$$\boldsymbol{w \cdot Y^{PFconvex}} = \frac{\boldsymbol{w}}{\boldsymbol{n_{\mathcal{J}}}} \sum_{l \in \mathcal{J}} \boldsymbol{i_{ij,s}} \tag{200}$$

where $\boldsymbol{n_j}$ is the number of lines and $i_{ij,s}$ is the squared current variable on the line between node *i* and node *j* ,expressed as a pu-value. The equation is the similar to eq. (120) , but with the possibility to adjust the weights. The given weight to the penalty factor should be high enough so that slack is removed from the relaxation, but at the same time should be not too high so that is optimized towards minimal curtailing and not towards minimal current.

Figure 10-14 shows the optimization results when the weight w is varied for each case study. The top plot of these figures shows the obtained objective value, consisting of the curtailed cost value and the value of the penalization term (indicated in red). The middle plot shows the total slack $\epsilon^{PFconvex}$ of the SOCP relaxation. The bottom plot shows the obtained curtailing cost of the optimization result Kcost, obtained from (224).

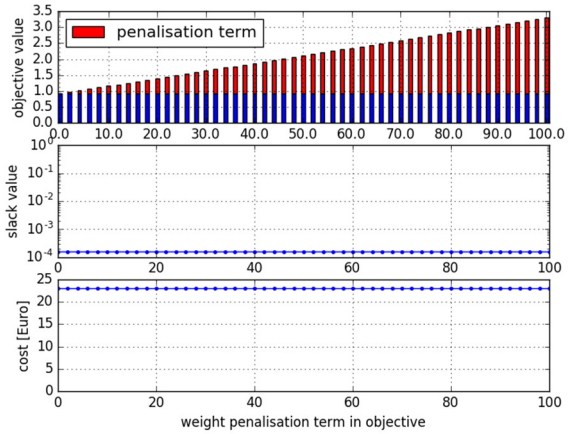

Figure 10-14 Sensitivity of penalization factor in the 'undervoltage' case study.

It can be seen from Figure 10-14 that for the 'undervoltage' case study, no penalty factor is needed in order to find a feasible, optimal solution. This complies with the observation that relaxation slack is found when additional 'non-physical' losses would be beneficial for a solution, however, undervoltages can never be solved by these additional losses. This can be seen by observing eq. (120) .

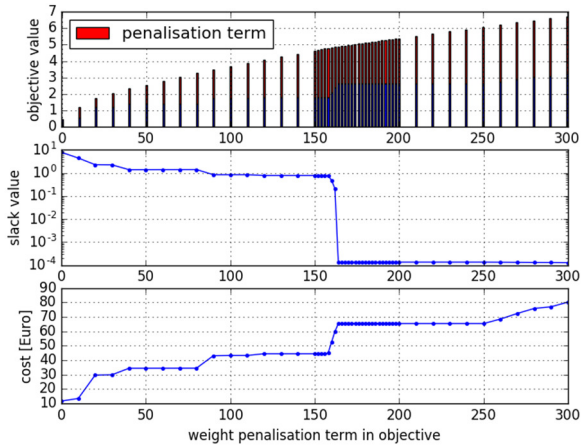

Figure 10-15 Sensitivity of penalization factor in the 'overvoltage' case study.

In the 'overvoltage' case study, the optimization result is quite robust in terms of penalty weight: the optimization result lies on the cone surface and does not change with a weight w ranging from ±164 to ±250. When using a penalty weight within this range, the obtained result is the optimal one.

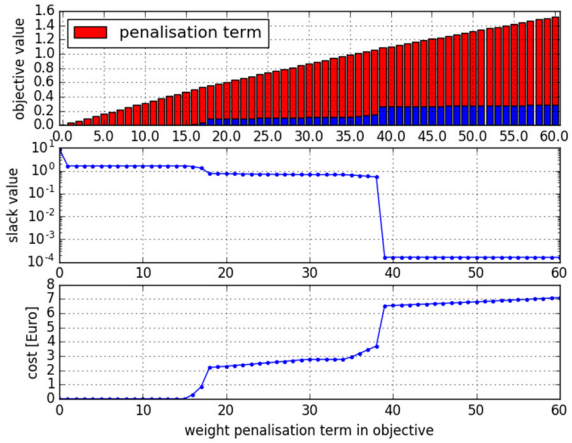

Figure 10-16 Sensitivity of penalization factor in the 'overcurrent' case study.

In the 'overcurrent' case study, however, the optimization is much less robust against the penalty weight: the result is only optimal (in terms of curtailing cost) with a penalty weight within a very small range around 39. This indicates that for every scenario and case study, the penalty weight should be carefully chosen so that the obtained result is feasible, and is optimal at the same time, especially when overvoltages and current limit constraint violations are found, since fake losses could be used for these two use cases to solve them, while for under-voltages it is not possible.

Relaxation and Approximation Approaches Compared

A comparison is made of the results found by the SOCP relaxation, the DC OPF approximation and the Simplified DistFlow approximation of the optimal power flow problem for the three case studies. A nonconvex AC optimal power flow is also added to the comparison.

10.4.4.1.1 'Undervoltage' Case Study

Figure 10-17 and Figure 10-18 show a comparison of the results found of the different OPF approaches of the 'undervoltage' case study. Figure 10-17 shows the active and reactive power consumed or generated by the flexible resources in the solutions obtained through the different optimization approaches. Figure 10-18 gives an overview of the resulting costs of each solution, the corresponding grid losses for each solution and the constraint violations found of the post-processed results of each optimization approach. From these results, we can conclude the following:

- The solution found by the DC OPF approximation is, although in cost the cheapest solution, not a feasible one. The overall number of constraint violations found in the original situation does not change by applying the DC OPF approximation.
- The solution found through the Simplified DistFlow approach is also not a feasible solution, but is still able to solve some of the constraints found in the original situation. Generally speaking, voltage drops are underestimated in the Simplified DistFlow approximation, hence the non-feasible solution. In this case study, the cost of the Simplified DistFlow solution is lower than the cost of the SOCP solution, but grid losses are higher.
- The SOCP approach yields a feasible solution with least grid losses and the lowest curtailment cost.
- The solution of the nonconvex AC OPF is not the optimal solution (cost is higher than the SOCP solution), indicating that in this case study the nonlinear solver reaches a local optimum.

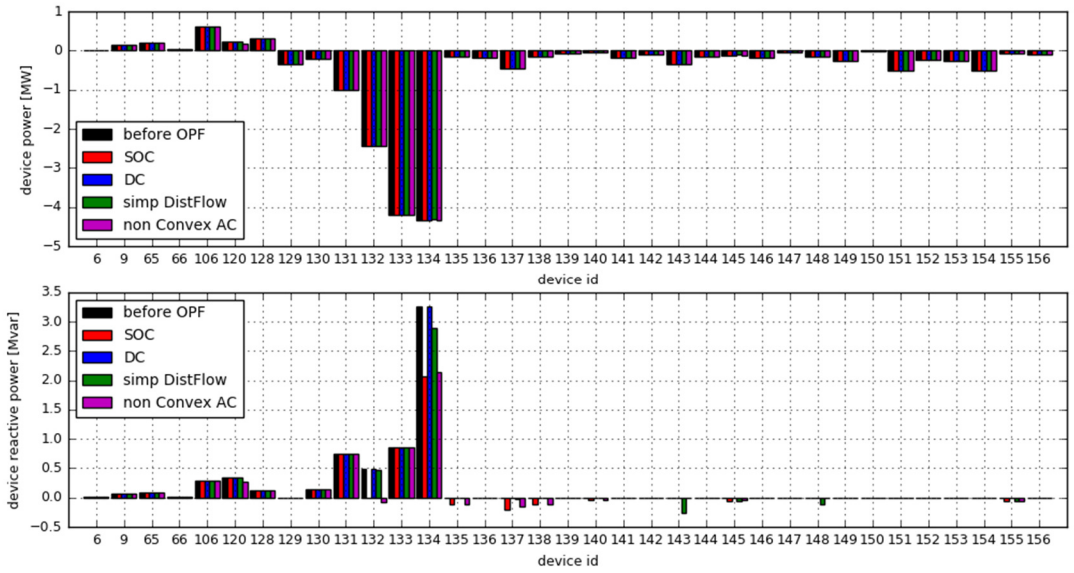

Figure 10-17 Comparison of solutions found by different formulations for the 'undervoltage' case study.

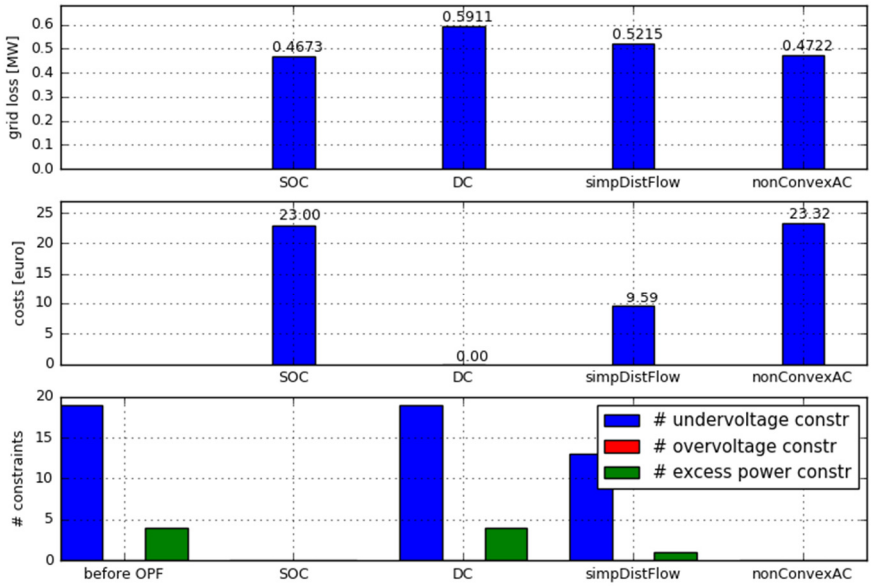

Figure 10-18 The resulting costs and grid losses of the different solutions in the 'undervoltage' case study.

10.4.4.1.2 'Overvoltage' Case Study

Figure 10-19 and Figure 10-20 show a comparison of the results found of the different OPF approaches of the 'overvoltage' case study. From these results, we can conclude the following:

- The solution found by the DC OPF approximation is, although in cost a very cheap solution, not a feasible one. This solution solves almost none of the constraint violations that were found in the original situation.

- The solution found through the Simplified DistFlow approach is a feasible solution. However, the cost of this solution is higher than the cost of the SOCP solution. This is mainly because the overvoltages are overcompensated in this solution, leading to a higher cost.

- The SOCP approach yields a feasible solution with the least grid losses. However, the result found by the (nonconvex) AC OPF has a slightly lower cost than the SOCP solution. In this case, the inclusion of the penalty term does not immediately lead to a feasible as well as global optimal solution, indicating numerical issues. These are probably caused by a badly scaled penalty factor. This indicates that, as mentioned in Section 4.4.4, scaling of the SOCP penalty is non-trivial. In terms of combined grid losses and curtailment cost, the SOCP solution still performs the best.

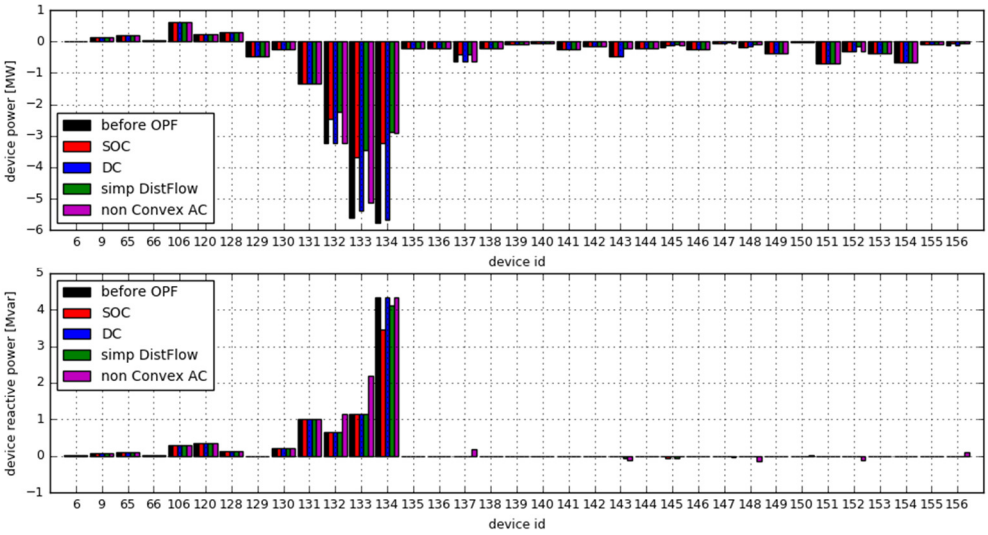

Figure 10-19 Comparison of solutions found by different formulations for the 'overvoltage' case study.

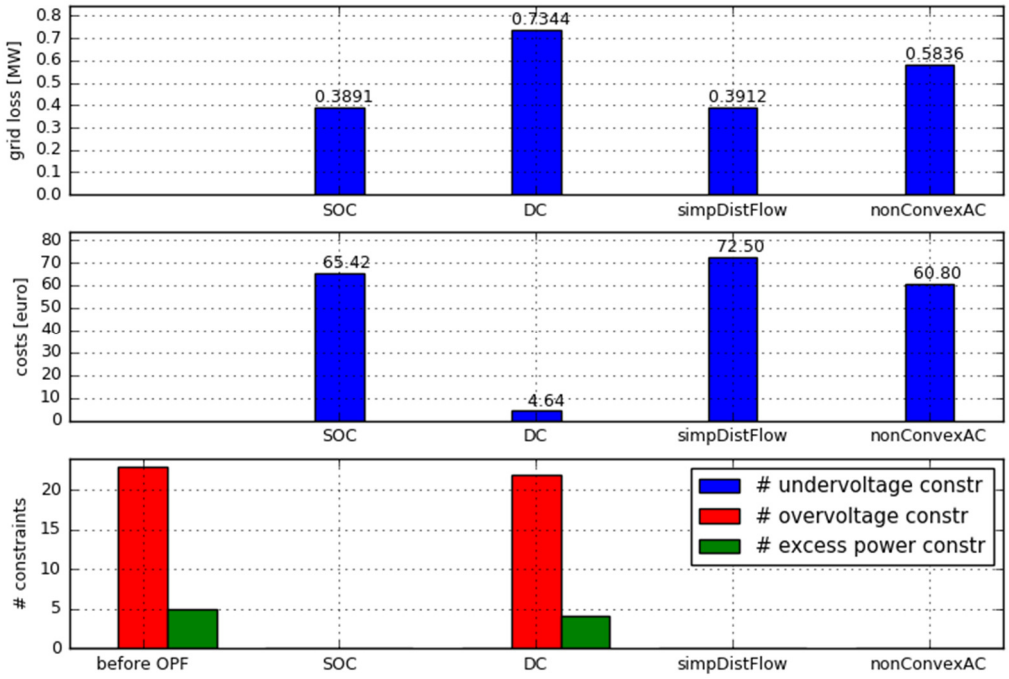

Figure 10-20 The resulting costs and grid losses of the different solutions in the 'overvoltage' case study.

10.4.4.1.3 'Overcurrent' Case Study

Figure 10-21 and Figure 10-22 show a comparison of the results found of the different OPF approaches of the 'overcurrent' case study. From these results, the following can be concluded:

- The solution found by the DC OPF approximation is, although in cost the cheapest solution, not a feasible one, as it fails to satisfy the bounds.
- The solution found through the Simplified DistFlow approach is a feasible solution in this case study. The cost of this solution is however higher than the cost of the SOCP solution.
- The SOCP approach yields a feasible solution with least grid losses.
- The cost of the nonconvex AC OPF quasi equals the cost of the SOCP solution, the grid losses of this solution are however higher than the solution found by the SOCP approach. In this case, numerical issues related to the scaling of the penalty factor lead to a slightly higher cost of the SOCP solution. However, in terms of combined cost and grid losses, the SOCP solution still performs better.

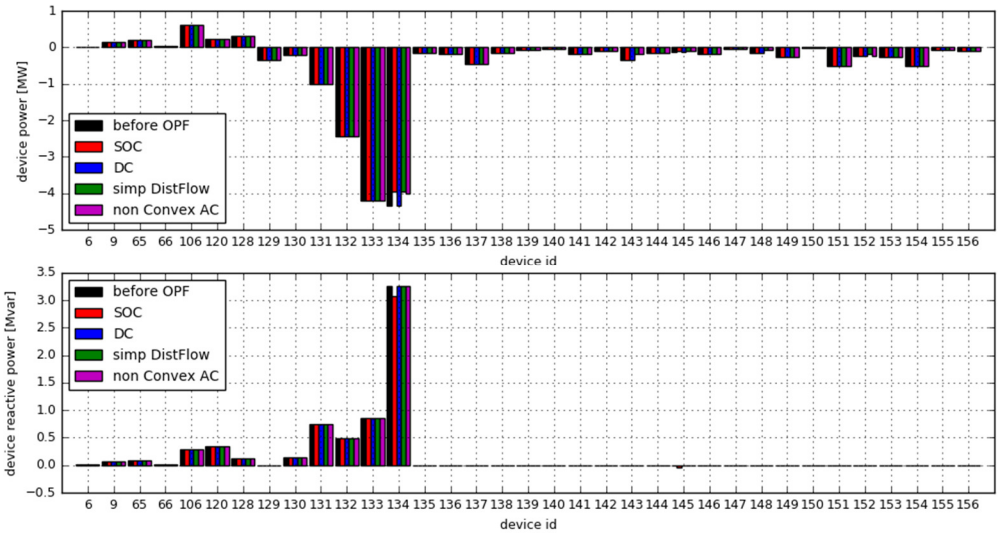

Figure 10-21 Comparison of solutions found by different formulations for the 'overcurrent' case study.

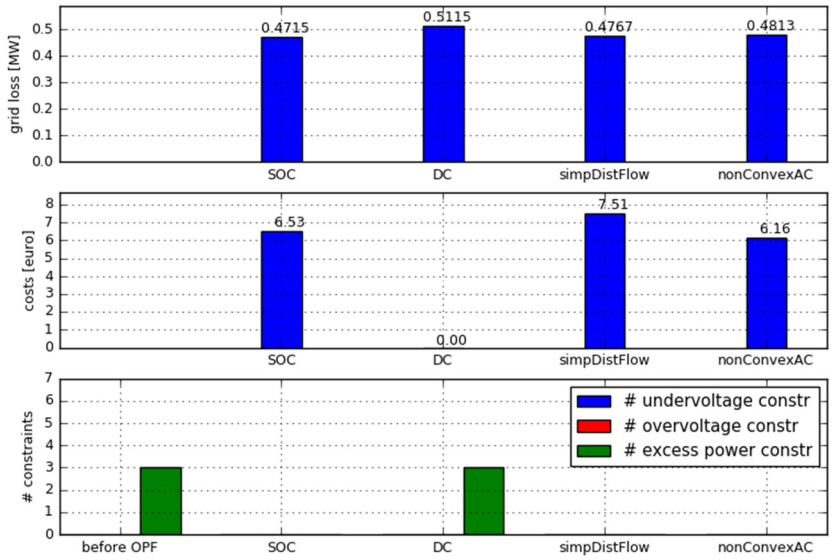

Figure 10-22 The resulting costs and grid losses of the different solutions in the 'overcurrent' case study.

10.4.4.1.4 Discussion

It can be concluded that the DC OPF approximation is not a suitable approach to solve optimal power flow problems in a distribution grid, since in many (or most) cases it will not yield feasible solutions. The reason for this is that reactive power is not properly accounted for in this approximation when used in distribution grid modeling.

Compared with the DC OPF, the Simplified DistFlow approximation yields much better results in terms of feasibility. Feasibility issues are mostly related to undervoltage issues, since these are under-compensated using the Simplified DistFlow approximation. In terms of solution cost, the solutions obtained by the Simplified

DistFlow approximation in many cases lead to higher costs than the optimal cost (using a full OPF with no approximation). This is mainly due to the fact that overvoltages are overcompensated in the obtained solutions.

The SOCP relaxation yields, in all cases, a feasible solution. The obtained solution is the guaranteed global optimal solution with respect to the combined minimum of cost and grid losses. Grid losses are accounted for in the objective because of the inclusion of the penalty term forcing the obtained solution to lie on the cone surface and thus be physically feasible. Finding a penalty factor that effectively leads to the global optimal solution in terms of curtailment cost proves to be non-trivial in 2 cases. In the case of undervoltage issues, the penalty factor is less critical, and it is thus easier to find the global optimum.

The nonconvex AC OPF does not give a guaranteed optimum, the solver may reach a local optimum, with a higher cost and higher losses than the solution found by the SOCP relaxation.

Ben-Tal Polyhedral Relaxation of SOCP

The Ben-Tal polyhedral relaxation technique [34] can be used to reformulate any SOCP problem as an equivalent LP problem to an arbitrary, chosen accuracy. The SOCP DistFlow formulation includes 3 SOC constraints (see section 4.3):

$$\left(P_{ij,s}\right)^2 + \left(Q_{ij,s}\right)^2 \leq i_{ij,s} \cdot u_i' \tag{201}$$

$$\left(P_{ij}\right)^2 + \left(Q_{ij}\right)^2 \leq (S_{ij}^{rated})^2 \tag{202}$$

$$\left(P_{ji}\right)^2 + \left(Q_{ji}\right)^2 \leq (S_{ji}^{rated})^2 \tag{203}$$

The polyhedral relaxation accuracy ϵ is a function of a user chosen setting ν:

$$\nu \geq 1, \nu \in \mathbb{N} \tag{204}$$

$$\epsilon(\nu) = \frac{1}{\cos(\frac{\pi}{2^{\nu+1}})} - 1$$

For all three case-studies, the three SOC constraints were relaxed using the Ben-Tal technique with a varying accuracy. Accuracy setting ν_1 is used to define the accuracy of the polyhedral relaxation of SOC constraint (201), while ν_2 is the accuracy setting of the polyhedral relaxation of SOC constraints (202) and (203). A different relaxation accuracy for the different SOC constraints makes sense, since power rating constraints, i.e. (202) and (203), can be treated as less strict constraints, while the accuracy of SOC constraint (201) defines the feasibility of the obtained result. It must be noted that the more accurate the result has to be, i.e. the higher the accuracy setting ν, more variables are introduced in the optimization problem, possibly leading to memory or other computational tractability issues.

Figure 10-23 and Figure 10-24 show the obtained results for the 'undervoltage' case study. It can be seen that for an accuracy setting of ν_1 = 4 and ν_2 = 3 relatively accurate results are obtained. Using these accuracy settings only one branch power constraint violation remains, but the power rating is only exceeded with a relatively low value. The undervoltage issues are reduced to 3 issues, but the remaining undervoltage is quite close to the voltage limit. Also, the cost of the obtained result differs from the SOCP obtained result with only 4%.

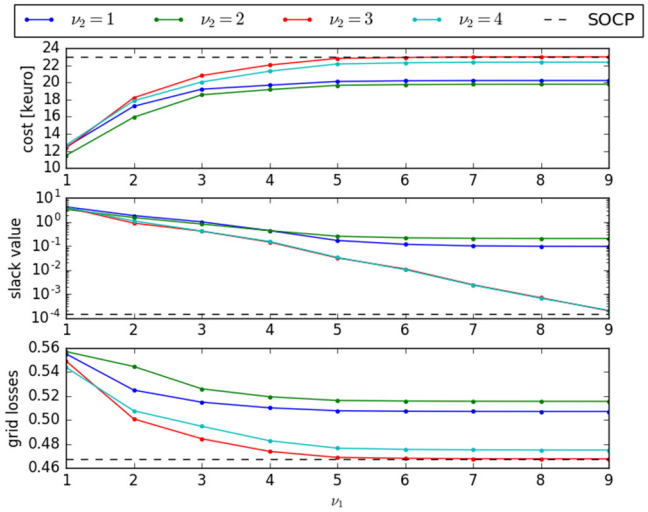

Figure 10-23 The resulting costs, slack value and grid loss with varying Ben-Tal accuracy setting for the 'undervoltage' case study. The obtained cost, slack value and grid loss of the SOCP result is also shown.

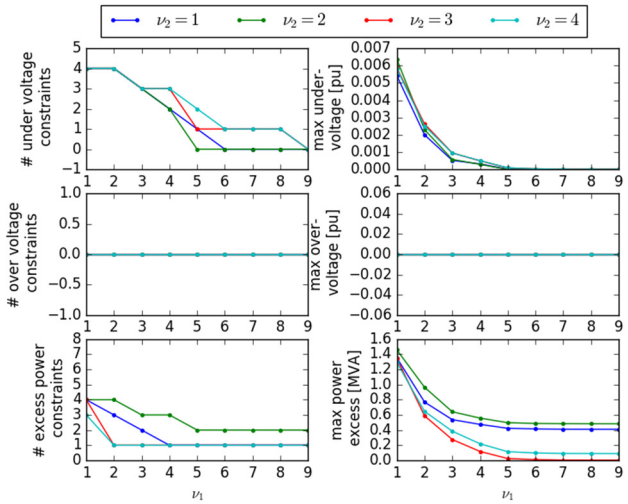

Figure 10-24 Feasibility of the solutions obtained with varying Ben-Tal accuracy setting in the 'undervoltage' case study. The left figures show the number of constraint violations found and the right figures show the biggest constraint violation.

Figure 10-25 and Figure 10-26 show the obtained results for the 'overvoltage' case study. In this case, an accuracy setting of ν_1 = 2 and ν_2 = 1 leads to relatively accurate results. Using these accuracy settings, no branch power constraint violation nor any overvoltage issue remains. Also, the cost of the obtained result differs from the SOCP obtained result with only 5%. It must be noted that the achieved accuracy does not necessarily increase monotonously with the accuracy settings given: note that the accuracy setting ν

determines an upperbound of the achieved accuracy, a lower accuracy can be reached using a lower accuracy setting ν.

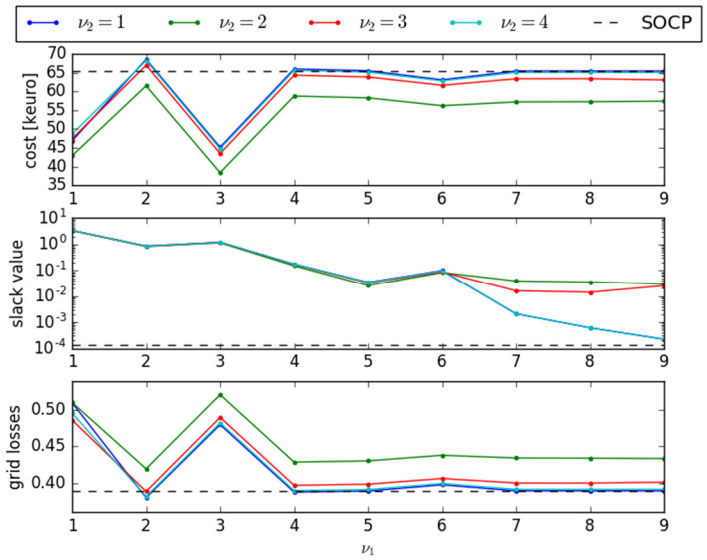

Figure 10-25 The resulting costs, slack value and grid loss with varying Ben-Tal accuracy setting for the 'overvoltage' case study. The obtained cost, slack value and grid loss of the SOCP result is also shown.

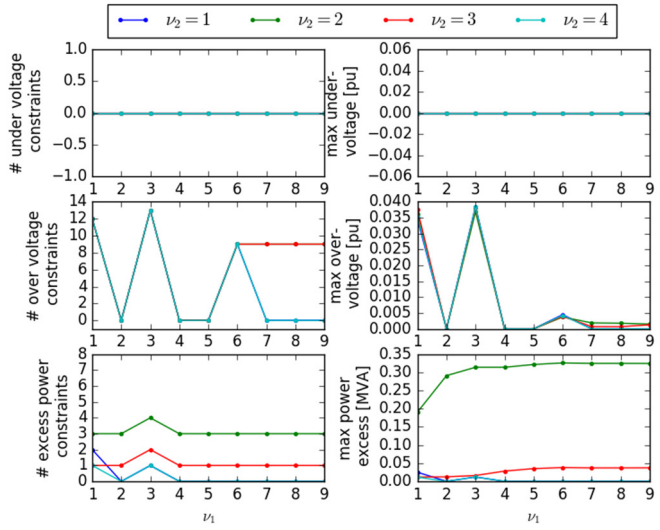

Figure 10-26 Feasibility of the solutions obtained with varying Ben-Tal accuracy setting in the 'overvoltage' case study. The left figures show the number of constraint violations found, the right figures show how large the biggest constraint violation is.

Figure 10-27 and Figure 10-28 show the obtained results for the 'overcurrent' case study. In this case, an accuracy setting of ν_1 = 2 and ν_2 = 1 leads to relatively accurate results. Using these accuracy settings, no branch power constraint violation remains. Also, the cost of the obtained result differs from the SOCP obtained result with 7%.

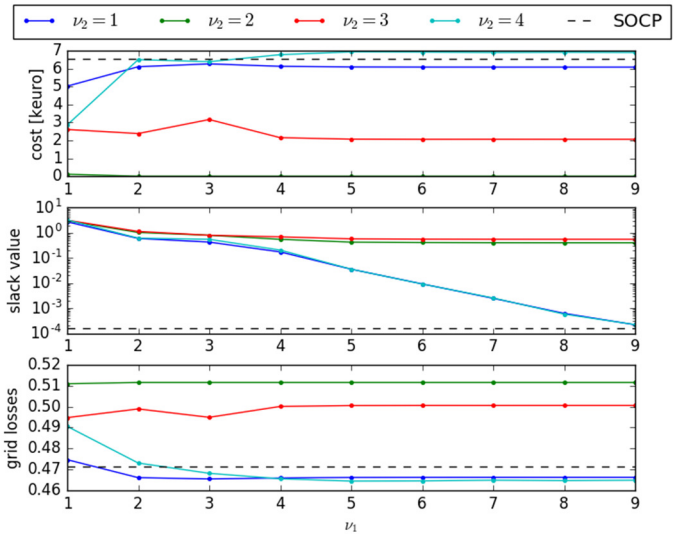

Figure 10-27 The resulting costs, slack value and grid loss with varying Ben-Tal accuracy setting for the 'overcurrent' case study. The obtained cost, slack value and grid loss of the SOCP result is also shown.

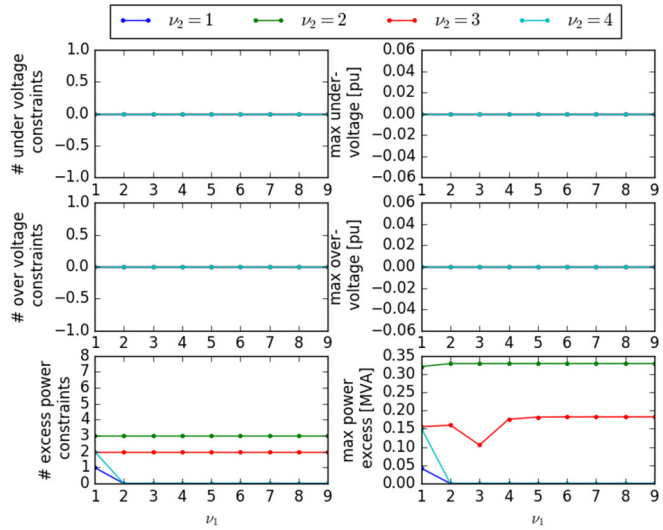

Figure 10-28 Feasibility of the solutions obtained with varying Ben-Tal accuracy setting in the 'overcurrent' case study. The left figures show the number of constraint violations found, the right figures show how large the biggest constraint violation is.

To conclude, in all tested case studies, relatively accurate Ben-Tal relaxation results are obtained with relatively low accuracy settings. Accuracy settings of ν_1 and ν_2 = 4 in all tested cases lead to acceptable results. This implies that without the inclusion of much more extra variables, LP solvers can be used to solve the SOCP problem without losing too much accuracy. A lower value of accuracy setting might be better, depending on the specific case study, since the accuracy setting only determines an upper bound of the achieved accuracy.

10.4.5 Verification Study of the Inactive Constraints Method

The inactive constraints method as network simplification method for transmission grid modeling is illustrated in this chapter. The method is applied to the available networks, in order to find the inactive lines. To make the verification more general, the method is applied to large range of load values. The load is treated as a variable between 10% and 300% (depending on the network considered) of the nominal value. In this way, the method is validated in different loading conditions.

Given a fixed AS needs, the use of medium voltage resources for AS can reduce the use of the high voltage resources to provide these AS. The impact of the medium voltage resources also depends on their position.

Finally, we have to take into account that we are considering the balancing market. In this market, the changes of the production/consumption, which are caused by relieving network congestions and short-term fluctuations of sustainable power sources, are only a few percent of the total load (assuming a 2020 world), so the balancing should not introduce great variation of the power flow. This assumption might be challenged in a furture scenario wth much more RES into the system. For this preliminary analysis, only the high voltage generators are taken into account. This simplified approach is considered to be sufficient to highlight the weakest areas of the transmission network.

Danish Network

The results for the two asynchronous areas of the Danish network are reported in Figure 10-29. It can be seen that in all the loading conditions, the lines with active constraints are usually no more than 10% (which are about 40 lines) of the total. The nominal load in this case is about 5 GW.

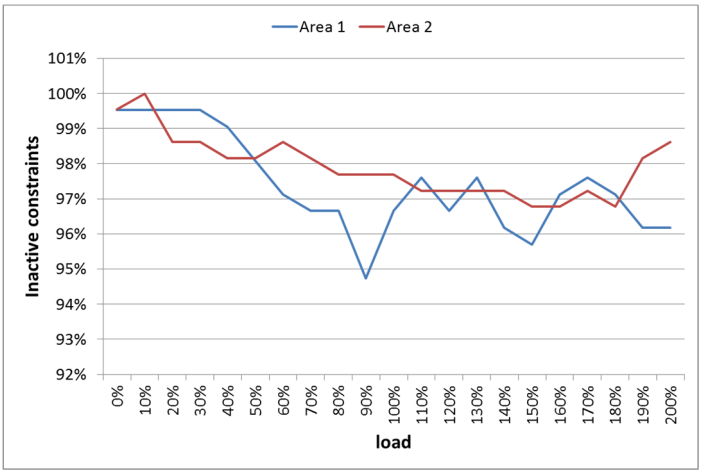

Figure 10-29: Inactive constraints in the two asynchronous Danish network areas

Spanish Network

10.4.5.1.1 Base Case

The results for the Spanish network are reported in Figure 10-30. In this network, there are more active constraints than in the Danish network: The lines with active constraints are usually no less than 20% (about 600 lines). The nominal load in this case is about 40 GW.

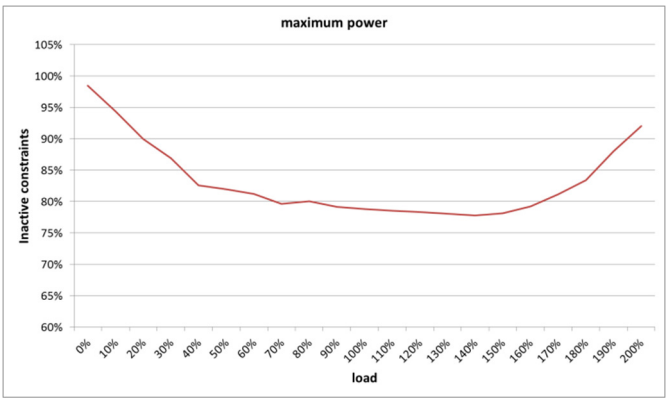

Figure 10-30: Inactive constraints in the Spanish network

10.4.5.1.2 Limited Maximum Power

Not all the active power of the generator is usually available in the balancing market, but only a small fraction of it. Therefore, the calculations are repeated considering that the generators can increase the active power of only the 20% (conventional value) of the maximum power.

It can be seen (Figure 10-31) that in this condition the percentage of lines with inactive constraints increases to about 90%. Only for high values of the load (almost 80 GW), the percentage of active constraints increases above 10% (about 300 lines). With the new maximum capability, the number of lines with inactive constraints are lower for very high loading situations. In fact, the current limit violations are due to the high loads, where the lower values of the generators capabilities increase the probability of the current flow at high load situations hits the limits.

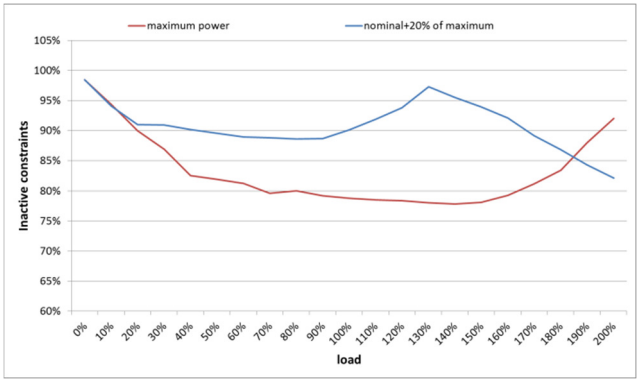

Figure 10-31: Inactive constraints in the Spanish network with adjusted maximum generator capability

Also, considering that a small fraction of the line capacity has to be preserved for the reactive power, it is clear that the reduction of the number of lines is considerable.

10.4.5.1.3 Statistical Analysis

To study further the inactive constraints method, a statistical analysis is carried out. The total load is increased from 10% to 200% and for each load scenario 50 cases are analyzed multiplying each single load by a random number between the 75% and 125%. Considering these stochastic variations, the number of lines with inactive constraints decreases about 5%

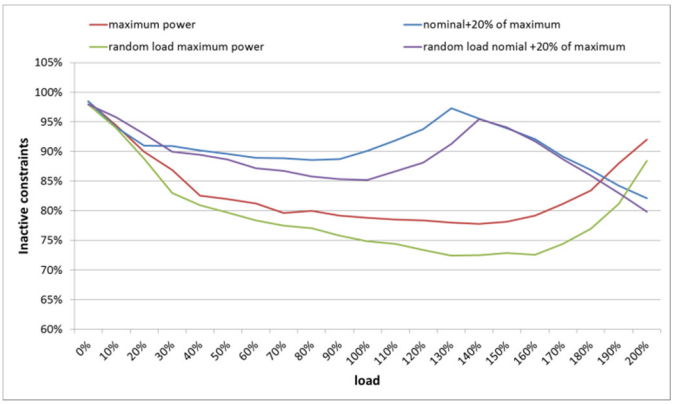

Figure 10-32: Inactive constraints in the Spanish network with stochastic load variation

10.4.5.1.4 Limiting the Area of the Network

If the reduced number of variables is seen as still being too high after network reduction has been applied, an alternative is to control only the branches on a certain zone, for example the zone of the pilot. In the example case of the Spanish pilot, only about 40 lines with active constrains have to be considered.

10.4.6 Verification Study of the DC Approximation for Transmission Grid Modeling

It is necessary to verify that the DC approximation does not introduce too large errors in the power flow calculation. For this purpose, some tests are carried out in different conditions of operation.

In this verification study, the calculated error concern the active power flow. All errors are given as mean values. The calculated AC power flow is taken as the reference value, and the deviation of the calculated DC power flow approximation from the AC power flow is considered as error. All relative errors are expressed with respect to the maximum power rating.

The total load (and generation) is varied with a load-scaling factor, ranging from 50% to 150% of the nominal power, with 11 steps of 10%. Fr each step, 10 random configurations are made, where each load and

generator are made variable with a Gaussian distribution with a standard deviation of 20%. This gives 110 different cases to calculate.

The resulting error data are three-dimensional depending on the applied load-scaling factor, the line number and the random distribution. For visualization purposes, the data are plotted as sets of curves, and two possibilities are used:

- A curve for each combination of line number and random distribution, with the load-scaling factors on the horizontal axis
- A curve for each combination of load-scaling factor and random distribution, with the line numbers on the horizontal axis

Spanish Network

Studying the Spanish network has shown, that the error between the DC and AC power flow, in terms of power flow on the lines, is low on average. However, in the area of the network near the slack bus, the error increases and become too relevant to be discarded (almost 500 MW). The following section reports the result of the methods introduced.

10.4.6.1.1 Method 1

The following procedure is performed for each random sample:

1. The loads and generators are obtained by the random procedure previously described.
2. One ACPF is performed to obtain the losses.
3. The losses are added proportionally to the generators. In this way, the balancing of the losses is distributed between all the generators and not only in the slack node (i.e. the losses would be attributed on all the nodes proportionally to the generation at those nodes, as opposed to a single, so called *slack*, node of the network).
4. The ACPF is repeated taking into account the new generation profile with the losses.
5. Flat losses are added proportionally to the load.
6. The DC power flow is computed.
7. The AC and DC power flow are compared.

The value of the flat loss-profile parameter is selected to 2.5%, which is about the percentage of losses in the Spanish network under normal conditions.

The mean error in this case is 4.1 MW. The mean percentage error, computed with respect the power limit of the lines is 1.3%.

The mean error is quite low, but it is not acceptable in some lines, in particular when there is a huge error near the slack bus (Figure 10-33; Figure 10-34), since the slack has to balance the losses.

The error is minimum when the load and the losses are near the nominal condition. They increase for the other loading conditions. The error becomes very high when the load increases (Figure 10-34), since the losses are quadratic with respect the currents. It is clear that it is necessary to take into account, at least in first approximation, the value of the losses to compute the exact value of the load.

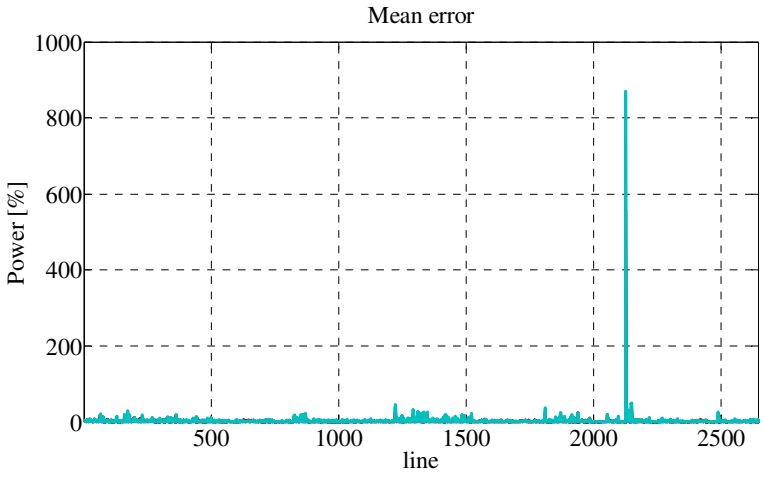

Figure 10-33: Relative error vs. line number (Method 1, Spain)

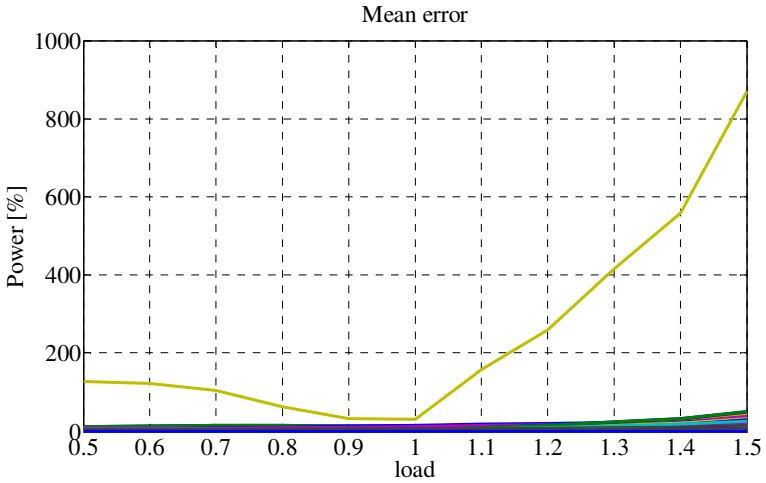

Figure 10-34: Relative error vs. load scaling factor (Method 1, Spain)

10.4.6.1.2 Method 2

In order to reduce the error, the losses are not kept fixed, but are computed in each considered condition of operation. The procedure is described by the following steps:

1. The loads and generators are obtained by the random procedure previously described.

2. One ACPF is performed to obtain the losses.

8. The losses are added proportionally to the generators. In this way, the balancing of the losses is distributed between all the generators and not only in the slack node (i.e. the losses would be attributed on all the nodes proportionally to the generation at those nodes, as opposed to a single, so called *slack*, node of the network).

3. The ACPF is repeated taking into account the new generation profile with the losses.

4. The losses computed at the previous step are added proportionally to the load.

5. The DC power flow is computed.

6. The AC and DC power flow are compared.

Using this method, the error strongly decreases: the mean error in this case is 3.3 MW and the mean percentage error, computed with respect the power limit of the lines is 1.1%. Besides, the power error on the lines is always lower than 150 MW and the large error near the slack node disappears. The 95-percentile error is below 12.7 MW and 4.1% (Figure 10-35; Figure 10-36), the number of lines with high error is limited. The line with the maximum absolute errors correspond to the line with the highest power flow (Figure 10-37), but considering the percentage error, the errors in these lines is below the 5%. This is good, since the highest absolute error corresponds with the lines with the highest capacity.

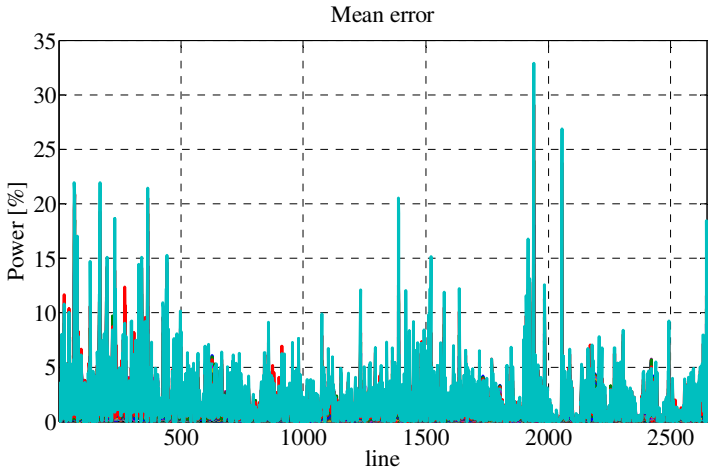

Figure 10-35: Relative error vs. line number (Method 2, Spain)

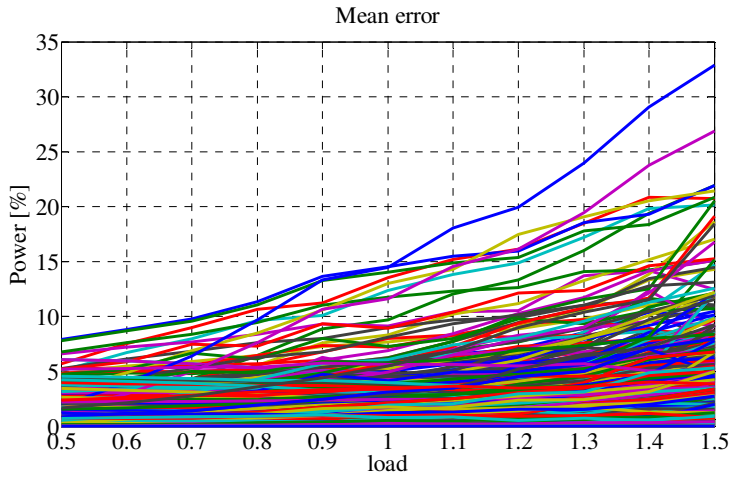

Figure 10-36: Relative error vs. load scaling factor (Method 2, Spain)

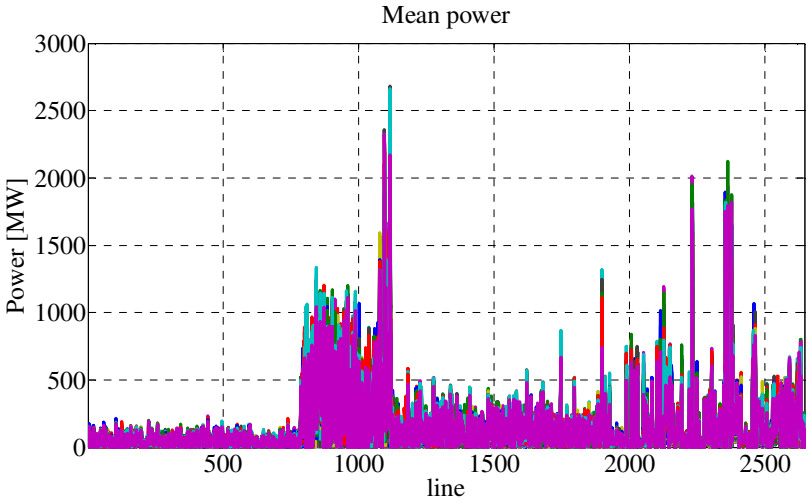

Figure 10-37: Mean active power flow vs. line number (Method 2, Spain)

10.4.6.1.3 Method 3

In this case, the losses in the DC power flow are not added proportionally to the load, but the losses of each line are assigned to the two ending busses. This should increase the accordance between the two models. The procedure follows:

1. The loads and generators are obtained by the random procedure previously described.
2. One ACPF is performed to obtain the losses.
9. The losses are added proportionally to the generators. In this way, the balancing of the losses is distributed between all the generators and not only in the slack node (i.e. the losses would be attributed on all the nodes proportionally to the generation at those nodes, as opposed to a single, so called *slack*, node of the network).

3. The ACPF is repeated taking into account the new generation profile with the losses.
4. The losses, computed at the previous step, of each line are added to the ending busses of the line.
5. The DC power flow is computed.
6. The AC and DC power flow are compared.

The error decreases with respect to the previous cases: the mean error in this case is 2.3 MW and the mean percentage error, computed with respect to the power limit of the lines is 0.84%. Besides, the power error on the lines is always lower than 140 MW and the large error near the slack node disappears. The 95-percentile error is below 8.4 MW and 3.4% (Figure 10-38; Figure 10-39), the number of lines with high error is limited. This method demonstrates very good agreements between the two calculation methods.

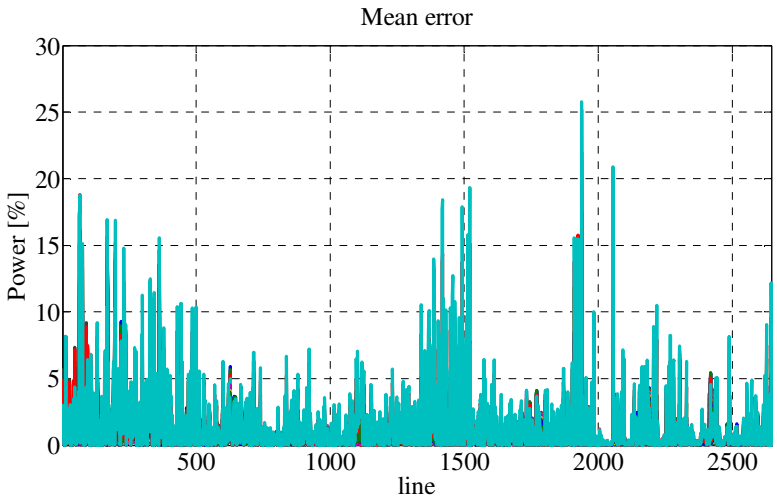

Figure 10-38: Relative error vs. line number (Method 3, Spain)

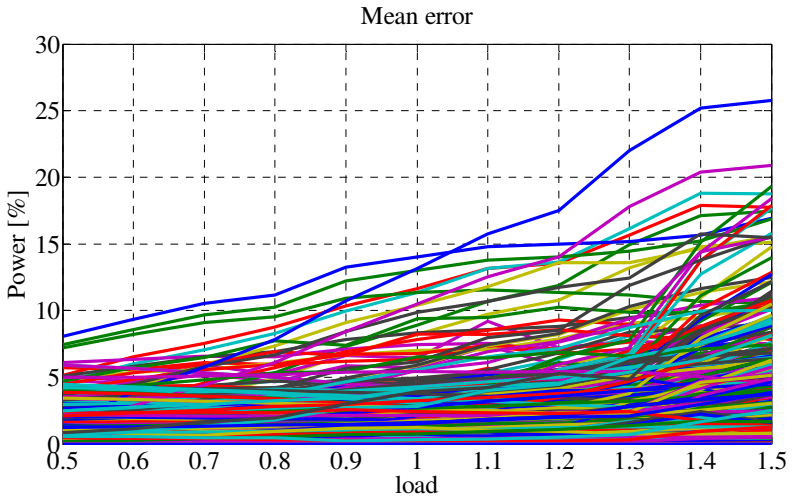

Figure 10-39: Relative error vs. load scaling factor (Method 3, Spain)

10.4.6.1.4 Method 3 with IIC

The mean error in this case is 2.3 MW and the mean percentage error, computed with respect to the power limit of the lines is 0.84%. Besides, the power error on the lines is always lower than 100 MW and the great error near the slack node disappears. The 95-percentile error is below 8.7 MW and 3.3% (Figure 10-40; Figure 10-41), the number of lines with high error is limited.

The two methods present very similar results, so it is difficult to say which method is better. In this specific case, the previous method performs a little better.

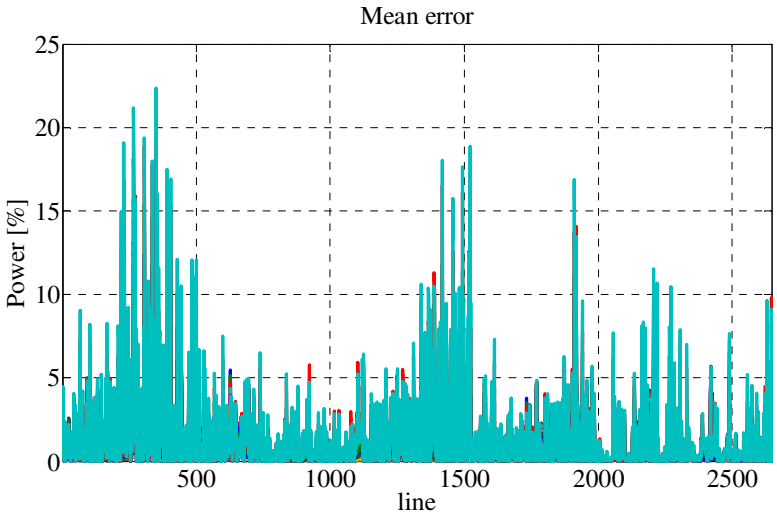

Figure 10-40: Relative error vs. line number (Method 3 with IIC, Spain)

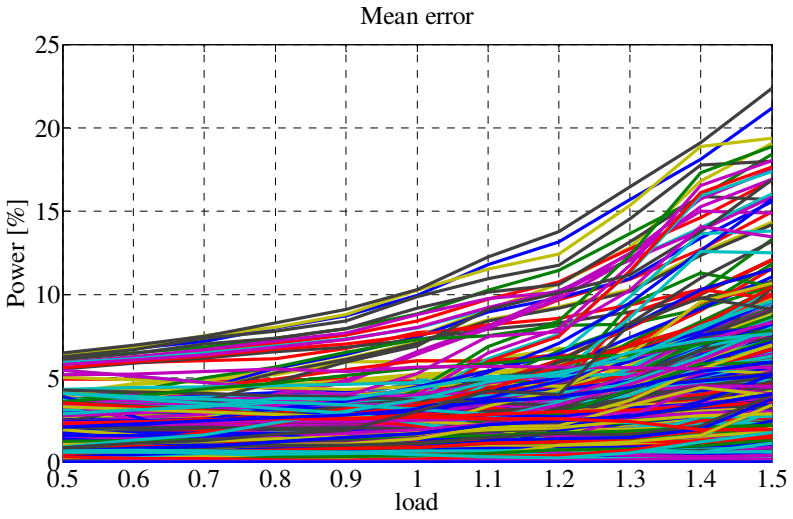

Figure 10-41: Relative error vs. load scaling factor (Method 3 with IIC, Spain)

10.4.6.1.5 Method 4

This method is like the method 2, but the losses are added proportionally to the generator productions. The mean error in this case is 3.4 MW and the mean percentage error, computed with respect to the power limit of the lines is 1.15%. Besides, the power error on the lines is always lower than 150 MW and the large error near the slack node disappears. The 95-percentile error is below 12.8 MW and 4.2%, the number of lines with high error is limited.

10.4.6.1.6 Method 5

This method is like the method 2, but the losses are added 50% proportionally to the generator productions and 50% to the load. The mean error in this case is 3.0 MW and the mean percentage error, computed with respect to the power limit of the lines is 1.05%. Besides, the power error on the lines is always lower than 140 MW and the large error near the slack node disappears. The 95-percentile error is below 11.1 MW and 3.7%, the number of lines with high error is limited.

Danish Network

The tests are repeated for the two parts of the Danish network. The error between the AC and DC power flow is smaller for this network, so the analysis is simpler. Only method 3 is used here. The errors for the west and east part of the network are reported in Figure 10-42 and Figure 10-43 respectively. The lower error is probably due to the smaller dimension of the network, the lower losses and generally higher x/r ratio.

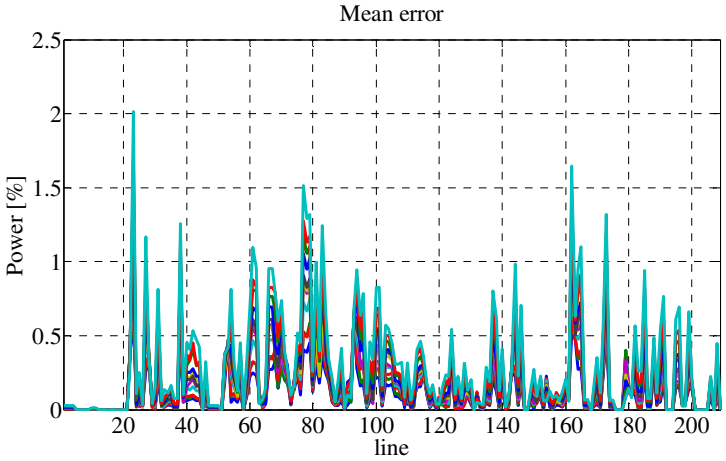

Figure 10-42: Relative error vs. line number (Method 3, western Denmark)

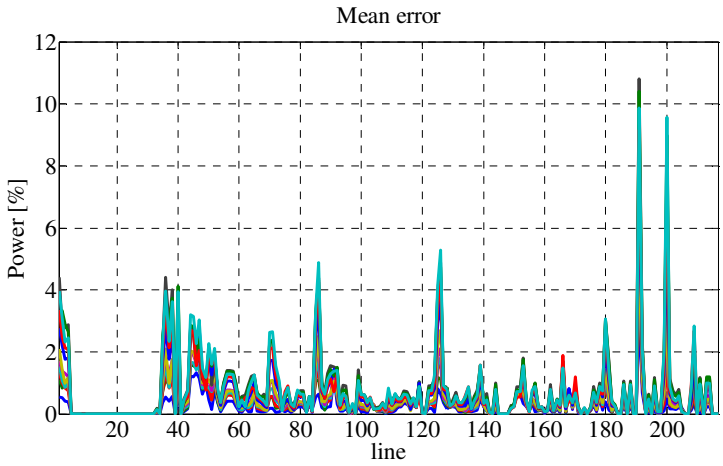

Figure 10-43: Relative error vs. line number (Method 3, eastern Denmark)

Summary

The DC approximation is a good approximation for these networks. The errors are limited also for the simpler methods. The principal open point is the contribution of the losses. In fact, the AC and DC approximation return the same results only if the losses are correctly taken into account. There are principally two ways to take into account the losses in the project framework:

- The balancing market simulates the network condition in the real-time market. Then the input data (profiles of load and generators) should already take into account the losses. Then it is possible to add the losses in the DC approximation with different methods (proportionally to the load or to the generation). However, since the AC power flow is not performed, it is more difficult to associate the losses to the lines (future investigation).

- The input data do not take into account the losses (for example if the data are from day ahead market and it does not take into account the losses). In this case, it is not necessary to add the losses in the DC formulation.

10.5 Mathematical Formulation of Market Clearing

10.5.1 Coupling of Physics and Economics

S_{nt} represents the forecast net node apparent-power injection at time step *t*, at node *n,* after the market session, i.e. considering the activated bids. It represents the sum of all injections **directly** at that node (i.e. not the flow coming from or going to other nodes), from which we subtract the sum of all offtakes **directly** at that node. In particular, the injections coming from and/or offtakes to neighboring nodes are not included. The following constraint expresses that S_{nt} is the sum of $\hat{S}_{nt}$, the forecast apparent power injection for this time step *t*, and S_{nt}^{m}, the compensating power injections that the Integrated Reserve market decides for solving any imbalance and/or congestion problems.

$$S_{nt} = \hat{S}_{nt} + S_{nt}^{m} \tag{205}$$

Then, the coupling of (network) physics and (market) economics is formulated using (206). This constraint links the apparent-power injections of the considered market in node n at time t, to the accepted active and reactive power quantities for all bids.

$$S_{nt}^{m} = \sum_{a}\sum_{b}\sum_{\beta} q_{nabt\beta,active} \cdot x_{nabt\beta,active} + j \cdot q_{nabt\beta,reactive} \cdot x_{nabt\beta,reactive} \tag{206}$$

In (206), both left and right hand sides are complex quantities (defining $j = \sqrt{-1}$), so it equates both the real and imaginary part, representing active and reactive power respectively. Note also that the physical limits on total injection will be formulated in terms of the total absolute apparent-power injection S_{nt}.

10.5.2 Network Constraints for Market Clearing

We define $\mathrm{S_{nmt}}$ as the power sent from node n to node *m* through the edge nm, and $\mathrm{R_{nmt}}$ as the power received in node n through edge mn. For each node *n,* and for each time step *t*, the power balance can be written as:

$$\sum_{m:n\to m} S_{nmt} = \sum_{m:m\to n} R_{nmt} + S_{nt} \tag{207}$$

The power received through edges, $\mathrm{R_{mnt}}$, is less than the power departing on the edge mn at node m, since power losses occur on the lines (or edges). In fact, more specifically

$$R_{nmt} = S_{nmt} - z_{mn} \cdot |I_{mnt}|^2 \tag{208}$$

where $\mathrm{z_{mn}}$ is the line impedance and $\mathrm{I_{mnt}}$ represents the electric current in the line. This we get:

$$\sum_{m:n\to m} S_{nmt} = \sum_{m:m\to n} (S_{nmt} - z_{mn}\cdot |I_{mnt}|^2) + S_{nt} \quad (209)$$

Now, S_{nt}^{m} can be expressed in terms of market bids as we saw in (206). Substituting this into (**209**) gives

$$\sum_{m:n\to m} S_{nmt} =$$

$$\sum_{m:m\to n} (S_{mnt} - z_{mn}\cdot |I_{mnt}|^2) + \hat{S}_{nt} \quad (210)$$

$$+ \sum_{a}\sum_{b}\sum_{\beta} q_{nabt\beta,active}\cdot x_{nabt\beta,active} + j\cdot q_{nabt\beta,reactive}\cdot x_{nabt\beta,reactive}$$

10.5.3 Adaptation of Prices to Avoid Unnecessary Acceptance

In order to prevent flexibility providers from making profit by just exchanging power among each other, an adaptation of bid prices is performed just before running the marking clearing algorithm, as explained below.

At first, the total imbalance of each subnetwork is computed. This allows us to identify which bid type, i.e. upward or downward, are necessary to balance the subnetwork. Depending on the sign of the imbalance, two different approaches are then used.

In case of negative imbalance, the minimum price among the bids in the right direction and the maximum price among the bids in the opposite directions are identified, as expressed by the following equations:

$$\psi = \min_{\beta\in\Pi^{pos}}\{p_\beta\} \quad (211)$$

$$\gamma = \max_{\delta\in\Pi^{neg}}\{-p_\delta\} \quad (212)$$

The modified price of negative bids is now expressed by means of the following equation:

$$\forall\delta\in\Pi^{neg},\ \ p_\delta^{new} = -\min(-p_\delta^{old}, \psi - \epsilon - \mu\cdot|\gamma + p_\delta^{old}|) \quad (213)$$

where ϵ and μ are very small positive numbers ($0 < \epsilon \ll 1, 0 < \mu \ll 1$).

In case of positive imbalance, the minimum price among the bids in the right direction and the maximum price among the bids in the opposite directions are given by the following equations:

$$\psi = \max_{\delta\in\Pi^{neg}}\{-p_\delta\} \quad (214)$$

$$\gamma = \min_{\beta\in\Pi^{pos}}\{p_\beta\} \quad (215)$$

The modified price of positive bids is now expressed by means of the following equation:

$$\forall \beta \in \Pi^{pos},\ \ p_{\beta}^{new} = max(p_{\beta}^{old}, \psi + \epsilon + \mu \cdot |\gamma - p_{\beta}^{old}|) \tag{216}$$

Using this trick, the prices of bids in the wrong quantity direction become uninteresting to be matched with any other bids. As a result, these bids are only accepted if they are able to solve another physical problem in the network (such as congestion and voltage problems).

An example of this price manipulations is further described. Consider the situation for which the subnetwork imbalance is 10 MW and the following bids are proposed to the market clearing:

- Bid 1: An upward bid of 20 MW at 30 €/MWh
- Bid 2: An upward bid of 10 MW at 10 €/MWh
- Bid 3: A downward bid of 15 MW at -70 €/MWh
- Bid 4: A downward bid of 10 MW at -50 €/MWh

The situation is illustrated in Figure 10-44.

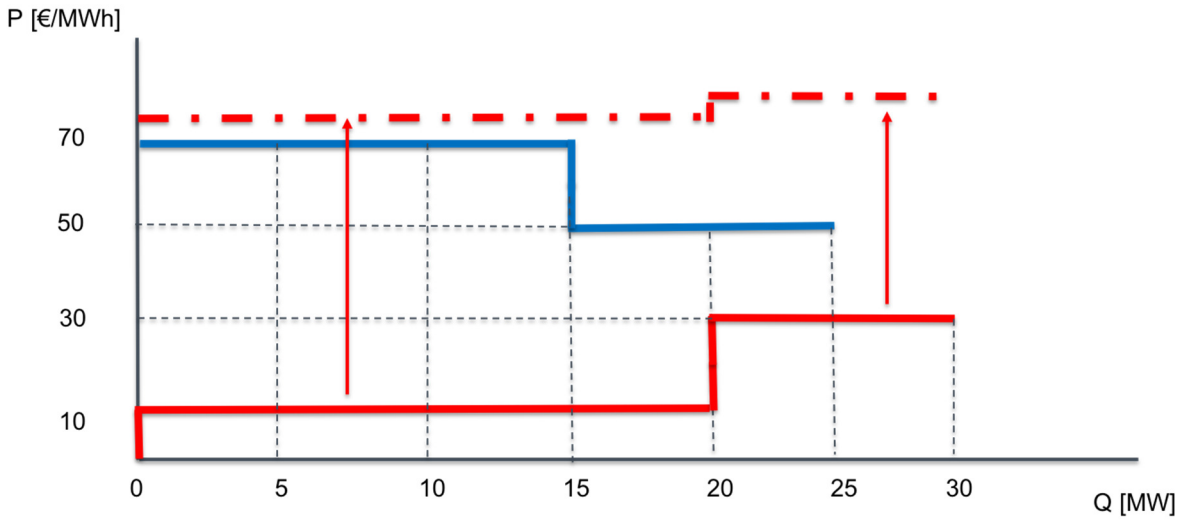

Figure 10-44: Example of avoidance of unnecessary activations

In our case, as the network imbalance is positive, the above introduced quantities take the following values:

$$\psi = 70\ €/\text{MWh}$$

$$\gamma = 10€/\text{MWh}$$

Taking a value of 0.001 for both ϵ and μ, the adapted prices for bid 1 and bid 2 are the following:

$$p_1^{new} = \max(30, 70 + 0.01 + 0.01 \cdot |10 - 10|) = 70.21 \text{ €/MWh}$$

$$p_2^{new} = \max(10, 70 + 0.01 + 0.01 \cdot |10 - 10|) = 70.01 \text{ €/MWh}$$

The modified upward bids are represented by dashed lines in Figure 10-44. This way, no intersection is possible between upward and downward bids and only downward bids would be selected in the market clearing, unless upward bids would be needed for solving congestion problems. Moreover, the merit order is also preserved.

10.5.4 An Example of Nodal Marginal Pricing

Consider the example of Figure 10-45 [133]. The system consists of two loads and three generators. Each line of the network has identical characteristics and line 1-3 has a flow limit of 120 MW. The demand and marginal cost of the generators are shown in the left part of the figure. The resulting prices are shown in the right part. A linearization of Kirchhoff's power flow laws through a standard DC power flow model implies that each MW of power shipped from any node to any other node will distribute itself so that one third takes the 'long' path (i.e. the path involving two lines) and two thirds will take the 'short' path (i.e. the path involving one line). It can be shown that the price is equal to 40 €/MWh, 80 €/MWh, and 120 €/MWh for locations 1, 2, and 3, respectively.

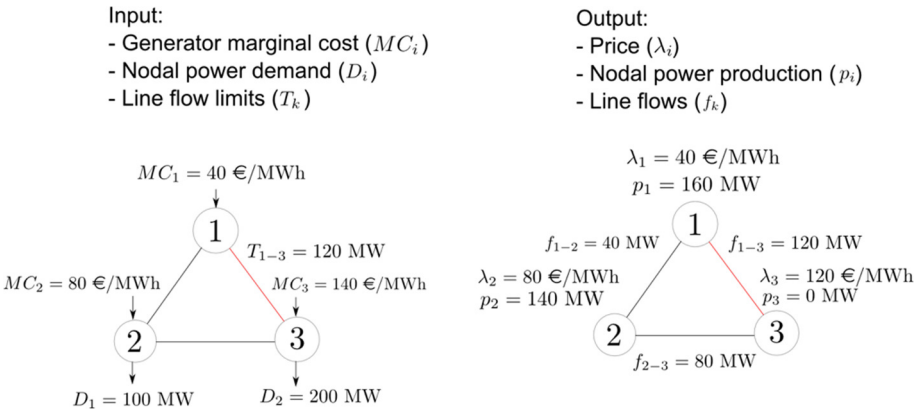

Figure 10-45 A three-node network. The network consists of lines with identical electrical characteristics. Line 1-3 has a transmission limit of 120 MW. Off-takes are inelastic and the marginal costs of generators are indicated on the figure.

The first thing to note is that the price is different for all three locations, and that even locations connected by an uncongested line (locations 1 and 2) have a different price. What is also noteworthy is that no generator in the network has a marginal cost of 120 €/MWh, nevertheless the price in location 3 is 120 $/MWh.

To see how this marginal cost emerges, note that the minimum cost dispatch that satisfies off-takes is equal to 160 MW in location 1 and 140 MW in location 2. In order to satisfy a marginal increase in off-

take in location 3 by 1 MW at minimum cost, while satisfying transmission constraints, we reduce the injection of generator 1 by 1 MW, and increase the injection of generator 2 by 2 MW, so as to satisfy the additional off-take while ensuring that the flow on line 1-3 remains at the 120 MW limit. This results in a marginal cost increase of 120 $/MWh, which is the nodal price at location 3. This price sends the correct signal to loads at location 3 about the marginal cost impact of their consumption.

The above example is used for the sake of illustration, but it is based on a mathematically formalized approach towards defining nodal prices. In particular, nodal prices are obtained as the dual optimal multipliers of power balance constraints in optimal power flow problems. Optimal power flow problems are solved routinely in short-term (day-ahead and real-time) operations, therefore the computation of nodal prices is fully compatible with existing operating practices and is well within the reach of existing computational software for industrial scale models. Nodal prices can then be used as the basis for settling longer-term forward contracts, and providing appropriate signals for the investment in transmission and generation infrastructure. In the above example, the price at node 1 is equal to 40 $/MWh, indicating a profitable investment opportunity for an increase in the capacity of line 1-3 which coincidentally increases the value of trade between producers in location 1 and consumers in location 3. Owing to its compatibility with existing operations and its sound theoretical foundations, nodal pricing has become a standard component of electricity market design in a number of markets worldwide, including the United States (e.g. PJM, Texas, MISO, NYISO, California ISO) and certain European markets (e.g. Poland and Greece).

10.5.5 An Example of Zonal Pricing

Consider the example of Figure 10-46 [134]. An aggregation of nodes 1 and 2 into a single generating zone creates the challenge of defining how much capacity can be carried from the injection zone to the off-take zone (which is comprised of location 3). With a view towards respecting the thermal limit of line 1-3 regardless of the configuration of production, we would impose a limit of 900 MW between zones, so as to ensure that even if all injections are sourced from location 1, the limit of line 1-3 is respected. However, this eliminates opportunities for trade, in case node 2 has cheaper injections than location 1. If, on the other hand, we wish to maximize opportunities for trade then we would define the transmission limit as 1800 MW (if all off-takes were to be sourced from location 2), however this would threaten the thermal limit of line 1-3 if it turns out that the power is sourced from location 1.

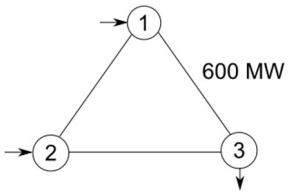

Figure 10-46 A three-node network with identical line characteristics, injections in nodes 1 and 2, and an off-take in node 3. Line 1-3 has a limit of 600 MW.

10.5.6 Pricing in the Presence of Binary Variables

Introducing binary variables that indicate on/off decisions into an optimal scheduling or dispatch problem (and, more generally, introducing features to the problem that render it non-convex) complicates the definition of market clearing prices, because market equilibrium, as described in the previous paragraph may not exist due to 'jumps' in agent decisions as a function of price. An alternative definition of market clearing price under such conditions has been debated extensively in the power system economics community. We list here a number of possibilities: (i) It is possible to proceed with a resolution of the convex relaxation of the scheduling problem and use the dual multipliers of the power balance constraints as locational prices; (ii) it is possible to solve the scheduling problem, fix decisions for the present interval, solve the dispatch problem with binary decisions fixed to their optimal value, and obtain the price from the power balance constraints; (iii) convex hull pricing [135] could be employed, (iv) the proposal of O'Neill [136] could be used, or (iv) a scheme like Euphemia [137] could be implemented, whereby the payments to paradoxically accepted bids are minimized. The relative advantages and disadvantages of these approaches are well documented in literature. These approaches remain to be tested in our numerical experiments. The approaches presented in section 10.5.9 pertain to convex optimization models and, hence, do not accommodate binary variables.

10.5.7 Algorithm for Calculating Prices with Possible Indeterminacies

First, the primal problem is solved and quantities are found. Then, the algorithm for finding cleared price p^* at node n goes as follows:

Every totally-accepted and partially-accepted bid is sorted according to the merit order. This should result in all partially-accepted bids being at the end of the sequence, and for the bids with the same p, the partially-accepted one should come after the totally-accepted ones. For each node n, we concentrate on the last accepted bids, β^{last} (note that we use the plural form "bids", because the last accepted bid could exist for bith $q > 0$ and $q < 0$). If there exist a partially accepted bid in β^{last} (such that $0 < x < 1$), the cleared price is found by looking at the value of the price in that bid:

$$p^* = p^*\left(x^{\text{partial}}_{\beta\in\beta^{\text{last}}}\right) \tag{217}$$

If β^{last} contains no partially-accepted but only totally-accepted bids ($x = 1$), then there is a price indeterminacy. In such a case, the cleared price is located in the middle of the p_1 values for the β^{last} with $q > 0$ and the β^{last} with $q < 0$:

$$p^* = {}^1\!/_2 \cdot \left(p_1^{q<0} + p_1^{q>0}\right) \tag{218}$$

An example is shown in Figure 10-47. In this case, the bids a_1 and b_1 are the last totally-accepted bids.

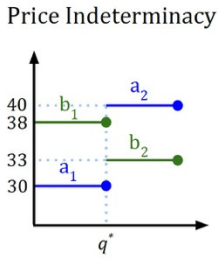

Figure 10-47 Price indeterminacy at the vertical edge of the crossing.

Therefore, the cleared price is calculated as

$$p^* = {}^1\!/_2 \cdot (38 + 30) = 34$$

10.5.8 DC versus AC on 2-node Example

In order to illustrate the influence of the exact representation of AC power flow equations on locational marginal prices, consider the two-node system example of Figure 10-48.

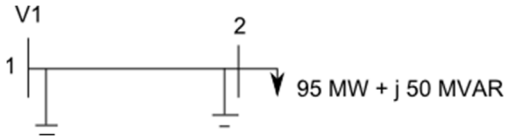

Figure 10-48 A two-node network with an injection at constant voltage at node 1 and an inelastic off-take at node 2. The basis is 100 MW. The per-unit characteristics of the line are R = 0.0065 and X = 0.062. The marginal cost at node 1 is 50 €/MWh.

An optimal DC power flow formulation of the model, where reactive power and real power losses are ignored and where voltage is normalized to 1 per unit[21], would result in a marginal price equal to 50

[21] The basis for voltage is irrelevant since all relevant quantities can be scaled accordingly, what matters is that voltage is not explicitly optimized.

€/MWh at location 2, as long as the capacity of the transmission line is greater than 0.95 per unit. An AC formulation can be described as:

$$v_2 - 2(0.0065 flowP + 0.062 flowQ) + l(0.0065^2 + 0.062^2) = v_1$$

$$\frac{flowP^2 + flowQ^2}{l} \leq v_2$$

$$q = 0.0065l - flowP$$

$$flowP + 0.95 = 0$$

$$q_{reactive} = 0.062l - flowQ$$

$$flo\ \ Q + 0.5 = 0$$

where v_i is the voltage magnitude squared in location i, $flowP$ is the real power flow over the line, $flowQ$ is the reactive power flow over the line, $q_{reactive}$ is the reactive power injection in node 1, and l is the current magnitude squared. The locational marginal price at node 2 becomes 50.679 €/MWh. The difference compared to the DC model is due to the real power losses that occur over the line connecting nodes 1 and 2.

10.5.9 Three Approaches for Pricing with AC Power Flow models

The above example illustrates the complexity introduced by the AC power flow equations. This is crucial for the intuitiveness of derived nodal prices, which will help to justify the differences in the nodal prices. In a general network, it is important to be able to explain how different factors contribute to the formation of price. We have developed three different approaches (see [138]) towards answering this question, with each approach providing a different point of view for the same problem.

Method 1: Contribution of Constraints to Price Formation

The first method generalizes the approach of Schweppe, Caramanis and Bohn [99], [100]. The price at a certain location is obtained as the contribution of a global power balance term, a term linked to congestion, a term related to binding voltage constraints, and a term related to binding transmission constraints:

$$\lambda = \begin{array}{c}\text{GlobalBalanceConstraintTerm} + \text{VoltageConstraintTerm} + \\ \text{TransmissionConstraintTerm} + \text{CongestionTerm}\end{array} \quad (219)$$

Each of the four terms above depend on network parameters (for example, impedance and reactance of lines) and the partial derivative of the decision variables with respect to a net injection of real power in the node whose price we are computing. This partial derivative becomes analytically complex to derive even for the simple two-node network of Figure 10-48, and is practically impossible to derive analytically

for a network with arbitrary topology. Therefore, each of these terms needs to be approximated numerically by re-solving the optimal power flow problem with a slight perturbation in the amount of power injection in the node whose price we are computing.

The key to the above result is to use a well-known result in power system analysis: all power flows can be described as a function of the root node voltage magnitude, and real and reactive power injections at the nodes. In intuitive terms, this means that if we were told the voltage magnitude at the root and the real and reactive power injections at all locations of the network then we could determine the power flows over the entire network. We can then write out the optimization problem in terms of the root voltage magnitude, real injections and reactive injections. Relaxing the voltage constraints, transmission constraints, and global power balance constraint of the problem yields a Lagrangian function, whose first-order conditions with respect to real power injection can be used to derive the relationship above (eq. (**219**)).

Method 2: Contribution of Losses to Price Formation

The starting point of the second method is the sensitivity interpretation of prices: the real power price of a certain location is the sensitivity of cost to a marginal change in real power injections in that same location. Since cost can be expressed as a function of total real power, which in turn can be expressed as the sum of real power consumption plus losses in the entire network, we obtain the following (see [138]):

$$\lambda \simeq \lambda_m(1 + \sum_{i \in E} \frac{d\ Losses_i}{d\ D_n}) \tag{220}$$

where λ_m is the marginal cost of the marginal generator, E is the set of lines of the network, and $\frac{d\ Losses_i}{d\ D_n}$ is the total derivative of the real power losses with respect to real power consumption in the location whose price we are computing. The marginal generator is the generator that is producing strictly above its technical minimum and strictly below its technical maximum, and whose output would be expected to change in order to satisfy a change in the real power consumption for the location whose price we are computing. As in the case of the previous method, the full derivatives cannot be computed analytically and need to be approximated numerically.

It is worth noting that the relation above is not exact, since it does not account for the second-order effect that non-marginal generator real power adjustments have on the objective function. Nevertheless, experimental experiences on a CIGRE 15-bus network shows that it predicts prices with an accuracy which is no worse than 0.1 €/MWh. Additional tests on networks of different sizes and topologies would have to be performed in order to verify the precision of the above formula.

The above decomposition provides the most intuitive way of understanding the formation of price. Once we understand how changes in real power injection at a certain location impact real power losses on

lines, we can explain how each of these loss terms contributes towards the formation of price. Note that these contributions may be positive or negative. A negative contribution to losses occurs when real power injection at a certain location brings the voltage magnitude of this location closer to that of its neighbors. (I.e. if the neighbors have a higher voltage magnitude than the node whose price we are computing). The contribution to losses becomes positive otherwise. (I.e. the neighbors have a lower voltage magnitude than the node whose price we are computing). Note that the price formation involves the entire network, and cannot be explained only in terms of the lines that are adjacent to the node whose price is being computed.

Method 3: Recursive Relation

The third method breaks down the price as follows (see [138]):

$$\lambda = \alpha \cdot \lambda_A + \beta \cdot \mu + \gamma \cdot \mu_A \tag{221}$$

where λ_A is the price of real power of the ancestor node, μ is the price of reactive power of the node in question, and μ_A is the price of reactive power of the ancestor node. The constants α, β and γ depend on network parameters and the decision variables of the optimal power flow solution, and can therefore be easily computed once the mathematical program has been solved. Stated otherwise, the price at the current node can be expressed as a linear combination of the reactive power price at the current node, and the price of real and reactive power of the ancestor node. This provides us with a recursive relation for computing prices from the top to the bottom of a radial network. Experimental experience suggests that the term $\alpha \cdot \lambda_A$ has the greatest influence in the formation of the price.

Cross-comparison of Three Methods

The three methods described above can be compared in terms of how intuitive they are in explaining prices, how easily the price breakdown can be computed (how many times the optimal power flow needs to be solved and whether the conic relaxation is adequate or a non-linear power flow needs to be solved), and exactness (whether the derived identities are exact and whether these identities can be computed in closed form or need to be approximated numerically). Table 10-1 summarizes the relevant information. It highlights the tradeoffs in the three methods, since there is no dominant method in all criteria.

	Physical intuition	Scalability of computation	Exactness
Method 1: Constraint contribution	+	- (two NLPs, or two SOCPs if conic relaxation is tight)	+ (partial derivatives need to be approximated numerically)
Method 2: Losses	++	+ (two SOCPs even if conic relaxation is not tight)	- (original identity is approximate, and total derivatives need to be approximated numerically)
Method 3: Recursive	-	++ (one SOCP)	++ (valid even if conic constraint is not tight)

Table 10-1 Comparison of three methods.

Our recommendation for the preferable approach is method 2, based on losses, since it is the method best grounded on physical intuition (very important in practice in the power markets, e.g. DA market in Europe), while being acceptably accurate and scalable. It only requires twice the amount of computation compared to method 3, and relies on the resolution of an SOCP relaxation within an operationally acceptable timeframe. The accuracy of the method has been verified through experiments: for the CIGRE 15-node network, the method predicts prices with an accuracy of 0.1 €/MWh.